AN INVESTIGATION OF THE ROLE OF THE EPSTEIN-BARR VIRUS-ENCODED PROTEIN, EBNA1, IN THE REGULATION OF EBER EXPRESSION

By

Thomas John Owen

A thesis submitted to The University of Birmingham

for the degree of

DOCTOR OF PHILOSOPHY

Cancer Research UK Institute for Cancer Studies

School of Cancer Sciences

The University of Birmingham

September 2009

ABSTRACT

The Epstein-Barr virus (EBV)-encoded RNAs (EBERs) are abundantly expressed in all EBV-associated malignancies, although the precise mechanisms by which EBV is able to achieve such high levels of EBER expression have not been fully determined. Abundant EBER expression has previously been demonstrated to be important for the oncogenic potential of the EBERs to be realised in epithelial cells. This study aimed to elucidate further how EBV achieves abundant EBER expression. Firstly, experimental analysis focussed on the possible direct correlation between EBV genomic copy number and levels of EBER expression. These initial experiments revealed that no direct link between EBV genomic copy number and levels of EBER expression was evident, suggesting that EBV may be influencing the cellular environment. Previously, EBV has been demonstrated to induce a variety of cellular EBER-associated transcription factors, and the remainder of the study focussed on determining the role of EBV nuclear antigen 1 (EBNA1) in inducing changes to the cellular environment to allow high levels of EBER expression. EBNA1 was found to induce the transcription of cellular RNA polymerase (pol) II and pol III transcription factors associated with EBER expression and levels of the cellular transcripts transcribed by the EBER-transcribing pol III were increased. Cell systems were generated which allowed EBNA1 to be expressed transiently in EBER-expressing cells, with such expression resulting in increased EBER expression, demonstrating directly that EBNA1 is able to increase levels of EBER expression. EBNA1 promoter binding studies were conducted, revealing EBNA1 to be present at the promoter regions of transcriptionally induced genes, affording mechanistic insight into EBNA1's mode of action. The results of this study prove significant not only in determining how EBV expresses such high levels of EBERs, but also in that EBNA1 is shown to influence several cellular factors directly implicated in oncogenesis.

ACKNOWLEDGEMENTS

I would like to take the opportunity to thank Cancer Research UK for funding my research. I would also like to thank Professor Lawrence Young for giving me the opportunity to work within his group and for his intellectual support during the course of this project.

I would also like to give special thanks to Dr John Arrand for his help, guidance, patience, and supervision of the course of this project.

The support and encouragement of the whole NPC group has also proved invaluable, especially the bench supervision and technical guidance provided by Dr John O'Neil.

Finally, I would like to thank my parents and my beautiful fiancée Natasha for their endless love, support and tolerance which has enabled me to complete this project.

Abbreviations

AIDS	Acquired immunodeficiency disease
AP-1	Activator protein 1
APS	Ammonium persulphate
ATF-2	Activating transcription factor 2
ATL	Adult T-cell leukaemia
BARTs	BamHI A rightward transcripts
BCR	B-cell receptor
BL	Burkitt's lymphoma
BSA	Bovine serum albumin
CGH	Comparative genomic hybridisation
ChIP	Chromatin immunoprecipitation
CMV	Cytomegalovirus
CRE	cAMP Responsive Element
CREB	Cyclic AMP response element-binding protein
Ct	Cycle threshold
CTAR	C-terminal activation region
CTLs	Cytotoxic T-lymphocytes
DS	Dyad symmetry
EBERs	EBV-encoded RNAs
EBNA	EBV nuclear antigen
EBNA-LP	EBNA-leader protein
EBP2	EBNA binding protein 2
EBV	Epstein-Barr virus
EMSA	Electromobility shift assays
ERK	Extracellular-regulated kinase

FACS	Fluorescence-activated cell sorting
FBS	Foetal bovine serum
FITC	Fluorescein isothiocyanate
FR	Family of repeats
GC	Gastric carcinoma
Gly/Ala	Glycine-Alanine
GSK-3	Glycogen synthase kinase-3
HBV	Hepatitis B Virus
HCC	Hepatocellular carcinoma
HCV	Hepatitis C Virus
HHV	Human Herpes Virus
HINGS	Heat inactivated goat serum
HIV-1	Human immunodeficiency virus-1
HL	Hodgkin's lymphoma
HLA	Human leukocyte antigen
HLH	Helix-loop-helix
HPVs	Human papillomaviruses
HRS	Hodgkin/Reed-Sternberg
HSV	Herpes Simplex Virus
HTLV-1	Human T-cell leukaemia virus type 1
IF	Immunofluorescence
IFN	Interferon
IL	Interleukin
IM	Infectious mononucleosis
IP	Immunoprecipitation
IR	Internal repeat
ISH	*In situ* hybridisation staining

KSHV	Kaposi's sarcoma-associated herpesvirus
LANA	KSHV latency-associated nuclear antigen
LB	L-Broth
LCL	Lymphoblastoid cell line
LD	Lymphocyte depleted
LMP	Latent membrane protein
LTRs	Long terminal repeats
LZ	Leucine zipper
MC	Mixed cellularity
MCM	Minichromosome maintenance
MDCK	Madin-Darby Canine Kidney
MHC-I	Major histocompatibility class-I
miRNAs	MicroRNAs
NF-κB	Nuclear factor kappa B
NK	Natural killer
NLS	Nuclear localisation signal
NPC	Nasopharyngeal carcinoma
NS	Nodular sclerosing
OHL	Oral hairy leukoplakia
ORC	Origin recognition complex
ORF	Open reading frame
PAGE	Polyacrylamide gel electrophoresis
PBS	Phosphate buffered saline
PCR	Polymerase Chain Reaction
PELs	Primary effusion lymphomas
PFA	Paraformaldehyde
PKR	Protein kinase R

pol II	RNA polymerase II
pol III	RNA polymerase III
PTLD	Post-transplant lymphoproliferative disease
Rb	Retinoblastoma protein
RIG-I	Retinoic acid-inducible gene-1
RNP	Ribonucleoprotein
SCC	Squamous cell carcinoma
SCID	Severe combined immunodeficient
SDW	Sterile distilled water
SV40	Simian Virus 40
TAM	Tyrosine-based activation motif
TBP	TATA-binding protein
TBS	Tris-buffered saline
TGFβ	Transforming growth factor β
TNFR	Tumour necrosis factor receptor
TR	Terminal repeats
TRF2	Telomeric repeat binding factor 2
TSG	Tumour suppressor gene
VAHS	Virus-associated haemophagocytic syndrome
VZV	Varicella-zoster virus
WHO	World Health Organisation
XMRV	Xenotropic murine leukemia virus-related virus

CONTENTS

Title of section **Page**

LIST OF TABLES

LIST OF FIGURES

Title of figure **Page**

[Figures in this digital copy are located at the end of the document]

Title of figure **Page**

Chapter 4

Title of figure **Page**

Title of figure **Page**

Title of figure **Page**

Title of figure **Page**

Chapter 1

Introduction

Chapter 1 – Introduction

1.0 The Biology of Cancer

Although cancer as a disease was recognised several thousand years ago, it was not until the 19th century that scientific oncology was born. An historical perspective of cancer is succinctly provided by several interesting review articles (Kardinal and Yarbro 1979; Diamandopoulos 1996). In the past quarter of a century, cancer research has advanced hugely and at a rapid rate, generating a complex and diverse body of evidence demonstrating that dynamic changes to the genome are responsible for the disease. Two classes of cancer gene have been identified through their alteration (mutation) in cells and the oncogenic phenotypes these mutations elicit *in vitro* (Bishop et al. 1996); proto-oncogenes possessing a dominant gain of function, and tumour suppressor genes with a recessive loss of function. Evidence suggests that tumourigenesis is a multistep process, determined by genetic and environmental factors, that reflects the progressive alterations that drive the transformation of normal human cells into malignant derivative cells (Hanahan and Weinberg 2000). For the transformation into a malignant cell, it has been proposed that any normal cell must evolve six "hallmarks" of cancer, or acquired capabilities (in addition to genomic instability which represents the means that enables the 6 biological endpoints to be reached), namely: 1) self-sufficiency in growth signals; 2) insensitivity to anti-growth signals; 3) evasion of apoptosis; 4) limitless replicative potential (immortalisation); 5) sustained angiogenesis; 6) tissue invasion and metastasis (Hanahan and Weinberg 2000). Each of these novel capabilities acquired during tumour development breaches one or more of the multitude of anticancer mechanisms possessed by cells and tissues. As such the evolution of these traits is a long and cumulative process, with only cells that develop each of the capabilities reaching their full malignant

potential. The dynamic and complex nature of the process explains, at least in part, how more than 100 distinct types of human cancer may have developed, and why cancer is relatively rare during a human lifetime.

1.1 Viruses and Cancer

Oncogenic viruses are of huge importance in cancer research for two main reasons. Firstly, current estimates suggest viruses are involved in 15% to 20% of human cancers worldwide (Javier and Butel 2008), with this proportion likely to be significantly increased over the 21st century, given the years of research usually required for the viral causation of a given human cancer to be widely accepted (Butel 2000; Pagano et al. 2004). A large number of these cancer causative infections may in future be prevented through immunisation, a trend which is sure to grow beyond the current vaccination for hepatitis B virus (HBV) and human papillomaviruses (HPVs). Secondly, experimental analysis of tumour viruses has provided more general illumination of cancer, with many oncogenes and tumour suppressor genes first identified through studies of tumour viruses.

Tumour viruses can be subdivided, based upon whether an RNA or DNA genome is packaged into the infectious virus particle, into two categories; the RNA tumour viruses and DNA tumour viruses (Javier and Butel 2008).

1.2 RNA Tumour Viruses

Hepatitis C Virus (HCV) is a single stranded RNA virus of the Hepacivirus genus in the Flaviviridae family. It infects approximately 2% of the worldwide population and is the only positive-stranded RNA virus among human oncogenic viruses. Persistent infection with HCV is associated with hepatitis, cirrhosis, hepatic steatosis, and hepatocellular carcinoma (HCC) (Saito et al. 1990; Alter 1995; Lauer and Walker 2001; Poynard et al. 2003; Pawlotsky 2004).

Among patients infected with HCV, it is almost exclusively those with cirrhosis who develop HCC, and while it is currently thought that this major risk factor for malignant progression plays a key role in HCV-induced carcinogenesis, precise underlying mechanisms are yet to be elucidated fully (Fattovich et al. 2004). Multiple viral and cellular factors are likely to be involved, along with viral and environmental cofactors such as HBV infection and excessive alcohol consumption. Interestingly, HCV has been shown to cause genome instability, suggesting a mutator function for certain HCV proteins (Smirnova et al. 2006).

Human T-cell leukaemia virus type 1 (HTLV-1) was the first reported tumourigenic human retrovirus, first isolated from cultured human T-lymphoma cells in 1980 (Poiesz et al. 1980). Over several subsequent years, a rapid accumulation of evidence linking HTLV-1 with adult T-cell leukaemia (ATL) occurred (Levine 1991). HTLV-1 remains the only human retrovirus linked directly to a specific malignancy (Javier and Butel 2008), despite retroviral association with a variety of animal tumours. Contrary to typical animal retrovirus mechanisms, HTLV-1 does not cause cancer through transactivation of cellular proto-oncogenes or insertional mutagenesis of tumour suppressor genes. The viral *Tax* gene is the major oncogenic determinant of HTLV-1 (Matsuoka and Jeang 2007), and also encodes a protein essential for viral replication. Tax modulates expression of viral genes though the viral long terminal repeats (LTRs), and also induces dysregulation of multiple cellular transcriptional signalling pathways including activator protein 1 (AP-1) (Iwai et al. 2001; Peloponese and Jeang 2006), nuclear factor kappa B (NF-κB) (Chu et al. 1998; Sun and Ballard 1999), and cyclic AMP response element-binding protein (CREB) (Zhao and Giam 1992; Franklin et al. 1993; Kwok et al. 1996). Tax does not bind to promoter or enhancer sequences directly, but interacts with cellular transcriptional co-activators (Bex et al. 1998; Harrod et al. 1998; Scoggin et al. 2001).

Tat, a homologue of Tax in human immunodeficiency virus 1 (HIV-1), plays an important role in the pathogenesis of Kaposi's sarcoma (Blattner 1999).

Recently, Xenotropic murine leukemia virus-related virus (XMRV) has been described. A gamma retrovirus, XMRV was discovered in tumours from prostate cancer patients (Urisman et al. 2006), and although it is unclear whether XMRV is causally associated with prostate cancer, it may contribute to tumourigenesis through an indirect mechanism.

1.3 DNA Tumour Viruses

Human DNA tumour viruses are a diverse group consisting of viruses that vary in terms of structure, replication strategy and genome organisation, with some causing malignancies in their natural hosts (e.g. HBV, Epstein-Barr virus (EBV), HPV and Kaposi's sarcoma-associated herpesvirus (KSHV)), and others possessing transforming properties in cultured cells and heterologous animal models (e.g. human adenoviruses). DNA tumour virus oncogenes are often of viral rather than cellular origin, and are required for viral replication (Damania 2007). Analysis of DNA tumour virus oncoproteins has provided insight into viral mechanisms controlling mammalian cell growth. Although extensive description of each tumourigenic mechanism of individual DNA tumour viruses is beyond the scope of this thesis, key examples are discussed below.

Certain cellular tumour suppressors are targeted by evolutionarily distinct DNA tumour viruses using diverse mechanisms, highlighting the importance of these regulators in both the viral life-cycle and tumourigenesis. Two of the most significant and best described cellular tumour suppressors affected by infection of cells by DNA tumour viruses are p53 and retinoblastoma protein (Rb). Cellular tumour suppressor gene p53 was discovered through its association with the large tumour (T) antigen of Simian Virus 40 (SV40) (Lane and Crawford

1979; Linzer and Levine 1979). A variety of cellular stress stimuli induce activation and accumulation of p53, which in its role as a sequence-specific transcription factor regulates several important cellular factors (Braithwaite and Prives 2006) which control cell cycle, senescence, apoptosis and DNA damage. SV40 large T antigen, along with adenovirus E1B-55K protein and HPV protein E6, binds to and inactivates p53, opening a temporal window for virus replication, before a p53-mediated cellular anti-viral response is initiated by viral infection.

The *Rb* tumour suppressor gene was identified in the mid 1980s (Friend et al. 1986; Lee et al. 1987) and subsequently associations were established between Rb and adenovirus E1A protein, SV40 large T antigen, HPV E7 protein and polyomavirus large T antigen which lead to aberrant cell cycle control (DeCaprio et al. 1988; Whyte et al. 1988; Dyson et al. 1989). Binding of these viral oncoproteins to Rb results in the disruption of cellular complexes containing the transcription factor E2F, with release of E2F accompanied by the progression of the cell cycle from G_1 to S-phase and DNA synthesis. Active E2F that has been aberrantly freed by viral oncoprotein binding to Rb leads to unscheduled cellular proliferation of quiescent cells. Adenovirus, SV40 and HPV16 infected cells are associated with increased levels of free E2F and loss of cell cycle-dependent E2F regulation (Chellappan et al. 1992). Human herpesviruses are also known to modulate Rb function during infection, and this topic has been recently reviewed by Hume and Kalejta (2009). That dysregulation of the Rb/E2F pathway occurs in the majority of human tumours (Weinberg 1995) demonstrates the vast significance of DNA tumour viruses in cellular pathways important in tumourigenesis.

Immune evasion by DNA tumour viruses also plays a role in their tumourigenic pathogenesis. For example, down-regulation of major histocompatibility class-I expression by E1A of

adenovirus type 12 and the KSHV encoded proteins K3 and K5 (Guan et al. 2008; McLaughlin-Drubin and Munger 2008) has been demonstrated to play a role in the pathogenesis of these tumour viruses. Further, evasion of cytotoxic T lymphocytes (CTLs) by adenoviruses, KSHV and EBV means cells infected by these viruses are not killed in a CTL-dependent manner while EBV also encodes a homologue of interleukin 10 (vIL-10) which may be capable of suppressing cytotoxic T-cells (Marshall et al. 2004).

The listed mechanisms of DNA tumour virus function and viral oncogenes given above are by no means exhaustive, with further examples given throughout this thesis. Additionally, viruses other than those described have been implicated in human tumourigenesis. For example, Torque teno virus, a single-stranded circular DNA virus of the Circoviridae family, is associated with a number of human cancers (de Villiers et al. 2002) and Merkel cell polyomavirus is frequently found to be integrated in cells prior to tumour development in Merkel cell carcinoma, a rare but a highly aggressive neuro-endocrine carcinoma of the skin (Becker et al. 2009).

Further examples of tumour viruses and their mechanisms have been subject to recent review by Mclaughlin-Drubin and Munger (2008).

1.4 Human Herpesviruses

The taxonomy of herpesviruses has been updated by the International Committee on Taxonomy of Viruses (ICTV). The former family *Herpesviridae* has been split into three families, which have been incorporated into the new order *Herpesvirales* (Davidson et al. 2009). The revised family *Herpesviridae* retains the mammal, bird, and reptile viruses; the new family Alloherpesviridae incorporates the fish and frog viruses; the new family Malacoherpesviridae contains a bivalve virus. Although there are over 100 characterised

members of the *Herpesviridae* family, only eight herpesviruses are routinely isolated from humans; Herpes simplex virus type 1 (HSV-1), Herpes simplex virus type 2 (HSV-2), Varicella-zoster virus (VZV), EBV, Cytomegalovirus (CMV), Human herpesvirus 6 (HHV-6), Human herpesvirus 7 (HHV-7) and Kaposi sarcoma-associated herpesvirus (KSHV) (reviewed by Whitley 2006).

Four significant biological properties are shared by all human herpesviruses (Roizman and Pellett 2001): 1) Unique enzymes are encoded. These structurally diverse enzymes provide unique sites for inhibition by antiviral agents. 2) Viral DNA synthesis and assembly, and capsid assembly, are initiated in the nucleus. 3) Cell death accompanies release of progeny virus from infected cells. 4) Latent infection is established that is indicative of the tissue tropism of each family member.

Herpesviruses contain double stranded DNA, varying from 120 to 250kb in length, located at the central core, which is surrounded by a capsid in which 162 capsomers are arranged in icosapentahedral symmetry. The viral tegument adheres tightly to the outside of the capsid, with a lipid bilayer derived from host cell membranes loosely surrounding the capsid and tegument. Finally an envelope, consisting of cellular polyamines and lipids, and viral glycoproteins, coats herpesvirus virions.

Herpesviruses are grouped into subfamilies which identify evolutionary relatedness and summarise the unique properties of each member. Members of the *Alphaherpesviridae* have an extremely short (hours) replicative cycle, destroy the host cell and replicate in a wide variety of host tissues. These viruses have a propensity to replicate in neuronal tissue, meaning latent infection is established in sensory nerve ganglia. The alphaherpesvirus subfamily consists of HSV-1, HSV-2, and VZV.

Members of the *Betaherpesviridae* infect a restricted host range, and have long (days) replicative cycles, with slowly progressing infection in culture. Infection is characterised by the formation of giant multinucleated cells. Latent infections are established in secretory glands, cells of the reticuloendothelial system (phagocytic cells) and the kidneys. Betaherpesviruses include CMV, HHV-6 and HHV-7.

The *Gammaherpesviridae* include EBV and KSHV. Subfamily members are lymphotrophic, possessing the most limited limited host range of the *Herpesviridae*, and are characterised as having oncogenic potential. Some gammaherpesvirus subfamily members including murine gammaherpesvirus 68 and EBV possess dual tissue tropism, replicating in the respiratory and oropharyngeal epithelium respectively, before establishing latent infection in B-cells. Gammaherpesviruses can be further sub-categorised into the lymphocryptoviruses (gamma-1-herpesviruses) and rhadinoviruses (gamma-2-herpesviruses). Lymphocryptoviruses include EBV, rhesus lymphocryptovirus, and herpesvirus papio of baboons, while gamma-2-herpesviruses include KSHV, herpesvirus saimiri virus of squirrel monkeys and the murid herpesvirus MHV-68. This thesis will focus on the gamma-1-herpesvirus EBV.

1.5 Epstein-Barr Virus

Epstein-Barr Virus was the first reported human tumour virus. In the 1950s, a British surgeon, Denis Burkitt, working in East Africa was the first to describe the childhood tumour now known as Burkitt's lymphoma (BL) (Burkitt 1958). Strikingly, cases of the disease were found to follow closely the African malarial belt, leading Burkitt to suspect that a virus, perhaps transmitted by an arthropod vector, might be the etiologic agent for the novel childhood tumour (Burkitt 1962). In 1965, Tony Epstein, Yvonne Barr and colleagues were successful in establishing BL-derived cell lines, and in the visualisation by electron microscopy of herpesvirus-like particles from a small percentage of cells (Epstein et al. 1965).

This virus was subsequently shown to be antigenically and biologically distinct from other known human herpesviruses (Henle and Henle 1966) and was named EBV. Seroepidemiologic studies showed a worldwide distribution for EBV in human populations, with over 90% of adults testing positive for serum antibodies to EBV, and the proposed role of EBV in Burkitt's lymphoma was initially met with scepticism (Epstein 2001), although overwhelming evidence now supports the concept of EBV playing a central role in African BL (Pagano et al. 2004). Serological studies also identified EBV as the etiological agent of infectious mononucleosis (IM), and demonstrated that EBV infection was a common feature of another malignancy, undifferentiated nasopharyngeal carcinoma (NPC) (Henle et al. 1968; zur Hausen et al. 1970). The transformation potential of EBV was confirmed almost concurrently by demonstration of the ability of the virus to transform resting B-cells *in vitro* (Henle et al. 1967; Pope et al. 1968), leading to EBV being characterised as the first human tumour virus. Subsequent studies have implicated EBV in other malignancies including Hodgkin's lymphoma (HL), lymphoproliferative disorders in the immunocompromised, T-cell lymphomas and gastric carcinoma (GC). EBV and its role in oncogenesis have been reviewed extensively (Young and Murray 2003; Thompson and Kurzrock 2004; Young and Rickinson 2004), and will be discussed more fully later in this chapter.

The EBV particle shares features common to all human herpesviruses, with the outer envelope studded with viral glycoproteins used for attachment to host cells, fusion and subsequent entry. EBV preferentially infects B lymphocytes by binding the major viral envelope glycoprotein gp350 to the CD21 receptor on the surface of B-cells, and through the binding of glycoprotein gp42 to human leukocyte antigen class II molecules as a co-receptor (Nemerow et al. 1987; Borza and Hutt-Fletcher 2002).

The DNA genome extracted from virus particles is a double-stranded linear molecule of around 172kb. EBV was the first herpesvirus to be completely cloned and sequenced (Baer et al. 1984), with the prototype EBV strain B95-8 being obtained from patients with IM and passaged in marmoset leucocytes. The EBV genome is not a unique structure, with genomes containing a variable number of terminal repeats (TR) of 538 nucleotides in length, a short unique region of about 15 kb, and a long unique region of around 150kb in size. These regions are separated by varying number (5-12) of internal tandem repeats (each repeat unit being 3072bp in length), known as internal repeat (IR)-1. EBV also contains other smaller repeated sequences including IR2 and IR4. IR2 is 125 nucleotides long and is proximal to the left end of the long unique region. IR4 (102 nucleotides long) shows homology with IR2 and is located towards the right end of the long unique region. Additionally, a distinct repeating sequence (IR3) is located within the coding region for EBNA1 and consists of around 45 copies of the tandemly repeated sequence GGGGCAGGAGCAGGA, which encodes an array of alanine and glycine residues, giving rise to its alternative name of the 'Gly/Ala repeat' region. The EBV genome organisation is shown schematically in Figure 1.1. The EBV genome was sequenced from an EBV DNA BamHI fragment-cloned library (Baer et al. 1984), and as such open reading frames (ORFs), genes and sites for transcription or RNA processing are often referenced to specific BamHI fragments named according to size, with 'A' being the largest, through to the smaller 'Z'. Lowercase letters indicate the smallest fragments and a summary of the *Bam*HI fragments is presented in Figure 1.1B. Although the EBV DNA genome is linear, following infection terminal repeats are known to fuse, resulting in intracellular viral DNA being predominantly episomal and circular. However, the presence of integrants in early passage cell lines suggests that *in vivo* integration of EBV DNA occurs, a suggestion supported by evidence reporting the observation of integrated EBV genomes in

Figure 1.1 – **A)** General organisation of EBV DNA, adapted from Arrand (1998). U1 and U2 are the unique sequence regions of the genome which are interspersed with four internal repeat regions (IR1-4) and flanked by terminal repeats (TR).

B) Adapted from Young and Rickinson (2004). Location of open reading frames for the EBV latent proteins on the *Bam*HI restriction-endonuclease map of the prototype B95.8 EBV genome. The *Bam*HI fragments are named according to size, with 'A' being the largest, through to the smaller 'Z'. Lowercase letters indicate the smallest fragments. Notably, the LMP2 proteins (not marked on this map) are produced from mRNAs that splice across the terminal repeats (TRs) in the circularized EBV genome. This region is referred to as Nhet, to denote the heterogeneity in this region due to the variable number of TRs in different virus isolates and in different clones of EBV-infected cells.

C) Adapted from Young and Rickinson (2004). Location and transcription of the EBV latent genes on the double-stranded viral DNA episome. The origin of plasmid replication (OriP) is shown in orange and the large green solid arrows represent exons encoding each of the latent proteins with arrows indicating the direction in which the genes encoding these proteins are transcribed. The long outer green arrow represents EBV transcription during latency III (Lat III), in which all the EBNAs are transcribed from either the Cp or Wp promoter while the inner, shorter red arrow represents the EBNA1 transcript, which originates from the Qp promoter during Lat I and Lat II.

Figure 1.1

NPC tumour biopsies (Kripalani-Joshi and Law 1994). Integration of DNA has been implicated in carcinogenesis (e.g. HBV and HPV) although it is unclear whether integration of viral DNA is required for EBV-associated neoplasia, as the majority of EBV DNA found in tumour cells is episomal.

1.5.1 EBV infection *in vitro*

EBV has the unique ability to transform resting B-cells into permanent, latently infected lymphoblastoid cell lines (LCLs). This *in vitro* system has provided an invaluable model of the lymphomagenic potential of the virus. Each cell in an LCL carries multiple extrachromosomal copies of the viral episome and constitutively expresses a limited set of latent viral gene products: six nuclear antigens (EBNAs 1, 2, 3A, 3B, 3C and -LP); three latent membrane proteins (LMPs 1, 2A and 2B); the BamHI-A transcripts (BARTs); two small non-polyadenylated RNAs (EBERs) and viral microRNAs (miRNAs) (Thompson and Kurzrock 2004; Young and Rickinson 2004). This 'growth programme' pattern of gene expression is referred to as latency III and mimics what occurs *in vivo* upon infection of naïve, and possibly, memory B-cells. Patterns of EBV latent gene expression are discussed more fully in the subsequent section, 1.5.4.

LCLs show high levels of expression of the B-cell activation markers CD23, CD30, CD39 and CD70, and of the cell-adhesion molecules lymphocyte-function-associated antigens 1 and 3, and intercellular cell-adhesion molecule 1 (Rowe et al. 1987; Kieff and Rickinson 2001). Usually on resting B-cells, such markers are expressed at extremely low level or are absent, but transient induction of these markers to high levels can occur following activation into short-term growth by mitogenic or antigenic stimulation. This indicates that EBV-induced immortalisation can be elicited through the activation of the same cellular pathways that drive

B-cell proliferation in a physiological setting (Young and Rickinson 2004). The role of individual EBV latent genes in the *in vitro* transformation of B-cells has been investigated through the use of recombinant forms of EBV lacking single latent genes. Such studies have confirmed the absolute requirement for LMP1 and EBNA2 in transformation, and have highlighted crucial roles for EBNA3, EBNA-LP, and EBNA1 (Kieff and Rickinson 2001).

Although EBV infection of resting B-cells is usually tightly latent, a small number of cells within an LCL population will be undergoing spontaneous reactivation and lytic replication at any one time. Lytic replication can also be induced by the treatment of cells with chemical activators or cross-linking of the B-cell receptor (Shimizu et al. 1996; Feederle et al. 2000). Such stimulation results in the induction of lytic transactivators BZLF1 and BRLF1, through activation of transcription factors such as AP-1. These lytic transactivators subsequently mediate a switch from viral latency to classic herpesvirus lytic replication, which is observed to be almost identical in B-cells and epithelial cells despite the reported differences in latent infection *in vitro* (Feederle et al. 2000).

Examination of the early events following *in vitro* infection of primary epithelial cells and cell lines has been problematic for researchers, given that epithelial cells do not express cell surface molecule CD21 and, as such, are generally refractory to infection with EBV. Transfection of CD21 into epithelial lines has been utilised to allow the efficient infection of epithelial cells, with abortive lytic infection resulting (Li et al. 1992; Knox et al. 1996), a finding in contrast to the outcome of EBV-infection of CD21 expressing B-lymphocytes *in vitro*. However, some rare clones retaining EBV have previously been isolated by limiting dilution cloning (Knox et al. 1996) and by utilising recombinant EBV, thus allowing drug resistance selection of EBV-positive clones (Imai et al. 1995). The EBV-positive clones

which were generated in such experiments displayed a latency I or II type gene expression, similar to the EBV expression in the malignant cells of undifferentiated NPC.

Recently, a system has been developed in which EBV is efficiently delivered into epithelial cells by a process which involves the transfer from the surface of virus-loaded resting B cells (Shannon-Lowe et al. 2006). This system has been utilised to demonstrate that B-cell and epithelial cell types support different patterns of transcription, and that other differences between *in vitro* EBV-infection of B-cells and epithelial cells are apparent (Shannon-Lowe et al. 2009). For example, whereas infection of B cells with one or two copies of EBV results in rapid amplification of the viral genome to >20 copies per cell, such amplification was not observed after infection of primary epithelial cells or undifferentiated epithelial lines in this study. Furthermore, in epithelial cells, EBNA1 expression was detected in less than 50% of EBER-expressing cells, with the EBV genome subsequently being lost during prolonged culture. Such data highlight the influence of the host cell on the outcome of EBV infection with regard to genome expression, amplification, and maintenance.

1.5.2 EBV primary infection

Transmission of EBV from host to host is via saliva, with most children in the developing world becoming infected early in life, in most instances through familial contact (Gratama et al. 1990). However in the Western world, primary infection is often delayed, with the virus subsequently being acquired in adolescence or young adulthood, often resulting in IM. EBV induced IM is a self-limiting infection characterised by fever, malaise, lymphadenopathy and hepatosplenomegaly (Slots et al. 2006). In acute infection of B-lymphocytes, EBV expresses a protein complement that results in cell proliferation. In healthy individuals, this produces an EBV-specific CTL response, accounting for an ensuing fall in infected B-cells, with the

adaptive immune response eventually controlling primary infection. As such, EBV becomes latent and persists within memory B-cells for the lifetime of the carrier (Babcock et al. 1998), although periodic lytic reactivation of EBV occurs at mucosal sites and shedding of virus can be detected in healthy EBV carriers (Babcock et al. 1998; Ikuta et al. 2000).

The precise life cycle of EBV *in vivo* is still incompletely defined. EBV, transmitted by infected saliva, transits (through an unknown mechanism) the epithelium of tonsillar crypts before infecting naïve B-cells in underlying tissue (Thorley-Lawson 2005). This infection results in the expression of the EBV transforming growth programme (latency III) as observed in the transformation of resting B-cells *in vitro* (Babcock et al. 2000). Following the attachment of EBV to CD21 molecules on the surface of naïve B-cells, cellular CD21 becomes cross-linked, initiating an activation signal that prepares the cell for EBV infection. The tyrosine kinase *lck* is activated by EBV binding to CD21 and calcium is mobilised (Gordon et al. 1986; Cheung and Dosch 1991). An increase in mRNA synthesis follows, along with blast transformation, surface CD23 expression, homotypic cell adhesion and interleukin (IL)-6 production (Tanner et al. 1987; Alfieri et al. 1991; Tanner et al. 1996), before viral genome uncoating and delivery to the nucleus. Here, circularisation of viral DNA occurs, before a cascade of events is launched by gene expression from the viral W promoter (Wp). This cascade results in expression of all six nuclear antigens along with the three LMPs, with EBNA-LP and EBNA2 being the first detectable EBV proteins following infection (Hennessy and Kieff 1985; Sung et al. 1991). 24-48 hours post-infection, transcription shifts from Wp to the C promoter (Cp). EBNAs are then transcribed (from Cp) from the same transcriptional unit which is around 100kb in length, ending at the 3' end of the EBNA1-encoding gene. Initially, the switch from Wp to Cp expression was thought to coincide with an expansion of splicing patterns to allow expression of EBNA1 and EBNA-

3A, -3B, and -3C, although this splicing pattern is now known to precede the switch in promoter usage (Puglielli et al. 1997). Indeed, data suggest that these downstream EBNAs are involved in the regulation of Cp activation (Reisman and Sugden 1986; Radkov et al. 1997; Yoo et al. 1997). Further, each EBNA protein is involved in other transcriptional control processes, and EBNAs are known to participate in the activation of LMP expression, along with the induction of several cellular genes. Expression of viral gene products has the capacity to activate B-cells and drive their proliferation in the absence of antigenic stimulation. Activated lymphoblasts transit to a follicle and subsequently enter germinal centre reactions. During this transit down-regulation of EBNA2 occurs, with EBV adopting a more restricted pattern of gene expression (latency II) confined to EBNA1, LMP1, LMP2A, the EBERs and BARTs (Babcock et al. 2000).

1.5.3 EBV latency states

The analysis of a number of different EBV-positive cell lines, and of several EBV-associated malignancies, has led to the definition of four latency programmes in which the patterns of viral gene expression are distinct. These patterns of latent gene expression result from differential viral promoter activity, in addition to influences from host cellular factors, and are outlined below:

Latency 0 - proposed to occur in circulating memory B-lymphocytes. Expression of all EBV latent gene products is absent, with the possible exception of LMP2A and the EBERs.

Latency I - characterised by BL, where expression is limited to the EBER and BART RNAs, with EBNA1 expression being driven from the Qp promoter. Expression of all of the other EBNAs, LMP1 and LMP2 is not observed.

Latency II - characterised by NPC and EBV-positive HL. In addition to the expression of the EBERs, BART RNAs and Qp-driven EBNA1, LMP1 and LMP2 are detected to varying degrees. No expression of all other EBNAs is observed.

Latency III – characterised by LCLs (as outlined above) and post-transplant lymphoproliferative disease (PTLD). The full spectrum of latent gene products is expressed, including all six EBNA genes spliced from a single poly-cistronic transcript driven from the Cp/Wp promoter. Expression of all three latent membrane proteins, the EBERs, and the BART RNAs is also observed.

Whilst the outlined forms of viral latency are useful in defining distinct viral gene expression patterns, they are subject to variability. EBV gene expression is a dynamic process *in vivo*, with the virus often adapting itself to the cellular environment in which it infects, leading to subsequent changes in latent gene expression over time, if necessary. *In vitro* observations of drifting patterns of latent gene expression (Rowe et al. 1992) and atypical gene expression patterns in BL cells (Kelly et al. 2002) support the idea of EBV gene expression being a highly dynamic process.

1.5.4 EBV persistence *in vivo*

Following antigen stimulation, activated naïve B-cells enter the germinal centre before undergoing rounds of rapid proliferation. This process is associated with isotype switching and somatic hypermutation of immunoglobulin genes. During this process cells which show greatest avidity for antigen are actively selected, with cells showing weaker antigen binding undergoing apoptosis. Actively selected surviving cells leave the germinal centre as either memory cells or differentiated plasma cells. The process requires survival signals provided by T helper cells through CD40 ligand stimulation in addition to antigenic activation. It has been

proposed that down-regulation of EBNA2 is essential for differentiation of EBV infected naïve B-cells. LMP1 and LMP2A provide essential survival signals which may increase the probability and frequency of EBV infected cells reaching the memory cell pool (Thorley-Lawson 2001) with LMP1 mimicking the constitutively active CD40 receptor and LMP2A being a viral homologue of the B-cell receptor, providing cell survival signals. These viral signals replace the usual requirement for high-affinity binding to antigen (Young and Rickinson 2004).

Contrary to the proposed model of EBV infection and persistence described above, some reports have revealed that IM tonsil sections show no down-regulation of EBNA2 in memory B-cells (Kurth et al. 2000). Taking this evidence into account, it is theorised that EBV may gain access to the memory compartment through the direct infection memory B-cells, resulting in latency III gene expression and resultant expansion of latently infected cells. Down-regulation or shut off of EBV gene expression may subsequently occur in order to allow EBV infected memory cells to evade CTL-mediated killing (Kurth et al. 2000). Alternatively, it is possible that EBV may directly infect memory cells during primary infection, however such direct infection of memory cells by EBV in healthy carriers has never been detected (Babcock et al. 2000).

Although the precise mechanism of EBV-infection of the pool of memory B-cells has yet to be elucidated, subsequent events are better characterised. After entry into the peripheral circulation, EBV gene expression is repressed with EBV-infected memory B-lymphocytes displaying a latency 0 transcription programme (Babcock et al. 1999). Latency 0 has been proposed to occur in circulating memory B-lymphocytes with the absence of expression of all EBV latent gene products (with the possible exception of LMP2A and the EBERs) enabling

the avoidance of host immune detection and EBV persistence within the B-lymphocyte compartment (Babcock et al. 1998; Thorley-Lawson 2005). Upon the occasional division of the memory B-lymphocytes in which EBV persists, a type I latency programme is adopted by EBV, where EBNA1 is expressed, thus ensuring equal segregation of the viral genome (Thorley-Lawson and Gross 2004). EBV is also thought to change its pattern of gene expression on occasions where resting memory B-lymphocytes re-enter the tonsil from the peripheral circulation. Survival of antigen-specific memory B-lymphocytes requires an intact functional B-cell receptor (BCR) and it is postulated that unknown signals induce the adoption of latency II, resulting in the re-expression of LMP1 and LMP2. LMP2 is then able to provide the required BCR signal to ensure the survival of cells in the memory population (Thorley-Lawson 2001).

For the maintenance of EBV in the general population, the virus must intermittently replicate and be shed into saliva for host to host transmission to occur. EBV is reactivated into lytic replication by signals that induce terminal differentiation of B-lymphocytes into plasma cells, resulting in the release of infectious virions (Laichalk and Thorley-Lawson 2005). Given the migration of antibody-secreting plasma cells into mucosal epithelium, virions would be released onto the mucosal surface, in the case of tonsil, directly into saliva (Thorley-Lawson 2005).

EBV infection of epithelial cells *in vivo* remains poorly elucidated in comparison with *in vivo* EBV-infection of B-lymphocytes. Initial studies revealed the presence of EBV in desquamated oropharyngeal epithelial cells of patients with acute IM (Sixbey et al. 1984), and recent data have successfully detected EBV DNA, mRNA and protein in a small subset of epithelial cells derived from healthy EBV-positive donors (Pegtel et al. 2004). However, other data contradict these findings (Hudnall et al. 2005; Karajannis et al. 1997; Niedobitek et al.

1997), leaving the question of the importance EBV-infection of epithelial cells in EBV persistence open to debate.

1.5.5 EBV Strain Variation

Given the high prevalence of EBV infection across the world's population, potential for huge evolutionary variation of the virus exists. Analysis of EBV DNA from a large variety of sources has revealed that despite this potential, all strains of EBV are closely related, though two of the best characterised strains, the prototypic B95-8, and P3HR-1, are variants which possess significant deletions within their DNA sequence. B95-8 has a deletion of around 12.5 kb, encompassing IR4. P3HR-1 has a deletion of the EBNA2 region. DNA homology of EBV isolates correlates well with antigenic similarity on the envelopes of various strains, and the fact that no distinct serotypes have been reported. Although expected minor inter-isolate differences exist, the notion of disease-specific subtypes is not favoured.

In spite of the overall similarity between EBV isolates two distinct EBV types, EBV-1 and EBV-2, have been defined on the basis of specific sequence variation in the EBNA2 gene (Dillner et al. 1985; Hennessy and Kieff 1985; Mueller-Lantzsch et al. 1985; Rymo et al. 1985). This variation results in antigenically distinct forms of EBNA2, and subsequently type specific differences have been demonstrated to extend to EBNA3A, EBNA3B, EBNA3C, EBNA-LP and the EBERs (Rickinson et al. 1987; Arrand et al. 1989; Sample et al. 1990; McCann et al. 2001). EBV-1 has been demonstrated to be more efficient in the *in vitro* transformation of resting B-cells, with EBV-1 transformants proliferating more rapidly, reaching higher saturation densities and showing less dependence on cell concentration than EBV-2 transformants (Rickinson et al. 1987; Cohen et al. 1989). Despite variation in a number of EBV genes being reported between EBV-1 and EBV-2, EBNA2 variation has been shown to be sufficient to mediate such effects (Cohen et al. 1989; Tomkinson and Kieff

1992). However, both EBV-1 and EBV-2 appear to contribute to the pathogenesis of BL and NPC with equal efficiency, and the specific divergence at genetic loci seems to be confined to latent genes as proteins associated with productive infection show much greater conservation (Arrand 1998).

1.6 EBV-associated diseases

In addition to IM, the acute, self-limiting disease associated with primary EBV infection, the virus is implicated in the aetiology of several different lymphoid and epithelial malignancies. Characteristics of these malignancies, and the role of EBV in each, are outlined in this section.

1.6.1 EBV-associated B-cell lymphomas

1.6.1.1 Burkitt's lymphoma

Burkitt's lymphoma is a particularly aggressive lymphoma, the hallmark of which is a chromosomal translocation between chromosome 8 and either chromosomes 14, 2, or 22 (Dalla-Favera et al. 1982; Taub et al. 1982; Leder et al. 1983). Because of this translocation, the oncogene c-myc (chromosome 8) is juxtaposed to the immunoglobulin heavy-chain (chromosome 14) or light-chain genes (chromosomes 2 or 22), with this aberrant configuration resulting in dysregulation of c-myc expression. The relationship between EBV, Burkitt's lymphoma, and the c-myc translocation is complicated by the existence of two types of Burkitt's lymphoma: endemic and nonendemic. EBV is present in all cases of endemic BL (Young and Rickinson 2004; Bornkamm 2009), the high-incidence form of the tumour that affects children in areas of Africa and New Guinea in which malaria is holoendemic , and in up to 85% of cases in areas of intermediate incidence such as Brazil and North Africa (where

schistosomiasis may play an aetiological role, similar to malaria, in EBV associated BL) (Araujo et al. 1996). However, in low-incidence sporadic tumours (nonendemic BL) that are seen in children in the developed world, only 15% EBV positivity is observed. Although a c-myc translocation occurs in both endemic and nonendemic BL, the breakpoints within the genes involved, and presumably the mechanism mediating juxtaposition, vary between the types of BL (Baumforth et al. 1999).

The role of EBV in BL is strongly supported by observations of the Akata BL cell line. Akata subcultures that lose EBV show decreased growth and an inability to induce tumours in mice (Shimizu et al. 1994), with reinfection of such subcultures with EBV re-establishing the malignant phenotype (Komano et al. 1998). However, the primary importance of c-Myc deregulation as the key factor in BL pathogenesis is widely accepted, given data produced from a range of experimental systems (Polack et al. 1996; Kovalchuk et al. 2000). In addition, mutations to the p53 pathway and the retinoblastoma-like tumour suppressor are further common features of BL (Lindstrom and Wiman 2002). Irrespective of EBV status, the phenotype of BL cells is strikingly similar to that of germinal centroblasts, with the detection of ongoing Ig-gene mutation in tumour cells supporting the suggestion that they are of germinal centre origin. The crucial c-Myc translocation is also likely to have occurred through error in the somatic hypermutation process (Young and Rickinson 2004), with the juxtaposition of c-myc next to one of the three immunoglobulin enhancers shown to result in deregulated c-myc expression (Klein et al. 2007).

Monoclonal EBV is consistently detected in the cell populations of BL biopsies suggesting that infection occurs prior to the malignant outgrowth of the tumour (Neri et al. 1991). The majority of EBV-positive BL tumours show a highly restricted latency I form of infection at presentation, with viral antigen expression limited to that of EBNA1 (Rowe et al. 1987; Kelly

et al. 2002) meaning that EBV's method of contribution to the pathogenesis of BL remains a matter of speculation, given that the EBV antigens required for B-cell immortalisation *in vitro* are not expressed in BL cells *in vivo*. The virus may play an initiating role in which growth-transforming B-cell infections establish a pool of target cells that are at risk of a subsequent c-myc translocation, and this process has been successfully modelled *in vitro* (Polack et al. 1996). However, this study highlighted the apparent incompatibility of the EBV latency III-driven and c-myc-driven growth programmes in B-cells (Pajic et al. 2001), indicating that the progression to BL can occur only if the EBV programme is suppressed. The strength of selection against full expression of viral latent genes is illustrated by a subset of BLs in which the transcriptional features of latency III are retained, but the deletion of the EBNA2 gene of viral genomes has occurred, ablating conventional B-cell transforming capability (Kelly et al. 2002). However, despite the apparent incompatibility of EBV latency III and c-Myc growth programmes, recent data suggest that c-Myc transcriptional regulation is an active effector in EBV latency III growth programme (Faumont et al. 2009a).

It is possible that EBV might contribute to BL pathogenesis through the latency I-active genes themselves, with EBNA1 an obvious candidate, and experiments in which EBNA1 function was blocked in EBV-positive BL cell lines demonstrated that EBNA1 promotes cell survival (Kennedy et al. 2003). However, as subsequently discussed (Section 1.7.7), EBNA1's oncogenicity in mouse transgene assays (Wilson et al. 1996), and its contribution to *in vitro* B-cell transformation, remains controversial. Other observations in Akata BL cell lines that suggest the involvement of latency I gene products in BL pathogenesis include increased survival (and therefore viral persistence), mediated either by virus-induced downregulation of c-myc expression in low serum (Ruf et al. 1999), upregulation of the TCL1 oncogene (Kiss et al. 2003), or through the EBER-mediated induction of IL-10 (Takada and Nanbo 2001).

EBERs have also been demonstrated to upregulate BCL-2 expression, induce colony formation in soft agar, and induce tumours in nude transgenic mice (Komano et al. 1999; Kitagawa et al. 2000; Ruf et al. 2000), features reminiscent of EBV infected Akata cells relative to their negative counterparts (Komano et al. 1998). Although the wider relevance of these effects beyond the Akata Burkitt's lymphoma model system remains to be determined, and Akata BL cells have been observed to behave differently from other BL lines in culture (Shimizu et al. 1994; Shimizu et al. 1996), a proportion of the described effects of EBERs in Akata BL cells have also been observed in other BL lines such as BJAB, Daudi and Mutu (Yamamoto et al. 2000; Nanbo et al. 2002). Holoendemic malaria and HIV infection are associated with marked increases in tumour incidence. Both agents are able to act as chromic stimuli of the B-cell system, with HIV infection also resulting in persistent generalised lymphadenopathy that is characterised by exaggerated germinal centre activity. Such increased activity is proposed to enhance the chances of productive c-Myc translocations occurring (Young and Rickinson 2004). Both agents also disturb the balance between host cells and EBV, probably increasing the numbers of EBV-infected B-cells that are at risk of being recruited into germinal-centre reactions (Araujo et al. 1999). Despite the observed lack of consistent association of EBV with non-endemic BL, EBV is proposed to play a role in the pathogenesis of this sporadic form of BL. Such proposals are based upon the observation of rearranged EBV genomes in tumour biopsies. Rearranged genomes may consequently express BZLF1 (the lytic transactivator), resulting in loss of the virus. Further, any replicating virus may not be detected by EBER *in situ* hybridisation as EBER expression is downregulated during lytic replication (Greifenegger et al. 1998). As such, EBV may play a "hit and run" role in the development of nonendemic BL (Young and Murray 2003).

1.6.1.2 Hodgkin's lymphoma (HL)

Although the morphology of the pathognomonic Reed-Sternberg cells of HL was described over a century ago, it was not until recently that their origin from B lymphocytes was recognised. The demonstration that a proportion of cases of HL harbour EBV and that its genome is monoclonal in these tumours suggests that the virus contributes to the development of HL in some cases. HL is a complex granuloma where the clonal malignant Hodgkin/Reed-Sternberg (HRS) cells represent less than 2% of the tumour mass surrounded by a complex infiltrate of T- and B-cells, macrophages, eosinophils and plasma cells. The appearance of the non-malignant infiltrate distinguishes the nodular sclerosing (NS), mixed cellularity (MC), rarer lymphocyte depleted (LD), and a newly defined entity known as ''lymphocyte rich classical'' subtypes of HL (Kapatai and Murray 2007). In the developed world, EBV can be detected in 40-50% of HL cases within the HRS cells as a monoclonal population (Staudt 2000; Klein et al. 2007). This figure includes most MC and LD cases but only a minority of the NS tumours that make up the peak of HL incidence that is seen in the third decade of life in the developed world, and that first raised the issue of an infectious aetiology. In the developing world, HL appears to show an even higher overall association with EBV (Chang et al. 1993; Weinreb et al. 1996). The increased EBV positivity in HL in underdeveloped countries may be due to the existence of an underlying immunosuppression, similar to that observed for endemic BL, a theory supported by the higher EBV-positive rates in HL from HIV-infected patients (Uccini et al. 1990). Alternatively, the timing of EBV infection (which often occurs earlier in life in developing countries) might also be important (Kapatai and Murray 2007).

The existence of HL tumours in the absence of EBV infection presents the possibility that, when present, EBV is simply a 'passenger'. However, the chance of HL arising in an EBV-

positive cell by chance is slight, given that infected cells normally make up a small fraction of the total B-cell pool (Laichalk et al. 2002). Further, in EBV-positive tumours, the viral genome is present in each HRS cell, and exhibits a latency II pattern of gene expression (Deacon et al. 1993). Levels of LMP1 in HL appear extremely high indicating that this particular viral protein may play a pivotal role in the tumourigenic phenotype (Deacon et al. 1993), although whether EBV is able to contribute to the malignant phenotype at the time of tumour presentation is more difficult to determine, given that there are no EBV-positive HRS cell lines available as *in vitro* models that retain a latency II pattern of gene expression.

HRS cells show many characteristics of LMP1-induced phenotypic changes (Section 1.7.3), including the strong activation of NF-κB (and its associated downstream effects). Intriguingly, HRS cells of EBV-negative HL also show a similar phenotype, which, in a proportion of cases at least, seems to have been induced through the inactivation of inhibitor of IκBα (the physiological regulator of NF-κB activity), or through the amplification of the REL gene (which encodes an NF-κB family member (Kuppers 2002). That EBV-positive and EBV-negative tumours achieve this same endpoint by biologically distinct mechanisms indicates the importance of NF-κB deregulation in the pathogenesis of HL. Manipulation of HRS cells from tumour biopsies has demonstrated that these cells contain clonal rearrangements in their immunoglobulin genes, with DNA sequencing demonstrating a high level of crippling somatic mutations in the rearranged segments. Such data indicate that the HRS cell progenitor is derived from a germinal centre B-cell, rescued from apoptosis (Kanzler et al. 1996). EBV has been found to rescue BCR-negative germinal centre B-cells from apoptosis (Chaganti et al. 2005), most likely through LMP1 mimicking of CD40 which binds the CD40L on T-cells, thus inducing B-cell proliferation and survival. Further, LMP2A (also expressed as part of the latency II pattern of gene expression seen in HL) is a viral

homologue of the cellular BCR, and may provide tonic signalling in the absence of receptor cross-linking (Caldwell et al. 2000). Therefore, EBV may play a direct role in the development of HL by preventing apoptosis of the HRS progenitor in the absence of antigenic stimulation.

1.6.1.3 Lymphoproliferative disease in immunosuppressed individuals

The lymphoproliferations that arise following immunosuppression for transplant surgery are collectively known as PTLDs. Similar tumours are observed in other immunocompromised patients with certain forms of inherited immunodeficiency syndromes, such as X-linked lymphoproliferative syndrome and Wiscott–Aldrich syndrome, and in AIDS patients.

PTLDs are often of B-cell origin, and T-cells are required for the development of PTLD-like tumours in severe combined immunodeficient (SCID) mice, which suggests an important role for T-cell help in the growth of B-cell-derived PTLDs (Johannessen et al. 2000). Most cases of PTLD are EBV positive, and show a latency III pattern of gene expression (Young et al. 1989), appearing to represent an *in vivo* counterpart for the *in vitro* LCL model system, and therefore by implication PTLDs are likely to be primarily driven by EBV, with a decrease in chemotherapy usually being sufficient to induce regression (Timms et al. 2003). However, other patterns of EBV latent gene expression are sometimes observed in PTLDs, and EBV-negative forms of PTLDs have also been described. AIDS-related lymphoproliferative disorders are another group of heterogeneous diseases exhibiting strong association with EBV. These diseases occur as a consequence of HIV immunosuppression and include CNS and systemic B-cell lymphomas, and primary effusion lymphomas (PELs) which can be co-infected by KSHV (Thompson and Kurzrock 2004). Leiomyosarcomas (smooth muscle tumours) are not associated with EBV in immunocompetent hosts but have been strongly

correlated with viral infection in patients whose immune system is compromised by HIV or other factors. Such an association between leiomyosarcomas and EBV indicate that EBV is capable of infecting smooth muscle cells, a finding consistent with experimental evidence that the EBV receptor is present on those cells (McClain et al. 1995; Suankratay et al. 2005).

1.6.2 EBV-associated T- and natural killer cell lymphomas

The association of EBV with rare but specific types of T-cell and natural killer (NK)-cell lymphomas was completely unexpected when first identified (Jones et al. 1988; Harabuchi et al. 1990), given that the virus is so markedly B-lymphotropic upon *in vitro* exposure to human lymphocyte preparations. Although the mechanism by which EBV is able to access and infect these cell lineages *in vivo* is still undetermined, most evidence indicates that such infections are rare though when they occur, they confer a high risk of lymphoma development (Young and Rickinson 2004). T- and NK-cell lymphomas arising as a consequence of EBV infection appear highly malignant and have a poor clinical prognosis (Kanavaros et al. 1993; Harabuchi et al. 1996).

1.6.3 EBV-associated epithelial cell disorders

1.6.3.1 Oral hairy leukoplakia

Oral hairy leukoplakia (OHL) was first described in the 1980s (Greenspan et al. 1985; Reichart et al. 1989) and is a benign epithelial lesion that presents on lateral and dorso-lateral regions of the tongue (Slots et al. 2006). OHL causes no other symptom or medical/dental problems, and does not usually require treatment, though antiherpesviral treatment (with acyclovir) may lead to remission. Histologically, OHL shows vacuolated epithelial cells and little or no inflammatory infiltrate in the underlying connective tissue. OHL is almost

exclusively seen in immunocompromised individuals, particularly in HIV-infected patients in whom it may serve as an indicator of progression to AIDS.

Despite the well established association between EBV and OHL, the precise role that EBV plays in OHL development is not well understood. Both lytic and latent EBV antigens have been detected in lesions including EBNA1, EBNA2, EBNA-LP and LMP-1 (Sandvej et al. 1992; Webster-Cyriaque and Raab-Traub 1998; Webster-Cyriaque et al. 2000; Walling et al. 2004), although the consensus of opinion is that EBV does not establish a latent infection in the disorder. As previously mentioned, treatment of patients with acyclovir (to inhibit viral replication) results in significant resolution of OHL lesions. However, lesions reappear one to four weeks post-treatment, suggesting that viral replication is necessary for the pathogenesis of this disease (Walling et al. 2003). OHL lesions frequently contain multiple EBV strains (Walling and Raab-Traub 1994), suggesting that OHL may arise as a consequence of a repeated super-infection of EBV-infected cells present within differentiating epithelial layers (Webster-Cyriaque et al. 2000).

Significantly, although no formal link with OHL has been established, EBV has been demonstrated to associate with aggressive types of oral tumours, especially in immunosuppressed patients (Leong et al. 2001), however research is needed to determine the extent to which EBV participates in oral tumourigenesis, and to understand complex and varying interplay between the virus and the host cell environment in different types of oral cancer (Slots et al. 2006).

1.6.3.2 Nasopharyngeal Carcinoma

Nasopharyngeal carcinoma is a distinctive type of head and neck cancer that arises from surface epithelium, often presenting as a neck mass with symptoms of nasal obstruction and

loss of hearing. NPC has a characteristic ethnic and geographic distribution, with a low incidence of the malignancy in Caucasians from Europe, North America and other Western countries (1 case per 100,000 persons per year). However, NPC represents the most common tumour in Southern China, accounting for 20% of all adult cancers in this region (25-30 cases per 100,000 persons per year) (Yu and Yuan 2002) and is particularly apparent in individuals of Cantonese origin (Lo et al. 2004). Incidence rates of NPC are high in individuals of Chinese descent irrespective of where they live, and particularly in Cantonese males, suggesting a genetic predisposition to the disease (Young and Murray 2003). Undifferentiated nasopharyngeal cancer affects mostly individuals in their mid-40s, with men two- to three-fold more frequently affected than women (Vasef et al. 1997). Distant metastasis is the key contributor to NPC mortality, with thirty to sixty percent of patients with NPC eventually developing metastatic tumours (Spano et al. 2003). In terms of treatment strategies, NPC tends to be radio- and chemo-therapy sensitive, with initial treatments often encouraging. However, relapse and metastasis occur frequently (Spano et al. 2003; Brennan 2006).

In 1978, the World Health Organisation (WHO) classification distinguished NPC into three histopathological types based on the degree of tumour differentiation: Type I – a keratinising squamous cell carcinoma (SCC), similar to other head and neck cancers; Type II – a non-keratinising carcinoma; Type III – undifferentiated carcinoma (Shanmugaratnam 1978). Both type II and III are further characterised by the presence of a prominent cellular infiltrate and each type has a strong propensity to metastasise. Despite subsequent re-classification of NPC by the WHO in 1991, EBV researchers worldwide, rather strangely, still tend to refer to NPC types by the 1978 classification.

The well-differentiated keratinising (WHO type I) NPC makes up 20% of all NPC cases, with the remaining cases being non-keratinising, differentiated and non-differentiated (WHO

Types II and III) NPC. Prevalence of the different histological NPC types varies geographically, with keratinising SCC more common in Western countries, and WHO type III NPC accounting for more than 97% of all NPC cases in endemic regions such as Southern China (Marks et al. 1998). Undifferentiated NPC has a typical morphology with a prominent lymphocytic infiltrate. The interactions between tumour cells and these infiltrating lymphocytes is proposed to be critical in tumour propagation (Young and Rickinson 2004), with type II and III NPC being distinguished from other SCCs through their universal association with EBV.

The EBV-associated, undifferentiated form of NPC (WHO type III) shows the most consistent worldwide association with EBV. A link between EBV and undifferentiated NPC was suggested as early as 1966 on the grounds of serological studies (Henle and Henle 1970), and was later substantiated by the demonstration of EBV DNA in the tumour cells of NPCs through *in situ* hybridisation (zur Hausen et al. 1970). Subsequently, Southern blot hybridisation of DNA from NPC tissues revealed the monoclonal nature of the resident viral genomes, indicating that EBV infection occurs prior to clonal expansion of malignant cell populations (Raab-Traub and Flynn 1986). EBV has since been found to be associated with virtually all cases of undifferentiated NPC, despite its strong tropism for B lymphocytes (Young et al. 1988; Niedobitek et al. 1992). Further, it has been demonstrated that tumour-derived EBV DNA load in pre- and post-treatment patient serum was a good indicator of overall survival and chances of relapse (Chan et al. 2002). Association of EBV with more differentiated (types I and II) of NPC is not well established. Although EBV DNA has been detected (albeit at low copy number) in SCC biopsies by Southern blotting (Raab-Traub et al. 1987), it remains possible that the DNA detected in this study may have originated from B lymphocytic infiltrate. However, a more recent study detected EBER expression in the tumour

cells of 31 differentiated SCC biopsies using *in situ* hybridisation and the same study also reported the presence of monoclonal EBV episomes in SCC, and a pattern of viral gene expression reminiscent of that observed in undifferentiated NPC (Pathmanathan et al. 1995). Contrastingly, other studies have failed to detect EBV DNA or EBER expression by *in situ* hybridisation analysis of differentiated NPC biopsies (Niedobitek et al. 1992; Niedobitek et al. 1993), leading to a general school of thought that EBV infection of squamous NPC may occur in endemic regions, but is less likely to occur in areas of low NPC incidence (Spano et al. 2003).

Despite the strong evidence outlined above indicating that EBV plays a strong etiological role in NPC, EBV infection itself is not sufficient to induce tumourigenesis. This point is highlighted by the fact that despite most of the world's population being asymptomatically infected with EBV, NPC incidence is remarkably low in most regions. Experimental evidence reinforces such epidemiological observations, with a reservoir of EBV infection not being detectable in normal and low-grade nasopharyngeal pre-invasive epithelium (Pathmanathan et al. 1995). Extensive epidemiological studies have resulted in the identification of two important co-factors, other than EBV infection, in NPC pathogenesis: genetic predispositions and environmental cofactors.

Environmental cofactors such as dietary components (e.g. salted fish, high in volatile nitrosamines) are thought to be important in the aetiology of the disease (Yu et al. 1986). Indeed, rats fed Cantonese-style salted fish have been observed to develop nasal cavity carcinoma in a dose-dependent manner (Huang et al. 1978; Yu and Yuan 2002). The consumption pattern of such high-risk foods is entirely consistent with the geographical distribution of NPC, and a decreasing trend in NPC incidence (~30%) in Hong Kong over the last 25 years may be attributed to the change of traditional lifestyle, particularly the avoidance

of feeding salted fish to young children (Lo et al. 2004). Other environmental co-factors such as exposure to dust, smoke and chemical fumes also play a role in predisposing individuals to NPC (Yu et al. 1986; Yu and Yuan 2002), although while the use of Chinese medicinal herbs and phorbol ester contamination of water supplies have been suggested to increase the risk for NPC by reactivating EBV infection in the host, the association of NPC with other non-dietary factors such as cigarette smoking or formaldehyde exposure is either weak or disputed (Raab-Traub 2002; Lo et al. 2004).

The development and progression of NPC is thought to involve the accumulation of multiple genetic changes. Both genetic changes, such as gene amplification, deletion and mutation, and epigenetic changes (methylation events) are able to effect the development of NPC through altering the functions of genes involved in cellular processes such as proliferation, apoptosis, and differentiation (Lo and Huang 2002). Some interplay between genetic and environmental cofactors is postulated. A variant form of the cytochrome P450 enzyme, CYP2E1, which catalyzes the metabolic activation of low-molecular weight nitrosamines such as those detected in NPC-associated foods, has been identified which exhibits higher enzymatic activity. Chinese subjects possessing this genotype have a 2-fold increased risk of developing NPC (Hildesheim et al. 1995, 1997). Genome-wide analysis of NPC genetic alterations has been conducted, utilising a comprehensive complementary approach through the combination of combining comparative genomic hybridisation (CGH), array-based CGH, spectral karyotyping and high resolution deletion mapping on micro-dissected tumours to screen for allelic losses, copy number gains and specific amplifications throughout the entire NPC genome (Hui et al. 1999, 2002; Lo and Huang 2002; Wong et al. 2003). Such studies have consistently reported high frequencies of genetic loss on multiple chromosome arms, including 3p, 9p, 9q, 11q, 13q, 14q and 16q, with recurrent chromosomal gains observed on

chromosomes 1q, 3q, 8q, 12p and 12q. Of the reported alterations, the most common were deletion of 3p and 9p; regions correlating with known tumour suppressor genes located on 9p21 (p14 and p16) and 3p21.3 (RASSF1A) which have been shown to be defective due to promoter hypermethylation in NPC (Lo et al. 1996, 2001). Upon restoration of p16 and RASSF1A expression in NPC cell lines, a marked decrease in cell growth and reduction of soft-agar colony formation was observed, along with reduced tumourigenic potential following injection into athymic nude mice (Wang et al. 1999; Chow et al. 2004). Further, clonal cell populations with 3p and 9p deletions have been frequently detected in dysplastic lesions and even in histologically normal nasopharyngeal epithelia from Southern Chinese individuals (Chan et al. 2000, 2002a) and these deletions were observed at a higher frequency in high-risk Chinese populations compared with low-risk populations. Such observations suggest that these deletions are critical events which occur early in the development of NPC. Other promoter hypermethylation events occur on tumour suppressor gene (TSG) promoters in NPC including those on chromosome 11q (tumour suppressor in lung cancer TSLC1), 13q (endothelin receptor EDNRB) and 16q (E-cadherin). Included within the significant amplifications of some chromosome regions are oncogenes. Such regions include 3q (PI3K catalytic subunit and ΔN-p63), 7p (epidermal growth factor), and 8q (c-myc). More recently, micro-array analysis using biopsies from patients with EBV-positive undifferentiated NPC and from cancer-free controls revealed down-regulation of multiple TSGs not previously associated with this NPC, including the ataxia telangiectasia mutated (ATM) gene, which is known to be mutated in a variety of other tumours (Bose et al. 2009). An analysis of all genetic and epigenetic changes reported in NPC is beyond the scope of this thesis, although suitable review articles are readily available (Lo and Huang 2002). The genetic and epigenetic alterations identified following the establishment of a stable EBV infection and expression of

viral latent genes, are proposed to mediate the malignant development of NPC from a high-grade pre-invasive lesion to an aggressive and metastatic invasive carcinoma. This has led to the design of a multi-step model for the pathogenesis of NPC in which EBV infection provides an essential tumour-promoting function (Lo and Huang 2002).

EBV latent gene expression in NPC tumour cells is well characterised, with numerous studies reporting EBV to display type II latency gene expression, similar to that observed in HL cells. Expression of EBNA1, LMP2A, LMP2B, EBERs and the BARTs has been consistently demonstrated (Young et al. 1988; Niedobitek et al. 1992; Chen et al. 1995). LMP1 expression has also been reported in NPC cells, however expression of this viral latent gene product is variable, with around 20-30% of NPC biopsies analysed found to express LMP1 (Young et al. 1988; Niedobitek et al. 1992). LMP1 expression seems to be important in NPC, with LMP1-negative tumours reported to have gained additional compensatory cellular gene mutations (Spano et al. 2003).

1.6.3.3 Other EBV-associated lymphoepitheliomas

Given EBV's well established association with NPC, studies have examined a possible role for EBNA1 in other undifferentiated epithelial carcinomas, or lymphoepitheliomas. Although EBV has been detected in thymic and salivary gland tumours (Raab-Traub et al. 1991; Fujii et al. 1993), examination of breast lymphoepithelioma revelated no association with EBV (Dadmanesh et al. 2001). Further, any EBV association with these carcinomas appears to correlate with regions in which NPC is endemic (Raab-Traub et al. 1991; Fujii et al. 1993). EBV is also associated with rare NPC-like gastric lymphoepitheliomas, with 90% of cases showing EBV positivity (Tokunaga et al. 1993; Imai et al. 1994).

1.6.3.4 Gastric Carcinoma

In addition to the fairly well established association between EBV and gastric lymphoepitheliomas, numerous studies have also detected EBV in some conventional gastric adenocarcinomas (GC), of both the intestinal and diffuse histological subtypes (Shibata and Weiss 1992; Tokunaga et al. 1993; Imai et al. 1994). EBV-associated GC is a distinct subgroup of GC which occurs worldwide without regional or racial differences, and accounts for around 10% of all GC cases, with around 90,000 patients worldwide estimated to develop this kind of stomach cancer annually (Fukayama et al. 2008). The clinical features of EBV-associated GC include male predominance, relatively younger age and preponderant location in the proximal stomach. EBV-associated GC has a relatively favourable prognosis compared with EBV-negative GC (Fukayama et al. 2008).

In EBV-associated GC, studies have identified that monoclonal EBV is present in an episomal form, without integration into the host genome, and that the infection is latent with no viral replication. Mono or bi-clonal EBV has been observed in the carcinoma tissues at the intramucosal stage; however, at the stage of submucosal invasion, and in further advanced carcinoma, EBV is monoclonal (Fukayama et al. 1994; Imai et al. 1994; Uozaki and Fukayama 2008). Therefore, EBV infection occurs at the initial or a very early stage of carcinoma development (Fukayama et al. 2008), suggesting that EBV plays an important etiological role in tumourigenesis, a suggestion that is reinforced by the differing molecular and pathological phenotypes of EBV-negative and EBV-positive GCs. Tissue arrays comparing EBV-positive and EBV-negative GC biopsies have revealed substantial differences between the two tumour types. EBV-positive cases have been identified as showing a more frequent loss of SMAD4, E-cadherin, cyclin-dependent kinase inhibitor $p16^{INK4A}$ and O-6-methylguanine methyltransferase (Lee et al. 2004).

Despite such notable differences in the pathology of EBV-positive and -negative GC, the precise role of EBV in tumourigenesis remains poorly defined. A restricted pattern of viral gene expression is observed in GC similar to latency I gene expression observed in BL, but with LMP2A expressed in addition (Fukayama et al. 1994; Imai et al. 1994; Uozaki and Fukayama 2008). Although the precise pathogenic role of EBV in GC is yet to be determined, data demonstrating the absence of EBV infection in pre-malignant gastric lesions support the notion that viral infection may be a relatively late event in gastric carcinogenesis but once infection occurs, EBV is able to drive the clonal proliferation of malignant cells (Zur Hausen et al. 2004).

1.7 EBV latent gene products

A comprehensive review of each of the EBV-encoded latent gene products is beyond the scope of this thesis. The following section briefly introduces EBV latent gene products less pertinent to this particular project, before focussing on the two latent gene products most relevant to this thesis: EBNA1 and the EBERs.

1.7.1 EBNA2 and EBNA-LP

EBNA2 and EBNA-LP are temporally the first EBV latent proteins to be detected following EBV infection (Murray and Young 2002). The acidic phophoprotein EBNA2, although lacking intrinsic DNA binding activity, is a known transcriptional activator of viral genes (LMP1 and LMP2) and cellular genes (CD21 and CD23) (Wang et al. 1990; Kieff and Rickinson 2001), and plays a critical role in cell immortalisation. The conspicuous inability of an EBV strain, P3HR-1, which is deleted for the last two exons of EBNA-LP and the entire EBNA2 gene, to transform B-cells *in vitro* was the first observation that indicated that EBNA2 made a critical contribution to cellular transformation by EBV (Rabson et al. 1982).

Subsequent reintroduction of EBNA2 into this strain unequivocally confirmed the role of this viral latent gene product in transformation (Hammerschmidt and Sugden 1989). EBNA2 is also known to transactivate Cp, inducing the observed switch from Wp to Cp expression early in B-cell infection. EBNA2-responsive promoters are not bound directly by EBNA2, but rather by the ubiquitous cellular DNA-binding protein RBP-Jκ, which interacts with EBNA2 and binds the common core sequence (GTGGGAA) of EBNA2-responsive promoters (Grossman et al. 1994). The RBP-Jκ homologue in *Drosophila* is involved in signal transduction from the Notch receptor, a pathway that is important in cell fate determination in the fruit fly and has been implicated in the development of human T-cell tumours (Artavanis-Tsakonas et al. 1995), with EBNA2 being demonstrated to be capable of functionally replacing the intracellular region of Notch (Sakai et al. 1998). Conversely, activated forms of Notch have been shown to have the ability to substitute for EBNA2 in the promotion of B-lymphocyte transformation and the transactivation of EBNA2-regulated viral promoters (Hofelmayr et al. 1999; Strobl et al. 2000; Hofelmayr et al. 2001), although a recent study suggests differential effects of Notch and EBNA2 signalling on the proliferation and survival of EBV-infected B-cells (Kohlhof et al. 2009). The oncogene c-Myc is seemingly another important EBNA2 target, and is significant for EBV-induced B-cell proliferation (Kaiser et al. 1999; Zimber-Strobl et al. 1999).

EBNA-LP is a nuclear protein transcribed from the 5' leader sequences of the other EBNA RNAs (Kieff and Rickinson, 2001) and functions as a transcriptional co-activator with EBNA2 in regulating Cp and LMP1 promoters (Nitsche et al. 1997; McCann et al. 2001). The cooperation between EBNA2 and EBNA-LP does not seem to require direct or indirect complex between these two proteins (Peng et al. 2005). EBNA-LP enhancement of EBNA2 gene transactivation is instead suggested to occur through the displacement of HDAC4 and

associated transcriptional repressors (Portal et al. 2006). Although detectable in the cytoplasm, it has recently been established that nuclear-cytoplasmic shuttling is not required for efficient EBNA-LP co-activation function (Ling et al. 2009). In addition to these transcriptional co-activation activities, EBNA-LP may play a role in the evasion of IFN-mediated antiviral responses by EBV (Echendu and Ling 2008). Further, EBNA-LP has been found to interact with Rb and p53 *in vitro* (Szekely et al. 1993). However, EBNA-LP's ability to disrupt Rb and p53 signalling pathways *in vivo* and promote B-cell proliferation is controversial (Young and Murray 2003). EBNA2 and EBNA-LP have also been previously demonstrated to act cooperatively to drive progression of resting B lymphocytes into the G1 phase of the cell cycle (Sinclair et al. 1994).

1.7.2 EBNA3 family

The three members of the EBNA3 family, EBNA3A, 3B and 3C are encoded by genes that are adjacent on the viral genome. They are all hydrophilic nuclear proteins, containing heptad repeats of leucine, isoleucine or valine which act as dimerisation domains. Following EBV infection of B-lymphocytes, transcription of the EBNA3 genes occurs after EBNA2 and EBNA-LP. EBNA3A and EBNA3C have been demonstrated as being essential for EBV-mediated B-cell transformation *in vitro*, although EBNA3B is thought to be dispensable (Tomkinson et al. 1993). However, EBNA3B has been shown to enhance vimentin and CD40 expression (Silins and Sculley 1994).

The EBNA3 family are known transcriptional regulators, with EBNA3C inducing upregulation of both cellular (CD21) and viral (LMP1) gene expression (Allday and Farrell 1994), and repression of the Cp promoter (Radkov et al. 1997). This EBNA3C function is thought to require association with HDAC1, mSin3A and N-CoR co-repressors (Radkov et al.

1999; Knight et al. 2003). EBNA3C may also promote transformation through interaction with pRB and has also been reported to cooperate with oncogenic RAS in transforming rat embryo fibroblasts (Parker et al. 1996). More recently, EBNA3C has been demonstrated to interact with and enhance the stability of c-Myc (Bajaj et al. 2008). Further, EBNA3A and EBNA3C have been demonstrated to cooperate as the main determinants of the transcriptional down-regulation of the pro-apoptotic Bcl-2-family member Bcl-2-interacting mediator of cell death (Bim) in EBV-positive BL cells (Anderton et al. 2008).

EBNA3 family proteins have also been shown to cooperate in the specific inhibition of EBNA2-activated transcription, through direct interaction of their amino terminus with RBP-Jκ (Johannsen et al. 1996; Robertson et al. 1996). This suggests that EBNA2 and EBNA3 have cooperatively evolved to precisely regulate RBP-Jκ activity and consequent expression from cellular and viral promoters containing RBP-Jκ binding sites (Murray and Young 2001).

1.7.3 LMP1

LMP1, a 63 kDa integral membrane protein, is EBV's major transforming protein, behaving as a classical oncogene in rodent fibroblast transformation assays and being essential for the EBV-induced transformation of B-cells *in vitro* (Wang et al. 1985; Kaye et al. 1993). The pleiotropic effects of LMP1 expression in cells include the induction of cell surface adhesion molecules and activation antigens (Wang et al. 1990), upregulation of antiapoptotic proteins such as Bcl-2 and A20 (Henderson et al. 1991; Laherty et al. 1992), and stimulation of cytokine production (Eliopoulos et al. 1997; Eliopoulos et al. 1999). LMP1 functions as a constitutively active member of the tumour necrosis factor receptor (TNFR) superfamily, activating a number of signalling pathways in a ligand-independent manner (Gires et al. 1997;

Kilger et al. 1998). Further, LMP1 functionally resembles TNFR superfamily member CD40 and is able partially to substitute for CD40 *in vivo* (Uchida et al. 1999).

Structurally, LMP1 may be subdivided into three domains: (1) the N-terminal cytoplasmic tail, responsible for orienting and tethering of LMP1 to the plasma membrane; (2) the six hydrophobic transmembrane loops which are involved in self-aggregation and oligomerisation; (3) a long carboxy-terminal cytoplasmic region, possessing the majority of LMP1's signalling capacity. Further, two distinct functional domains referred to as C-terminal activation regions 1 and 2 (CTAR1 and CTAR2) have been identified based upon their ability to activate the NF-κB pathway (Huen et al. 1995). The activation of NF-κB contributes to an ever expanding range of phenotypic consequences of LMP1 expression. Indeed, LMP1 has recently been implicated in the regulation of DNA polymerase-β through the NF-κB pathway (Faumont et al. 2009b) and LMP1 has been shown to transactivate transcription of the oncogenic microRNA miR-155 through the NF-κB pathway (Gatto et al. 2008).

LMP1 also engages the MAP kinase cascade which results in the consequential activation of ERK, JNK and p38, and the stimulation of the JAK/STAT pathway (Kieser et al. 1997; Eliopoulos and Young 1998; Roberts and Cooper 1998; Eliopoulos et al. 1999; Gires et al. 1999). Many of these effects are a result of the ability of TNFR-associated factors (TRAFs) to interact directly with CTAR1 of LMP1, or indirectly through death domain protein TRADD to CTAR2 of LMP1 (Kieff and Rickinson 2001). The region between CTAR1 and CTAR2 (CTAR3) has been suggested to be responsible for the JAK/STAT pathway although this remains controversial, and deletion of this region has been shown to have no effect on the efficiency of B-cell transformation (Gires et al. 1999; Izumi et al. 1999). LMP1 also activates phosphatidylinositol 3-kinase (PI3K), a lipid kinase responsible for activating a diverse range of cellular processes in response to extracellular stimuli (Dawson et al. 2003) and induces a

hyperproliferative and inflammatory gene expression programme in cultured keratinocytes (Morris et al. 2008).

1.7.4 LMP2

The LMP2 gene encodes two distinct proteins of similar structure, LMP2A and LMP2B. Both proteins possess 12 transmembrane domains and a 27 amino acid cytoplasmic C-terminus, with LMP2A also having an additional 119 amino acid cytoplasmic amino-terminal domain (Longnecker and Kieff 1990). Neither LMP2A nor LMP2B is essential for the EBV-mediated transformation of B-cells *in vitro* (Longnecker 2000).

The amino-terminal domain of LMP2A contains eight tyrosine residues, two of which form an immunoreceptor tyrosine-based activation motif (TAM) (Fruehling and Longnecker 1997), similar to the TAM present in the B-cell receptor (BCR) which plays a central role in the mediation of lymphocyte proliferation and activation of the *src* family of protein tyrosine kinases (PTKs). The LMP2A TAM has been demonstrated to be responsible for blocking BCR-stimulated calcium mobilisation, tyrosine phosphorylation and the activation of EBV lytic cycle in B-cells (Miller et al. 1995) through interacting with PTKs and negatively regulating their activity through depleting the plasma membrane of Src and Syk PTKs (Fruehling and Longnecker 1997). Other data build upon these findings, and indicate that an additional tyrosine residue in the LMP2A amino-terminal domain is required for efficient binding of *src* family PTKs (Fruehling et al. 1998) and that LMP2A is phosphorylated *in vitro* on serine residues by MAP kinase (Panousis and Rowe 1997). Signalling of LMP1 was recently demonstrated to occur preferentially through the Src family kinase Lyn, due in part to Lyn's SH2 domain associating with LMP2A (Rovedo and Longnecker 2008). Further, LMP2A was shown to inhibit BCR-induced apoptosis and EBV reactivation in BL cell lines

(Fukuda and Longnecker 2005). In addition, LMP2A contains proline motifs capable of interacting with WW domain-containing proteins, with LMP2A found to interact with the Nedd4 family of ubiquitin ligases. This interaction is thought to lead to the increased turnover of Lyn (Ikeda et al. 2000).

Although not essential for B-cell transformation, expression of LMP2A in the B-cell compartments of transgenic mice abrogates normal B-cell development thus allowing immunoglobulin-negative cells to colonise peripheral lymphoid organs. These data suggest that LMP2A is able to drive survival and proliferation of B-cells in the absence of BCR signalling (Caldwell et al. 1998), and support a role for LMP2 in the modification of the normal B-cell development programme to favour the maintenance of EBV latency in the bone marrow and prevent inappropriate activation of EBV lytic cycle (Young and Murray 2003). Consistent with a cell survival role, LMP2A activates the PI3K/Akt pathway in epithelial and B-cells, providing protection against TGFβ induced apoptosis (Fukuda and Longnecker 2004).

LMP2B is proposed to have a regulatory role in the function of LMP2A (Longnecker 2000), with a more precise role for LMP2B in modulating LMP2A activity having recently been identified. Although LMP2B lacks the N-terminus of LMP2A it is still able to aggregate in the plasma membrane and may directly associate with LMP2A, with this association preventing the recruitment of the Lyn tyrosine kinase (Rovedo and Longnecker 2007).

LMP2A's role and function in epithelial cells is quite distinct from those seen in B-cells, with LMP2A phosphorylation in epithelial cells not involving PTKs, but instead being dependent on cell interactions with the extracellular matrix (Scholle et al. 1999). LMP2A has also been reported to repress NF-κB and STAT signalling and to have an importance in the modulation

of LMP1 expression (Stewart et al. 2004). This is in contrast to studies conducted in B-cells, where LMP2A was found to activate NF-κB in conjunction with LMP1 through promoting TRAF2 expression (Guasparri et al. 2008).

1.7.5 EBV-encoded BamHI A rightward transcripts (BARTs)

The BART RNAs are a heterogeneously spliced group of RNAs transcribed rightward from the BamHI A region of the EBV genome. BART RNAs have been detected in the peripheral blood of healthy EBV carriers (Chen et al. 1999) and in all EBV-associated diseases that have been examined (Raab-Traub et al. 1991; Deacon et al. 1993; Sugiura et al. 1996; Tao et al. 1998; Sugawara et al. 1999).

The BART RNAs were originally identified by the analysis of cDNA libraries established from an NPC tumour (Hitt et al. 1989; Gilligan et al. 1990b). Despite extensive analysis and supposition that due to their presence in EBV-associated malignancies they may play some role in EBV-mediated tumourigenesis, the function of the BARTs remains mysterious. Prior to the discovery of the EBV miRNAs, some open reading frames (ORFs) in the spliced BART cDNAs were investigated as potential protein-coding sequences. It was demonstrated that the RPMS1 and A73 ORFs could be translated *in vitro* from the spliced BART cDNAs isolated from C15 NPC tumour cells (Smith et al. 2000). Subsequently, it was shown that RNAs covering RPMS1 and A73 ORFs represent significant portions of the BART family of transcripts (de Jesus et al. 2003), with biochemical activities of artificially expressed RPMS1 and A73 proteins having been identified as having a possible role in EBV pathology (Smith et al. 2000; Zhang et al. 2001; de Jesus et al. 2003). RPMS1 was found to antagonise Notch1 and/or EBNA2 transcriptional activation, through competing for binding to the RBP-Jκ protein (Smith et al. 2000), with A73 found to bind to the RACK1 protein (Smith et al. 2000)

(known to act as a scaffold in Src family kinase signalling). Despite the existence of some evidence of an immune response to protein products of BART RNAs in EBV-infected humans (Gilligan et al. 1991; Kienzle et al. 1999), neither RPMS1 nor A73 has been identified in a natural EBV infection, resulting in their existence in real EBV infections remaining a controversial issue.

Although the majority of the EBV genome in C15 NPC tumour DNA is heavily methylated, an unmethylated region was found around the BART promoter and extended about 1 kb downstream, suggesting that the genome there is protected from methylation by the binding factors involved in the activity of the BART promoter (de Jesus et al. 2003).

1.7.6 EBV-encoded microRNAs (miRNAs)

In addition to the BART transcripts, the BART miRNAs are thought to be almost exclusively derived from introns prior to splicing of the BART primary transcripts (Edwards et al. 2008). EBV was initially reported to express five miRNAs from two separate regions of the EBV genome, the BamHI A (BART miRNAs) and the BamHI H (BHRFI miRNAs) regions (Pfeffer et al. 2004), although subsequent analysis has revealed EBV to be capable of expressing up to 22 miRNAs. However, many of these are encoded in DNA missing from the prototypic B95.8 genome (Cai et al. 2006; Grundhoff et al. 2006). The expression patterns of EBV miRNAs are complex, depending upon both cell type and the overall pattern of gene expression. For example, in NPC cell lines, the cluster of BART miRNAs is robustly expressed, whereas expression is much less abundant in most B-lymphocyte derived lines (Cai et al. 2006). Conversely, the BHRFI cluster of miRNAs is not detected in NPC cells, but is expressed in B-cells which exhibit a latency III pattern of gene expression (Xing and Kieff 2007). An additional level of complexity arises upon the induction of lytic EBV replication,

which induces expression of many but not all of the EBV-encoded miRNAs (Cai et al. 2006; Xing and Kieff 2007).

The importance of miRNAs in EBV infection is supported by the high degree of conservation of most miRNAs between rhesus lymphocryptovirus and EBV (Cai et al. 2006), although few functional targets have been definitively identified for EBV miRNAs. However, there is evidence that miRNA BART2 is able to regulate the EBV DNA polymerase gene (Barth et al. 2008), and that miRNA BART 1-5p and 17-5p can regulate LMP1 (Lo et al. 2007).

1.7.7 EBNA1

EBNA1 expression is observed in all EBV-infected cells, in which its role in the maintenance and replication of the episomal EBV genome is achieved through sequence-specific binding to the plasmid origin of viral replication, *OriP*. EBNA1 is expressed in all forms of viral latency and can be detected in all EBV-associated malignancies (Kieff and Rickinson 2001). Given these essential roles in maintenance of the EBV genome and ensuring correct genomic segregation into daughter cells, it comes as no surprise that EBNA1 has been one of the most intensely studied viral proteins. As previously outlined, the EBV genome is maintained predominently as an episome in latently infected cells. Replication of this viral episome is synchronised with that of the host cell chromosome, ensuring maintenance of EBV in progeny cells (Nonoyama and Pagano 1972). For replication of the EBV genome, requirement exists for two viral components: the latent origin of replication, the *cis*-acting element *OriP*; and the *trans*-acting element, EBNA1, which binds *OriP*. No other viral proteins are required for the replication of EBV in latently infected cells, a key observation in the explanation of consistent association of EBNA1 with viral latency and EBV-associated malignancies (Yates et al. 1984, 1985; Lupton and Levine 1985; Reisman and Sugden 1986; Lee et al. 1999). EBNA1 is also

known to act as a key viral transcriptional transactivator, having been demonstrated to activate both Cp and LMP1 promoters (Sugden and Warren 1989; Gahn and Sugden 1995). Additionally, EBNA1 has been shown to negatively regulate its own expression in latency I through the binding of two low-affinity EBNA1 sites downstream of the transcriptional start site of the Qp promoter (Sample et al. 1992). The absolute requirement for EBNA1 in episome maintenance and viral replication has complicated the study of EBNA1's role in the modulation of cellular gene transcription. Nonetheless, there is a growing body of evidence suggesting that EBNA1 is capable of regulating expression of cellular, as well as viral, gene expression and an involvement of EBNA1 in EBV-associated malignancies is postulated.

1.7.7.1 EBNA1 protein structure

EBNA1 is a multi-domain DNA binding phospho-protein of around 641 amino acids which is encoded by the *Bam*HI K region of the EBV genome. Distinct individual structural domains of EBNA1 have been characterised and are represented in the schematic of Figure 1.2. A significant portion of the amino-terminal half of EBNA1 is made up of a large domain containing a glycine-alanine (Gly/Ala) co-polymer repeat which shows variation in size between EBV isolates (Kieff and Rickinson 2001). Despite its significant structural presence, the Gly/Ala repeat region of EBNA1 has been shown to be dispensable for EBNA1 function, with deletion of the region not affecting the replication and transcription functions of EBNA1 *in vitro* (Yates and Camiolo 1988) or the ability of EBNA1 to immortalise B-lymphocytes (Lee et al. 1999). However the Gly/Ala repeat region does play an important role in evasion of the host immune response by EBNA1, efficiently inhibiting ubiquitin/proteasome-mediated degradation of EBNA1. This acts to prevent processing of EBNA1 polypeptides and subsequent presentation to CTLs by MHC class I molecules on the cell surface (Levitskaya et

al. 1997). Protection from degradation afforded by a Gly/Ala repeat is not restricted to viral proteins, as a minimal Gly/Ala repeat prevents the interaction of ubiquitinated IκBα with the proteasome (Sharipo et al. 1998).

EBNA1 possesses a nuclear localisation signal (NLS) which is located between amino acids 379 and 386. Nuclear import of EBNA1 may be mediated by the nuclear importin receptor Rch1/importin α as interaction of EBNA1 with such complexes has been identified *in vitro* (Fischer et al. 1997; Kim et al. 1997).

Mutation of the carboxy-terminus of EBNA1 abrogates EBNA1's ability to regulate viral replication and transcription (Yates and Camiolo 1988), suggesting that sequences encoded here are crucial for EBNA1 dimerisation and DNA binding. More recently, the crystal structure of the EBNA1 DNA binding domain was resolved, with two domains characterised (Bochkarev et al. 1996). A core domain, similar to the bovine papilloma virus E2 protein's DNA binding domain was identified, along with a flanking domain which contacts DNA sequences. The function of EBNA1's 34-amino-acid acidic tail, situated carboxy-terminal to the DNA binding/dimerisation domain, is yet to be elucidated.

Two DNA-linking regions (amino acids 40 to 89, and 328 to 377) of EBNA1 confer the ability of DNA-bound EBNA1 dimers to associate with other DNA-bound EBNA1 dimers, thus looping out intervening sequences (Mackey et al. 1995; Leight and Sugden 2000).

Figure 1.2 - The 641 amino acid structure of EBNA1 from the prototypical B95.8 strain of EBV. The amino terminal consists of a large domain of 328 amino acids containing the gly-ala repeat sequence, which prevents presentation of EBNA1 antigens by MHC class I molecules. Two positively charged regions within EBNA1 (amino acids 40-89 and amino acids 328-337) are referred to as linking region 1 and 2 respectively (LR1 and LR2) and are involved in DNA-linking. A nuclear localisation sequence is located between amino acids 379-386. Finally, the carboxy terminus encodes the sequences required for dimerisation and site-specific DNA-binding, in addition to a 38 amino acid acidic tail with unknown function. Also shown are sequences required in mediating DNA replication, segregation and transcriptional activation functions of EBNA1 through binding to *OriP*, and those involved in associating with human EBP2 and USP7. Viral replication requires the DNA binding/dimerisation domain and redundant contributions of both the 8-67 and 325-376 regions. Maintenance and segregation of the viral episome requires the DNA binding/dimerisation domain, residues 325-376 and is stimulated by residues 8-67. Transcriptional activation of viral promoters requires the DNA binding/dimerisation domain, residues 61-83 (shown as residues 67-81 for clarity in Figure) and 325-376, and is stimulated by residues 8-67. EBP2 binding is primarily mediated by amino acids 325-376 and is stimulated by residues 8 to 67, whereas USP7 binding requires residues 395-450.

DNA-binding motifs (AT hooks) that are proposed to enable EBNA1 to play a direct role in episome segregation (Sears et al. 2004) are found between residues 33 to 89, and residues 328 to 378.

Figure 1.2

1.7.7.2 Modulation of viral replication, episome segregation and transcription - *OriP* and EBNA1

EBV DNA replication initiates within the dyad symmetry (DS) element of *OriP*, which contains four binding sites for EBNA1 (Reisman et al. 1985; Gahn and Schildkraut 1989; Wysokenski and Yates 1989; Niller et al. 1995), whereas the partitioning of EBV episomes involves EBNA1 binding to the family-of-repeats (FR) element of *OriP*, which contains 20 EBNA1 binding sites (Lupton and Levine 1985; Reisman et al. 1985). EBNA1 binding to the FR element also enhances expression of other viral latency proteins (Reisman and Sugden 1986; Gahn and Sugden 1995).

EBNA1 binding to recognition sites in *OriP* is reasonably well understood, with the binding of an EBNA1-dimer to each site, and cooperative assembly on the four sites in the DS element (Frappier and O'Donnell 1991; Hearing et al. 1992; Summers et al. 1996). However, precise mechanisms of transcriptional and DNA replication activation by EBNA1 are more poorly defined. EBNA1 does not possess enzymatic activity, and as such these mechanisms are likely to involve the recruitment of cellular proteins, including the cellular origin recognition complex and minichromosome maintenance complex (Chaudhuri et al. 2001; Dhar et al. 2001; Schepers et al. 2001), to *OriP* and possibly the remodelling of EBV chromatin structure. EBNA1 is known to bind and destabilise nucleosomes formed on the DS element (Avolio-Hunter et al. 2001), presumably allowing the access of host DNA replication machinery to the EBV origin of replication. In addition to four EBNA1-binding sites, the EBV DS repeat element contains three copies of a nonameric telomere repeat sequence which contributes to *OriP* plasmid maintenance and DNA replication (Yates et al. 2000). EBNA1-dependent binding of telomeric repeat binding factor 2 (TRF2) to these repeats has been

demonstrated (Deng et al. 2002), although other telomeric regulatory factors have been identified to bind *OriP* and have an inhibitory function (Deng et al. 2002; Deng et al. 2003).

A substantial body of evidence supports the idea that EBNA1 is able to govern the partitioning of EBV episomes and FR-containing constructs, through the mediation of their attachment to cellular mitotic chromosomes. EBV episomes, *OriP* containing constructs and EBNA1 have all been observed to associate with condensed cellular chromosomes during mitosis (Grogan et al. 1983; Harris et al. 1985; Petti et al. 1990; Delecluse et al. 1993; Simpson et al. 1996), with the association of *OriP* plasmids demonstrated to be EBNA1-dependent (Kanda et al. 2001). Further, the *OriP* FR element has been demonstrated to be responsible for efficient segregation and mitotic chromosome attachment of DNA constructs (Krysan et al. 1989; Kanda et al. 2001). Additionally, deletion of amino acids 325-376 of EBNA1 disrupts segregation of FR-containing plasmids and EBNA1 association with mitotic chromosomes without affecting nuclear localisation of the protein DNA replication activity (Shire et al. 1999; Wu et al. 2000), and functional replacement of the N-terminal half of EBNA1 (which mediates chromosome attachment and *OriP* plasmid maintenance) with chromosome binding sequences from histone H1 is possible (Hung et al. 2001).

Evidence suggests that EBNA1 is able to achieve attachment to cellular mitotic chromosomes through binding (mediated by amino acids 325-376) to the human EBNA binding protein 2 (EBP2) on chromosomes (Shire et al. 1999; Wu et al. 2000), EBP2 being a cellular nucleolus component which, similarly to EBNA1, coats condensed cellular chromosomes during mitosis. The importance of EBP2 to EBNA1-mediated partitioning of FR-containing plasmids has been demonstrated through the requirement for human EBP2, EBNA1 and the *OriP* FR element in a reconstituted EBV segregation system in budding yeast (Kapoor et al. 2001).

Further, it was demonstrated that human EBP2 associates with yeast mitotic chromosomes in a cell cycle-dependent manner, resulting in subsequent EBNA1 recruitment to these chromosomes (Kapoor and Frappier 2003) and the necessity for EBP2 for the proliferation of human cells has also been shown (Kapoor et al. 2005). However, other evidence has been produced which is inconsistent with this model of EBP2-EBNA1 action. The observation that the amino terminus of EBNA1 contains DNA-binding motifs (AT hooks) that are found in a family of proteins that binds scaffold-associated regions on metaphase chromosomes has led to the proposal of a more direct role for EBNA1 (Sears et al. 2004), which would yield random partitioning.

The FR element of *OriP* also acts as an enhancer element following EBNA1 binding (Reisman and Sugden 1986), enhancing transcription from the Cp and LMP1 promoters (Sugden and Warren 1989; Gahn and Sugden 1995), although the mechanism by which this transcriptional enhancement is enabled is yet to be fully elucidated. Evidence suggests that EBNA1 domains responsible for DNA binding/dimerisation and DNA linking are required (Mackey and Sugden 1999; Ceccarelli and Frappier 2000; Wu et al. 2002a), however EBNA1's ability to associate with cellular proteins such as EBP2 via these linking regions opens the possibility that recruitment of additional cellular proteins by EBNA1 may occur through relocation of the EBV episome to transcriptional activation centres within the nucleus. Here, EBNA1 may facilitate the looping out of DNA sequences, linking the *OriP* FR element with a site proximal to promoters. Similar cellular examples of such looping out of DNA sequences exist, for example the p53-mediated transactivation of the muscle creatine kinase promoter (Jackson et al. 1998). Further, dimerisation of the E2 protein of HPV16, which also plays a central role in the regulation of regulating viral gene expression and replication, has recently been demonstrated to be responsible for DNA loop formation in the

regulatory region of the HPV genome (Hernandez-Ramon et al. 2008). The mitochondrial protein, p32/TAP, has also been demonstrated to associate with EBNA1 (Wang et al. 1997a) and shown to be important in the mediation of transcriptional activation via the FR of *OriP* (Van Scoy et al. 2000). However, other data suggest that the EBNA1-p32 interaction may be non-specific (Holowaty et al. 2003b). More recently, it has been demonstrated that EBNA1 can functionally interact with Brd4 in native and heterologous systems, that this interaction facilitates transcriptional activation by EBNA1 from the FR element (Lin et al. 2008), and that deletion of AT hook motifs within the DNA-binding domain of EBNA1 (previously proposed to play a role in episome segregation) decreases the transactivation ability of EBNA1. This finding suggests a significant transcriptional role for this DNA-binding motif (Singh et al. 2009).

The domains of EBNA1 involved in functional processes have been elucidated (and are represented diagrammatically in Figure 1.2), with the three EBNA1 functions having overlapping but different sequence requirements. Transcriptional activation requires residues 61 to 83 and 325 to 376 and is stimulated by residues 8 to 67; partitioning requires residues 325 to 376 and is stimulated by residues 8 to 67; and replication involves redundant contributions of both the 325-to-376 and 8-to-67 regions (Yates and Camiolo 1988; Kirchmaier and Sugden 1997; Ceccarelli and Frappier 2000; Wu et al. 2002a). Recently, further mechanistic studies on EBNA1 transcriptional activation have been performed, with zinc shown to be necessary for residues 61-83 of EBNA1 to activate transcription, and that this region of EBNA1 coordinates zinc through a pair of essential cysteine residues contained within it. Residues 61-83 were also shown to dimerise upon coordinating zinc, revealing that EBNA1 contains a second dimerisation interface in its amino-terminus (Aras et al. 2009).

Recent work has also suggested that phosphorylation sites of EBNA1 are involved in the regulation of its function. Ten specific phosphorylated EBNA1 residues were identified, and a phosphorylation deficient mutant derivative of EBNA1 was shown to be significantly reduced in its ability to maintain EBV plasmids in cells and activate transcription, despite the mutant retaining a long half-life and nuclear translocation ability (Duellman et al. 2009).

1.7.7.3 Viral promoter regulation of EBNA1

EBNA1 transcription is driven from four different viral promoters in EBV-infected cells. These promoters are termed Cp, Wp, Qp and Fp, and are located in the BamHI-C, BamHI-W, BamHI-Q, and BamHI-F regions of the viral genome respectively (Kieff and Rickinson 2001). Differential use of these promoters is observed during different latency programmes and lytic cycle in EBV-infected B-lymphocytes. In LCLs, where a latency III pattern of gene expression is seen, transcription of EBNA1 is initiated from Cp/Wp promoters, with the Qp promoter transcriptionally silenced. Qp activity is subject to EBNA1 autoregulatory control (Sample et al. 1992) along with control by multiple cellular factors, including cytokines and cell cycle factors, that play both positive and negative roles in regulating Qp activity (Sung et al. 1994; Davenport and Pagano 1999; Zhang and Pagano 1999, 2000; Liang et al. 2000). Preferential selection for usage of a particular EBNA1 promoter is observed in EBV-infected epithelial cells and EBV-associated malignancies where the established programme of latency varies from the latency III programme observed in LCLs. For example, EBNA1 is transcribed from the Qp promoter in type I and II latency programmes (BL, HL, NPC) (Kieff and Rickinson 2001), with silencing of the Cp/Wp promoters through methylation observed (Schaefer et al. 1997). During type I latency, EBNA1 transcription was initially thought to be driven from Fp, although this theory was based on findings in cells undergoing spontaneous

lytic replication (Sample et al. 1991; Schaefer et al. 1991) and subsequent analysis revealed EBNA1 transcription is initiated from Fp in lytically induced cells, and the Fp promoter was found to be localised 100-200bp upstream of Qp (Schaefer et al. 1995, 1997; Tsai et al. 1995; Nonkwelo et al. 1996).

1.7.7.4 The role of EBNA1 in the modulation of cellular transcription and tumourigenesis

Classically EBNA1 is regarded as a genome maintenance protein, though there is a growing body of evidence suggesting that it may contribute to the cell transforming properties of EBV. The role of EBNA1 in the development of EBV-associated malignancies remains controversial, and despite the accumulating support for its role in oncogenesis, several reports contradict such findings.

In one of the first studies implicating EBNA1 in cellular transformation, targeted expression of EBNA1 to the B-cell compartment in two lineages of transgenic mice resulted in lymphomas, which were reported to be phenotypically similar to lymphomas induced by dysregulated c-Myc (Wilson et al. 1996). However, the results of more recent similar transgenic studies failed to recapitulate these findings, as observations failed to demonstrate an association between EBNA1 and lymphoma development (Kang et al. 2005), although an increased susceptibility to pulmonary adenoma was observed in EBNA1-positive FVB mice (Kang et al. 2008). Consistent with EBNA1 not playing a role in cellular transformation, another report has shown that LCLs generated with EBV deleted for EBNA1 are indistinguishable from their EBNA1-positive counterparts and that when these EBNA1-deleted LCLs were injected into SCID mice, tumour growth was supported, indicating that EBNA1 is not mandatory for EBV's oncogenic potential (Humme et al. 2003). However it

should be noted that the frequency of LCL generation achievable with EBV deleted for EBNA1 was much lower than the frequency attained with wild type EBV.

Increased expression of recombination-activating genes 1 and 2 is observed in EBV-positive BL cells, compared with their EBV-negative counterparts, and has been demonstrated to be dependent on EBNA1 expression (Srinivas and Sixbey 1995), leading to the postulate that EBNA1 may contribute to the characteristic c-myc translocation of BL (Srinivas and Sixbey 1995; Wilson et al. 1996). Such an oncogenic role for EBNA1 in BL is seemingly consistent with findings that EBNA1 is the only viral protein consistently detected in this EBV-associated malignancy, and data which revealed that the use of a dnEBNA1 in EBV-positive BL lines resulted in decreased cell viability (Kennedy et al. 2003). However, alternative dnEBNA1 studies, conducted this time in LCLs with a stably integrated EBV genome, failed to show any dnEBNA1 induced changes in viral or cellular gene expression, other than a slight effect on EBER expression (Kang et al. 2001). Further, studies in which EBNA1 was expressed in EBV-negative BL cells failed to show any effect of EBNA1 expression upon cell growth, tumourigenicity and apoptosis in response to a range of stimuli (Komano et al. 1998; Ruf et al. 1999).

Recent studies of the role of EBNA1 in another B-cell malignancy, HL, have revealed induction of CD25 and CCL20, and down-regulation of transforming growth factor β (TGFβ)-target gene PTPRK in response to EBNA1 expression, contributing to the growth and survival of HL cells (Baumforth et al. 2008; Flavell et al. 2008).

The results of several other studies of EBNA1 function suggest that the protein plays a role in the modulation of cellular pathways involved in tumourigenesis. EBNA1 has been demonstrated to associate with a known suppressor of metastasis and cell migration, Nm23-

H1, in EBV-transformed LCLs, removing the protein's repressive effect of upon cell motility (Murakami et al. 2005). Further, EBNA1 interacts with the human deubiquitinating enzyme, USP7 (Holowaty et al. 2003a), through amino acids 395-450 (Holowaty et al. 2003a). USP7 is known to associate with p53, causing deubiquitination of this tumour suppressor protein and thus rescuing it from proteasomal degradation, ultimately leading to p53-mediated cell growth suppression (Li et al. 2002). As such, it is postulated that EBNA1 may contribute to host cell immortalisation by EBV through sequestration of USP7 and subsequent destabilisation of p53.

Much evidence also exists for EBNA1 playing a tumourigenic role in epithelial cells. EBNA1 has been observed to destabilise p53 (through USP7 interaction) and promote cell survival in epithelial cells (Saridakis et al. 2005), and EBNA1-expressing NPC-derived cells were reported to form large, highly metastatic and poorly differentiated tumours following injection into mice (Sheu et al. 1996). More recently, EBNA1-mediated disruption of PML nuclear bodies was observed in NPC cells, promoting the survival of cells with DNA damage. PML nuclear body disruption by EBNA1 was shown to be independent of p53, but dependent upon binding to cellular USP7, with EBNA1 expression leading to the impairment of several cellular processes (including DNA repair and apoptosis) that are PML-dependent (Sivachandran et al. 2008).

In contrast to previous data, suggesting no transactivation of cellular genes or integrated viral genes by EBNA1in LCLs (Kang et al. 2001), EBNA1 appears to be a potent transcriptional regulator in nasopharyngeal cells. In findings similar to those previously mentioned in HL (Flavell et al. 2008), EBNA1 has been shown to regulate the TGFβ pathway negatively, through an increase in the turn-over of the mothers against decapentaplegic homologue 2 (SMAD2) transcription factor. As TGFβ is a widely regarded tumour suppressor, inactivation

of TGFβ signalling by EBNA1 may contribute to the development and metastatic nature of NPC (Wood et al. 2007). EBNA1 has also been found to modulate the AP-1 transcription factor pathway (O'Neil et al. 2008).

Recently, EBNA1 has been identified to bind to promoter regions of cellular genomic DNA in EBV-positive B-cells (Dresang et al. 2009), and although no EBNA1-dependent activation of reporter constructs from these promoters was observed, these findings may prove of huge significance in elucidating future mechanisms of EBNA1-mediated modulation of cellular transcription and tumourigenesis.

1.7.8 EBERs

In addition to the EBV latent protein complement, two small non-polyadenylated and non-coding RNAs, EBER1 and EBER2, are detected in all forms of viral latency, and are frequently used as a diagnostic marker for EBV infection. The EBERs are transcribed from the EcoRI-J fragment of the EBV genome, and are 167 and 172 nucleotides in length respectively. EBERs are abundantly transcribed in latently infected cells, with up to 10^7 copies of the EBERs present in each cell (Lerner et al. 1981a; Arrand and Rymo 1982; Nanbo and Takada 2002). However, despite their abundant and ubiquitous expression, the EBERs are not essential for the EBV-induced transformation of B-lymphocytes (Swaminathan et al. 1991; Yajima et al. 2005; Wu et al. 2007).

The EBERs are similar in size and gene organisation to two small adenovirus RNAs, VAI and VAII. Other similarities between EBERs and VA RNAs exist, with both being transcribed by RNA polymerase III (pol III) and binding the same cellular proteins. This suggests that EBERs and VA RNAs may perform analogous functions in infected cells. The VA RNAs have been shown to be critical for adenovirus replication by rescuing cells from the shutdown

of protein translation mediated by the cellular kinase PKR, which is induced by interferon and activated by double-stranded RNAs produced during replication of many viruses (Hovanessian 1989; Ghadge et al. 1994). Further, *in vitro* analysis of adenovirus mutant constructs, in which VA RNAs were replaced by EBERs, revealed the EBERs to be capable of functionally substituting for the VA RNAs (Bhat and Thimmappaya 1983; 1985).

Following EBV infection of B-lymphocytes, temporally the EBERs are the last EBV latent gene products to be expressed (Rooney et al. 1989; Alfieri et al. 1991). Further, the P3HR-1 virus (which is transformation defective) is able to express the EBERs in BL cells, but not resting B-cells, highlighting the requirement for an activated cellular environment for EBER expression to occur (Rooney et al. 1989). Despite being transcribed at approximately equal rates EBER1 is often reported as being more abundant than EBER2 in latently infected cells, possibly due to EBER1 possessing a longer half-life, of around 9 hours compared with EBER2's half-life of less than an hour (Clarke et al. 1992; Komano et al. 1999). Indeed a recent study, although not addressing EBER2 half-life, estimated the half-life of EBER1 to be even longer, at around 25 hours (Fok et al. 2006b). A switch from latent to lytic infection is accompanied by a significant down-regulation of EBER transcription, and although the mechanism behind this down-regulation of EBER transcription is currently undetermined, such a switch is consistent with the absence of EBER expression in the permissive EBV lesion oral-hairy leucoplakia (OHL) (Gilligan et al. 1990a; Greifenegger et al. 1998).

The EBERs are thought to localise predominantly to the nucleus, although some evidence suggests that they are detectable in the cytoplasm. One of the first studies to examine EBER localisation used *in situ* hybridisation assays and reported EBER expression to be confined to the nucleus (Howe and Steitz 1986), although a later report using more sensitive techniques

(confocal microscopy) suggested that the EBERs were present in the cytoplasm during some phases of the cell cycle, with EBER localisation varying remarkably with the phases of the cell cycle (Schwemmle et al. 1992). Further analysis using *in situ* hybridisation supported the notion that the EBERs are mainly nuclear, although differences in the localisation of EBER1 and EBER2 were reported, with no colocalisation of the two molecules found, such analysis suggesting distinct roles for EBER1 and EBER2 (Teramoto et al. 1998). More recently, EBER localisation was again addressed, with the EBERs found not to shuttle out of the nucleus, possibly as a consequence of their failure to bind exportin 5 (Fok et al. 2006a). As such, it is widely accepted that the EBERs are subject to nuclear localisation, though the possibility of leakage to the cytoplasm should not be completely discounted.

A high degree of secondary structure is adopted by EBER1 and EBER2, involving long stems and loops due to strong intra-molecular bond formation (Nanbo and Takada 2002). This complex structure of the EBERs enables interaction with dsRNA binding proteins that are thought to be important for EBER function, an observation that is supported by the high levels of EBER1 and EBER2 sequence conservation reported among EBV isolates (Arrand et al. 1989). The EBERs are reportedly able to associate with four cellular proteins: (1) La antigen; (2) ribosomal protein L22; (3) protein kinase R (PKR); and (4) retinoic acid-inducible gene-1 (RIG-I) (Lerner et al. 1981a; Clarke et al. 1991; Toczyski and Steitz 1991; Nanbo et al. 2002; Samanta et al. 2006). The EBERs are detected in ribonucleoprotein (RNP) complexes with La antigen using autoreactive sera from systemic lupus erythematosus patients (Lerner et al. 1981a), with these RNP complexes also containing L22 (Toczyski and Steitz 1991). EBER sequestration of L22 in the nucleus has also been observed, with the EBERs preventing L22 from being incorporated into ribosomal machinery (Toczyski et al. 1994). Although it is possible that EBER interactions with La and L22 may affect RNA splicing and translation,

the precise physiological role of the interaction between the EBERs and these cellular proteins remains unidentified. The association of the EBERs with two dsRNA binding proteins of the innate immune system, PKR and RIG-I, is well studied and of known significance in explaining EBER function.

Despite not being required for EBV reactivation, replication, virion release, infectivity, viral gene expression and the transformation of B-lymphocytes *in vitro*, the EBERs have been demonstrated to increase transformation efficiency by approximately 100 fold and promote LCL growth at low cell densities (Swaminathan et al. 1991; Yajima et al. 2005; Wu et al. 2007). It is now understood that these effects are dependent on EBER2, rather than EBER1 expression, and are mediated in part by the enhanced secretion of IL-6 which acts as both an autocrine growth factor and an inhibitor of apoptosis (Wu et al. 2007). EBER expression in BL cells has also been demonstrated to induce tumours when cells are injected into nude mice. Further, EBER expression in BL cells induces anchorage-independent growth, resistance to apoptosis, enhanced proliferation and the secretion of type I interferon (IFN) along with the autocrine growth factor IL-10 (Komano et al. 1999; Kitagawa et al. 2000; Ruf et al. 2000, 2005; Yamamoto et al. 2000; Nanbo et al. 2002; Samanta et al 2006), with the secretion of these cytokines being shown to be dependent on the activation of RIG-I by the EBERs (Samanta et al. 2006, 2008). EBERs appear to confer resistance to apoptotic stimuli through binding to, and inactivation of, PKR (Ruf et al. 2005; Wang et al. 2005b).

The biological effects of the EBERs are not restricted to lymphocytes: work with epithelial cells has shown that the EBERs induce the expression of insulin-like growth factor 1 (Iwakiri et al. 2003, 2005). Induction of the expression of these autocrine growth factors in epithelial cells as well as lymphocytes hints at the transforming role the EBERs may play in EBV pathology. Furthermore, stable expression of EBERs in immortalised nasopharyngeal

epithelial cells confers resistance to apoptotic stress, with EBER expression also preventing p38 and c-Jun phosphorylation in response to dsRNA suggesting inhibition of AP-1 (Wong et al. 2005). EBER expression in intestinal 407 epithelial cells has also been reported to prevent FAS-mediated apoptosis (Nanbo et al. 2005). However, EBER expression has been found to be insufficient to transform pre-malignant nasopharyngeal cells, with the EBERs failing to induce anchorage-independent growth or induce tumours in nude mice (Wong et al. 2005), although in a more recent study, high levels of EBER expression in MDCK cells (but not NPC-KT cells) induced growth in soft agarose (Yoshizaki et al. 2007).

The increase in various cytokines following EBER expression (Kitagawa et al. 2000; Iwakiri et al. 2003, 2005; Yang et al. 2004) has been determined to be at the level of mRNA, implicating induction of transcription or transcript stabilisation by the EBERs, although in the absence of evidence for direct or indirect interaction with promoter sequences or mRNAs, a plausible mechanism for the action of EBERs to induce highly gene specific effects is still lacking (Swaminathan 2008). Supporting the idea of EBER-induced changes to cellular transcription, recently published data suggest a cellular transcription response to EBER2 expression in HEK293 cells, with significant changes in patterns of gene expression observed (Eilebrecht et al. 2008).

Cellular non-coding RNAs have increasingly come to be recognised as playing important regulatory roles in cellular transcription, with a recent report describing how PIP7S, a nuclear La-related protein, binds and stabilises 7SK RNA, which is involved in regulating transcriptional elongation by pol II (He et al. 2008). Some speculation exists that the EBERs could be viral counterparts of cellular non-coding RNAs, playing a significant part in regulation of a multitude of cellular functions (Swaminathan 2008).

1.7.8.1 Transcriptional regulation of EBER expression

Although transcribed exclusively by RNA polymerase (pol) III, the EBER promoters contain a hybrid of pol II and pol III elements. A schematic of the EBERs and their transcriptional regulatory regions is shown in Figure 1.3, with both EBER1 and EBER2 possessing similar promoter regions significant for their expression including intragenic A and B blocks (typical of type 2, pol III promoters) (Rosa et al. 1981; Arrand and Rymo 1982), an upstream TATA box, and upstream ATF-2 and Sp1 binding sites (typical pol II promoter regions) (Howe and Shu 1989; 1993; Felton-Edkins et al. 2006). In addition, EBER1, but not EBER2, has two E-boxes 130bp upstream of its transcriptional start site to which c-Myc has been shown to bind both *in vitro* and *in vivo* (Niller et al. 2003), although the importance of these binding sites has been questioned by a study which demonstrated that excision of these sites had no effect upon EBER expression (Wensing et al. 2001). The promoter for EBER2 has been analyzed by testing mutated promoters in transfection assays (Howe and Shu 1989; 1993), with results showing that deletion of 5' sites that would be expected to bind Sp1 and ATF-2 together reduced transcription by more than 90%. Additionally, deleting the TATA box reduced expression even further and mutations in either the Sp1 or TATA box regions reduced expression by 80%, whereas mutating the ATF-2 site reduced expression by 50%. Subsequently similar experiments have been conducted to analyse the effects of disrupting the promoter regions upstream of EBER1, with results confirming the importance of these regions to EBER1 expression, and suggesting that the ATF-2 binding site is of particular importance. The same study revealed that the presence of *OriP* and EBNA1 increased EBER transcription two- to four-fold, but had a much smaller effect than has been observed on the Cp or LMP1 promoters, which are conventional RNA polymerase II promoters (Wensing et al. 2001).

Figure 1.3 - Promoter regions of EBER1 and EBER2. 'A' and 'B' denote internal A- and B-blocks, typical of type II, pol III promoter regions to which pol III specific transcription factor TFIIIC binds. Upstream elements include TATA box (-23 to -28), Sp1 (-56 to -77) and ATF (-40 to -55) binding sites (CRE motif). Notably, EBER1, though not EBER 2 possesses a c-Myc binding site (consisting of two E-boxes) at -149 to -130 relative to its transcriptional start site. Deletion of the 5' sites that would be expected to bind Sp1 and ATF-2 together has been shown to reduce EBER transcription by more than 90%. Additionally, deleting the TATA box reduces expression even further and mutations in either the Sp1 or TATA box regions reduces expression by 80%, whereas mutating the ATF-2 site reduces expression by 50% (Howe and Shu 1989, 1993).

Figure 1.3

Several observations suggest that the massive expression of EBER genes in EBV-transformed cells is not simply due to inherent strength of the EBER promoters, but instead requires EBV-induced changes to the cellular environment, with previous studies suggesting a strong influence of trans-acting factors in controlling the transcription of the EBERs. Stable transfection of EBER1 alone allowed maximal expression of 10^5 transcripts per cell, whereas latent infection with the EBV genome can result in 10^7 EBER1 transcripts per cell (Lerner et al. 1981b; Laing et al. 2002). Significant EBER expression only becomes apparent 36 h after infection, following the appearance of other EBV latent gene products (Rooney et al. 1989). Further, when latently infected cells switch to lytic viral replication, transcription of the EBERs decreases dramatically (Greifenegger et al. 1998).

EBV-induced changes to the cellular environment that appear to contribute to achieving high levels of EBER expression have recently been identified and described (Felton-Edkins et al. 2006). EBV was shown to induce the cellular transcription factors TFIIIB and TFIIIC (leading to induction of general cellular pol III-mediated transcription) and the typical pol II transcription factor ATF-2, that enhance expression of EBER1 and EBER2. Cellular factors seemingly induced by EBV and involved in the transcription of the EBERs (pol III transcription, ATF-2, c-Myc) are discussed more fully later in this introductory section.

Methylation, or rather hypomethylation, has also recently been shown to play a possible role in EBER regulation. CpG-methylation is known, in most cases, to block the activity of pol II transcribed promoters, and although the role of DNA methylation in the regulation of pol III transcribed promoters is less clear, a recent study found that *in vitro* methylation of EBER1 and EBER2 promoters blocked the binding of c-Myc and ATF-2 to the 5' regions of these genes, silencing their expression (Banati et al. 2008). This is significant as the EBER locus is invariably hypomethylated in cell lines, with the tight binding of nuclear proteins and

constitutive transcription proposed to keep the EBER locus methylation free, even in NPC cells that carry otherwise highly methylated episomes (Minarovits et al. 1992). These data also seem to confirm further the importance of typical pol II promoter regions upstream of EBER1 and EBER2.

EBV copy number may also play a role in determining levels of EBER expression. This topic is addressed in Chapter 3.

1.7.8.1.1 RNA polymerase III transcription

The EBERs, and other viral non-coding RNAs (e.g. adenovirus VA RNAs), are transcribed exclusively by pol III, meaning an understanding of pol III transcription, and its links with cancer and viral infection, is critical in appreciating the role of pol III in expression of these abundantly expressed viral gene products.

Archaea and prokaryotes utilise just a single RNA polymerase in the transcription of their genes, but in eukoryotes this cellular transcription is divided between three RNA polymerases, pol I, pol II and pol III. All protein-encoding genes, along with many genes for non-coding RNAs are transcribed by pol II, with pol I and III specialised to the exclusive expression of non-coding RNAs. Despite this restriction, pols I and III are known to contribute up to 80% of all nuclear transcription in rapidly proliferating cells (White 2008). Pol I is unique among the nuclear RNA polymerases in transcribing only one set of genes: the large, tandemly repeated, ribosomal RNA (rRNA) genes, and thus in having to recognise a single promoter structure. Pol II promoters can be divided into a core region, defined as the minimal region capable of directing transcription *in vitro*, and a regulatory region. The regulatory regions are highly varied in structure, which reflects the highly varied synthesis patterns of cellular proteins and the need for exquisite and complex regulation of these

patterns. Comprehensive reviews of the complexities of pol II transcription are available (Orphanides et al. 1996; Woychik and Hampsey 2002; Juven-Gershon et al. 2008).

Pol III promoters are more varied in structure than the uniform RNA polymerase I promoters, though not as diverse as the RNA polymerase II promoters. They have been divided into three main types (see Figure 1.4), two of which are gene-internal and generally TATA-less (types 1 and 2), and one of which is gene-external and contains a TATA box. EBERs can be characterised as having elements typical of both type 2 and 3 pol III promoter types, with additional typical pol II transcription factor binding elements also present. The cellular 7SL genes have an upstream promoter arrangement similar to the EBER genes, as well as important internal promoter sequences (Ullu and Weiner 1985; Kleinert et al. 1988; Howe and Shu 1993; Muller and Benecke 1999).

The promoters of pol III templates that are located within the transcribed region are bound directly by TFIIIC, a large complex of six subunits, TFIIIC-220, -110, -102, -90, -63 and the newly characterised (Dumay-Odelot et al. 2007) TFIIIC-35. By contrast, the type 1 internal promoters (exclusive to the 5S rRNA gene) are recognised by a polypeptide called TFIIIA that provides a binding site for TFIIIC. TFIIIC functions to recruit TFIIIB, a complex composed of the TATA-binding protein (TBP) and the Brf1 and Bdp1 polypeptides, which is responsible for the subsequent recruitment of pol III and its positioning over the transcription start site. Pol III itself has 17 subunits and is the largest RNA polymerase known (White 2008). A comprehensive review of pol III recruitment to its target promoters is available (Schramm and Hernandez 2002), and provides insight into the mechanistic complexities and variations of pol III recruitment to each promoter type. Recent data have addressed pol III recruitment *in vivo*, and provide support for the *in vitro* models previously described (Kenneth et al. 2008).

RNA polymerase III is dedicated to the transcription of an eclectic collection of genes whose main common features are that they encode structural or catalytic RNAs and that they are invariably shorter than 400bp, a length limit consistent with the elongation properties of pol III, which recognises a simple T-residue run as a termination signal (Schramm and Hernandez 2002). Pol III products include transfer RNAs (tRNA), 5S rRNA, and 7SL RNA, which is needed to insert proteins into membranes as part of the signal recognition particle. Further products include the U6, MRP and H1 RNAs, required to process mRNA, rRNA and tRNA, respectively (Dieci et al. 2007). Pol III also synthesises 7SK, Alu and B2 RNAs, which can regulate pol II transcription and have been implicated in the expression of a subset of human miRNAs (White 2008).

Pol III products are aberrantly over-expressed in a broad variety of cancers. In 1974, hyperactivity of pol III in mice with cancer was observed, in the first such report associating increased pol III activity and cancer (Schwartz et al. 1974). Subsequently, abnormally high levels of pol III products have been observed in a wide variety of transformed cell types, including human ovarian carcinomas (Winter et al. 2000), with one study reporting elevated levels of 7SL RNA samples from 19 types of cancer (Chen et al. 1997). Such compelling data make a strong association between aberrant expression of pol III transcripts and cellular transformation (White 2004).

The molecular mechanisms that result in increased polIII output in transformed cells and cancers can be classified into three general categories: (1) release from repression by tumour suppressors; (2) activation by oncogene products; and (3) increased expression of pol III-associated transcription factors (Marshall and White 2008). Multiple mechanisms may contribute to an overall increase in pol III activity in any given cancer.

Figure 1.4 – Adapted from Felton-Edkins et al. (2006). Summary of the promoter types employed by pol III. The arrow indicates the transcription start site, with PSE denoting proximal sequence element and CRE denoting cAMP-response element. A schematic of the EBER promoter type is included for comparison. Type 1 and 2 promoters possess only internal transcription factor finding sites, with type 1 promoters consisting of A- and C-blocks, and type 2 promoters consisting of A- and B-blocks. Conversely, type 3 promoters consist entirely of promoter binding sites upstream of the transcriptional start site, with a PSE and TATA box constituting such a promoter type.

Figure 1.4

Release from tumour suppressor genes may be the most common mechanism by which pol III activity is increased in cancers, given that it involves tumour suppressors such as PTEN, p53 and Rb, whose activities are known to be reduced in a large proportion of malignancies. PTEN is able to inhibit pol III transcription through its lipid phosphatase activity, counteracting signalling through the PI3K pathway (Woiwode et al. 2008). TFIIIB is also a target for p53, Rb, and Rb-like proteins RBL1 and RBL2, which bind it directly and prevent it from recruiting pol III to promoters (Chesnokov et al. 1996; Sutcliffe et al. 1999; Sutcliffe et al. 2000; Crighton et al. 2003; Hirsch et al. 2004). Other tumour suppressor genes are crucial in mediating the binding of both p53 and Rb to TFIIIB (Scott et al. 2001; Morton et al. 2007), and TFIIIB is also known to be bound and repressed by Maf1 (Willis and Moir 2007; Goodfellow et al. 2008), which although yet to be defined as a tumour suppressor, is known to inhibit anchorage-independent growth in glioblastoma cells (Johnson et al. 2007).

TFIIIB is also regulated by a variety of oncogenic proteins which are able to stimulate, rather than repress, its activity. Many oncogenic proteins are able to affect TFIIIB through the subversion of negative regulation imposed by Rb and/or p53 (Marshall and White 2008); for example the HPV oncoproteins E6 and E7 have been demonstrated to stimulate pol III transcription through the inactivation of p53 and the Rb family respectively (Sutcliffe et al. 1999; Stein et al. 2002). Ras, Raf, PI3K and Akt operate through oncogenic signalling pathways which are able to alter the phosphorylation state of pol III machinery (Wang et al. 1995; Chesnokov et al. 1996; Felton-Edkins et al. 2003), and c-Myc acts directly on TFIIIB stimulating its activity through a physical and genetic interaction (Gomez-Roman et al. 2003). Induction of c-Myc increases target occupancy by both TFIIIB and pol III, an effect that correlates with localised acetylation of histone H3, a modification that is associated with active transcription (Kenneth et al. 2007). Recently published data suggest that pol III

induction makes a significant contribution to c-Myc-mediated cell transformation (Johnson et al. 2008).

Over-expression of pol III transcription machinery was first observed for TFIIIC, which has been found to be increased in culture following infection or transformation by several DNA tumour viruses, including adenovirus, SV40 virus and EBV (Hoeffler et al. 1988; Larminie et al. 1999; Felton-Edkins and White 2002; Felton-Edkins et al. 2006). Further, levels of TFIIIC have been demonstrated to be abnormally elevated in both NPC (Dr JR Arrand, personal communication) and human ovarian carcinomas (Winter et al. 2000). This is not a response to altered proliferation, as TFIIIC levels are not influenced by growth factors or cell cycle arrest (Winter et al. 2000; Scott et al. 2001). Over-expression of TFIIIB subunits has also been found in human cervical and colon carcinomas, and can be induced in culture by oncogenic viruses (such as EBV, and the X oncoprotein of HBV), and the cellular oncoprotein Ras (Wang et al. 1995; Johnson et al. 2003; Daly et al. 2005; Felton-Edkins et al. 2006). Further, other virus-encoded proteins such as HTLV-1 tax protein, have been shown to activate cellular pol III transcribed genes (Gottesfeld et al. 1996) with others, such as Influenza A virus matrix protein 1, known to interact with pol III machinery components (Huang et al. 2009).

In recent years, evidence linking aberrant pol III activity to cancer (outlined above) has strengthened considerably, with data now suggesting that increased pol III transcription is capable of, and necessary for, promotion of proliferation and oncogenic transformation in some cellular contexts (Johnson et al. 2008; Marshall et al. 2008). These findings, although in need of confirmation in terms of their generality, are of huge significance and interest, especially given the well established role of oncogenic viruses in pol III dysregulation.

1.7.8.1.2 c-Myc: An EBER-associated cellular transcription factor

The c-Myc proto-oncogene is one of the most frequently activated oncogenes and is estimated to be involved in 20% of all human cancers (Dang 1999; Nesbit et al. 1999). Deregulation of c-Myc expression occurs in cancers through chromosomal translocation, viral insertions, amplification, deletions, insertions, and/or mutation of cis-elements (Meyer and Penn 2008).

A comprehensive review of the biology of c-Myc is beyond the scope of this thesis, though such reviews are readily available (Meyer and Penn 2008). However, it is important to introduce at least certain aspects of c-Myc biology, given that c-Myc has been demonstrated to bind upstream of the EBER1 transcriptional start site *in vitro* and *in vivo* (Niller et al. 2003). The brief introduction to c-Myc that follows is based around its role as a transcriptional activator, and the regulation of its expression and activity.

In the late 1980s, strong evidence was produced to suggest that c-Myc was able to function as a regulator of gene transcription (Luscher and Eisenman 1990; Marcu et al. 1992), being both a positive and negative regulator of cellular gene expression. Sequence-specific DNA binding and transcriptional activity of c-Myc were revealed through the characterisation of two important domains of the protein: the leucine zipper (LZ) domain (Landschulz et al. 1988) and the helix-loop-helix (HLH) domain (Murre et al. 1989), with both these regions found to be essential for c-Myc-mediated cellular transformation (Stone et al. 1987; Dang et al. 1989). Direct transcriptional activity of c-Myc was then demonstrated (Kato et al. 1990) before DNA binding of c-Myc was formally observed (Blackwell et al. 1990; Prendergast and Ziff 1991). Subsequently, c-Myc's partner protein, the ubiquitously expressed Max, was identified, with c-Myc-Max heterodimers demonstrated to bind a CACGTG E-box motif with high affinity (Blackwood and Eisenman 1991), and c-Myc-Max heterodimerisation was shown to be

essential for c-Myc transformation (Amati et al. 1993). Although c-Myc appears dedicated to Max, Max itself is able to bind other members of the Mxd family through the LHL-LZ region (Ayer et al. 1993), with these interactions providing a mechanism of functional regulation of c-Myc (Billin and Ayer 2006; Nair and Burley 2006; Wahlstrom and Henriksson 2007).

Recent estimates suggest that c-Myc could regulate as many as 15% of all genes in the human genome (Dang et al. 2006), by utilising a multitude of mechanisms, including recruitment of histone acetylases, chromatin modulating proteins, basal transcriptional factors and DNA methyltransferase (McMahon et al. 1998; Cheng et al. 1999; Eberhardy and Farnham 2002; Fernandez et al. 2003; Kanazawa et al. 2003; O'Connell et al. 2003; Orian et al. 2003; Brenner et al. 2005). c-Myc targets can therefore be classified into distinct subgroups whose regulation may involve some or all mechanisms through which c-Myc affects transcription, with the cis-regulatory modules for individual subgroups likely to contain binding sites for other specific transcription factors which cooperate with c-Myc (Dang et al. 2006).

The identification of the Mxd family of proteins has allowed further insight into the protein interactions that regulate c-Myc's transcriptional function. When bound to Max, Mad (and other family members) bind consensus E-box sequences and compete for binding with c-Myc/Max heterodimers. Mad/Max dimers repress transcription through the recruitment of the chromatin-modifying co-repressor complex (which contains Sin3, N-CoR, and the class I histone deacetylases HDAC1 and 2) to the promoters of target genes, resulting in deacetylation of histone tails and a closed chromatin conformation which prevents the transcriptional activation that occurs through E-boxes (Ayer et al. 1995; Alland et al. 1997). In contrast to the ubiquitous expression of Max, Mad proteins are induced during terminal differentiation (Ayer and Eisenman 1993), and consistent with these data, chromatin

immunoprecipitation (ChIP) experiments have revealed a switch from c-Myc-Max binding to Mad-Max binding during cellular differentiation (Bouchard et al. 2001; Xu et al. 2001).

c-Myc is also able to inhibit transcription through direct interference with other factors known to activate gene expression. For example, c-Myc binds to and interferes with the transcriptional activator Miz-1, thereby causing trans-repression of specific Miz-1 target genes (Wanzel et al. 2003; Wu et al. 2003).

The search for physiological and pathological c-Myc target genes has intensified significantly in recent years, with searches evolving from hypothesis-driven, low throughput studies of candidate c-Myc target genes, to high throughput microarray technologies for the discovery of c-Myc responsive genes (O'Connell et al. 2003). Despite these impressive advances, much work must yet be undertaken to achieve a complete understanding of c-Myc responsive genes and how they relate to tumourigenesis. c-Myc responsive genes that are reported consistently in different cell types, systems and species can be identified from the c-Myc target gene database (http://www.myccancergene.org). Although c-Myc is thought to influence up to about 15% of genes and despite the functional range of specific genes altered, c-Myc affects specific classes of genes involved in cellular metabolism, protein biosynthesis, cell cycle regulation, cell adhesion, apoptosis, intercellular signalling (such as angiogenesis) and the cytoskeleton (Dang et al. 2006). c-Myc has also been implicated in regulation of pols I and III, thus influencing genes involved in ribosome biogenesis and protein synthesis. c-Myc binds TFIIIB, directly activating pol III transcription, with ChIP experiments verifying that c-Myc directly binds the pol III-transcribed tRNA and 5S rRNA genes (Gomez-Roman et al. 2003). Significantly, recent data demonstrate that transformation by c-Myc can be compromised by blocking pol III transcriptional induction (Johnson et al. 2008). Interestingly, recent data generated in *Drosophila*, using a dMyc (homologue of c-Myc) mutant unable to

interact with Max, revealed that Max-independent stimulation of pol III transcription occurred, and that despite a loss of influence upon pol I and II transcription, this dMyc mutant retained substantial biological activity (Steiger et al. 2008). The extent to which pol III regulation can account for the biological activity of dMyc in Max-depleted flies remains to be determined, but no other Max-independent targets have yet been identified (Kenneth and White 2009). Further non-coding cellular RNAs, miRNAs, are regulated by c-Myc. Several loci that encode miRNAs are bound by c-Myc *in vivo* (O'Donnell et al. 2005; Chang et al. 2008), with studies identifying c-Myc promoter binding as leading to the repression of miRNAs whose expression can reduce tumourigenesis (Chang et al. 2008), and c-Myc-mediated induction of miRNAs that are able to stimulate tumour angiogenesis (Dews et al. 2006).

The expression and activity of c-Myc is tightly regulated in non-transformed cells and designed to respond quickly to proliferative cues from the extracellular signals. Initial studies of c-Myc established a direct link between mitogenic stimulation of quiescent cultured cells and a rapid induction of mRNA encoding c-Myc, with maximal mRNA levels of this immediate early response gene being reached within 2 hours of mitogen treatment where protein synthesis was inhibited (Kelly et al. 1983). Further, mRNA encoding c-Myc, and c-Myc protein have both been demonstrated to possess short half-lives (Dani et al. 1984; Hann and Eisenman 1984), and anti-proliferative signals trigger a rapid down-regulation of c-Myc expression (Campisi et al. 1984; Gonda and Metcalf 1984; Lachman and Skoultchi 1984; Dean et al. 1986). A multitude of signal transduction pathways and numerous transcriptional and post-translational regulatory mechanisms have evolved to tightly control c-Myc expression. Evidence that deregulation of c-Myc mRNA expression is able to drive cancer development has been demonstrated through the use of transgenic mouse models (Adams et

al. 1985; Leder et al. 1986). The c-Myc promoter is a point of convergence for multiple signalling cascades involved in transcriptional regulation of c-Myc, and comprehensive reviews of the c-Myc promoter region have recently been published (Levens 2008; Wierstra and Alves 2008). Dysregulation of c-Myc transcription can occur directly and indirectly, resulting in cellular proliferation and transformation (Roussel et al. 1991; Afar et al. 1994; Barone and Courtneidge 1995; He et al. 1998; Oster et al. 2002; Cheng et al. 2006; Weng et al. 2006). In addition to dysregulation of transcription, c-Myc mRNA turnover is also altered by an array of signals, adding a further layer of complexity to the regulation of c-Myc mRNA levels (Jones and Cole 1987; Bernstein et al. 1992). Post-transcriptional modification of c-Myc occurs through phosphorylation events. Research has focussed on the phosphorylation of two specific residues of the c-Myc protein, Thr58 and Ser62. These residues are important for transformation and regulate both c-Myc stability and activity (Hann 2006; Vervoorts et al. 2006). Proliferative stimuli activate specific kinases that phosphorylate Ser62, increasing the stability of c-Myc. Phospho-Ser62 is subsequently able to act as a platform for phosphorylation of Thr58 by glycogen synthase kinase 3 (GSK-3), enabling the tumour suppressor FBW7 to bind leading to the direct ubiquitination of c-Myc and consequent proteasomal degradation. Additional mechanisms of c-Myc regulation have also been identified including the discovery of a short form of c-Myc, arising from variation in translational initiation sites (Spotts et al. 1997), and cap-independent translation of c-Myc (Cobbold et al. 2008).

Significantly, recently published data suggest c-Myc (along with NF-κB) is one of the two main transcription factors responsible for the phenotype, growth pattern, and biological properties of cells driven into proliferation by EBV, with c-Myc shown to be activated in the latency III programme of EBV-immortalised B-cells (Faumont et al. 2009a). Interaction of

EBV and c-Myc growth programmes in BL has been outlined in the previous section discussing EBV-associated malignancies (1.6.1), and the influence of a variety of oncogenic viruses on c-Myc is discussed in Chapter 4.

1.7.8.1.3 ATF-2

ATF-2 is postulated to play a significant role in EBER regulation, given that mutation of the ATF-2 binding sites upstream of EBER1 and EBER2 has been demonstrated significantly to reduce levels of EBER expression (Howe and Shu 1989; 1993; Wensing et al. 2001).

The ATF/CREB family of proteins consists of sixteen cellular stress-responsive transcription factors, divided into six subgroups according to their sequence similarity (Hai and Hartman 2001). These proteins all share common features, including the bZIP element, which enables homo- and hetero-dimerisation and binding to specific DNA sequences (Hai et al. 1989). As with c-Myc, a comprehensive review of ATF-2 is beyond the scope of this work, however suitable review articles are available (Vlahopoulos et al. 2008).

The ATF-2 promoter contains Sp1 elements and a CRE-like element in the region -50 to +90, relative to the ATF-2 gene's transcriptional start site. These regions are important for basal promoter activity. However activation of ATF-2 is achieved through post-translational modifications upon stress stimuli. In unstimulated cells, ATF-2 is maintained in a transcriptionally inactive form by intramolecular interactions between its own activation domain and its bZIP domain (Li and Green 1996). In response to stress stimuli, ATF-2 is phosphorylated by multiple cell signalling pathways at amino acids Thr69 and Thr71. Phosphorylated ATF-2 forms dimers that bind to specific DNA sequences on target gene promoters, activating their expression (Gupta et al. 1995; Livingstone et al. 1995; Ouwens et al. 2002). ATF-2 is able to form homodimers or selective heterodimers with other members of

the ATF/CREB family and Fos/Jun family, with these dimers preferentially binding the 8-base palindromic CRE (cAMP Responsive Element) consensus sequence $T^{G}{}_{T}$ACGTCA promoters (Hai et al. 1989), although ATF-2 has been shown to bind other elements, including the AP-1 element (De Cesare et al. 1995; Song et al. 2006).

Activated ATF-2 complexes stimulate a broad spectrum of targets that are implicated in cancer including cell cycle molecules such as cyclin D1 (Beier et al. 1999), invasion related molecules such as matrix metalloproteinase 2 (MMP2) which is able to degrade components of the extracellular matrix (Song et al. 2006), cytokines such as IL-8 (Eliopoulos et al. 1999), cell adhesion molecules such as E-selectin (Read et al. 1997), and anti-apoptotic factor Bcl-2 (Ma et al. 2007).

The c-Jun transcription factor is an unusual target of ATF-2, as it is both a target and a co-operator of ATF-2. c-Jun is another bZIP protein, which belongs to the Jun protein family, and through its bZIP domain it forms either dimers with other members of the Jun family (c-Jun–JunB, c-Jun–JunD heterodimers), as well as heterodimers with Fos family members. The dimers that Jun members form are called AP-1 proteins and bind to the AP-1 element located in numerous genes. AP-1 has been subject to comprehensive review (Shaulian and Karin 2002; Hess et al. 2004).

A fine-tuned network of interacting bZIP proteins (including ATF-2) is involved in response to cellular stress stimuli. Interactions between ATF-2 and bZIP proteins involve: (1) regulation of other bZIP proteins' transcription; (2) antagonism with other bZIP monomers for selective dimer formation; (3) antagonism between bZIP dimers for binding to the same responsive element; (4) co-operation between bZIP dimers for binding to the same responsive element; and (5) selection of the responsive element according to the overall cellular bZIP

content (Vlahopoulos et al. 2008). Deregulation of these interactions leads to alterations in cellular processes such as proliferation, differentiation and apoptosis, resulting in the acquisition of cancerous characteristics. Given that ATF-2 is implicated in each of these types of interaction affecting target gene regulation, it can be regarded as a major cell fate modulator.

Through the described interactions with other bZIP proteins, ATF-2 has been clearly identified as playing a role in oncogenesis, with *in vitro* studies in human cancer cell lines, as well as *in situ* studies revealing a well documented activation of ATF-2 in several cancer types (Vlahopoulos et al. 2008). Phosphorylated ATF-2 is overexpressed in benign prostatic hyperplasia and, more intensely, in prostate tumours, suggesting that ATF-2 enhances survival and cell proliferation, promoting cancer progression (Ricote et al. 2006). Further, reduced levels of ATF-2 have been demonstrated to predispose mice to mammary tumours (Maekawa et al. 2007). ATF-2 also has been implicated in differentiation-related cell-cycle arrest and apoptosis in several leukaemia cell lines (Wu et al. 2002b; Wang et al. 2005a) and is proposed to play a role in central nervous system tumours (Tindberg et al. 2000), melanomas (Berger et al. 2003), lung cancer (Woo et al. 2002), hepatic cancer (Zhao et al. 2005) and NPC (O'Neil et al. 2008). Further, transgenic mouse studies have provided *in vivo* evidence linking ATF-2 and skin cancer development (Cho et al. 2004).

1.8 Aims and Objectives

Although the precise mechanisms by which EBERs may function in oncogenesis are not yet resolved, it is clear that EBERs are an important component of the EBV latent gene complement. The EBERs are the most abundant viral latent gene products. However, precisely how EBV is able to exploit the well defined cellular transcriptional mechanisms by

which the EBERs are transcribed is yet to be fully elucidated. Previously EBV has been demonstrated to induce transcription factors associated with EBER expression, including pol III transcription factors and ATF-2. Thus, the main aim of this study was to further increase understanding of how high levels of EBER expression are achieved by EBV, with much of the work being conducted in an epithelial cell background. High levels of EBER expression are thought to be crucial for oncogenic activity of EBERs in epithelial cells, with a recent study suggesting that high, but not low, levels of EBER expression could cause MDCK cells to form colonies in soft agar (Yoshizaki et al. 2007).

Initial studies in the project involve assessing the relationship between EBV copy number and levels of gene expression, to examine if high levels of EBER expression could be explained simply by multiple copies of EBER template being present in the form of multiple EBV episomes per cell. Previous evidence suggests that there may be a correlation between EBV copy number and rate of EBER transcription, albeit in a very small scale study (Metzenberg 1989), although other evidence suggests that the levels of expression of other EBV latent gene products do not correlate with genomic copy number (Metzenberg 1989; 1990; Sternas et al. 1990).

Subsequently, this project focuses on an investigation of the possibility that the ubiquitously expressed EBV latent protein EBNA1 plays a role in the induction of EBER-associated cellular transcription factors, and ultimately influences levels of EBER expression in *in vitro* cell line models derived from epithelial cell carcinomas. As previously discussed, observations suggest that high expression levels of EBER genes in EBV-transformed cells is not simply due to inherent strength of the EBER promoters, suggesting a strong influence of trans-acting factors in controlling the transcription of the EBERs (Lerner et al. 1981a; Rooney et al. 1989; Greifenegger et al. 1998; Laing et al. 2002). Given previous reports of EBNA1

being able to induce the transcription of cellular genes, including some of those involved in EBER expression (Wood et al. 2007; O'Neil et al. 2008), the role of EBNA1 as a trans-acting factor in EBER regulation is fully investigated, and given the reported EBNA1-mediated transcriptional induction of cellular genes, EBNA1 promoter binding studies are conducted. Such studies allow mechanistic analysis of EBNA1 function, particularly in terms of regulation of cellular EBER-associated transcription factors.

Chapter 2

Materials and Methods

Chapter 2 – Materials and Methods

2.1 Molecular cloning

2.1.1 Plasmids

The commonly used cloning vector pUC19 was obtained from New England Biolabs. It contains an ampicillin resistance cassette. UC refers to the University in which it was created (University of California).

The plasmid pOTEII HUMPU-GFP was obtained from Dr JR Arrand. It contains *OriP* and cassettes that express EBNA1 and GFP. It also expresses the puromycin resistance cassette described by Chen and Arrand (2003).

The pUC19 Puro plasmid was generated by excising the puromycin resistance cassette from pOTEII HUMPU-GFP with SalI and inserting at the SalI site of pUC19 (as detailed in Chapter 4).

pEcoRI-J and BamHI-X (Arrand et al. 1981) containing, respectively, the EBV EcoRI-J and BamHI-X fragments of EBV DNA were obtained from Dr JR Arrand.

The pUC19-EBERs plasmid was generated by inserting the 1kb SacI – EcoRI subfragment from the EcoRI-J fragment within pEcoRI-J into the corresponding sites of pUC19. Subsequently, the puromycin resistance cassette from pOTEII HUMPU-GFP was inserted at the SalI site (as detailed in Chapter 4).

For generation of pUC19-Puro-EBERs-ΔX, the X-box c-Myc binding site was excised from the pUC19-EBERs plasmid using SacI and PmlI, excising bases -352 to -125 relative to the EBER1 transcriptional start site (as detailed in Chapter 4).

The common cloning vector pSG5 is a high copy number eukaryotic expression vector and was obtained from Stratagene UK.

The EBNA1 expression plasmid pSG5-EBNA1 (Sample et al. 1992) was obtained from Dr J Sample.

The c-Myc reporter plasmid pX-CMVp-Luc plasmid and its respective control plasmid p-CMVp-Luc (Niller et al. 2003) were obtained from Dr H-H Niller.

The Renilla luciferase reporter plasmid (pRL-TK) was obtained from Promega.

The AP-1 reporter plasmid pAP1-Luc was obtained from BD Biosciences. pTAL-Luc is a commonly used control for studying putative enhancers that are inserted upstream of the luciferase reporter gene and was obtained from Clontech.

The dominant-negative EBNA1 expression vector EBNA1-M1 (Marechal et al. 1999) was obtained from Dr J-C Nicolas.

To generate the c-MycER expression plasmid, a plasmid containing a functionally-inducible c-Myc gene (a fusion between the hormone binding domain of the oestrogen receptor and c-Myc) (Littlewood et al. 1995) was obtained from Dr. C Tselepis. An EcoRI fragment containing the fusion (c-MycER) was ligated into pcDNA3.1/zeo (Invitrogen).

Vectors expressing shRNA directed against c-Myc (pGIPZ 152051) and ATF-2 (pLKO.1 13713) were both obtained from OpenBiosystems, as was the non-silencing pGIPZ shRNA control (RHS4348).

The plasmid backbone for HaloCHIP cloning (pFC14K) was obtained from Promega. For the plasmid map, see Figure 5.11.

The cloning vector pCR8-TOPO was obtained from Invitrogen. pCR8-TOPO contains a topoisomerase cloning site, spectinomycin resistance cassette and sequencing priming sites to allow easy sequencing of PCR-derived inserts. A plasmid map is available online (http://tools.invitrogen.com/content/sfs/vectors/pcr8gwtopo_map.pdf).

2.1.2 Solutions

L-Broth (LB): 10g L-broth base (Gibco) was dissolved in 500ml SDW and was sterilised by autoclaving.

Agar plates: 7.5g Agar was dissolved in 500ml of LB before autoclaving. Agar was melted prior to use and allowed to cool to approximately 50^{o}C before adding any antibiotic. Plates were poured and once set were inverted and stored at 4^{o}C until use.

Ampicillin: 100mg/ml stock was prepared in SDW, sterilised through a 0.45µm filter and stored as 5ml aliquots at -20^{o}C. The working concentration of ampicillin in plates and media was 100µg/ml.

Kanamycin: 100mg/ml stock was prepared in SDW, sterilised through a 0.45µm filter and stored as 2ml aliquots at -20^{o}C. The working concentration of kanamycin in plates and media was 30µg/ml.

2.1.3 Restriction endonuclease digestion

For a typical restriction endonuclease digestion reaction, 5µg of purified DNA was digested in a total volume of 20µl with the appropriate restriction enzymes and buffers (Roche Diagnostics, Germany; New England Biolabs, UK; Promega, UK). Briefly, a reaction

consisted of 2µl of 10x BSA stock (10mg/ml), 2µl of 10x restriction enzyme buffer, 1µl of each restriction enzyme (typically 10 Units) and nuclease-free water up to a final volume of 20µl. The reaction mixture was incubated for 1.5 hours at 37ºC water bath and if required, reactions were stopped by heating the sample at 65°C for 20 minutes. Digested DNA was analysed by agarose gel electrophoresis.

2.1.4 Ligation of DNA insert into vectors

Ligation reactions were carried out using T4 DNA ligase (Promega, UK). Vector and insert DNA were added, typically in a ratio of 1:3 (vector:insert, DNA totalling 0.2µg), to a total volume of 20µl, consisting of 2µl 10x T4 ligase buffer, 1µl T4 ligase and sterile water up to a final volume of 20µl. The reaction was incubated at 16ºC overnight to allow ligation to occur.

2.1.5 Bacterial transformation of competent cells

5µl of ligation reaction (Section 2.1.4) was used to transform 100µl DH5α competent or Top10 F supercompetent cells (Invitrogen, UK) in a 1.5ml microcentrifuge tube. Competent cells, having been stored at -80°C, were thawed on ice before the addition of ligation reaction DNA. Cells were gently mixed with the ligation reaction, avoiding pipetting up and down, incubated on ice for 30 minutes, heat shocked for 60 seconds at 42ºC and then immediately transferred onto ice and incubated for a minimum of 5 minutes. 250µl of LB (Section 2.1.2.) was added to cells before incubation at 37ºC for 1 hour in an orbital incubator. The complete transformed cell mixture was then spread onto LB-agar plates (see Section 2.1.2) with 100µg/ml ampicillin or 30µg/ml kanamycin where required. Plates were inverted and incubated at 37º C overnight before examination of the plates for drug-resistant colonies the following day.

2.1.6 Isolation of DNA from bacterial cultures

2.1.6.1 Mini-preps

Colonies present on bacterial transformation plates were picked with a sterilised pipette tip and incubated in 3ml LB supplemented with the required antibiotic for 16 hours at 37^{o}C in an orbital shaker. To extract plasmid DNA, 1.5ml of the bacterial culture was processed with the Qiagen Mini-prep kit according to the manufacturer's protocol (Qiagen, UK). DNA was stored at 4°C until subsequent screening by restriction digestion.

2.1.6.2 Maxi-preps

To produce abundant amounts of plasmid DNA, 500µl of screened and validated mini-prep culture was incubated at 37^{o}C for 16 hours with 300ml LB supplemented with the required antibiotic. The culture was pelleted before lysis and plasmid DNA was recovered using the Quiagen Maxi-prep kit. The manufacturer's protocol was followed precisely and pelleted, purified plasmid DNA was resuspended in TE buffer (10mM Tris-HCl pH 8, 1mM EDTA). DNA concentration was determined using a NanoDrop 1000 spectrophotometer (Thermo Scientific) and diluted to a stock concentration of 1µg/µl before storage at -20°C.

2.1.7 Preparation of glycerol stocks of plasmid-expressing bacteria

Following maxiprep propagation (described above), aliquots of culture were taken for the preparation of glycerol stocks. These were generated by thoroughly mixing 800µl of liquid culture with 200µl sterile glycerol and stored at -80^{o}C

2.1.8 DNA Sequencing

DNA sequencing was performed for the identification of insert DNA and to check for any possible mutations and rearrangements introduced during PCR amplification or cloning. Sequencing was performed using a well-established protocol. Briefly, for each sample PCR

reactions were set up in duplicate containing 100ng DNA, 2µl Ready Reaction Premix (Applied Biosystems), 2µl Big Dye sequencing buffer (Applied Biosystems) and 3.2pmol (1µl) appropriate primer. These reactions were adjusted to 20µl with nuclease-free PCR grade water. PCR reactions were carried out in a thermocycler with the following conditions:

96°C for 1min

96°C for 10secs
50°C for 5secs } x 25 cycles

60°C for 4mins

4°C HOLD

PCR reactions were subsequently cleaned up in the following manner. 2µl of 125mM EDTA was added to each reaction along with 2µl of 3M sodium acetate and 50µl of 100% ethanol. Tubes were mixed by inverting 5 times before incubation at room temperature for 15 minutes and subsequent centrifugation at 4°C (45 minutes at 2000g) to pellet the PCR product. Supernatant was carefully aspirated and 70µl of 70% ethanol was added to each pellet to wash the DNA before centrifugation at 4°C (1650g for 15 minutes) to pellet the DNA once more. Supernatant was aspirated before pellets were air dried at 37°C for 30 minutes. HiDi formamide buffer (Applied Biosystems) was used to resuspend the dry pellets (10µl per sample) and samples were then stored at 4°C until use.

Samples were loaded into a 96 well plate before the plate was itself loaded into the 3130xl Genetic Analyzer sequencing machine (Applied Biosystems). Samples were run using instrument protocol ‘standard sequence’ and analysis protocol ‘3100POP6_BDTv3kB’. Data were collected and analysed using Chromas Version 1.45 (http://www.technelysium.com.au/chromas14x.html). Where 2 sequences were compared for

homology, following Chromas analysis, the NCBI website sequence alignment tool was utilised (http://www.ncbi.nlm.nih.gov/blast/bl2seq/wblast2.cgi).

2.2 Tissue culture

2.2.1 Tissue culture media

RPMI 1640 liquid (1x) supplemented with 2mM L-Glutamine and adjusted to pH 7.0 was purchased in sterile 500ml bottles from GIBCO (Invitrogen, UK) and stored at 4°C until use.

2.2.2 Tissue culture reagents

Foetal bovine serum (FBS) of South American origin, pre-screened for mycoplasma and viruses, was purchased in sterile 500ml bottles from GIBCO (Invitrogen, UK) and aliquoted into 50ml aliquots before storage at -20°C.

Ciprofloxacin solution was purchased from Bayer. Filter sterilisation was carried out before use at 2.5ml/500ml media.

Geneticin (G418) powder was purchased from Sigma-Aldrich. 5g was dissolved in 100ml sterile distilled water before filter sterilisation and storage in 5ml aliquots at 4°C. Penicillin/streptomycin (pen/strep) solution (10,000 units/ml penicillin-G and 10mg/ml streptomycin) were purchased from Sigma-Aldrich and filter sterilised before use at 2.5ml/500ml media.

Acyclovir powder was purchased from Sigma-Aldrich, and used to supplement culture medium at a concentration of 200μM.

1 x Trypsin solution (containing 2.5g/L trypsin (0.25%) and 0.38g/L EDTA) was purchased in 100ml sterile bottles from GIBCO (Invitrogen, UK). 10ml aliquots were stored at -20°C.

Phosphate buffered saline (PBS) tablets were purchased from Oxoid Ltd. To produce PBS solution (8g/L NaCl, 0.2g/L KCl, 1.15g/L Na_2HPO_4, 0.2g/L KH_2PO_4), 10 tablets were dissolved in 1L of distilled H_2O. Aliquots of 500ml were sterilised by autoclaving for 10 minutes at 115°C.

2.2.3 Cell lines

Ad/AH cells are derived from a nasopharyngeal adenocarcinoma.

AGS cells are a gastric carcinoma derived cell line.

Hone-1 cells are an NPC derived line that were originally EBV-positive but lost the viral genome during culture.

X50-7 is an LCL expressing the full array of EBV latent genes.

Other LCLs used in obtaining copy number/EBER expression data (See Chapter 3) were generated within the University of Birmingham and were kind donations from various members of University of Birmingham staff.

Akata rEBV is a Japanese BL-derived line latently infected with an Akata strain of EBV which has a neomycin resistance cassette to allow selection of stably infected cells (Shimizu et al. 1996). Unlike most EBV-positive BL lines, Akata retains the type I latency pattern.

Akata BL is a sub clone of the EBV-positive line which has lost the virus through limited dilution in culture (Shimizu et al. 1994).

BJAB is an EBV-negative BL-derived line

Ad/AH-rEBV is an Ad/AH cell line stably infected with an Akata strain of EBV which has a neomycin resistance cassette to allow selection of stably infected cells. This line was kindly provided by Dr VHJ Wood (Stewart et al. 2004).

Ad/AH-, AGS- and *Hone-1-EBNA1* and *-neomycin (neo) control* lines were kindly provided by Dr. VHJ Wood, and were generated by transfection of an EBNA1, or neo control, plasmid into the parental lines followed by drug selection and isolation of individual clones (Wood et al. 2007).

Ad/AH-neo and -EBNA1-c-MycER lines were kindly provided by Dr. CW Dawson, and were generated by transfection of the c-MycER plasmid into Ad/AH neo or EBNA1 lines, followed by drug selection and isolation of individual clones.

Ad/AH-Puro and –Puro-EBERs lines were generated by transfection of pUC19-Puro or pUC19-Puro-EBERs plasmids (generation of these plasmids is described in Chapter 4) into Ad/AH parental cells, followed by drug selection with puromycin. Polyclonal populations of cells were generated.

Ad/AH-Puro-EBERs-ΔX lines were generated by transfection of pUC19-Puro-EBERs-ΔX plasmid (generation of these plasmids is described in Chapter 4) into Ad/AH parental cells, followed by drug selection with puromycin. Polyclonal populations of cells were generated.

2.2.4 Culture conditions

All B-cell lines were maintained in RPMI 1640 supplemented with 10% FBS, ciprofloxacin and pen/strep. For experiments where it was necessary to prevent lytic outgrowth of virus, cells were maintained in culture media supplemented with acyclovir for a minimum of 2 weeks prior to harvest. Ad/AH, AGS and Hone-1 lines were maintained in RPMI 1640

supplemented with 5% FBS, ciprofloxacin and pen/strep. To ensure viral genome maintenance, Akata rEBV cells were drug selected at 600μg/ml G418 and Ad/AH-rEBV cells were drug selected at 400μg/ml G418. Maintenance of EBNA1 expression in Ad/AH and AGS lines was achieved by drug selecting at 400μg/ml G418, Hone-1 lines were selected at 200μg/ml G418. c-MycER plasmid maintenance in Ad/AH-neo and -EBNA1 cells was ensured by drug selection at 62.5μg/ml zeocin (Invitrogen, UK).

2.2.5 Maintenance of cell lines

All cell lines were maintained at 37°C in incubators supplied with 5% CO_2.

Adherent cells (Ad/AH, AGS, Hone-1) were grown in 75cm^2 tissue culture flasks purchased from Iwaki. Upon reaching 90-95% confluence, spent media were removed before washing with PBS solution. 4ml of 1X trypsin was added and cells were subsequently incubated at 37°C for 5 to 10 minutes to allow cell detachment from the adherent flask surface. To neutralise the trypsin reaction, 10ml of RPMI 1640 supplemented with 5% FBS was added before centrifugation of cells at 1500rpm for 5 minutes to pellet cells. Cell pellets were resuspended in 10ml of RPMI 1640 supplemented with 5% FBS, and 2ml of cell suspension was taken into a fresh 75cm^2 flask to achieve a 1 in 5 dilution of original cell numbers. 18ml of RPMI 1640 supplemented with 5% FBS was added and drug selection was applied if required.

Non-adherent cells (Akata, LCLs) were grown in 25cm^2 tissue culture flasks purchased from Iwaki. Lines were maintained in 10ml of growth medium, with cells being passaged twice weekly by removal of 8ml cell suspension and replacement with 8ml fresh complete growth medium to achieve a 1 in 5 dilution of original cell numbers. At each passage, drug selection was applied if necessary.

Cell suspensions of both adherent and non-adherent cells were used to perform haemocytometer counts and the required volumes added to the appropriate vessel for experiments.

2.2.6 Cryopreservation

For both adherent and non-adherent lines, cell suspensions were pelleted as described in Section 2.2.5. Pellets were resuspended in 1ml of freezing solution (complete growth medium, FBS and DMSO in a 5:4:1 ratio) and 1ml cell suspensions were added to cryovials (Nunc). Cryovials were transferred to a Mr Frosty (Nalgene) before storage at -80°C to enable gradual freezing. Cryovials were transferred to the gas phase of a liquid nitrogen freezer (-140°C) 24 hours later for long term storage.

Cells cryopreserved in the above manner were revived by rapid thawing at 37°C following which cell suspensions were transferred to a Universal tube (Sterilin, UK) and appropriate complete growth medium was added in a dropwise manner. Suspensions were seeded into tissue culture flasks as described in Section 2.2.5 following a 5 minute incubation at room temperature. If required, drug selection was applied 48 hours post-revival.

2.2.7 Crystal Violet staining

To assess cell viability following drug selection, crystal violet staining was used. Cells were plated into 6 well plates and grown to 80% confluence before drug selection for an appropriate amount of time (typically between 24 and 72 hours). Subsequently, cells were washed with 1x PBS, before fixing with 4% paraformaldehyde (PFA) at room temperature for 5 minutes. Following fixation, cells were washed three times with PBS before addition of 0.05% crystal violet solution. Cells were stained for 30 minutes before several washes with

distilled water to remove excess crystal violet solution, and subsequent inversion and drying. At this point, cells were examined by microscopy and photographed.

2.3 Immunofluorescence (IF) staining

Adherent cells were trypsinised and counted as described in Section 2.2.5. Cells ($1x10^4$) were seeded onto sterile Teflon coated slides (Henley) and left to adhere for 48 to 72 hours in 150mm culture dishes. Desiccation was prevented by the addition of PBS solution to the culture dishes. Once adherent, cells were washed with PBS before fixation in 4% PFA pH 7.4 for 10 minutes. Following fixation, cells were again washed in PBS and permeabilised in 0.5% Triton X-100 for 5 minutes. After a further PBS wash, cells were treated with 50µl of 20% heat inactivated goat serum (HINGS) diluted in PBS in a humidified chamber for a minimum of 1 hour in order to prevent non-specific antibodybinding. Primary antibodies diluted in 20% HINGS to a working concentration (see Table 2.1) were then applied to cells and incubated overnight at 4°C. Slides were washed 3 times in PBS with gentle agitation before the area around the wells was dried using filter paper (Whatman, UK). Alexa Fluor secondary antibody (Molecular Probes), of corresponding species to the primary antibody, conjugated to a 594nm (red) fluorochrome was diluted 1 in 1000 in 20% HINGS and applied to slides at room temperature for an hour in the dark. Slides were washed 3 times more in PBS before mounting using DABCO pH 8.6 (90ml glycerol, 10ml PBS, 2.5g DABCO ((1,4-diazabicyclo[2.2.2]octane) powder, Sigma-Aldrich). Cells were stored in the dark at -20°C for a minimum of 24 hours to reduce background staining prior to visualisation by fluorescence microscopy. To control for background staining, cells were stained with secondary antibody alone, with the primary antibody incubation step being replaced with extended blocking with 20% HINGS.

2.4 Immunoblotting

2.4.1 Sample preparation

Once ready for harvest, cells were washed once in PBS and lysed in 100-500µl RIPA buffer (25 mM Tris-HCl pH 7.6, 150 mM NaCl, 1% NP-40, 1% sodium deoxycholate, 0.1% SDS) depending on the size of the tissue culture vessel and the confluence of cells. Collection of cell lysates was achieved using cell scrapers (Sarstedt, Germany) and samples were transferred to pre-chilled 1.5ml microcentrifuge tubes on ice before sonication of samples to ensure disruption of cellular components and full cell lysis. Concentration of protein in samples was determined using a commercial protein assay kit (Biorad 500-0112). Briefly, 5µl of Bovine Serum Albumin (BSA) protein standards prepared in sterile distilled water (SDW) (0, 0.1, 0.2, 0.5, 1 and 2µg/µl) and 5µl sample diluted 1 in 5 using sterile H_2O were aliquoted, in triplicate, into a 96 well microtitre plate. 25µl of reagent A followed by 200µl of reagent B were added to each well and incubated for 2min at room temperature with gentle shaking. The absorbance of the samples was then read on a BioTek automated microtitre plate reader at 620nm. The values obtained were used to construct a standard curve for the BSA standards from which the sample protein concentrations were determined. Depending on the abundance of the protein being examined, and the quality of specific primary antibody, 30-100µg of protein lysate was used for immunoblotting. Samples were prepared for loading by diluting 1:3 in Laemmli loading buffer (250mM Tris-HCl pH 6.8, 8% w/v SDS, 40% glycerol, 0.05% w/v bromophenol blue, 10% β-mercaptoethanol). Diluted samples were heated to 95°C for 5 mins to denature samples before being chilled immediately on ice. Cooled samples were centrifuged briefly to pellet cell debris before loading on to SDS-polyacrylamide gels.

2.4.2 SDS-polyacrylamide gel electrophoresis (SDS-PAGE)

SDS-PAGE was performed using the Mini-PROTEAN 3 electrophoresis kit (Bio-Rad, UK). To achieve optimum fractionation, gels were cast containing a percentage of acrylamide best suited to the molecular weight of the protein subject to analysis. Typical gels contained a mixture of an appropriate percentage (v/v) of acrylamide stock solution (30% w/v acrylamide and 0.8% v/v bis-acrylamide) (Bio-Rad, UK), 25% v/v resolving buffer (1.5M Tris-HCl pH 8.8, 0.4% w/v SDS and 0.24% v/v TEMED) and distilled H_2O which was added last to adjust the mixture to the required volume. Polymerisation was catalysed by the addition of 20% ammonium persulphate (APS) to a final concentration of 0.1%, prior to filling of the gel cassettes. Surface air bubbles were removed by overlaying the solution with 100% ethanol, which was subsequently rinsed away with SDW before blotting paper was used to absorb any excess moisture. Once the resolving gel was fully polymerised, a stacking gel consisting of 4% acrylamide and 50% v/v stacking buffer (0.75M Tris-HCl pH 6.8, 0.2% w/v SDS and 0.12% v/v TEMED) adjusted to the required volume using distilled H_2O was prepared. 20% APS was added to a final concentration of 0.15% to catalyse polymerisation before gel combs were carefully inserted. Once the gel was fully set, gel combs were removed and the gels were placed into an electrophoresis tank and submerged in running buffer (30g Tris, 144g glycine and 10g SDS in 10L distilled H_2O). Protein samples were loaded alongside molecular weight rainbow marker (Amersham) and electrophoresis was carried out at 130V until the dye front had reached the bottom of the gel.

2.4.3 Protein transfer and immunoblotting

Once resolved by electrophoresis, proteins were transfered to a nitrocellulose membrane using the Mini Trans-blot wet transfer system (Bio-Rad, UK). The gel and transfer membrane were placed between two sponges and filter papers, soaked in transfer buffer (30g Tris, 144g

glycine, 2L methanol and 8L distilled H_2O) and pressed to remove any air bubbles. This sandwich was then placed into a transfer kit filled with transfer buffer before transfers were conducted at 90V on ice for 90 minutes.

Following complete transfer of proteins, membranes were soaked in either 5% BSA in Tris-buffered saline (TBS)-Tween (20mM Tris-HCl, pH7.4, 500mM NaCl, 0.05% Tween-20) or 5% skimmed milk in TBS-Tween depending on the nature of the primary antibody to be used. 5% BSA was used to block non-specific interactions for all phospho-specific antibodies, with 5% skimmed milk being used for all total protein-specific antibodies. Blocking was performed with agitation overnight at 4°C or for an hour at room temperature. Following this blocking step, membranes were transferred to the relevant blocking buffer containing the appropriate concentration (Table 2.1) of primary antibody and incubated with agitation overnight at 4°C. Blots were then washed three times in TBS-Tween at room temperature with agitation before incubation with the relevant HRP-conjugated secondary antibody (Table 2.1) in 5% skimimed milk blocking buffer at room temperature with agitation for an hour. Blots were washed as before then incubated with ECL reagents (1:1 ratio of reagents 1 and 2) which allow detection of protein-antibody conjugated complexes (Amersham). Visualisation of these complexes was achieved by wrapping blots in Saran Wrap, and exposing to X-ray film (Amersham). The X-ray film was developed using an automated film processor (X-Ograph Ltd).

Table 2.1 Antibodies used for immunoblotting (WB) and immunofluorescence (IF)

Protein	**Primary antibody**	**Species**	**Applic-ation**	**Dilution**	**Secondary antibody & dilution**
β Actin	β actin Sigma-Aldrich (A5441)	Mouse	WB	1:20000	1:1000 Anti-Mouse HRP
Total Akt	Akt Cell Signaling Technology (9272)	Rabbit	WB	1:500	1:1000 Anti-Rabbit HRP
Total ATF-2	ATF-2 Santa Cruz Biotechnology (sc-242)	Mouse	WB, IF	1:1000 for WB, 1:250 for IF	1:1000 Anti-Mouse HRP for WB, 1:1000 Anti-Mouse 594 for IF
pATF-2 (Thr 69/71)	Phospho-ATF-2 (Thr69/71) Cell Signaling Technology (9225)	Rabbit	WB, IF	1:1000 for WB, 1:250 for IF	1:1000 Anti-Rabbit HRP for WB, 1:1000 Anti-Rabbit 594 for IF
c-Jun	c-Jun Cell Signaling Technology (19162)	Rabbit	WB	1:1000	1:1000 Anti-Rabbit HRP
c-Myc	c-Myc Santa Cruz Biotechnology (sc-40)	Mouse	WB	1:750	1:1000 Anti-Mouse HRP
pATF2 (Thr71)	Phospho-ATF-2 (Thr71) Cell Signaling Technology (9221)	Rabbit	WB	1:1000	1:1000 Anti-Rabbit HRP
EBNA1	A.M. (Young et al. 1988)	Human serum	WB	1:200	1:8000 Protein A HRP
EBNA1	R4 (gift from Dr Lori Frappier)	Rabbit	IF	1:1000	1:1000 Anti-Rabbit 594
Total ERK	P44/42 MAPK Cell Signaling Technology (9102)	Rabbit	WB	1:1000	1:1000 Anti-Rabbit HRP
pERK	Phospho-p44/42 MAPK Cell Signaling Technology (9101)	Rabbit	WB	1:500	1:1000 Anti-Rabbit HRP
Total GSK3β	GSK-3β Santa Cruz Biotechnology (sc-81462)	Mouse	WB	1:1000	1:1000 Anti-Mouse HRP
pGSK3β	Phospho-GSK-3β (Ser9) Cell Signaling Technology (9336)	Rabbit	WB	1:500	1:1000 Anti-Rabbit HRP
HaloTag	Anti-HaloTag® pAb Promega (G9281)	Rabbit	WB	1:1000	1:1000 Anti-Rabbit HRP
Sp1	Sp1 Santa Cruz Biotechnology (sc-59)	Rabbit	WB	1:500	1:1000 Anti-Rabbit HRP

Table 2.1 ctd Antibodies used for immunoblotting (WB) and immunofluorescence (IF)

Protein	Primary antibody	Species	Applic-ation	Dilution	Secondary antibody & dilution
TFIIIC 110	4286 (Felton Edkins et al. 2006)	Rabbit serum	WB	1:1000	1:1000 Anti-Rabbit HRP
TFIIIC 102	3238 (Felton Edkins et al. 2006)	Rabbit serum	WB	1:1000	1:1000 Anti-Rabbit HRP
TFIIIC 90	1898-64 (Felton Edkins et al. 2006)	Rabbit serum	WB	1:1000	1:1000 Anti-Rabbit HRP
Tubulin	Santa Cruz Biotechnology (sc-8035)	Rabbit	WB	1:500	1:1000 Anti-Rabbit HRP
USP7	USP7 Bethyl Labs (BL-851)	Rabbit	WB	1:1000	1:1000 Anti-Rabbit HRP

2.5 Electromobility shift assays (EMSA)

2.5.1 Nuclear and cytosolic protein extracts

Epithelial cells were grown in 10cm^2 dishes and harvested once cells were 80-90% confluent. Nuclear and cytosolic protein extractions were then conducted using the NE-PER Nuclear and Cytoplasmic Extraction kit (Pierce) following the manufacturer's instructions. Briefly, cells were harvested from 10cm^2 dishes by addition of 100µl ice-cold CERI (Cytosolic Extraction Reagent I) and scraping into pre-chilled microcentrifuge tubes, stored on ice. To each sample, 5.5µl CERII was added before mixing by vortex and storing on ice. To pellet the nuclear fraction, samples were centrifuged at 16,000g for 5 minutes, and the supernatant consisting of the cytosolic fraction was transferred to a fresh microcentrifuge tube and stored at -80°C until use. The pellet containing cell nuclei was resuspended in 50µl of NER reagent and this suspension was stored on ice for 40 minutes. Within this 40 minute incubation, samples were vortexed every 10 minutes (at highest setting for 15 seconds) to break nuclei open. Subsequent centrifugation of samples (16,000g for 10 minutes) pelleted nuclear membrane fragments with the nuclear protein fraction (supernatant) being removed and placed in a fresh

microcentrifuge tube and stored at -80°C until use. Protein concentrations were determined as previously described (Section 2.4.1).

2.5.2 Casting of native polyacrylamide gels

Preparation of native polyacrylamide gels (native-PAGE) used 13.3ml of 30% w/v acrylamide (Bio-Rad), 44ml of 1x TBE (10.8g Tris, 4.5g boric acid 0.74g EDTA in 1L distilled H_2O), 22.7ml of distilled H_2O and 45µl of TEMED. Polymerisation was initiated by addition of 450µl of 20% APS before addition of the gel mixture to novex cassettes (Invitrogen, UK) and careful insertion of a gel comb. Once cast, gels were wrapped in 1X TBE soaked paper towels and Saran Wrap and stored at 4°C until use.

2.5.3 Preparation of EMSA probes

Oligonucleotides end-labelled with an IRDye-700 (MWG-Biotech) infrared dye were diluted to 100pmol/µl with PCR grade H_2O. 5µl of the sense and anti-sense oligonucleotides for each probe set were mixed with 90µl of restriction buffer B (Roche). Probes were annealed by incubation for 10 minutes in a hot-block at 95ºC before the hot-block was turned off, with samples being allowed to cool to room temperature in the hot-block overnight. Subsequently, annealed probes were removed from the heating block and placed in the dark at -20ºC. Oligonucleotide sequences are provided in Table 2.2.

Table 2.2 Oligonucleotides used for EMSA.

Probe	**Oligonucleotide sequence**
c-Myc X-Box wild type	Sense 5'- CGACCGCGCCACCAGATGGCACACGTGGGGGAAAT -3' Antisense 3' - GCTGGCGCGGTGGTCTACCGTGTGCACCCCCTTTA -5'
c-Myc X-Box MUTANT	Sense 5' - CGACCGCGCCACCAGAGAGCACACGGAGGGGAAAT- 3' Antisense 3' - GCTGGCGCGGTGGTCTCTCGTGTGCCTCCCCTTTA - 5'

2.5.4 EMSA binding reactions and visualisation

The following binding reaction master mix was prepared for n+2 samples: 2µl 10x binding buffer, 2µl 25mM DTT containing 2.5% Tween, 1µl polyI.dC (1µg/µl), 1µl annealed EMSA probe. 6µl of master mix was added per sample together with 5µg of nuclear extract before total volume adjustment to 20µl with PCR grade H_2O. Samples were gently mixed and incubated in the dark for 20 minutes to allow protein-DNA complexes to form before addition of 2µl DNA loading buffer (0.025g bromophenol blue, 0.025g Xylene Cyanol FF and 6ml glycerol made up to 20ml with H_2O) to each sample. After gentle mixing, samples were loaded onto pre-cast native-PAGE gels which had been subject to electrophoresis for 30 minutes at 70V in 0.5X TBE prior to loading in order to remove gel contaminants. Gel electrophoresis was subsequently conducted in the dark at 70V for 1-2 hours depending on dye front progression before detection of protein-DNA complexes using the Odyssey Infrared imaging system (Li-Cor biosciences). The IR scanner was set to 700nm to detect IRDye-700 labelled probes, and offset focus was set to 2.5mm to account for gel and plate thickness.

2.6 Nucleic acid transfection of mammalian cells

Liposome transfection of eukaryotic cells was conducted using lipofectamine reagent (Invitrogen, UK). TurboFect reagent (Fermentas) was also used to tranfect cells in some instances. TurboFect *in vitro* transfection reagent is a sterile solution of a proprietary cationic polymer in water. The polymer forms compact, stable, positively charged complexes with DNA. These complexes protect DNA from degradation and facilitate gene delivery into eukaryotic cells. Both methods of transfection frequently resulted in a transfection efficiency of between 50% and 80% in epithelial cells.

Examples of transfection volumes given below were scaled up or down based on guidelines provided by reagent manufacturers depending on the size of tissue culture vessel used.

2.6.1 Lipofectamine reagent transfection of epithelial cells

The efficiency of transfection using lipofectamine reagent was enhanced by the addition of plus reagent (Invitrogen, UK). This additional reagent allows DNA to pre-complex before the addition of the lipofectamine reagent. Briefly, for 6-well plates, cells were seeded at a density of 2-3x10^5 and allowed to adhere for 48 hours. As such, on the day of transfection, cells were approximately 70-90% confluent. Amounts of DNA transfected varied as was required experimentally, but typically, 1µg DNA was diluted in 100µl serum-free and antibiotic-free Opti-MEM (Invitrogen, UK) before the addition of 6µl plus reagent. DNA complexes were allowed to form by incubation at room temperature for 15 minutes. Meanwhile, 4µl lipofectamine was diluted in 800µl serum-free and antibiotic-free Opti-MEM. Following DNA complex formation, the diluted lipofectamine reagent was added, and a 15 minute incubation at room temperature allowed liposome formation. Cells to be transfected were washed once in serum-free and antibiotic-free Opti-MEM before the addition of the 900µl transfection mix. The mix was applied dropwise and plates were gently swirled to ensure even distribution of complexes before transfer to a 37°C incubator for 3 hours. Subsequently, wells were topped up with antibiotic-free Opti-MEM, supplemented with 10% FBS (2ml per well). Cells were fed 24 hours post transfection with appropriate complete growth medium and subsequently harvested at necessary time points.

2.6.2 TurboFect reagent transfection of epithelial cells

The transfection protocol for TurboFect reagent resembled the method used for liposome transfection, however incubation steps varied slightly to allow effective transfection of DNA.

Briefly, for 6-well plates, cells were seeded at a density of 2-3x10^5 and allowed to adhere for 48 hours. As such, on the day of transfection, cells were approximately 70-90% confluent. Amounts of DNA transfected varied as was required experimentally, but typically, 2µg DNA was diluted in 400µl serum-free and antibiotic-free Opti-MEM before the addition of 6µl TurboFect reagent. Transfection mixtures were left for 20 minutes to allow the TurboFect polymer to form compact, stable, positively charged complexes with DNA. During this 20 minute incubation, cells were washed once with serum-free and antibiotic-free Opti-MEM before 600µl of serum-free and antibiotic-free Opti-MEM was added to each well. Following complex formation, the transfection mix was added to the 600µl Opti-MEM in each well. The mix was applied dropwise and plates were gently swirled to ensure even distribution of complexes before transfer to a 37°C incubator for 3 hours. Subsequently, wells were topped up with antibiotic-free Opti-MEM, supplemented with 10% FBS (2ml per well). Cells were fed 24 hours post transfection with appropriate complete growth medium and subsequently harvested at necessary time points.

2.7 Luciferase reporter assays

The Dual-Luciferase Reporter Assay System (Promega, UK) was used to conduct reporter assays. This system allows the activities of both firefly (*Photinus pyralis*) and Renilla (*Renilla reniformis*) luciferases to be measured from the same sample since the luciferases possess different emission wavelengths. Renilla activity was used to provide an internal control for cell viability and transfection efficiency, whereas firefly luciferase was measured to assess the activity of the experimental factor of interest.

Transfection of cells was conducted using the lipofectamine protocol described in Section 2.6.1. Cells were co-transfected with 0.5µg of firefly reporter plasmid DNA (test promoter or empty vector to account for background luminescence) and 0.5µg of Renilla plasmid DNA. Harvest of cells typically occurred 48 hours post transfection. Cells were lysed in 500µl passive lysis buffer (Promega, UK), with complete lysis and homogenisation of samples being achieved through vigorous pipetting. 20µl of each homogenised sample was loaded in triplicate into a 96 well plate. To determine luciferase activity, 50µl LARII (Promega, UK) was added to each sample and the firefly luciferase activity was immediately measured using a Victor plate reader (Wallac, USA). Quenching of firefly activity and stimulation of Renilla activity was achieved by addition of 50µl Stop and Glo reagent (Promega, UK) to each sample. Renilla activity was immediately measured following this addition using a Victor plate reader.

Firefly luciferase activity was normalised against Renilla luciferase activity for each sample and luciferase activity from an appropriate firefly control plasmid was deducted to account for background luminescence. Reporter plasmids and their control vectors are listed in Table 2.3.

Table 2.3 Luciferase reporter and control constructs.

	Test plasmid	**Control plasmid**
Renilla luciferase	p-RL-TK	N/A
c-Myc reporter	pX-CMVp-Luc	p-CMVp-Luc
AP-1 reporter	pAP1-Luc	pTAL-LUC

2.8 RNA extractions

RNA extractions were conducted using the EZ-RNA isolation kit (Geneflow, UK). Guidelines given by the manufacturer were followed accurately to extract RNA and the following given volumes were scaled up or down depending on the volume of the tissue culture vessel used in each experiment. Cells were grown to a confluence of 70-90% before harvesting. For a $10cm^2$ dish, cells were harvested by lysis in 500µl of denaturing solution. Cells were scraped and collected into 1.5ml microcentrifuge tubes and incubated at room temperature for 5 minutes to ensure cell lysis. Subsequently, an equal volume of denaturing solution (500µl) was added and the sample mixed by vigorous vortexing for 15 seconds. Samples were left at room temperature for 10 minutes before centrifugation at 4°C (12,000rpm for 15 minutes) to separate the aqueous phase from the organic phase and interphase. The aqueous phase was then removed into a clean microcentrifuge tube and 500µl isopropanol was added to precipitate RNA. Precipitation occurred at -20°C overnight. Precipitated RNA was pelleted by centrifugation at 4°C (12,000rpm for 10 minutes) before the pellet was washed in 75% ethanol. RNA was repelleted by brief centrifugation and the ethanol carefully aspirated. The pellet was air dried before resuspension in PCR grade nuclease-free water. RNA concentration was determined using a NanoDrop 1000 spectrophotometer (Thermo Scientific) and samples diluted to 0.5µg/µl before storage at -80°C until used.

2.9 DNA extractions

Total DNA was extracted from cultured cells using the DNeasy spin column kit (Qiagen). Manufacturer's instructions were followed precisely following pelleting of cells by centrifugation and resuspension in PBS and proteinase K-mediated lysis (addition of 20 µl of

600 mAU/ml proteinase K solution). DNA concentrations were measured using a NanoDrop 1000 spectrophotometer.

2.10 Dual RNA and DNA extractions

In some instances, it was necessary simultaneously to extract both RNA and DNA from the same samples. In these cases, the Allprep DNA/RNA mini kit (Qiagen) was used according to the manufacturer's instructions.

2.11 Reverse Transcription Polymerase Chain Reaction (RT-PCR)

2.11.1 cDNA synthesis

cDNA was generated from RNA using Superscript III reverse transcriptase (Invitrogen, UK). Superscript III is derived from moloney murine leukaemia virus. For each reaction, 1µg RNA was added to a 0.2ml PCR tube along with 0.4µg random primers (Promega, UK) and 1µl of 10mM dNTP mix (Invitrogen, UK) and the volume adjusted to 13µl with PCR grade H_2O. The mixture was heated to 65°C for 5 minutes to denature the dsRNA then cooled on ice. Once cool, 4µl of 5x first strand buffer, 1µl of 0.1M DTT, 1µl of 40 units/µl RNaseOUT (Invitrogen, UK) and 1µl of 200 units/µl Superscript III was added to the tube and mixed by pipetting. cDNA synthesis was performed in a thermal cycler under the following conditions:

25°C for 5 minutes

50°C for 1 hour

70°C for 15 minutes

The cDNA mix was then diluted 1 in 5 (by addition of 80µl PCR grade H_2O) and stored at 4°C (for short term storage) or -20°C (for long term storage).

2.11.2 RT-PCR

For each RT-PCR reaction, the following components were assembled for each sample in a PCR tube: 5µl (50ng) diluted cDNA, 1µl 100pmol forward primer, 1µl 100pmol reverse primer, 25µl 2x GoTaq Green Master Mix (Promega, UK) and 18µl PCR H_2O. The GoTaq master mix contains Taq polymerase, PCR buffer, 400µM dNTP mix, 3mM $MgCl_2$ and DNA loading dye. PCR conditions consisted of an initial denaturation step (typically 5 minutes at 95°C), followed by a varying number of cycles of the following steps:

Denaturation – typically 30 to 60 seconds at 95°C

Annealing – 30 to 60 seconds at specific annealing temperature (see Table 2.4)

Extension – typically 30 to 60 seconds at 72°C

Samples were also subjected to a final extension period of 5 to 10 minutes at 72°C before being held at 4°C prior to agarose gel electrophoresis (Section 2.11.3).

Primers for RT-PCR were synthesised by Sigma-Aldrich and are presented in Table 2.4 along with specific annealing temperatures used for each primer set and the product size expected.

Table 2.4 PCR primers and accompanying annealing conditions and product sizes.

Gene	**Primer oligonucleotides 5' – 3'**	**Annealing temp (°C)**	**Product size (bp)**
ATF-2	Forward: CACACAACTCCACAGACCCAAA Reverse: GGAGCCATAACGATCTGTGAAA	55	494
Brf1	Forward: AATTCTGTGAGCCTCTTCCGTAGTG Reverse: AGACCCATGCTTGTACATTCCACG	60	95
c-Myc	Forward: AACCAGAGTTTCATCTGCGACCCG Reverse: TTGTGCTGATGTGTGGAGACGTGG	53	590

Table 2.4 ctd PCR primers and accompanying annealing conditions and product sizes

* denotes sequential annealing temperatures, ** From Felton Edkins et al. 2006.

Gene	**Primer oligonucleotides 5' – 3'**	**Annealing temperature (°C)**	**Product size (bp)**
EBER1	Forward: AGGACCTACGCTGCCCTAGA Reverse: AAAACATGCGGACCACCAGC	55	166
GAPDH	Forward: GCCTCCTGCACCACCAACTG Reverse: CGACGCCTGCTTCACCACCTTCT	52	250
TBP**	Forward: GCCAGAGTTATTTCCTGGTTT Reverse: CCCAGATAGCAGCACGGTAT	52	410
Bdp1**	Forward: GCTGATAGAGATACTCCTC Reverse: CCAGAGACAAGAATCTTCTC	60	293
TFIIIC 220**	Forward: TCCAGCGAGACCGTCACACC Reverse: GGATTGAGTGTTGCTGGGCT	62	144
TFIIIC 110**	Forward: CCAGAAGGGGTCTCAAAGTCC Reverse: CTTTCTTCAGAGATGTCAAAGG	62	303
TFIIIC 102**	Forward: GCAGAAGTAACATCATTGGC Reverse: CCTACTAATGTCCGTTATCTGTGG	61, 58, 50*	184
TFIIIC 90**	Forward: AAACAGAAGTTGCTGAGTGC Reverse: ATGGTCAGGCGATTGTCC	55, 62*	210
TFIIIC 63**	Forward: ATGGCTTGAAGTCCTCCTCCTCC Reverse: CCGAGATGTTCTACCAGTTATGCG	69, 62, 50*	300
5S RNA**	Forward: TTTACGGCCACACCACCCTG Reverse: AAAGCCTTCAGCACCCTGTA	58	107

Table 2.4 ctd PCR primers and accompanying annealing conditions and product sizes.

Gene	Primer oligonucleotides 5' – 3'	Annealing temperature (°C)	Product size (bp)
7SL** RNA	Forward: GTGTCCGCACTAAGTTCGGCATCAATATGG Reverse: TATTCACAGGCGCGATCCCACTACTGATC	70	150
$tRNA^{tyr}$**	Forward: CCTTCGATAGCTCAGCTGGTAGAGCGGAGG Reverse: CGGAATTGAACCAGCGACCTAAGGATGTCC	65	84

In some instances where increased assay sensitivity was required, semi-quantitative RT-PCR followed by Southern blotting was conducted. Semi-quantitative RT-PCR involved incrementally increasing the number of PCR cycles conducted, with samples taken at each cycle increment for analysis by gel electrophoresis of optimal cycle number. This analysis ensured samples used were in the linear range, with cycle numbers being selected where sufficient application had occurred, but saturation had not been reached. This ensured any differences in samples were observed, and were maximal. Where optimal conditions were attained, the gels from electrophoresis were prepared for Southern blotting. The procedures involved are outlined in Section 2.13.

2.11.3 Agarose gel electrophoresis

Fractionation, resolution and visualisation of PCR products were conducted on 1-2% w/v agarose gels, dependent on size of PCR product. Agarose powder was weighed and dissolved in the appropriate volume of 1x TBE by boiling in a glass conical flask. The solution was cooled to around 50°C before ethidium bromide was added to a final concentration of 0.5µg/µl. The solution was subsequently poured into a sealed gel casting tray and a gel comb inserted. Once set, the gel was placed into a horizontal gel electrophoresis tank (Eurogentec, USA) and the gel comb removed. The tank was filled with 1x TBE and 20-40µl of PCR

product was loaded into each well alongside an appropriate DNA size marker ladder (Geneflow, UK). Gel electrophoresis was typically performed at 130V for 1hr prior to visualisation of ethidium bromide stained bands using a UV transilluminator.

2.11.5 RT-qPCR for cellular genes

RT-qPCR for cellular genes was performed using ready synthesised Taqman primer and probe (FAM labelled) mixes purchased from Applied Biosystems (see Table 2.5). Each multiplexed RT-qPCR reaction consisted of 5µl (50ng) of cDNA, 1µl of ABI test primers and probe mix, 0.5µl of huGAPDH primer and probe (VIC labelled) mix, 10µl of 2x sensimix (Quantace) and DEPC water to 20µl. Reactions were performed in technical triplicate and analysed on an ABI 7500 Fast Real-time PCR machine. Cycle threshold (Ct) values were obtained by determining the point at which amplification occurred above background in the linear range of amplification for each reaction. The test primer data were then normalised against the multiplexed GAPDH data to obtain the dCt values and the average determined for each triplicate to obtain the mean dCt. ddCt values were calculated by subtracting the control dCt value from the "test" dCt, before fold changes from control to test samples were calculated using the formula 2^{-ddCt}.

Table 2.5 Applied Biosystems primer and probe master mixes.

Gene	ABI QPCR Primer/Probe Reference Number
TFIIIC220	Hs01121460_m1
TFIIIC110	Hs01086775_m1
TFIIIC102	Hs01066489_m1
TFIIIC90	Hs01034271_m1
TFIIIC63	Hs01030747_m1
BDP1	Hs00372575_m1

BRF1	Hs00377388_m1
TBP	Hs00920494_m1

2.12 Southern Blot analysis of EBV genome copy number

LCLs were maintained as described in Section 2.2.5, and DNA was extracted using phenol/chloroform before ethanol precipitation.

2.12.1 Southern Blotting Solutions

Denaturing solution: 1.5M NaCl, 0.5M NaOH

Neutralisation solution: 1.5M NaCl, 0.5M Tris-HCl pH7.2, 0.001M EDTA

20 X SSC: 3M NaCl, 0.3M Sodium Citrate

Prehybridisation solution: (For 100ml) – 70ml ddH_2O, 30ml 20 X SSC, 0.5g Milk powder.

2.12.2 Sample preparation

For each LCL, 10µg of isolated DNA was digested with BamHI restriction endonuclease. Digested samples were run on 0.8% agarose gels (containing ethidium bromide) before UV visualisation of DNA to ensure DNA had migrated an adequate distance, and to assess equal loading of samples.

Following visualisation, agarose gels were prepared for capillary transfer of DNA to N+ Hybond membrane (Amersham, UK) by soaking in denaturing solution for 30 minutes at room temperature with agitation. Denaturing solution was then replaced with neutralising solution and gels were incubated at room temperature with agitation for another 30 minutes. Following neutralisation a blotting platform was prepared as illustrated in Figure 2.1. Transfer was allowed to take place overnight before disassembly of the blotting apparatus. The nylon membrane was subsequently placed onto a sheet of 3mm paper soaked in 0.4M NaOH for 20

minutes to immobilise the transferred DNA onto the membrane, before storage in Saran Wrap at 4°C until use.

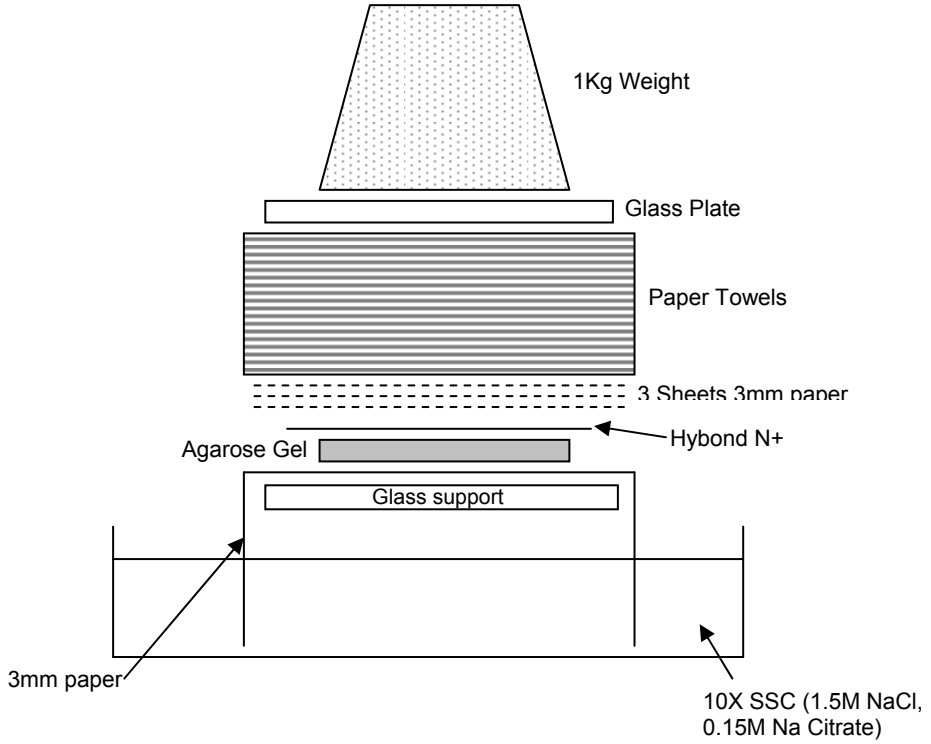

Figure 2.1

2.12.3 Probe preparation

To produce an EBV genomic DNA Southern blot probe, pBamHI-X plasmid DNA was digested with BamHI. This allowed gel isolation of the BamHI-X fragment of the plasmid which was subsequently used to generate radioactive probes. This was achieved using a Random Primed DNA Labelling Kit (Roche Applied Science), closely adhering to the manufacturer's instructions. Briefly, 25ng linear template DNA (BamHI-X) was denatured by heating to 95°C for 10 minutes before being placed on ice. Subsequently dNTP mixture was added (containing dATP, TTP and dGTP) along with reaction buffer, Klenow enzyme and 50 µCi [α-^{32}P]dCTP (Redivue aqueous solution, Amersham Biosciences, UK). The reaction was mixed and incubated at 37°C for at least 30 minutes to allow labelling of DNA.

Unincorporated radiolabelled nucleotides were removed using Sephadex G-50 DNA Grade NICK columns (GE Healthcare), according to the manufacturer's instructions.

2.12.4 Probe hybridisation, washing and visualisation

Membranes with immobilised DNA were incubated in prehybridisation solution (prehyb) in a hybridisation oven set to 68°C for 2-3 hours prior to addition of labelled probe. Immediately prior to addition to membranes, labelled probes were denatured for 2 minutes at 98°C. Denatured probes were then added to hybridisation tubes containing prehyb and membrane(s), and incubated overnight at 68°C to allow hybridisation of labelled probe to DNA. Following incubation, membranes were washed, again in a hybridisation oven at 68°C. The washes were carried out sequentially as follows:

2 X 30 minute washes in 2 X SSC, 0.1% SDS

2 X 30 minute washes in 0.2 X SSC, 0.1% SDS

Final rinse in 1 X SSC (removes SDS which may interfere with visualisation)

Following post-hybridisation washes, membranes were removed from hybridisation tubes and wrapped using Saran wrap before being placed in autoradiography cassettes. For visualisation and quantification, either autoradiography film was placed in the cassette with the membranes (for 24-48 hours, stored at -80°C) before developing and densitometry (Section 2.18).

2.13 Southern blotting following semi-quantitative RT-PCR

Agarose gels from electrophoresis of RT-PCR products were prepared for capillary transfer of DNA to N+ Hybond membrane (Amersham, UK) as previously described (Section 2.12.1). Preparation of probes for specific RT-PCR products was carried out by performing RT-PCR with the same primer sets used experimentally, using Ad/AH genomic DNA as a template.

Following gel electrophoresis, bands were gel isolated for use as Southern blotting probes, and prepared using a Random Primed DNA Labelling Kit (Roche Applied Science) as previously described (Section 2.12.3).

2.14 Quantitative PCR (qPCR) for EBV genome load

qPCR for EBV genome load was carried out using EBV-POL specific primer probe sets (Gallagher et al. 1999; Junying et al. 2003). To allow precise quantification of average EBV genome copies in each cell line, a calibration curve was prepared and results were analysed on the basis of this standard curve. DNA was extracted (Qiagen Allprep DNA/RNA minikit) from LCLs which had been maintained as described in Section 2.2.5.

2.14.1 DNA standards

Namalwa BL (which contains two integrated EBV genome copies per cell (Lawrence et al. 1988)) was used as a standard to prepare a calibration curve. DNA was isolated as described (Section 2.9), and the concentration determined. An aliquot of DNA was subsequently adjusted to give a final concentration of 132ng/µl, corresponding to 40,000 EBV copies per µl, based on the assumption that: (a) each cell contains 6.6pg DNA and (b) each Namalwa cell contains 2 viral genomes. From the 40,000 EBV genome stock, serial dilutions were prepared and stored at 4°C until use. Stock DNA was aliquoted and stored at -20°C.

2.14.2 PCR reaction

qPCR for EBV genome load was carried out using primer/probe sets (given in Table 2.6) for the EBV POL (BALF5) gene, and the human β-2 microglobulin gene which served as an endogenous cellular control.

PCR reactions were set up using the following components per 25µl reaction:

12.5µl Taqman Universal 2X Master Mix

2.5µl EBV POL forward primer (2µM stock)

2.5µl EBV POL reverse primer (2µM stock)

1µl EBV POL FAM-labelled probe (5µM stock)

0.5µl β-2M forward primer (3µM stock)

0.5µl β-2M reverse primer (4µM stock)

0.5µl β-2M VIC-labelled probe (5µM stock)

5µl DNA template (DNA concentration 1ng-100ng/µl)

25µl reactions were loaded into 96-well plates and analysed using ABI 7500 Fast Real-time PCR machine.

Table 2.6 qPCR primer/probe sets used in analysis of EBV copy number

Gene	**Forward Primer (5'-3')**	**Reverse Primer (5'-3')**	**Probe (5'-3')**
EBV POL (BALF5)	CTTTGGCGCGGATCCTC	AGTCCTTCTTGGCTAGTCTGTTGAC	CATCAAGAAGCTGCTGGCGGCC
β-2 microglobulin	GGAATTGATTTGGGAGAGCATC	CAGGTCCTGGCTCTACAATTTACTAA	AGTGTGACTGGGCAGATCCACCTTC

2.14.3 Data Analysis

Copy number quantification was achieved using calculations based on the standard curves generated from Namalwa BL DNA. To generate standard curves, for both β-2M and EBV POL, Ct Values were plotted against the log of number of EBV copies in each diluted sample. An example of the curves generated is shown in Figure 2.2.

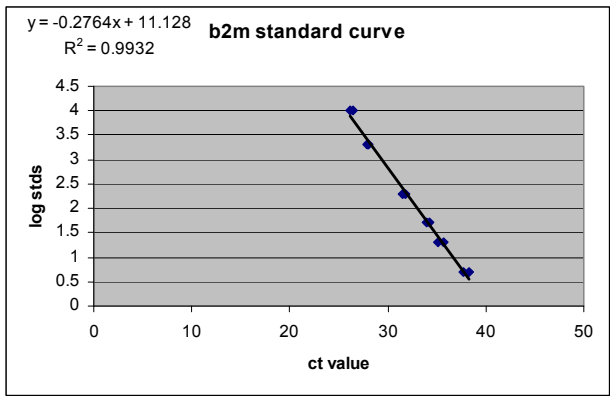

Figure 2.2

The formula from each β-2 microglobulin standard curve (line of best fit) was used, along with sample Ct values, to quantify the amount of β-2 microglobulin present in each individual sample (Ct value = X; β-2 microglobulin value = Y). The anti-log of this value was taken and used as each sample's final value for β-2 microglobulin. The same procedure was applied to Ct values for EBV POL, using standard curves generated from the Namalwa DNA using the EBV POL probe. EBV POL values for each sample were made relative to β-2 microglobulin values (by division) to generate the average number of EBV genome copies per cell. Each sample was analysed in technical and biological triplicate, with average values taken.

2.15 Methods of EBER detection

2.15.1 *In situ* hybridisation staining (ISH) for EBER expression

The presence of EBERs was detected *in situ* using a peptide nucleic acid (PNA), fluorescein isothiocyanate (FITC) labelled, fluorescent probe (Dako, Y5200) which is able to bind small nuclear RNA (snRNA) EBER1 and EBER2 transcripts. As for IF staining, adherent cells were trypsinised and counted as described in Section 2.2.5. Cells ($1x10^4$) were seeded onto sterile Teflon coated slides (Henley) and left to adhere for 48 to 72 hours in 150mm culture dishes, with desiccation prevented by the addition of PBS solution to the culture dishes. Cells were then washed with PBS before fixation in 4% PFA pH 7.4 for 10 minutes and immersion in RNase-free water multiple times. From this point, the manufacturer's protocol for EBER ISH using tissue sections was faithfully followed. Slides were placed in a humidity chamber before the addition of Proteinase K to each well to permeabilise the cells. Following a 20 minute incubation, cells were immersed in pure water and then 95% ethanol, before being air dried in the humidity chamber. A drop of either EBER PNA Probe/Fluorescein (DAKO, Y5200) or negative control PNA Probe/FITC (provided in DAKO kit, K5201) was applied to

each well of the slides before coverslips were added, and slides were incubated in a humidity chamber at 55°C for 90 minutes. The negative control probe allowed analysis of background staining in each well. Coverslips were removed before slides were immersed in Stringent Wash Solution (provided in DAKO kit, K5201) which had been pre-warmed to 55°C. Slides were incubated for 20 minutes at 55°C with constant shaking and then adjusted to room temperature by a 10 second immersion in TBS. Slides were replaced into the humidity chamber before a drop of Anti-FITC/AP (provided in DAKO kit K5201) was added to each well. Following incubation for 30 minutes, the antibody was tapped off and slides were immersed twice in TBS for 3 minutes then twice in RNase-free water for 1 minute. Having been placed back in the humidity chamber, a drop of substrate (provided in DAKO kit K5201) was added to each well prior to incubation for 30-60 minutes. At this point, slides were immersed in tap water for 5 minutes before mounting with coverslips and microscopy.

2.15.2 Detection of EBER RNA by flow cytometry

EBERs were also detected by flow cytometry, using the same PNA, FITC labelled, fluorescent probe (Dako, Y5200) that was utilised in EBER ISH (as described in Section 2.15.1). In order to avoid ribonuclease activity, all solutions were prepared using nuclease-free water. For each sample, approximately 2 x 10^6 cells were washed in PBS before centrifugation to pellet cells. Cells were fixed in 1ml 5% v/v acetic acid in 4% PFA before an aliquot of 1 x 10^6 cells was removed and centrifuged. After discarding the supernatant, cells were permeabilised at room temperature for 10 minutes in 50µl permeabilisation buffer (0.5% Tween 20 in 1X PBS). To ensure a formamide and buffer concentration similar to the hybridisation buffer that contains the EBER probe, 100µl DEPC water, 75µl formamide and 25µl formamide buffer (100mM NaCl, 50mM Na_2EDTA, 500mM Tris-HCl pH 7.5) were added to the cells. This step increases probe binding, and following incubation for 5 minutes

this equilibration step was ended by centrifugation of cells and aspiration of the supernatant. Subsequently, 50µL EBER PNA probe (Dako) in hybridisation buffer (10% w/v dextran sulphate, 10mM NaCl, 30% v/v formamide, 0.1% w/v $Na_4P_2O_7$, 0.2% w/v polyvinylpyrrolidone, 0.2% w/v ficoll, 5mM NaEDTA, 50mM Tris-HCl pH 7.5) was added and probe binding was carried out at 56˚C for 1 hour before addition of 1mL permeabilisation buffer and incubation at 56°C for a further 10 minutes. Cells were pelleted by centrifugation, with unbound probe then being washed from cells by incubation at 56˚C for 30 minutes in 1mL permeabilisation buffer. Finally cells were pelleted by centrifugation before resuspension in permeabilisation buffer ready for flow cytometry. The percentage of EBER-positive cells was measured using a Beckman Coulter XL flow cytometer. Fixed cells were gated on forward and side scatter and the EBER expression was detected though the FITC channel. The threshold of detection was set at 2% for EBV-negative cells. For each sample, 5,000 cells were counted and the percentage of positively stained cells recorded.

2.15.3 Northern blot analysis of levels of EBER expression

RNA was extracted (Qiagen Allprep DNA/RNA minikit) from LCLs which had been maintained as described in Section 2.2.5. Simultaneously DNA from the same sample was extracted and was used for qPCR analysis of EBV genome load.

2.15.3.1 Denaturing acrylamide gel preparation

Denaturing acrylamide (10%) gel mix (15ml – sufficient for one gel) was prepared by mixing 7.2g Urea (Sigma-Aldrich), 1.5ml 10 X TBE, 3.75ml 40% acrylamide (acrylamide:bis acrylamide = 19:1) and adding nuclease-free water to a total volume of 15ml. Subsequently, 75µl 10% APS and 15µl TEMED were added and following brief mixing, gels were poured into cassettes.

2.15.3.2 Electrophoresis and Transfer

10μg of RNA was mixed with loading dye prior to loading. Electrophoresis was conducted in 1 X TBE at 90V and was terminated once the dye front had migrated the full length of the gel. To assess the quality of samples and separation of the RNA, gels were stained with ethidium bromide and examined using a transilluminator before transfer. Following this assessment, RNA was transferred to a nylon membrane (N+ Hybond, Amersham) by electroblotting in 0.25 X TBE buffer, at 200mA for a minimum of 90 minutes. After blotting, the membrane was kept damp by wrapping in Saran Wrap, before the RNA was UV crosslinked to the membrane using a commercial crosslinking device (120mJ burst over 30 seconds).

2.15.3.3 Probe Preparation

A plasmid containing the EcoRI-J fragment of EBV genomic DNA was digested with EcoRI to yield a 3kb fragment which was excised following gel electrophoresis and used to generate radiolabelled probe for EBERs. This was achieved using a Random Primed DNA Labelling Kit (Roche Applied Science), as described in Section 2.12.3. The U4 small RNA probe was generated by PCR amplification of the U4 gene (Forward primer 5'-CGTGCCAATGAGGTTTATCC-3', Reverse primer 5'- AAAATTGCCAATGCCGACTA-3') followed gel electrophoresis and excision of the PCR product and use of the Random Primed DNA Labelling Kit (Roche Applied Science), as described in Section 2.12.3.

2.15.3.4 Probe hybridisation, washing and visualisation

Probe hybridisation, washing and visualisation were carried out as described for Southern blotting, in Section 2.12.4.

2.15.4 Quantitative RT-PCR for EBER1 and EBER2

Quantitative reverse transcription PCR (qRT-PCR) was conducted to determine the levels of EBER 1 and EBER2 in LCLs. This was performed on cDNA generated from RNA extracted as previously described (Section 2.15.3) in a gene-specific manner (Shannon Lowe et al. 2009).

2.15.4.1 DNase Treatment of RNA

Due to the extremely sensitive nature of qRT-PCR reactions for EBER1 and EBER2, DNase treatment of extracted RNA was conducted to ensure no genomic DNA was present, which might yield false positive results. 1µg RNA was incubated with DNase and buffer (DNA-*free* kit, Ambion, UK), in a reaction of 25µl total volume, at 37°C for 30 minutes before 2.5µl stop solution was added to the reaction. The mixture was then centrifuged at 10,000rpm for 90 seconds to remove the stop solution, before 20µl of the reaction was removed to a fresh microcentrifuge tube. 10µl of the reaction (400ng) was used per subsequent cDNA reaction.

2.15.4.2 cDNA synthesis

The 400ng of RNA was placed into a 0.5ml microcentrifuge tube and denatured by incubation at 90°C for 5 minutes then placed on ice. For each sample, mastermixes were prepared with and without Reverse Transcriptase enzyme (AMV RT, Roche), using gene specific primers (given in Table 2.7):

With RT

2µl specific DNA primer (10µM)	0.2µl RNase inhibitor
2µl dNTPs	1.3µl SDW
4µl 5 x RT Buffer	0.5µl RT

Without RT

2µl specific DNA primer
2µl dNTPs
4µl 5 x RT Buffer
0.2µl RNase inhibitor
1.8µl SDW

10µl of appropriate RT (or no RT) mix was then added to the ice cold denatured RNA, and the mixtures were incubated at 42°C for 1 hour before RT was inactivated by heating samples to 90°C for 5 minutes. cDNA samples were subsequently diluted to 5ng/µl by the addition of 60µl SDW.

2.15.4.3 X50-7 cDNA standard curves

Standard curves were plotted based on serial dilutions of X50-7 cDNA. From a starting point of 5ng/µl, cDNA samples of concentrations 1ng/µl, 200pg/µl, 40pg/µl and 8pg/µl were made.

2.15.4.4 PCR reactions

Separate mastermixes for both EBER1 and EBER2 were prepared for each sample. Example 20µl mastermix (for either EBER1 or EBER2):

12.5µl Taq MM
2.5µl EBER Forward Primer
2.5µl EBER Reverse Primer
1µl EBER probe
0.5µl GAPDH mix (primers and probe)
1µl DEPC water

20µl of the mastermix was added to each well of a 96 well plate as required. 5µl of X50-7 standard or experimental sample was added to appropriate wells, before brief

centrifugation of plate and loading into real-time PCR analyser. Details of primer/probe set sequences are given in Table 2.7:

Table 2.7 EBER1, EBER2 and GAPDH primer/probe and cDNA primer sets

Assay	Oligo	Sequence 5'-3'
EBER1	Forward	TGCTAGGGAGGAGACGTGTGT
	Reverse	TGACCGAAGACGGCAGAAAG
	Probe	AGACAACCACAGACACCGTCCTCACCA
	cDNA primer	GACCACCAGCTGGTAC
EBER2	Forward	AACGCTCAGTGCGGTGCTA
	Reverse	GAATCCTGACTTGCAAATGCTCTA
	Probe	CGACCCGAGGTCAAGTCCCGG
	cDNA primer	GGACAAGCCGAATACC
GAPDH	Forward	GAAGGTGAAGGTCGGAGTA
	Reverse	GAAGATGGTGATGGGATTTC
	Probe	CAAGCTTCCCGTTCTCAGCC
	cDNA primer	GATCTCGCTCCTGGAA

2.15.4.5 Data Analysis

Levels of EBER expression were determined relative to levels of EBER1 and EBER2 expression empirically determined in X50-7 cells. Standard curves were generated using serial dilutions of X50-7 cDNA for GAPDH, EBER1, and EBER2. For each gene assay, Ct Values were plotted against the log of ng/µl X50-7 cDNA in each diluted sample. The formula from the standard curve was applied to each sample's Ct value for the appropriate variable, before the anti-log of this value was taken and used as each sample's unknown for the variable. EBER unknowns (EBER1 and EBER2

analysed separately) were then normalised against the internal GAPDH control unknown (by division) to generate the relative level of expression of EBER1 and EBER2, relative to X50-7. Each sample was analysed in both biological and technical triplicate, with average values being reported.

2.16 Chromatin Immunoprecipitation (ChIP)

ChIP was performed using a commercial kit, EZ ChIP™ (Catalog # 17-371) obtained from Upstate (USA). The EZ ChIP™ kit contains reagents optimised for immunoprecipitation of chromatin from mammalian cells including controls to ensure successful performance of this assay. The included positive control antibody is a mouse monoclonal antibody to RNA Polymerase II and detects RNA Polymerase II of human, mouse, rat and yeast. The negative control is Normal Mouse IgG, which controls for the nonspecific immunoselection of chromatin by immunoglobulins. Control primers and 10X PCR Buffer are included for detection of a 166 base pair region of the human GAPDH promoter by PCR. Not provided in the kit are specific antibodies to precipitate proteins of interest and appropriate isotype control antibodies. Antibody chEBNA1 was kindly provided by Professor Paul Lieberman (The Wistar Institute, Philadelphia USA) for specific immunoprecipitation of EBNA1, having been successfully used for this purpose previously. chEBNA1 is a polyclonal rabbit antibody against EBNA1. As a non-specific isotype control, a polyclonal rabbit antibody to E-Cadherin was used (Santa Cruz Biotechnology Inc. USA, H-108). Protocols followed were as given in the Upstate user guide and are briefly outlined below.

2.16.1 Buffers and solutions provided and used in the EZ-ChIP kit

Stored at 4°C:

Salmon Sperm DNA/Protein G Agarose, Catalog # 16-201C. One vial containing 1.5ml packed beads with 600µg sonicated salmon sperm DNA, 1.5mg BSA and approximately 4.5mg recombinant Protein G. Provided as a 50% gel slurry for a final volume of 3ml per vial,suspended in TE buffer, pH 8.0, containing 0.05% sodium azide.

ChIP Dilution Buffer, Catalog # 20-153. One vial containing 24ml of 0.01% SDS, 1.1% Triton X-100, 1.2mM EDTA, 16.7mM Tris-HCl, pH 8.1, 167mM NaCl.

Low Salt Immune Complex Wash Buffer, Catalog # 20-154. One vial containing 24ml of 0.1% SDS, 1% Triton X-100, 2mM EDTA, 20mM Tris-HCl, pH 8.1, 150mM NaCl.

High Salt Immune Complex Wash Buffer, Catalog # 20-155. One vial containing 24ml of 0.1% SDS, 1% Triton X-100, 2mM EDTA, 20mM Tris-HCl, pH 8.1, 500mM NaCl.

LiCl Immune Complex Wash Buffer, Catalog # 20-156. One vial containing 24ml of 0.25M LiCl, 1% IGEPAL-CA630, 1% deoxycholic acid (sodium salt), 1mM EDTA, 10mM Tris, pH 8.1.

TE Buffer, Catalog # 20-157. Two vials, each containing 24ml of 10mM Tris-HCl, 1mM EDTA, pH 8.0.

0.5M EDTA, Catalog # 20-158. One vial containing 250µl of 0.5M EDTA, pH 8.0.

5M NaCl, Catalog # 20-159. One vial containing 500µl of 5M NaCl.

SDS Lysis Buffer, Catalog # 20-163. One vial containing 10ml of 1% SDS, 10mM EDTA, 50mM Tris, pH 8.1.

1M Tris-HCl, pH 6.5, Catalog # 20-160. One vial containing 500µl of 1M Tris-HCl, pH 6.5.

10X Glycine, Catalog # 20-282. One vial containing 24ml of 1.25M Glycine.

10X PBS, Catalog # 20-281. One vial containing 24ml of 10X PBS.

Stored at -20°C:

Protease Inhibitor Cocktail II, Catalog # 20-283. Two vials, each containing 110µl of 200X Protease Inhibitor Cocktail II in DMSO.

RNase A, Catalog # 20-297. One vial containing 45µl of 10mg/ml RNase A in sterile water.

Proteinase K, Catalog # 20-298. One vial containing 60µl of 10mg/ml Proteinase K in 10mM Tris-HCl, pH 8.0, 10mM $CaCl_2$.

1M NaHCO3, Catalog # 20-296. One vial containing 500µl of 1M NaHCO3.

10X PCR Buffer, Catalog # 20-295. One vial containing 200µl of 750mM Tris-HCl, pH 8.8, 200mM (NH4)2SO4, 0.1% Tween®-20, 25mM $MgCl_2$.

2.16.2 *In vivo* cross-linking and lysis

Adherent epithelial cells were grown in 10cm^2 dishes to a confluence of ~80-90% before *in vivo* cross-linking with formaldehyde. 270µl of freshly prepared 37.5% formaldehyde was added to the 10ml growth medium in each 10cm^2 dish to give a final concentration of 1% formaldehyde for cross-linking. Following a gentle swirl, plates were incubated at room temperature for 10 minutes. Following the cross-linking, any unreacted formaldehyde was quenched by the addition of 1ml 1.25M glycine. Plates were subsequently swirled and incubated at room temperature for 5 minutes before being placed on ice, and having all media aspirated. Cells were then washed 3 times with 10ml ice cold PBS, before the addition of 1ml ice-cold PBS

containing protease inhibitors. Cells were then scraped into microcentrifuge tubes and spun at 700 x g for 5 minutes to pellet the cells. Supernatant was removed and 1ml SDS lysis buffer was used to resuspend cell pellets. Lysates were aliquoted (400µl) into microcentrifuge tubes and either used immediately or stored at -80°C.

2.16.3 Sonication to shear DNA

Prior to the immunoprecipitation (IP) step, cells require breaking open and chromatin within the cells must be sheared into manageable fragments. This is achieved through sonication of the samples. Shearing DNA to 200-1000bp in length provides a high degree of resolution during the detection steps at the end of the procedure. Optimal conditions for shearing cross-linked DNA to 200-1000bp in length are dependent on a number of factors. These include cell type and concentration, sonicator equipment and setup, power settings, and the number of pulses used. As such, the sonication conditions described below were determined empirically to give fragments of 200-1000bp (see Chapter 5). The conditions outlined were applied to each set of experimental samples.

Samples were kept on ice throughout sonication to ensure that overheating (which may denature chromatin) did not occur. Each 400µl sample was sheared using a Misonix XL2000 sonicator (Misonix, New York, USA) set to power setting 10. 10 pulses of 10 seconds were used for each sample, with 30 seconds between each pulse to allow the sample to cool. Following sonication, samples were centrifuged at 12,000 x g for 10 minutes to remove any insoluble material before a 5µl aliquot was taken and subjected to gel-electrophoresis to ensure fragmentation of DNA into 200-1000bp fragments had occurred. Each sample was then divided into 100µl aliquots

(containing ~2 x 10^6 cells), sufficient for an immunoprecipitation, and stored at -80°C until use.

2.16.4 Immunoprecipitation of Cross-linked Protein/DNA

All IP procedures were conducted in a temperature controlled room at 4°C. 100µl aliquots of sample were prepared for IP by the addition of 900µl dilution buffer. To pre-clear the chromatin, 60µl of Protein G Agarose (50% slurry) was added to each sample and samples were incubated with rotation for 1 hour at 4°C. Agarose was pelleted by centrifugation at 3000 x g for 1 minute and supernatant was transferred to a fresh microcentrifuge tube. 10µl (1%) of the supernatant was removed and saved as input at 4°C until the completion of the IP procedure. Immunoprecipitating antibodies (see Table 2.8) were subsequently added to the appropriate supernatants and samples were incubated overnight with rotation at 4°C. The following morning, antibody/antigen/DNA complexes were collected by the addition of 60µl of Protein G Agarose and incubated for 1 hour with rotation at 4°C. Protein G Agarose was pelleted by centrifugation at 3000 x g for 1 minute and the supernatant was aspirated and discarded. Protein G Agarose-antibody/antigen/DNA complexes were washed by resuspension in 1ml each of the buffers in the sequence listed below:

Low Salt Immune Complex Wash Buffer – *1 Wash*

High Salt Immune Complex Wash Buffer – *1 Wash*

LiCl Immune Complex Wash Buffer – *1 Wash*

TE Buffer – *2 Washes*

Beads were washed by incubation with rotation for 5 minutes in each of the wash buffers, with Protein G Agarose-antibody/antigen/DNA complexes being pelleted after each wash by centrifugation at 3000 x g for 1 minute. All wash supernatants were carefully aspirated and then discarded.

Table 2.8 Antibodies used for immunoprecipitation.

Protein	**Immuno-precipitating antibody**	**Species**	**Working Concentration**
EBNA1	chEBNA1	Rabbit	7.5µl per IP
E-Cadherin (chEBNA1 isotype control)	E-Cad (Santa Cruz, H-108, sc7870)	Rabbit	7.5µl (1.5µg) per IP
RNA Polymerase II	Anti-RNA Polymerase II CTD448	Mouse	1µg per IP
Mouse IgG	Mouse IgG	Mouse	1µg per IP

2.16.5 Reversal of Cross-links of Protein/DNA complexes to free DNA

All tubes (IP samples and inputs) were supplemented with 8µl 5M NaCl and incubated at 65°C overnight to reverse the DNA-Protein cross-links. All samples were subsequently treated with RNase A for 30 minutes at 37°C before proteinase K digestion of remaining protein at 45°C for 2 hours.

2.16.6 Purification of DNA

DNA purification was required to remove chromatin proteins and prepare the DNA for detection steps. Purification was conducted using the DNA spin columns provided in the EZ-ChIP kit. The final volume of purified DNA eluate was ~50µl.

2.16.7 DNA detection by PCR

Immunoprecipitated-promoter region DNA was initially detected by PCR. This was conducted in the same manner as RT-PCR (Section 2.11.2), with the single difference that DNA was assayed directly, instead of cDNA being reverse-transcribed from cellular RNA and used as a template. Primer design was carried out (unless otherwise stated) for promoter regions of genes of interest. Promoter regions were identified using online search engines and typically primers were designed in regions up to 500bp upstream of the transcriptional start site of the gene of interest. Bearing in mind

the resolution of the ChIP assay (200-1000bp), primers designed in such regions should comfortably detect any promoter DNA that had been precipitated.

Primers for PCR were synthesised by Sigma-Aldrich and are presented in Table 2.9 along with specific annealing temperatures used for each primer set and the product size produced.

Table 2.9 PCR primers and accompanying annealing conditions and product sizes.

Gene (promoter region)	**Primer oligonucleotides 5' – 3'**	**Annealing temperature (°C)**	**Product size (bp)**
GAPDH	Forward: TACTAGCGGTTTTACGGGCG Reverse: TCGAACAGGAGGAGCAGAGAGCGA	59	166
ATF-2	Forward: CCCAAACCTCACCTAACCCGAAG Reverse: CTCGGGCGCTCATGATTGGACAA	59	397
c-jun	Forward: CCCACAAGTGGGGAAACAACAA Reverse: GCTACCAGTCAACCCCTAAAAATA	59	488
c-myc	Forward: TCCTCTCTCGCTAATCTCCGC Reverse: CCCTCCGTTCTTTTTCCCG	55	117
EBV DS repeat	Forward: CCGTGACAGCTCATGGGGTGGGAGAT Reverse: CAATCAGAGGGGCCTGTGTAGCTACCG	59	246

2.16.8 DNA detection and quantification by Real-Time quantitative PCR (qPCR)

For increased detection sensitivity, and accurate quantitative analysis of levels of promoter DNA precipitated, qPCR was carried out. Samples were analysed in biological and technical triplicate, with an input sample, isotype control sample, and experimental (chEBNA1) sample being analysed (in biological and technical triplicate) per initial lysate. 20µl reactions were assembled using 10µl 2X Sensimix mastermix (Quantace Ltd), 1µl of each primer (from stock concentration of 10µM) and optimal probe concentrations, which were determined empirically (see Chapter

5). 5µl of sample DNA was used per reaction, and reactions were set up in 96 well plates before analysis using an ABI 7500 Fast Real-time PCR machine. Primer/Probe sets used for each promoter region are given in Table 2.10.

Table 2.10 qPCR primer/probe sets used in ChIP analysis

Gene (promoter region)	**Primers 5′ – 3′**	**5′ FAM / 3′ TAMRA-labelled probe 5′ – 3′**
c-jun	Forward: GAGACCGCCCCTAAACTTAAGTC Reverse: CCCTTAAGGTGGCTCTGTGAA	TTAGGCTCGCCCCCACCTGGG
junB	Forward: TAACCCTCATTTCTGCTTTTTGG Reverse: AAACCCCTGAGGTACCCAGAATAC	CCCAATGGATTGTCAGTCCTCCTACCC
junD	Forward: CAGGATCCAAGCGCTTTCAG Reverse: CCCCGCGTGTGATTGC	ACCCTCCTCTCCCCTCCCGTCTCTT
c-fos	Forward: CAAGGGTAAAAAGGCGCTCTCT Reverse: ATTCGCACCTGGTTCAATGC	CCCATCCCCCCCGACCTCG
fosB	Forward: GGGATTCCCTCTGACGTCATT Reverse: GTGACGCAATTAGCCATATAAGGA	TAGGATACCAAACAAACACTCCGCCG
fra1	Forward: CAGTGCGCCGAGATCGA Reverse: AGGGTTACAAAAATGGTGGCATAT	ACTCCAGCCTGGGTGACAGAGACCC
fra2	Forward: TCACCCGAAAGCGAGGAA Reverse: CGTTGCCAAAGATGGTCATTT	CCCGCACTCGCGTCCTCTAACG
ATF-2	Forward: AAACCTCACCTAACCCGAAGCT Reverse: TTCCGTCACTTCCCAGCACTA	AACGCAGCCTACTTTTACCCACCTCCC
c-myc	Forward: CCCGGGTTCCCAAAGC Reverse: CCAGACCCTCGCATTATAAAGG	TCTCTCGCTAATCTCCGCCCACCG

Table 2.10 ctd. qPCR primer/probe sets used in ChIP analysis

Gene (promoter region)	**Primers 5′ – 3′**	**5′ FAM / 3′ TAMRA-labelled probe 5′ – 3′**
EBV-DS	Forward: GCCACTGCCCTTGTGACTAAA Reverse: CCCATGAGCTGTCACGGTTT	CACTACCCTCGTGGAATC CTGACCCC
GAPDH	Forward: CGCCCCCGGTTTCTATAAA Reverse: GTCGAACAGGAGGAGCAGAGA	TGAGCCCGCAGCCTCCCG

Cycle threshold (Ct) values were determined by ascertaining the point at which amplification occurred above background in the linear range of amplification for each reaction. The average of each technical triplicate was taken to obtain the mean dCt value for each sample and ddCt values were subsequently calculated by subtracting the relative input sample dCt value from the respective control or experimental sample dCt. Data were made relative to the input samples (which had a ddCt value of 0) by applying the formula 2^{-ddCt} to each control and experimental sample data set (N-fold value). Fold change from isotype control antibody to experimental antibody samples was calculated by simple division of these N-fold values. Statistical significance of fold changes was established using the Student's t-test.

2.17 HaloCHIP

The HaloCHIP system (Promega UK) is a novel method which captures covalently formaldehyde cross-linked protein:DNA complexes from transiently transfected cells. It is an antibody-free system and can be regarded as a robust and efficient alternative to the standard chromatin immunoprecipitation system described in Section 2.16. A DNA-binding protein, in this instance EBNA1 (or an EBNA1 mutant), is fused to the HaloTag protein (which mediates a covalent interaction with a resin-based ligand) using standard molecular biology techniques (see Chapter 5). The recombinant

construct is subsequently transfected into cells for transient expression. Following expression of the recombinant construct, procedures are similar to that described for chromatin immunoprecipitation (Section 2.16). The HaloCHIP protocol is outlined briefly below.

2.17.1 Buffers and Solutions Provided and used in HaloCHIP kit

HaloCHIP™ Blocking Ligand**:** 5mM fluorescent TMR HaloTag® Blocking Ligand in DMSO (excitation: 555nm; emission: 580nm)

HaloLink™ Resin equilibration buffer: 1X TE Buffer (pH 8.0), 0.1% IGEPAL® CA-630

High Salt Wash Buffer**:** 50mM Tris-HCl (pH 7.5), 700mM NaCl, 1% Triton® X-100, 0.1% sodium deoxycholate, 5mM EDTA

Lysis Buffer**:** 50mM Tris-HCl (pH 7.5), 150mM NaCl, 1% Triton® X-100, 0.1% sodium deoxycholate

Reversal Buffer: 10mM Tris-HCl (pH 8.0), 1mM EDTA, 300mM NaCl

TE Buffer (pH 8.0): 10mM Tris-HCl (pH 8.0), 1mM EDTA

2.17.2 *In vivo* cross-linking and lysis

Cells grown in 10cm^2 dishes and were crosslinked with 0.75% formaldehyde 24 hours post transfection with recombinant constructs. At this point, cells were typically 80-90% confluent. Other than the slightly reduced concentration of formaldehyde used, crosslinking procedures were identical to that given in Section 2.16.2. Following glycine neutralisation and several washes with ice cold PBS, each 10cm^2 dish of cells was scraped in 2ml of PBS into 15ml tubes. Cells were centrifuged at 2000 x *g* for 5

minutes at 4°C before the supernatant was removed and cell pellets were frozen at -80°C for at least 10 minutes (storage of cell pellets was possible at this stage of the procedure). After thawing at room temperature, cells from a $10cm^2$ dish were resuspended in 700µl of ice cold lysis buffer and mixed briefly by vortexing before incubation on ice for 15 minutes. Mechanical disruption was then used to lyse the cells by passing the cells through a 25-guage needle 4-6 times.

2.17.3 Sonication to shear DNA

Sonication of the cells was conducted in a very similar manner to that described in Section 2.16.3. However, in HaloCHIP experiments, samples were sonicated in 700µl aliquots of lysis buffer (i.e. each $10cm^2$ dish was sonicated and processed as an individual sample). The kit manufacturer's recommendations suggest a slightly larger average fragment size of DNA for these experiments. However, given the increased volume of aliquots in sonication, it was empirically determined that sonication conditions (i.e. number of pulses, sonicator power settings) should remain the same, or very similar to those described in Section 2.16.3.

2.17.4 Capture and Release of DNA

Sonicated samples were centrifuged at 14000 x *g* for 5 minutes at 4°C before careful aspiration of supernatant. A 30µl aliquot of supernatant was removed and retained at 4°C until the purification steps described below and used as an "input" control in subsequent DNA analysis. Samples were then divided into 2 x 300µl aliquots, one used as a control sample and one used as the experimental sample. To the control sample only, 0.5µl of blocking ligand was then added (final concentration 8.3µM). The blocking ligand binds to the HaloTag covalent binding site, preventing subsequent covalent pull down of fusion proteins in the control sample. Both control

and experimental samples were then incubated at room temperature for 30 minutes, whilst being mixed using a tube rotator. During this 30 minute incubation period, HaloLink Resin was prepared for use:

75µl resin was dispensed into two 1.5ml microcentrifuge tubes (per sample, 1 for control, 1 for experimental). Resin was centrifuged at 800 x *g* for 2 minutes and supernatant discarded. Resin was equilibriated by resuspension 3 times in equilibration buffer. Following the final suspension, buffer was aspirated just before the 30 minute incubation of samples was complete.

The entire experimental sample was then added to one tube containing equilibrated resin, and the entire control sample was added to the other tube. Samples were then incubated with constant mixing using a tube rotator for 3 hours at room temperature. Samples were centrifuged at 800 x *g* for 2 minutes at room temperature and the supernatant was discarded. Finally, samples were washed sequentially for 5 minutes at room temperature with constant mixing on a tube rotator in 1ml of each of the buffers in the order stated:

- Lysis Buffer
- Nuclease-Free Water (2 washes)
- High Salt Wash Buffer (15 minute incubation)
- Nuclease-Free Water (3 washes, the final wash being incubated for 15 minutes)

2.17.5 Reversal of Cross-links of Protein/DNA complexes to free DNA

Following removal and discard of the final wash solution, 300µl reversal buffer was added to each tube with the resin and mixed by gentle pipetting. Samples were then incubated at 65°C overnight to reverse the crosslinks. Resin was centrifuged at 800 x

g for 2 minutes and the supernatant containing the released DNA was transferred to a fresh tube.

2.17.6 Purification of DNA

Eluted DNA was purified using a commercially available DNA purification spin column kit (Purelink PCR Purification Kit, Invitrogen). Half the sample was purified per protocol, with a final elution volume of 50µl.

2.17.7 DNA detection by PCR

Purified DNA samples were analysed using PCR analysis as described in Section 2.16.7. Primers were designed in the same manner as previously stated with the exception of cellular polIII transcribed genes (5S RNA, 7SL RNA, $tRNA^{tyr}$). Due to the short length and small upstream regulatory regions of these genes, primers were designed within the region of the gene itself rather than 500bp upstream. TFIIIC110 and TFIIIC220 subunit promoter primer sequences were taken from Felton-Edkins et al. (2006). Primers for PCR were synthesised by Sigma-Aldrich and are presented in a previous table (Table 2.9), and the following table (Table 2.11) along with specific annealing temperatures used for each primer set and the product size expected.

Table 2.11 PCR primers and accompanying annealing conditions.

Gene (promoter region)	**Primer oligonucleotides 5' – 3'**	**Annealing temp (°C)**	**Product size (bp)**
TFIIIC220	Forward: GTTTGCAGTTCCCCTGGTTAC Reverse: CTTCGTCCAACAACGACTCC	58	260
TFIIIC110	Forward: TCTCCCCTTTTTGACACTGC Reverse: AGGGGGAGGAGTAATTGTGG	58	354
TFIIIC102	Forward: CGGTTCCTTGCTCTTGCT Reverse: GCATCGCCTCACTTTCTT	55	217
TFIIIC90	Forward: GCGGGTAGGGACAAGACT Reverse: CCCAGACAGGCTTTAGTT	56	217
TFIIIC63	Forward: GCCAACACCGACAGAATA Reverse: CGGAGGATAATAAGACACAAA	58	308

Table 2.11 ctd PCR primers and accompanying annealing conditions.

Gene (promoter region)	**Primer oligonucleotides 5' – 3'**	**Annealing temp (°C)**	**Product size (bp)**
5S RNA	Forward: TTTACGGCCACACCACCCTG Reverse: AAAGCCTTCAGCACCCTGTA	58	107
tRNAtyr	Forward: CCTTCGATAGCTCAGCTGGTAGAGCGGAGG Reverse: CGGAATTGAACCAGCGACCTAAGGATGTCC	65	84
7SL RNA (gene)	Forward: GTGTCCGCACTAAGTTCGGCATCAATATGG Reverse: TATTCACAGGCGCGATCCCACTACTGATC	70	150
7SL RNA (promoter)	Forward: CCGTGGCCTCCTCTACTTG Reverse: TTTACCTCGTTGCACTGCTG	58	202
Brf1	Forward: GCAAGGAGGTCAGGCACT Reverse: CCTTCCACGGCTACCTCT	58	367
Bdp1	Forward: GTTTCTTCACACCAGCATT Reverse: GCTACTGAGACTGGGTTA	56	236
TBP	Forward: CGCCCCTCCTTACCTAT Reverse: CAATCTGTTACCTGGGTC	55	242

2.17.8 DNA detection and quantification by quantitative PCR (qPCR)

For increased detection sensitivity, and accurate quantitative analysis of levels of precipitated promoter DNA, qPCR was carried out in some instances. Samples were analysed in biological and technical triplicate as described in Section 2.16.8.

2.18 Densitometry

Densitometry was conducted on autoradiograph and UV transilluminator images using ImageJ 1.37V. ImageJ is a public domain, Java-based imaging-processing program developed at the National Institutes of Health, available online (http://rsbweb.nih.gov/ij/). Bands were analysed in technical triplicate, normalising against background image levels and, if appropriate, internal controls. In all instances, densitometry was conducted in biological triplicate, with average results reported.

2.19 Statistics

Statistical significance of data was established using the Student's *t*-test, following designation of the variance of samples as either equal or unequal using an *f*-test.

Chapter 3

EBV genome copy number and EBER expression

Chapter 3 - EBV genome copy number and EBER expression

It has previously been demonstrated that EBV-positive cell lines show significant variation in the average number of EBV viral episomes maintained per cell (copy number) (Metzenberg 1989; 1990; Sternas et al. 1990; Jeon et al. 2009) and levels of EBER expression also vary significantly from cell line to cell line. Although differences in a multitude of cellular and viral factors could explain the variation in levels of EBER expression, perhaps the most simplistic explanation is that of EBV genomic copy number variation being directly responsible for fluctuations in levels of EBER expression between various cell lines, that is, the rate of transcription of EBERs increases monotonically with the average genome copy number. Assuming a constant rate of degradation of EBER expression in each cell background, this monotonic increase in the rate of EBER transcription based upon increase in EBV genome copy number would lead to increased accumulation of EBERs in cell lines with high average genome copy numbers. Consistent with this hypothesis, previous data have shown that increasing the copies of EBER genes (from 1 to 10 copies) expressed by a plasmid vector significantly increased levels of EBER expression (Komano et al. 1999). Further, and perhaps more pertinently, in a small panel of LCLs with vastly differing copy numbers, EBER transcription has been demonstrated to correlate with the amount of EBV genomic DNA in each LCL (Metzenberg 1989). However, this was a very small scale study (with only three LCLs of vastly differing copy number analysed), and a study of EBER transcription rate rather than overall levels. Therefore further investigation of the relationship between EBV copy number and levels of EBER expression are warranted. Preliminary attempts at such investigation have previously been carried out, with results appearing to agree with the hypothesis (Dr. JR Arrand, personal communication). This explanation of variation in levels

of EBER would perhaps be in line with the high levels of EBER expression that are detectable in EBV-infected cells, given that multiple episomal copies of the EBV genome are usually carried.

This chapter further explores the relationship between the average EBV genome copy number maintained in a range of LCLs, and the levels of EBER expression that are observed in each cell line. A variety of techniques, both traditional and more modern, for detection and quantification of the EBV genome and EBER1 and EBER2 are employed, with the techniques found to be most sensitive used in an ultimate comparison between average EBV genome copy number and levels of EBER expression.

3.1 Results

3.1.1 Measuring average EBV genome copy number

3.1.1.1 Southern blotting

Initial attempts at quantification of EBV genome copy number in the panel of LCLs focused on Southern blotting for the EBV genome. This well-established technique for detection of EBV genomic DNA, using a radio-labelled BamHI-X fragment of the EBV genome is outlined in Section 2.15, and the results are presented in Figures 3.1 and 3.2. LCL DNA was quantified before equal loading of each DNA sample, as detected by ethidium bromide staining (Figure 3.1A). Ideally, blotting for the BamHI-X fragment would have been conducted in parallel with blotting for a suitable internal control, however probes to enable this level of standardisation were not available at the time of experimentation. Figure 3.1 is illustrative of results obtained in these experiments, with changes in the intensity of bands seen in Figure 3.1B representing variations in EBV genome copies in each LCL. No EBV

Figure 3.1 – Southern blotting for EBV genomic DNA using DNA extracted from a panel of LCLs grown in media supplemented with acyclovir to prevent lytic outgrowth of virus. **(A)** UV transilluminator image of an ethidium bromide stained agarose gel, showing a panel of DNA samples extracted from LCLs and digested with BamHI enzyme. Such analysis was utilised to assess the consistency of sample loading. **(B)** Autoradiogram illustrative of Southern blotting for EBV genomic DNA across the panel of LCL samples. A Radio-labelled BamHI-X fragment of the EBV genome was used to probe. The autoradiogram presented is representative of a 2 hour exposure.

Figure 3.2 – Densitometric analysis of the Southern blot data presented in Figure 3.1B. The average value of 3 technical repeats is shown, with error bars representing the standard deviation of these repeats.

Figure 3.1 and 3.2

genome DNA is detected in EBV-negative cell line BJAB, with the LCL samples showing only slight variation in band intensity. Sample JS carries the smallest detectable EBV genome load, with samples DA and LMC producing the most intense bands for EBV genomic DNA. To quantify the results, densitometric analysis was conducted (Figure 3.2) and the data replicate the visual analysis of the Southern blot shown in Figure 3.1B. However, absolute quantification of average numbers of copies of the EBV genome is not possible in this instance, with results given as arbitrary units. Given the only slight variations in EBV genomic DNA between LCLs detectable using this method, alternative methods for EBV genome detection and quantification were identified that would prove to be more sensitive, and able to provide more exact quantification of the average EBV genomic load in each LCL.

3.1.1.2 qPCR measurement of average EBV genomic load

qPCR analysis of average EBV genome load in each LCL relied upon the generation of standard curves from DNA of known EBV genomic load. This DNA was taken from Namalwa BL cells, which contain two integrated EBV genome copies per cell. Based on assumptions outlined in Section 2.15, it was possible to perform serial dilutions to generate a set of DNA standards with a known number of EBV genome copies, per microlitre volume of sample. Using these samples of known EBV genomic copy number, standard curves were generated (Figure 3.3) for internal cellular control DNA (β-2 Microglobulin) and EBV genomic DNA (EBV POL gene) which enabled quantification of the average EBV genome load in each LCL from subsequent qPCR data analysis. Figure 3.4 shows the average EBV genome copy number found for each LCL in the panel investigated. Consistent with Southern blotting, EBV genomic DNA was not detected in BJAB-cells. However, in contrast to Southern blotting data, a large variation in average copy number is seen, ranging from less than 5 copies per cell, for X50-7 samples, to greater than 35 copies per cell, for NB and DA

Figure 3.3 – Example standard curves (Namalwa BL DNA) for **(A)** β_2-Microglobulin and **(B)** EBV POL qPCR analysis. Ct values (average values of technical triplicates) are plotted against the log of each standard value. The line of best fit is included, as is the formula of the line, and the R^2 value for each curve. Both (A) and (B) are single examples of curves that were generated alongside every experimental data set, with analysis of each data set being reliant upon a standard curve that was produced from DNA standards analysed in the same run.

Figure 3.3

Figure 3.4 – qPCR results indicating the average measured EBV genome load for each LCL across a panel of 10 LCLs, along with BJAB as an EBV-negative control. Each sample was tested in biological and technical triplicate, with average values presented. Error bars are representative of the standard deviation of biological replicates.

Figure 3.5 – FITC FACS staining for EBERs in BJAB (both stained and unstained cells plotted), Namalwa BL and Raji cells.

Figure 3.6 – Example of Northern blotting conducted for EBER1 and U4 (small RNA loading control). For analysis of EBER expression levels, a radio-labelled EcoRI-J fragment of the EBV genome was used as a probe, and a PCR product based on U4 gene template was radio-labelled and employed in the Northern blot analysis of U4 snRNA levels.

Figures 3.4 3.5 and 3.6

samples. This increase in the range of detected EBV genome copies reflects the greater sensitivity of this qPCR assay, compared with Southern blotting.

3.1.2 EBER expression level analysis

3.1.2.1 EBER FITC FACS staining

FACS analysis of EBER expression was employed in an attempt to quantify levels of EBER expression in the panel of LCLs. Initial experiments were conducted with BJAB-cells (negative control), Namalwa BL cells and Raji cells. EBER1 and EBER2 are known to be abundant in Raji cells (Schwemmle et al. 1992), and were included as a positive control. Contrastingly, EBER expression in Namalwa BL cells is very low (Minarovits et al. 1992). This cell line was analysed to assess the sensitivity of the assay, i.e. to establish if the technique enabled the detection of low levels of EBER expression and the ability to detect small differences in EBER expression between cell lines. Results shown in Figure 3.5 reveal that although EBER FITC FACS staining was successful in detecting strongly EBER-positive Raji cells, weakly EBER-positive Namalwa BL cells were not detected as such. Indeed, the results for stained BJAB-cells and Namalwa BL cells are strikingly similar. EBER FITC FACS staining was not therefore a suitable method of EBER quantification in this instance. Although useful in determining the number of strongly EBER-positive cells in a population, the technique was not able to distinguish between a cell population with weak EBER expression and a cell population completely lacking EBER expression.

3.1.2.2 Northern blotting

EBER expression analysis by Northern blotting is a well established technique, similar in terms of applications and sensitivity to Southern blotting for EBV genomic DNA. Figure 3.6 is exemplary of the quality of results obtained through use of this method. A striking aspect of

these results is that only a single band is detected for the EBERs. This is notable, as the radio-labelled probe (EcoRI-J fragment of EBV genome) detects both EBER1 and EBER2. However, along with U4, an internal small RNA control (detected by a separate radio-labelled probe), only one, and not the two predicted EBER-specific bands, was detected by Northern blotting. This results was most probably due to insufficient resolution of RNA to allow detection of distinct EBER1 (167bp) and EBER2 (172bp) bands.

Substantial variation in EBER expression was observed across the LCL panel, along with high levels of EBER expression in Raji samples (included as a positive control). EBERs were not detected in BJAB samples (negative control), although they also went undetected in Namalwa BL samples. This result suggests that the sensitivity of the assay is not sufficient to detect very low levels of EBER expression, meaning small differences in levels of EBER expression between LCLs in the panel may not be apparent using this method.

Densitometric analysis of Northern blotting was conducted (Figure 3.7), allowing quantitative evaluation of results. EBER data were normalised to the internal cellular control (U4) and in agreement with qualitative analysis of the Northern blots, substantial variation in levels of EBER expression was apparent. However, given the lack of sensitivity of the assay (undetected EBER expression in Namalwa BL samples), and lack of distinction between EBER1 and EBER2, alternative and more sensitive methods for EBER detection and quantification were identified, which were able to provide more exact quantification of EBER1 and EBER2 expression across the LCL panel.

Figure 3.7 – Densitometric analysis of Northern blotting for EBER expression levels, normalised to U4 small RNA loading control for each sample. Each sample was analysed in biological triplicate (average values presented), with technical repeats of densitometry performed for each replicate. Error bars represent standard deviation of biological replicates for each cell line.

Figure 3.8 – Example standard curves (X50-7 RNA/cDNA) used in the qRT-PCR analysis and quantification of EBER1 (A) and EBER2 (B) levels in panel of LCLs. Ct values are plotted against log of each standard with line of best fit included. Also presented are the formula and the R^2 value for each curve. Both (A) and (B) are single examples of curves that were generated alongside every experimental data set, with the analysis of each data set being reliant upon a standard curve that was produced from cDNA standards analysed in the same experimental set. GAPDH standard curves were also produced and utilised in quantification of GAPDH as the internal cellular control.

Figures 3.7 and 3.8

3.1.2.3 qRT-PCR for EBER1 and EBER2

qRT-PCR was used to measure accurately and sensitively the levels of EBER1 and EBER2 in the LCL panel. As with qPCR for EBV genome load, measurement of EBER expression was reliant upon data analysis based upon standard curves. In this instance cDNA generated from X50-7 RNA was serially diluted to generate standard curves for EBER1, EBER2 and GAPDH (as internal cellular control). Results reported are normalised to respective cellular GAPDH levels and are relative to EBER expression levels in X50-7 cells. Figure 3.8 shows example standard curves generated for EBER1 (Figure 3.8A) and EBER2 (Figure 3.8B) using the X50-7 cDNA standards. qRT-PCR analysis of EBER1, EBER2 and GAPDH levels in the LCL panel was followed by analysis using standard curves with average results for EBER expression shown in Figure 3.9. Figure 3.9A illustrates the considerable variation in levels of EBER1 expression that was observed across the LCL panel. Variation of EBER expression levels is greater than that observed using Northern blotting, confirming the highly sensitive nature of this method of EBER detection. Validity of standard curve-based quantification of EBERs was established by the analysis, as an experimental sample, of the levels of EBER1 and EBER2 in the X50-7 RNA sample. For both EBER1 and EBER2, experimental values for X50-7 RNA, relative to the value derived from the standard curve generated from X50-7 RNA, were approximately 1. Figure 3.9B reveals a similar level of variation of EBER2 expression, though variations in levels of EBER2 expression do not necessarily correlate to those seen for EBER1. This lack of correlation between levels of EBER1 and EBER2 expression in a minority of samples (most notably AO and JT) is more easily assessed when EBER1 and EBER2 expression data are analysed together in Figure 3.9C, illustrating that although in many LCLs EBER1 and EBER2 are expressed at similar levels, substantially higher levels of EBER1 than EBER2 were detected in some samples.

Figure 3.9 – qRT-PCR analysis of EBER1 (A), and EBER2 (B) levels in LCL panel. EBER1 and EBER2 data are also presented in tandem (C) to allow comparative evaluation. Average results from biological and technical triplicates normalised to internal cellular control (GAPDH) are plotted relative to X50-7 EBER1 and EBER2 levels. Error bars are representative of standard deviation of biological repeats.

Figure 3.9

3.1.3 Comparison of average EBV genome copy number and level of EBER expression

Figure 3.10 compares the average EBV genome copy number across the panel of LCLs (previously presented in Figure 3.4) with the average measured levels of EBER1 and EBER2 (previously presented in Figure 3.9) across the same panel of LCLs. From this scattergraph it is apparent that across this panel of 10 LCLs, there is no direct correlation between average EBV genome copy number and levels of EBER1 or EBER2, with no discernable trend connecting levels of EBER1 or EBER2 expression with EBV genome copy number. These data are not consistent with the hypothesis that the variation in levels of EBER expression across a panel of LCLs can be attributed to similar variation in EBV genome copy number across these cell lines.

3.2 Discussion

The above data describe the analysis of levels of EBER expression in a panel of LCLs in direct comparison with the average EBV genomic load per cell. Prior to this study, direct comparison of EBER expression and EBV copy number had not been conducted on a similar scale, and the results provide significant insight into the relationship between EBV genomic load and levels of EBER expression in LCLs.

Although the overall aims of this thesis relate to EBER expression in epithelial cells, a panel of lymphoid cells was used in these experiments. LCLs are an invaluable *in vitro* model of EBV infection and were utilised here for a number of reasons. Firstly, compared with *in vitro* EBV-positive epithelial cell systems, a large range of LCLs was readily accessible for analysis. This allowed generation of a data set large enough confidently to draw conclusions from experimental data obtained. Additionally, a large range of EBV copy numbers and levels

Figure 3.10 – Scattergraph plotting average EBV genome copy number (X-axis) against relative level of EBER1 and EBER2 expression (Y-axis) in a panel of LCLs. Average EBV genome copy numbers and EBER1 and EBER2 data are derived from qRT-PCR analysis

Figure 3.10

of EBER expression had previously been observed in a LCL panel, with an apparent correlation between the two being observed in small datasets (Dr JR. Arrand, personal communication). Consistent with this, a previous study of the rate of EBER transcription in cell lines with varying EBV genome copy number revealed a correlation between these variables (Metzenberg 1989).

Importantly, LCLs used in the analysis of EBV copy number were maintained in acyclovir-containing media, preventing any lytic outgrowth of virus. Although the percentage of lytically infected cells within an LCL population is typically very low, this small subpopulation of cells can make a significant contribution to the overall EBV DNA content of a transformed cell line, given the 100- to 1000-fold amplification of the viral genome during lytic replication (Hammerschmidt and Sugden 1988).

Southern blotting has traditionally been used in the quantification of EBV copy number in LCLs. However, given the lack of availability of a suitable internal control probe, and the very small levels of variation observed in the panel of LCLs (Figures 3.1 and 3.2) utilised in this experimental sample set, it was necessary to employ more sensitive techniques in analysis of EBV copy number. Accurate analysis of EBV genome load by qPCR has been described previously (Gallagher et al. 1999; Junying et al 2003) and this methodology was adapted for quantification of EBV copy number in the panel of LCLs. This qPCR analysis was substantially more sensitive than Southern blotting, as illustrated by the greater variation in EBV copy number results obtained using qPCR analysis (Figure 3.4). Additionally, precise quantification of average EBV genome copies per cell was possible, although this precision was heavily reliant upon the assumption that the Namalwa cells used in the generation of standard curves possessed two integrated copies of the EBV genome. Given that EBV genomes are integrated, variation in EBV copy number between cells in a Namalwa

population is minimal compared with cell lines where the genome is episomally maintained (and unequal genome segregation can occur). Confirmation that the Namalwa cells uniformly possessed two integrated EBV genome copies could have been conducted using fluorescence *in situ* hybridisation (FISH) (Shannon-Lowe et al. 2009).

Direct comparison between results obtained using Southern blotting and qPCR analysis reveals both consistency and inconsistency in results of differing analysis of the same cells lines. For instance, although using qPCR analysis, X50-7 had the lowest observed average EBV copy number, using Southern blotting, similar results were not obtained and comparable inconsistency was observed for sample HK286. However, both Southern blotting and qPCR copy number analysis revealed sample DA to have the highest average EBV copy number, and analysis by each method of several other LCLs showed comparable results.

The levels of variation in average copy number as measured by qPCR were comparable with variation previously reported, with up to 10-fold differences in average EBV copy number being found. Previously, much higher copy number LCLs had been reported (e.g. Metzenberg (1990)), however such high copy number LCLs were not present in the sample set used here. It would be interesting to analyse such high copy number LCLs for both copy number and EBER expression, to elucidate if in such extreme cases high copy number consistently led to high levels of EBER expression.

Analysis of EBV copy number was carried out for the average number of genome copies per cell. However, within an LCL population, EBV copy number heterogeneity exists due to occasional inequality in EBV episome segregation. As such, the average value obtained cannot be applied to each cell in the population, as some cells may carry many fewer episomes than the average number, and others many more. Assessment of LCL heterogeneity

for EBV genome copy number was not conducted in the panel of LCLs analysed, and it would be valuable to carry out FISH analysis to examine the full extent of variation in EBV copy number from cell to cell, within each LCL of the panel analysed by qPCR.

Initial attempts at analysis of EBER expression levels using FACS analysis were not successful. As briefly discussed in the results section, this method of EBER detection was not able to distinguish between cell populations expressing low levels of EBERs and those where expression was entirely absent (Figure 3.5). However, FACS analysis of EBER expression remains a valuable tool in quantification of the number/percentage of EBER-positive cells within a population, and indeed sorting of EBER-positive populations of cells, providing levels of EBER expression are sufficient to be detected.

Northern blotting analysis was successful in quantification of EBER expression levels across the LCL panel, although lack of resolution meant levels were determined as a single value, rather than separate values for EBER1 and EBER2 expression. Adaptation of experimental procedures may have resulted in increased resolution; however alternative (and more sensitive) methods of EBER detection (RT-qPCR) were employed in place of validation of adapted experimental procedures. Analysis of EBER levels by Northern blotting was perhaps more reliable than Southern blotting quantification of EBV copy numbers, given the use of small nuclear control U4. This allowed normalisation of data to an internal cellular control, meaning any discrepancies in loading were overcome. Sensitivity of Northern blotting was not sufficient to allow detection of EBER expression in Namalwa cells (Figures 3.6 and 3.7), suggesting not only that low levels of EBER could not be detected, but also that any small differences in EBER expression would not be quantified using this method of analysis.

RT-qPCR analysis of EBER expression levels proved to be accurate and sensitive, resulting in quantified levels of both EBER1 and EBER2 for each LCL. Data were generated using standard curves based upon serial dilutions of X50-7 cDNA, and as such results were relative to EBER expression levels in X50-7 cells. Analysis of X50-7 RNA as an experimental sample was conducted, with relative levels of expression of EBER1 and EBER2 found to be around 1 (Figure 3.9), demonstrating accuracy and reliability of RT-qPCR analysis of EBER expression. EBER expression analysis was also more sensitive using RT-qPCR, with Namalwa EBER expression being detected (data not shown, levels of EBER1 were 0.06-fold of X50-7 levels, EBER2 levels were 0.05-fold of X50-7 RNA levels). Additional evidence of increased sensitivity is provided by the greater variation in results for EBER expression from RT-qPCR experiments, compared with Northern blotting. However, the panel of LCLs was not identical for both these sets of experiments, and sensitivity of Northern blotting results may have been diminished by the lack of separate detection of EBER1 and EBER2.

Separate analysis of EBER1 and EBER2 levels allowed comparative evaluation of EBER1 and EBER2 levels in individual LCLs. Previously, conflicting data have been produced from such evaluation, with some studies finding EBER1 expressed at higher levels than EBER2 (e.g. Metzenberg (1989)), and others reporting EBER2 is expressed at higher levels than EBER1 (e.g. Jat and Arrand (1982)). Comparative evaluation of EBER1/2 levels across this LCL panel was also conflicting, with some samples showing substantially greater expression of EBER1 than EBER2 relative to X50-7 (e.g. samples AO, JT), though the majority of samples showed similar levels of EBER1 and EBER2 expression, again relative to X50-7. Given these findings, it can be concluded that the majority of LCLs in the panel express EBER1 and EBER2 in a similar ratio to X50-7, though this ratio is not identified. If Northern blotting resolution had been sufficient to allow separate detection of EBER1 and EBER2,

evaluation of EBER1:EBER2 expression ratio could have been conducted. Comparative levels of EBER1 and EBER2 expression are significant, given reports of each RNA possessing specific and diverse roles within EBV latent infection (Wu et al. 2007).

As with qPCR for EBV copy number, it should be noted that average levels of EBER expression were analysed and that levels of EBER expression in individual cells within an LCL population vary. Assessment of EBER expression heterogeneity was not conducted, and it would be valuable to carry out ISH analysis of EBER expression to examine the full extent of variation in EBER levels from cell to cell within each LCL of the panel analysed by RT-qPCR.

RT-qPCR analysis of the levels of EBER expression in LCLs was carried out following the generation of gene-specific cDNA, as outlined in the methods section of this thesis (see Section 2.20). It should be noted that by using gene specific cDNA in the assay, the analysis of levels EBER expression is dependent upon the reliability of generation of specific cDNA for EBER1, EBER2 and GAPDH genes, as variability in the generation of any of these gene-specific cDNAs would lead to discrepancies in the final analysis of levels of EBER expression.

Ultimate comparison of EBER expression levels with average EBV copy number across the panel of LCLs revealed no correlation between the two variables (Figure 3.10). This finding conflicts with expectations from previous data illustrating increasing the number of EBER genes substantially increased EBER expression levels (Komano et al. 1999). However, such data were produced using consecutive copies of the EBER genes in a single expression vector, compared with multiple copies of the EBER genes carried on separate EBV episomes, as was the case in the analysis presented above. Previously published data had reported a

correlation between EBV copy number and rate of EBER transcription in a very small panel of LCLs (Metzenberg 1989). Data reported in this study seem to be in conflict with such reports, assuming equal rates of EBER degradation. Given the larger experimental sample set and more sensitive methods of analysis of both EBER expression and EBV copy number, confidence is afforded that the data presented in this chapter are reliable, and that in this panel of LCLs at least, no correlation between average EBV genome copy number and levels of EBER expression existed. This lack of correlation of EBV genome copy number and latent gene product expression has precedence, with previous studies having demonstrated a lack of correlation between levels of several EBV latent gene products and EBV copy number (Metzenberg 1989; 1990; Sternas et al. 1990).

Analysis of EBER levels in comparison to EBV genomic DNA levels is of interest in clinical situations, given that the gold standard assay for EBV infection in tumour biopsies targets EBERs by *in situ* hybridisation in paraffin-embedded tissue sections (Gulley 2001; Gulley and Tang 2008). In gastric adenocarcinoma, levels of EBV DNA levels are reported generally to reflect EBER status (Ryan et al. 2009). However, the sensitivity of EBER staining in detection of EBV-positive tumours has been questioned following molecular and immunohistochemical assays revealing that EBV is present in some EBER-negative tumours (Lauritzen et al. 1994; Chen et al. 2002; Gan et al. 2002; Grinstein et al. 2002; Korabecna et al. 2003). Findings presented here demonstrating no direct correlation between EBV genome copy number and levels of EBER expression *in vitro* are perhaps of interest when considering methods of EBV detection in tumour samples.

The lack of correlation between EBV genome copy number and levels of EBER expression reported in this chapter enhanced the necessity to examine other factors involved in the regulation of EBER expression. Given that EBV has been shown to induce EBER-associated

cellular transcription factors (Felton-Edkins et al. 2006), subsequent chapters examine mechanisms by which EBV is able to enhance EBER expression in epithelial cells, and which latent gene product may be responsible for induction of EBER expression during EBV latent infection.

Chapter 4

EBNA1 induces EBER expression through EBER-associated cellular transcription factors

Chapter 4 – EBNA1 induces EBER expression through EBER-associated cellular transcription factors

Several oncogenic viruses, including EBV, have been demonstrated to stimulate RNA polymerase III (pol III)-mediated transcription by the induction of increased levels of pol III-specific transcription factors (Hoeffler et al. 1988; Gottesfeld et al. 1996; Wang et al. 1997b; Larminie et al. 1999; Felton-Edkins and White 2002; Felton-Edkins et al. 2006), as outlined in Section 1.7.8.1.1. In addition, EBER-associated transcription factors c-Myc and ATF-2, (Figure 1.3) which are more often associated with RNA polymerase II (pol II) transcription, are also influenced by a number of viral factors. Adenovirus E1A associates with the chromatin regulator p400 promoting its interaction with c-Myc. This interplay between c-Myc and p400 has two important consequences: (1) stabilisation of c-Myc through interfering with its ubiquitylation; (2) promotion of complex formation between c-Myc and p400 on c-Myc target genes, resulting in their activation. As such, E1A is able to elicit, in part, a c-Myc-like cellular response that contributes to adenovirus function in apoptosis and cellular transformation (Chakraborty and Tansey 2009). The HBV X protein has also recently been demonstrated to upregulate expression of c-Myc in HepG2 cells, with this upregulation in expression being shown to correlate with increased cell proliferation (Yang et al. 2008). The small T-antigen of SV40 virus has been found to inactivate protein phosphatase 2A (PP2A), which dephosphorylates c-Myc at Ser62 before ubiquitination, therefore exerting its oncogenic potential through preventing the dephosphorylation of c-Myc, resulting in its stabilisation (Yeh et al. 2004). Further, the HCV ARFP/F protein has been demonstrated to enhance the gene trans-activation activity of c-Myc, apparently by antagonising the inhibitory effect of c-Myc interacting protein MM-1 (Ma et al. 2008) and HPV proteins E6 and E7 have

both been identified as interacting with c-Myc complexes and mediating c-Myc transcriptional activity (McMurray and McCane 2003; Patel et al. 2004).

Human herpesviruses are also known to influence c-Myc, in terms of both stability and function. KSHV's EBNA1 homologue LANA acts to stabilise c-Myc, preventing phosphorylation of c-Myc at Thr58 (Bubman et al. 2007; Liu et al. 2007), and independently stimulates phosphorylation of c-Myc at Ser62, an event which transcriptionally activates c-Myc (Liu et al. 2007). Further, KSHV encodes a homologue of cellular interferon regulatory factor vIRF-3 which has been shown to have a direct involvement in the activation of c-Myc-mediated transcription (Lubyova et al. 2007).

Several human tumour viruses have been demonstrated to affect ATF-2 levels and functional activity, and to influence the AP-1 transcription factor family. Various members of the AP-1 and ATF/CREB families of transcription factors, including c-Jun, are targets for the adenovirus E1A protein. E1A stimulates transcription regulated by c-Jun/ATF-2 heterodimers through increasing levels of phosphorylated c-Jun (Hagmeyer et al. 1995). The core protein of HCV has recently been demonstrated to increase AP-1 transcription factor levels, and induce ATF-2 in hepatoma cell lines (Hassan et al. 2009), with the X protein of HBV also known to interact with ATF-2 (Zhang et al. 2006) Reoviruses are known to be capable of AP-1 induction (Tyler et al. 2001). In human herpesviruses, early infection with KSHV has been demonstrated to induce several cellular transcription factors including ATF-2 and c-Jun (Sharma-Walia et al. 2005), whilst EBV is known to induce levels of AP-1. Firstly, LMP1 has been demonstrated to activate c-Jun/AP-1 and ATF-2 (Kieser et al. 1997; Eliopoulos et al. 1999) and more recently EBNA1 has been shown to induce both the transcription of the genes, and activity of the proteins, of members of the AP-1 family, including ATF-2 (O'Neil et al. 2008). Another recent study reported increased levels of ATF-2 in EBV-infected B-lymphocytes and epithelial cells (Felton-Edkins et al. 2006).

Given that EBV stimulates polIII transcription and the observation that EBERs are temporally the last EBV latent gene products to be expressed following EBV infection of a B-lymphocyte (Rooney et al. 1989; Alfieri et al. 1991), it is tempting to propose that an EBV latent gene product could be involved in the regulation of EBER expression through the induction of EBER-associated cellular transcription factors. In addition to EBNA1's ability to to induce the transcription of the genes and the activity of the proteins of members of the AP-1 family (O'Neil et al. 2008), it is also known to have transcriptional regulatory properties on the viral Cp, Qp and LMP1 promoters (Sugden and Warren 1989; Sample et al. 1992; Gahn and Sugden 1995). Further, previously published Affymetrix array analysis (Wood et al. 2007) revealed an induction of RNA encoding the 102kd subunit of TFIIIC (TFIIIC-102) in response to EBNA1, indicating that this EBV latent gene product may be responsible for TFIIIC induction.

This chapter explores the hypothesis that EBNA1 may be the EBV latent gene product involved in the regulation of both classic pol II and pol III transcription factors associated with EBER expression, and that expression of EBNA1 leads to increased transcription of the EBERs.

4.1 Results

4.1.1 Generation of Ad/AH-Puro and Ad/AH-Puro-EBERs cell lines

In order to study the effect of EBNA1 upon EBER expression, cells were generated which expressed EBER1 and EBER2 (from their native promoters) in the absence of EBNA1, enabling the impact of EBNA1 expression in these cells to be investigated. To achieve this, a non-*OriP*-based system for EBER expression was required, ensuring that EBNA1 was not required for EBER plasmid maintenance. Such an expression vector was constructed using pUC19 as a plasmid backbone. It was appropriate to include a drug resistance cassette in the

expression vector, given the goal of generating a polyclonal population of cells that stably express the EBERs. The first step of the cloning procedure for this expression vector was insertion of a puromycin resistance cassette into pUC19. The puromycin drug resistance marker was chosen due to the high sensitivity of Ad/AH cells to puromycin, along with the consideration that expression vectors with other drug resistance cassettes would be used in conjunction with this expression vector in later experiments. The puromycin resistance cassette (1.2kb) was excised by SalI endonuclease digestion from pOTEII GFP-HUMPU before ligation of the insert into pUC19 vector that had been linearised with the same restriction endonuclease. Diagnostic cuts were used to screen miniprep DNA taken from bacterial colonies, with SalI acting to excise the inserted puromycin cassette, (Figure 4.1). The generated plasmid is subsequently referred to as pUC19-Puro.

pUC19-Puro-EBERs plasmid was generated by insertion of the 1kb SacI-EcoRI sub-fragment from the EcoRI-J fragment of the EBV genome into corresponding SacI and EcoRI sites located within the multiple cloning site (MCS) of pUC19-Puro. Diagnostic cuts were once again used to screen miniprep DNA, with EcoRI and SacI endonuclease digestion yielding fragments of 3.9 kb and 1kb (Figure 4.2).

Purified pUC19-Puro-EBERs plasmid DNA was subsequently transiently transfected into Ad/AH cells to assess EBER1 expression levels. RT-PCR analysis (Figure 4.3A) revealed titratable increases in the level of EBER1 expression upon transient transfection of increasing amounts of pUC19-Puro-EBERs into Ad/AH cells, indicative of EBER expression from the pUC19-Puro-EBERs vector in the absence of EBNA1. The plasmid map for pUC19-Puro-EBERs is given in Figure 4.3B.

Following demonstration of transient EBER expression from the pUC19-Puro-EBERs vector (Figure 4.3A), this construct was used to generate a polyclonal population of cells stably

Figure 4.1 – Restriction endonuclease analysis of pUC19-Puro construct miniprep DNA. SalI digestion of DNA yields 2.7Kb and 1.2Kb fragments, confirming the insertion of the 1.2Kb puromycin resistance cassette (from pOTEII GFP-HUMPU) into the pUC19 vector.

Figure 4.2 – Restriction endonuclease analysis of pUC19-Puro-EBERs construct miniprep DNA. Digestion of plasmid DNA with SacI and EcoRI endonucleases yields fragments of 3.9Kb and 1Kb, confirming the insertion of the EcoRI-J fragment into the pUC19-Puro construct.

Figure 4.3A – RT-PCR analysis confirming the expression of EBER1 in Ad/AH parental cells following transient expression of pUC19-Puro-EBERs (lanes 2-5). Cells were transfected with increasing amounts of plasmid DNA (from 0.1µg to 1µg), with RNA harvest at 24 hours post-transfection, followed by cDNA synthesis and RT-PCR analysis. EcoRI-J plasmid (lane 6) was used as a transient control, with untransfected Ad/AH-rEBV cells (which stably express EBER1 at a high level) also included as a further positive control.

Figure 4.3B (Plasmid Map) – Plasmid map detailing the significant elements of pUC19-Puro-EBERs plasmid. EcoRI-J fragment (EBERs and upstream regulatory region) and puromycin resistance cassette are presented as red arrows, with accompanying text highlighted.

Figures 4.1-4.3

expressing EBERs. Before drug selection for a population of EBER-expressing cells, the appropriate concentration of puromycin with which to treat Ad/AH cells to allow selection was ascertained. Figure 4.4 shows crystal violet staining of Ad/AH cells following treatment with increasing amounts of puromycin. Results indicate that 0.5µg/ml of puromycin was required for complete cell death of non-drug-resistant Ad/AH cells. Following transfection of Ad/AH cells with 0.5µg pUC19-Puro-EBERs (or control plasmid pUC19-Puro), cells were left untreated for 48 hours to allow expression of the puromycin acetyl transferase (PAC) gene. 48 hours post-transfection, cells were treated with 0.5µg/ml puromycin for 2 weeks before RNA was harvested from a population of cells and RT-PCR analysis of EBER1 and EBER2 expression was undertaken (Figure 4.5). The Ad/AH-Puro-EBERs cell line is demonstrated to express stably both EBER1 and EBER2, with Ad/AH-Puro cells expressing neither EBER1 nor EBER2.

As clonal selection was not employed in the generation of Ad/AH-Puro-EBERs, a polyclonal population of cells was present. As such, it was unclear (from RT-PCR analysis) if the polyclonal population of cells was highly heterogeneous for EBER expression, and contained few, highly EBER-positive cells, or if the population was more uniform with the majority of cells being weakly EBER-positive. To determine the heterogeneity of EBER expression in Ad/AH-Puro-EBERs cells, *in situ* EBER hybridisation was carried out (Figure 4.6). Panels A and B show *in situ* EBER staining in Ad/AH and Ad/AH-rEBV cells respectively. Strong nuclear staining for EBERs was observed in Ad/AH-rEBV cells, with only background staining, equivalent to staining seen with use of a negative control (sense strand) probe (panels E-H) seen in Ad/AH parental cells. Similar negative staining was seen in Ad/AH-Puro cells (panel C). Panel D reveals nuclear staining for EBERs in Ad/AH-Puro-EBERs cells. Fairly uniform staining is seen across all cells in this population, although levels of EBER expression are significantly lower than those observed in Ad/AH-rEBV cells. Ad/AH-

Figure 4.4 – Crystal violet staining of Ad/AH parental cells treated with varying amounts of puromycin, ranging from 0.1µg/ml to 0.5µg/ml. Puromycin was added to growth media for 48 hours before cell fixation with 3.5% paraformaldehyde and crystal violet staining of viable cells. Images are presented at 40x magnification.

Figure 4.5 – RT-PCR analysis of EBER1 and EBER2 expression in Ad/AH cells stably transfected with pUC19-Puro and pUC19-Puro-EBERs constructs (following puromycin drug selection). No Reverse Transcriptase (No RT) control refers to RNA samples taken from Ad/AH-Puro-EBERs cells and subjected to standard cDNA procedures with the RT omitted (ensuring no cDNA is made). This cDNA-free control enables the demonstration that EBER1 and EBER2 primers used in the PCR assay are detecting RNA products of vector plasmid DNA, and not the plasmid DNA template itself.

Figure 4.6 – A-D: *In situ* EBER staining of Ad/AH (A), Ad/AH-rEBV (B), Ad/AH-Puro (C) and Ad/AH-Puro-EBERs (D) cells. E-H Negative-control probe staining of Ad/AH (E), Ad/AH-rEBV (F), Ad/AH-Puro (G), and Ad/AH-Puro-EBERs (H) cells. Images were captured at a magnification of 60X (Panels A-D) or 40X (Panels E-H).

Figures 4.4-4.6

Puro-EBERs cells are therefore characterised as a polyclonal population of cells, with stable, fairly homogeneous low levels of EBER expression.

4.1.2 Analysis of RNA polymerase III transcription in EBNA1-expressing epithelial cells

The effect of EBNA1 expression on RNA polymerase III transcription was examined using a panel of epithelial cells (Ad/AH, AGS and Hone-1) which stably expressed either an empty vector (with neomycin drug resistance - neo) or EBNA1. In some instances, rEBV-infected cells of these lineages were used in the analysis of EBNA1 function. Validation of EBNA1 expression levels in cell lines was conducted using immunofluorescence staining. Fluorescence microscopy images are presented in Figure 4.7.

Previously EBV has been demonstrated to induce pol III activity via enhancement of TFIIIC expression in both lymphoid and epithelial cells (Felton-Edkins et al. 2006), although the viral gene product responsible for this induction remained unidentified. Previously published Affymetrix array analysis (Wood et al. 2007) revealed a 2.6-fold induction of RNA encoding the 102kd subunit of TFIIIC (TFIIIC-102) in response to EBNA1, indicating that this EBV latent gene product may be responsible for TFIIIC induction. Initial studies aimed to replicate results previously reported (Felton-Edkins et al. 2006), and investigate the role of EBNA1 in the induction of EBER-associated transcription factors. Figure 4.8 shows semi-quantitative RT-PCR analysis (followed by Southern blotting) of levels of three cellular pol III transcripts, 7SL RNA, 5S rRNA and $tRNA^{Tyr}$, in Akata BL and Ad/AH EBV-negative and -positive cell lines, along with Ad/AH-neo and -EBNA1 cells. The data presented were generated following preliminary experiments which determined the linear range of PCR amplification for each transcript analysed. In agreement with previous data, levels of all three cellular pol III transcripts were increased in both epithelial and lymphoid cells infected with EBV. In Ad/AH-EBNA1 cells, levels of all three cellular pol III transcripts were enhanced to a similar level, compared with Ad/AH-neo control cells. In addition to

Figure 4.7 – Immunofluorescence staining for EBNA1 in epithelial cell panel: (A) Ad/AH Parental; (B) Ad/AH-rEBV; (C) Ad/AH-neo c.1; (D) Ad/AH-EBNA1 c.3; (E) AGS-neo; (F) AGS-EBNA1; (G) Hone-1-neo; (H) Hone-1-EBNA1. Images shown are at 100X magnification.

Figure 4.7

Figure 4.8 – Semi-quantitative RT-PCR followed by Southern blotting to analyse the levels of cellular pol III-transcribed genes 7SL RNA, 5S rRNA and $tRNA^{tyr}$ in EBV-negative and EBV-positive Akata BL, Ad/AH parental, Ad/AH-rEBV, Ad/AH-neo c.1 and Ad/AH-EBNA1 c.3 cells. The cellular housekeeping gene GAPDH is included as an internal RNA polymerase II-transcribed control.

Figure 4.9 – RT-PCR analysis of TFIIIC subunit (TFIIIC-220, -110, -102, -90 and -63) mRNA levels in Ad/AH, AGS and Hone-1 cells stably expressing EBNA1 or a neomycin control cassette. Levels of EBNA1 mRNA are also assessed by RT-PCR. GAPDH is included as an internal cellular control.

Figures 4.8 and 4.9

confirming previously reported results, these data reveal that EBNA1 may be responsible, at least in part, for increased expression of endogenous pol III products induced by EBV.

Subsequent analysis of pol III transcription factors was conducted in EBNA1-expressing derivatives of three distinct epithelial carcinoma cell models (Ad/AH, AGS and Hone-1) to examine mechanisms by which EBNA1 could induce expression of cellular pol III transcripts. Initial studies centred on TFIIIC subunits, given that previous microarray analysis had revealed transcriptional induction of TFIIIC subunits in EBNA1-expressing cells (Wood et al. 2007) and that EBV has been demonstrated to induce pol III activity via TFIIIC expression (Felton-Edkins et al. 2006). RT-PCR analysis of the levels of RNA encoding the five TFIIIC subunits previously shown to be EBV responsive (TFIIIC-220, -110, -102, -90 and -63) was conducted across the epithelial cell panel and results are presented in Figure 4.9. Transcriptional induction of TFIIIC subunits varied, but was observed for multiple subunits in EBNA1-expressing derivatives of each cell line, at levels similar to those previously observed in EBV-infected epithelial cells (Felton-Edkins et al. 2006). In each cell line, EBNA1 was found to raise the expression of at least two TFIIIC subunits, with induction of TFIIIC subunits being most pronounced in cells of the Ad/AH lineage. Analysis of the levels of TFIIIC subunit proteins was restricted by a lack of suitable antibodies. However, immunoblotting for TFIIIC-110, -102 and -90 was conducted in Ad/AH-neo and -EBNA1 cells (Figure 4.10) and revealed induction of all three subunits in Ad/AH-EBNA1 cells.

In contrast to the TFIIIC data, and in agreement with the array analysis of Ad/AH-neo and Ad/AH-EBNA1 cells (Wood et al. 2007), there was no consistent increase in the RNA encoding TFIIIB transcription factors Bdp1, Brf1 and TBP across epithelial cell lines expressing EBNA1, as shown by RT-PCR (Figure 4.11) suggesting that EBNA1 can have a selective effect on the expression of TFIIIC. Such data are in agreement with previously

Figure 4.10 – Immunoblot analysis of the levels of TFIIIC-110, -102 and -90 in Ad/AH-neo and EBNA1 cells. Immunoblotting for EBNA1 is also shown, with β-Actin included as a loading control.

Figure 4.11 – RT-PCR analysis showing mRNA levels of TFIIIB subunits Bdp1, Brf1 and TBP in Ad/AH, AGS and Hone-1 cells stably expressing EBNA1 or neomycin control cassette. EBNA1 mRNA levels were also assessed and GAPDH was included as an internal cellular control.

Figures 4.10 and 4.11

published work showing that there was no consistent increase in levels of TFIIIB subunit mRNA across a panel of EBV-infected cells (Felton-Edkins et al. 2006).

To examine more precisely the levels of TFIIIB and TFIIIC subunit mRNA expression in Ad/AH, AGS and Hone-1 cells expressing EBNA1, RT-qPCR was conducted (Figure 4.12). This sensitive quantitative analysis afforded further confidence in results previously obtained, and enabled quantification of the changes in levels of expression of TFIIIB and TFIIIC subunit mRNA between neo control cells and EBNA1-expressing cells. In general, results obtained using RT-qPCR mirrored those seen using RT-PCR analysis, with no significant fold-change increase in expression seen for TFIIIB subunit mRNAs in EBNA1-expressing cells. In AGS-EBNA1 cells, a statistically significant increase in the expression of two TFIIIC subunit mRNAs (TFIIIC-220 and -110) was observed, compared with AGS-neo cells. However, more consistent significant increases in expression of TFIIIC subunit mRNA were observed in both Ad/AH and Hone-1 cells expressing EBNA1. RT-qPCR analysis of Ad/AH-EBNA1 cells revealed significantly greater levels of mRNA for all TFIIIC subunits examined except TFIIIC-63, a result consistent with RT-PCR analysis (Figure 4.9). Analysis of Hone-1-EBNA1 cells revealed, without exception, significantly greater levels of mRNAs for all TFIIIC subunits examined. These data are not in complete agreement with RT-PCR data (Figure 4.9), which suggested a less consistent induction of TFIIIC subunit mRNA levels in EBNA1-expressing Hone-1 cells. However, given the greater sensitivity of RT-qPCR compared with the qualitative analysis provided by RT-PCR and the reproducibility of the quantitative data, it is likely that a consistent induction of all TFIIIC subunit mRNAs does occur in Hone-1-EBNA1 cells. It is noted that the magnitude of fold change in TFIIIC subunit mRNA levels is fairly low, between 1.5 and 2 in all cases. Despite this modest increase in expression levels, the statistical analysis revealing significance confirms the importance of these quantitative data in reinforcing results seen using RT-PCR analysis.

Figure 4.12 – RT-qPCR analysis of levels of expression of TFIIIC and TFIIIB subunit mRNA in Ad/AH, AGS and Hone-1 cells stably expressing EBNA1 or neomycin control cassette. Fold change values are between neo control cells and EBNA1-expressing cells. All RT-qPCR data are means of three biological replicates analysed in technical triplicate. Error bars represent the standard deviation in fold change between biological replicates. Asterisks indicate that the fold change between neo control and EBNA1 cells is statistically significant, as determined by the student T-test. *$P \leq 0.05$; **, $P \leq 0.01$. Also included in the figure is the RT-PCR analysis from Figures 4.9 and 4.11 for easy comparison of qualitative and quantitative data sets.

Figure 4.12

Consistent with data shown in Figure 4.8, induction of cellular pol III transcripts 7SL RNA, 5S rRNA and $tRNA^{Tyr}$ was demonstrated by RT-PCR analysis in EBNA1-expressing derivatives of the panel of epithelial cells (Figure 4.13). Densitometric analysis of these data and comparative analysis of data from Felton-Edkins and co-workers confirmed that levels of induction in EBNA1-expressing cells, and EBV-infected cells were comparable. Increases in each pol III-transcribed gene from uninfected to EBV-infected cells, and from neo- to EBNA1-expressing cells, was measured as being between 1.5- and 2-fold in each instance. These data confirm the apparent downstream significance of the induction of TFIIIC subunit expression observed across EBNA1-expressing epithelial cell lines.

4.1.3 Analysis of EBER-associated RNA polymerase II (pol II) transcription factors in EBNA1-expressing epithelial cells

As previously discussed in the introductory section, although the EBERs are transcribed exclusively by pol III, the EBER promoter regions contain a hybrid of pol II and pol III elements. Pol II elements of EBER promoters are well characterised, and include a TATA-box, Sp1 and ATF-2 binding sites (Howe and Shu 1989; 1993; Felton-Edkins et al. 2006), and EBER1 (although not EBER2) possesses two E-boxes upstream of its transcriptional start site (see Figure 1.3), to which c-Myc has been demonstrated to bind (Niller et al. 2003). The pol II elements of EBER promoter regions have been shown by several studies to be necessary to allow high levels of EBER expression to occur (Howe and Shu 1989; 1993; Wensing et al. 2001), although some evidence suggests that the c-Myc binding site upstream of EBER1 is dispensable (Wensing et al. 2001).

Having established EBNA1's ability to affect typical cellular pol III transcription factors involved in EBER expression, this study went on to examine the role of EBNA1 in the

Figure 4.13 – RT-PCR analysis of the levels of cellular polIII-transcribed genes $tRNA^{tyr}$, 5S rRNA and 7SL RNA in Ad/AH, AGS and Hone-1 cells stably expressing EBNA1 or a neomycin control cassette. EBNA1 mRNA levels were also analysed with GAPDH included as an internal cellular control.

Figure 4.14 – Immunoblotting for cellular transcription factor Sp1 in Ad/AH parental, Ad/AH-rEBV and Ad/AH-EBNA1 cells. β-Actin is included as a loading control, and EBNA1 immunoblot analysis illustrates the level of EBNA1 expression in each cell line.

Figures 4.13 and 4.14

regulation of typical pol II cellular transcription factors known to be involved in the regulation of EBER expression.

4.1.3.1 Sp1

Immunoblotting analysis revealed levels of Sp1 protein were unchanged by rEBV infection or EBNA1 expression in Ad/AH cells (Figure 4.14), suggesting that EBNA1 does not influence EBER expression through Sp1 regulation.

4.1.3.2 ATF-2

ATF-2 has previously been identified as an EBER-associated typical pol II transcription factor that is upregulated in EBV-infected epithelial cells and, in addition, it is known to bind and activate the promoter of the gene encoding TFIIIC-220 (Felton-Edkins et al. 2006). Further, ATF-2 induction in EBNA1-expressing epithelial cells has been demonstrated (O'Neil et al. 2008). RT-PCR analysis (Figure 4.15) confirmed a robust induction of ATF-2 mRNA in a panel of EBNA1-expressing epithelial cells. Subsequent immunoblot analysis of levels of total ATF-2 protein in the same panel of EBNA1-expressing cells (Figure 4.16) showed induction of ATF-2 protein in Ad/AH-EBNA1 and AGS-EBNA1 cells, although no induction of ATF-2 protein levels was observed in Hone-1-EBNA1 cells. In agreement with these data, immunofluorescence staining for total and dual-phosphorylated (and activated) ATF-2 in Ad/AH, Ad/AH-rEBV and Ad/AH-EBNA1 cells revealed robust induction in the levels of total and dual-phosphorylated ATF-2 in Ad/AH-EBNA1 cells (Figure 4.17), with levels of induction observed being at least the equivalent of those seen in Ad/AH-rEBV cells and similar to levels seen upon TPA treatment of Ad/AH cells. Further immunoblot analysis of ATF-2 levels in Ad/AH cells (Figure 4.18) revealed not only a robust increase in levels of total ATF-2 in Ad/AH-EBNA1 cells, but also confirmed that significant induction of mono-(Thr71) and dual-phosphorylated (Thr69/71) ATF-2 occurs.

Figure 4.15 – RT-PCR analysis of ATF-2 mRNA levels in Ad/AH, AGS and Hone-1 cells stably expressing EBNA1 or a neomycin control cassette. EBNA1 mRNA levels were also assessed and GAPDH is included as an internal cellular control.

Figure 4.16 – Immunoblotting for total levels of ATF-2 in Ad/AH, AGS and Hone-1 cells stably expressing EBNA1 or neomycin control cassette. β-Actin is included as a loading control, with EBNA1 immunoblotting illustrative of EBNA1 levels in the cell lysates.

Figures 4.15 and 4.16

Figure 4.17 – Immunofluorescence staining for total and dual-phosphorylated ATF-2 in Ad/AH cells. **A-D**: Immunofluorescence for total ATF-2 in Ad/AH (A), Ad/AH-rEBV (B), Ad/AH-neo c.1 (C) and Ad/AH-EBNA1 c.3 (D) cells; **E-H**: Immunofluorescence for dual-phosphorylated ATF-2 (Thr69 and Thr71) in Ad/AH (E), Ad/AH-rEBV (F), Ad/AH-EBNA1 c.3 (G) and TPA stimulated Ad/AH (H) cells. Images shown are at a magnification of 400X.

Figure 4.17

Figure 4.18 – Immunoblot analysis of total ATF-2, mono-phosphorylated (Thr71) ATF-2 and dual-phosphorylated (Thr69/Thr71) ATF-2 in Ad/AH-neo and Ad/AH-EBNA1 cells. β-Actin is included as a loading control and levels of EBNA1 expression in cell lysates is also shown.

Figure 4.19 – RT-PCR analysis of the level of ATF-2 mRNA in Ad/AH-rEBV cells following transient transfection of cells with shRNA targeted against ATF-2. Along with a pSG5 transfection control, a titration of shRNA against ATF-2 from 0.5µg to 2.5µg was transfected into Ad/AH-rEBV cells, with RNA samples taken 72 hours post transfection for analysis. GAPDH is included as an internal cellular control.

Figure 4.20 - RT-PCR analysis of levels of EBER1 and EBER2, and ATF-2 mRNA in Ad/AH-rEBV cells following transient transfection of cells with 2.5µg shRNA targeted against ATF-2. Data are representative of experiments conducted in at least biological triplicate.

Figures 4.18-20

To assess the impact of EBNA1-mediated induction of ATF-2 upon EBER expression, a converse approach was adopted, transiently expressing shRNA against ATF-2 in Ad/AH-rEBV cells before analysing consequential levels of EBER1 and EBER2. Figure 4.19 shows RT-PCR conducted following an initial titration of shRNA against ATF-2 into Ad/AH-rEBV cells. Reduction in levels of ATF-2 was titratable, with the greatest reduction in levels of ATF-2 mRNA being observed with transfection of 2.5µg of expression vector DNA. Figure 4.20 is representative of multiple RT-PCR assays for EBER1 and EBER2 levels in Ad/AH-rEBV cells following transient expression of 2.5µg shRNA to ATF-2. shRNA targeting ATF-2 robustly reduced ATF-2 expression (measured as a 2-fold reduction in levels by densitometry) and, as a result, expression of both EBER1 and EBER2 was significantly diminished (by 3.5- and 3.1-fold respectively, by densitometric analysis). Such data confirm the importance of ATF-2 in the regulation of EBER expression in epithelial cells.

To influence EBER expression, nuclear location of ATF-2 is necessary. To confirm increased levels of nuclear ATF-2, nuclear and cytosolic fractions of Ad/AH-neo and Ad/AH-EBNA1 cell lysates were taken for immunoblot analysis, the results of which are seen in Figure 4.21. A clear increase in the levels of nuclear ATF-2 is observed in the Ad/AH-EBNA1 nuclear lysate, compared with the Ad/AH-neo nuclear lysate, with little cytosolic ATF-2 present in both Ad/AH-neo and Ad/AH-EBNA1 samples.

4.1.3.3 c-Myc

c-Myc has been shown to bind to E-box sites upstream of the EBER1 gene (Niller et al. 2003), and through its interaction with TFIIIB, c-Myc can directly activate many cellular pol III-transcribed genes (Gomez-Roman et al. 2003). Further, transcriptional induction of c-Myc has been demonstrated in EBNA1-expressing Ad/AH cells (Wood et al. 2007). Confirmation of this upregulation is shown by RT-PCR analysis (Figure 4.22), with levels of c-Myc mRNA

Figure 4.21 – Immunoblot analysis of total levels of ATF-2 in nuclear and cytosolic extracts, taken from Ad/AH-neo and EBNA1 cells. Sp1 and tubulin are nuclear and cytosolic proteins respectively and immunoblot analysis of levels of these proteins is included to demonstrate successful separation of nuclear and cytosolic fractions of cell lysates.

Figure 4.22 – RT-PCR analysis of c-myc mRNA levels in Ad/AH, AGS and Hone-1 cells stably expressing EBNA1 or neomycin control cassette. EBNA1 mRNA levels are also assessed with GAPDH included as an internal cellular control.

Figure 4.23 – Immunoblot analysis of total levels of c-Myc in Ad/AH-neo, Ad/AH-EBNA1 and Ad/AH-rEBV cells. β-Actin is included as a loading control and levels of EBNA1 expression are also shown.

Figures 4.21-4.23

in AGS and Hone-1-neo and -EBNA1 cells also assayed. Although induction of c-Myc mRNA was confirmed in Ad/AH-EBNA1 cells, no such induction was observed in AGS or Hone-1-EBNA1 cells.

Immunoblot analysis of c-Myc protein levels was conducted in Ad/AH-neo, Ad/AH-EBNA1 and Ad/AH-rEBV cells (Figure 4.23). Intriguingly, despite induction of mRNA in Ad/AH-EBNA1 cells, levels of c-Myc protein were robustly reduced in both Ad/AH-EBNA1 and Ad/AH-rEBV cells, compared with levels observed in Ad/AH-neo cells.

To assess if this reduction in levels of c-Myc protein in Ad/AH-EBNA1 cells, despite an induction of c-Myc mRNA, corresponded to a change in c-Myc-mediated transcriptional activation, dual luciferase reporter assays were conducted. The results of these assays (Figure 4.24) reveal increased transcriptional activity of c-Myc in EBNA1-expressing cells.

Having established that the transcriptional activation capacity of c-Myc is increased in EBNA1-expressing cells despite a reduction in protein levels, nuclear and cytosolic fractions of Ad/AH, Ad/AH-rEBV and Ad/AH-EBNA1 cell lysates were taken, to assess if increases in c-Myc-mediated transcription could be attributed to increased nuclear localisation of c-Myc. Figure 4.25 shows immunoblotting for c-Myc using these nuclear and cytsolic cell fractions, and reveals no differences in the intracellular localisation of c-Myc in Ad/AH, Ad/AH-rEBV and Ad/AH-EBNA1 cells.

Given the apparent complex nature of the regulation of c-Myc activity in Ad/AH-EBNA1 cells and c-Myc's involvement in regulating EBER expression, Ad/AH-neo and -EBNA1 cells stably expressing an inducible c-Myc fusion protein (c-MycER) were utilised in further examination of c-Myc function in EBNA1-expressing Ad/AH cells. Immunoblot analysis using an antibody which detected both endogenous c-Myc and c-MycER fusion protein revealed that levels of both c-MycER, and endogenous c-Myc were reduced in EBNA1-

Figure 4.24 – Dual luciferase reporter assays conducted in Ad/AH-neo, Ad/AH-rEBV and Ad/AH-EBNA1 cells. Levels of c-Myc transcriptional activation activity (from X-box consensus sequence) are shown, relative to levels of activity observed in Ad/AH-neo cells. Cells transfected with c-Myc luciferase reporter plasmid and Renilla control plasmid were harvested 24 hours post transfection. Levels of c-Myc luciferase reporter activity were normalised to transfection control (Renilla) before being made relative to levels of c-Myc luciferase reporter activity in Ad/AH-neo cells. The results presented are means of biological and technical triplicates, with error bars representative of the standard deviation of biological repeats.

Figure 4.25 - Immunoblot analysis for total levels of c-Myc in nuclear and cytosolic extracts, taken from Ad/AH-neo, Ad/AH-rEBV and EBNA1 cells. Sp1 and tubulin are nuclear and cytosolic proteins respectively, with immnoblotting for these proteins included to demonstrate successful separation of nuclear and cytosolic fractions of cell lysates.

Figures 4.24 and 4.25

expressing cells (Figure 4.26). Analysis of the transcriptional activation capacity of c-Myc was expanded to these cell lines, with dual-luciferase reporter assays for c-Myc-mediated transcriptional activation conducted following functional induction of the c-Myc fusion protein with 4-hydroxytamoxifen (4-OHT) (Figure 4.27). Enhanced c-Myc activity was observed in both neo- and EBNA1-expressing cells, with induction being considerably stronger in EBNA1-expressing cells compared with their neo counterparts. This is consistent with there being an increased transcription-enhancing activity of c-Myc in the presence of EBNA1. Indeed, basal levels (without 4-OHT stimulation) of c-Myc transcriptional activation capacity are increased 5-fold in EBNA1-expressing cells compared with neo control cells. In both Ad/AH-neo and -EBNA1 cells, the increase of c-Myc activity in response to 4-OHT treatment was titratable, with increased 4-OHT concentrations resulting in increased levels of c-Myc-induced transcriptional activation.

In an attempt to uncover an explanation for the reduced levels of c-Myc protein in EBNA1-expressing cells, proteins involved in the regulation of c-Myc protein stability were analysed by immunoblotting in an Ad/AH cell panel. A schematic of the regulation of c-Myc stability is shown in Figure 4.28. Figure 4.29 examines levels of total and phosphorylated extracellular signal-regulated kinases 1/2 (ERK) in untreated/stimulated samples from Ad/AH, Ad/AH-rEBV, Ad/AH-neo and Ad/AH-EBNA1 cells. ERK is responsible for an initial (stabilising) phosphorylation event (Ser62) of c-Myc (Pulverer et al. 1994; Sears et al. 2000). Across all samples, no significant variation in levels of total ERK was demonstrated, though levels of p-ERK were slightly increased in unstimulated Ad/AH-rEBV cells compared with other unstimulated cells. However, following osmotic shock, TPA stimulation, and anisomycin stimulation, levels of p-ERK were reduced in EBNA1-expressing cells (Ad/AH-rEBV and Ad/AH-EBNA1). Total levels of Akt (which phosphorylates and inactivates GSK3β) remained unchanged in EBNA1-expressing Ad/AH cells (Figure 4.30), though levels of total

Figure 4.26 – Immunoblot analysis of the levels of c-MycER (inducible c-Myc fusion protein) and endogenous c-Myc in Ad/AH-neo and EBNA1 cells stably expressing the c-MycER fusion protein. β-Actin is included as a loading control and levels of EBNA1 expression are also shown.

Figure 4.27 – Dual luciferase reporter assays conducted following transient transfection (with a c-Myc luciferase reporter plasmid) of Ad/AH cells stably expressing c-MycER and either EBNA1 or neomycin control cassette. Cells were treated with 0nm, 250nm, 500nm or 1000nm 4-Hydroxytamoxifen for 24 hours before cell lysis and performance of assay. Levels of c-Myc transcriptional activation activity (from X-box consensus sequence) are shown, relative to levels of activity observed in (untreated) Ad/AH-neo cells. Levels of c-Myc luciferase reporter activity were normalised to a transfection control (Renilla), before being made relative to levels of c-Myc luciferase reporter activity in untreated Ad/AH-neo cells. Results presented are means of biological and technical triplicates, with error bars representative of the standard deviation of biological repeats.

Figures 4.26 and 4.27

Figure 4.28 – Schematic of the regulation of c-Myc stability, adapted from Sears et al. (2000). c-Myc is phosphorylated on residue Serine-62 by ERK (the phosphorylation activity of ERK is controlled by Raf/MEK pathways). Subsequently, c-Myc can be phosphorylated on residue Threonine-59 by GSK-3, which can be inactivated by phosphorylation events controlled by PI3-kinase/Akt signalling pathways. Dual phosphorylated c-Myc (at Serine-62 and Threonine-59) is subject to ubiquitination and subsequent proteasomal degradation.

Figure 4.29 – Immunoblot analysis of the levels of expression of total and phospho-ERK1/2 in Ad/AH, Ad/AH-rEBV, Ad/AH-neo and Ad/AH-EBNA1 cells. Cells were left untreated or stimulated by osmotic shock (0.2M NaCl for 20 minutes prior to harvest), TPA treatment (60ng/ml TPA for 16 h prior to harvest) or anisomycin treatment (50ng/ml for 1 hour prior to harvest). β-Actin is included as a loading control.

Figures 4.28 and 4.29

Figure 4.30 – Immunoblot analysis of the levels of total Akt, phospho- and total-GSK3β in Ad/AH, Ad/AH-rEBV and Ad/AH-EBNA1 cells. β-Actin is included as a loading control with levels of EBNA1 expression (as assessed by immunoblotting) also shown.

Figure 4.31 – Immunoblotting for levels of c-Myc in Ad/AH-neo and Ad/AH-EBNA1 cells following treatment with 2 μg/ml cyclohexamide (CHX) for 0, 30, 60 and 120 minutes.

Figure 4.32 – Fluorescence microscopy images of GFP expression in Ad/AH-rEBV cells 48h post transfection with shRNA against c-myc '152051' (152051 expression plasmid also carries a GFP expression cassette which is constitutively expressed). Images show GFP expression following transfection of cells with 0μg, 1μg and 2μg of 152051 plasmid DNA.

Figures 4.30-4.32

and phospho-GSK3β were increased in EBNA1-expressing cells (Figure 4.30). c-Myc protein stability in Ad/AH-neo and -EBNA1 cells was assessed using cyclohexamide as an inhibitor of protein synthesis (Figure 4.31). These data reveal no significant reduction in the stability of c-Myc in Ad/AH-EBNA1 cells, compared with Ad/AH-neo cells, a result which adds no explanation for the decreased levels of c-Myc protein in EBNA1-expressing Ad/AH cells.

To assess the impact of EBNA1-mediated induction of c-Myc upon EBER expression, a converse approach was once more adopted, with shRNA against c-Myc transiently expressed in Ad/AH-rEBV cells before analysis of consequential levels of EBER1 and EBER2. The expression plasmid (152051) encoding the shRNA against c-Myc also constitutively expressed GFP, and this GFP marker was used to monitor transfection efficiency and efficacy. Fluorescence microscopy images of Ad/AH-rEBV cells transiently transfected with the shRNA vector (Figure 4.32) confirm successful transfection of expression vector, with a high percentage of GFP positivity in cell populations transfected with 2μg of expression vector plasmid DNA. Figure 4.33 illustrates the effect of transiently expressing shRNA to c-Myc in Ad/AH-rEBV cells. c-Myc mRNA levels are significantly reduced by transient transfection of 1μg of the expression vector, and completely ablated by transient transfection of 2μg of plasmid DNA. Transient transfection with 2μg of plasmid DNA was observed to be sufficient to significantly reduce levels of EBER1, and cause a moderate reduction in EBER2 levels. Densitometric analysis of the data from multiple experiments revealed the reduction in levels of EBER1 to be approximately 1.9-fold, with EBER2 levels being reduced only 1.2-fold. Levels of $tRNA^{Tyr}$ were also significantly reduced (2.5-fold by densitometry), a result which concurs with previously published data demonstrating the direct role c-Myc plays in upregulating cellular pol III transcription (Gomez-Roman et al. 2003). The lack of reduction in levels of EBER and $tRNA^{Tyr}$ expression following ablation of c-Myc expression by transfection of cells with 1μg of shRNA plasmid DNA is attributed to an insufficient

Figure 4.33 – RT-PCR analysis of the levels of EBER1, EBER2, c-myc mRNA and $tRNA^{Tyr}$ in Ad/AH-rEBV cells transiently transfected with pSG5, non-silencing control shRNA, or shRNA to c-myc. Cells were transfected with 1μg and 2μg of test plasmid with RNA subsequently extracted 48h post transfection, before cDNA synthesis and RT-PCR analysis was conducted. GAPDH is included as an internal control.

Figure 4.34 – RT-PCR analysis of EBER1 expression levels, confirming levels of EBER1 are equivalent in Ad/AH-Puro-EBERs and Ad/AH-neo-c-MycER-Puro-EBERs cell lines. GAPDH is included as an internal control.

Figures 4.33 and 4.34

reduction in levels of c-Myc protein that this level of shRNA expression resulted in, although this was not experimentally assessed. In parallel to anti-c-Myc shRNA experiments, non-silencing control shRNA was also transiently expressed in Ad/AH-rEBV cells, with no resultant effect on levels of c-Myc mRNA, or EBER expression (Figure 4.33).

To examine the effect of enhanced c-Myc-mediated transcriptional activation upon EBER expression, Ad/AH cells expressing both c-MycER and EBERs were generated by transfection of Ad/AH-neo-c-MycER cells with pUC19-Puro-EBERs plasmid. Following puromycin drug selection over a two week period, cells were assayed by RT-PCR for EBER1 expression (Figure 4.34). Roughly equivalent levels of EBER1 are seen for Ad/AH-Puro-EBERs cells and Ad/AH-neo-c-MycER Puro-EBERs cells, indicating successful generation of a population of cells, stably expressing both EBERs and c-MycER. To confirm that functional induction of c-MycER remained intact in these cells, dual luciferase reporter assays were conducted (Figure 4.35). Cells were subsequently used to evaluate the impact of functional induction of c-MycER on levels of EBER expression. Figure 4.36 shows RT-PCR analysis of levels of EBER1 and EBER2 following treatment of Ad/AH-neo-c-MycER-Puro-EBERs cells with 4-OHT for 6, 24 and 48 hours. Although no change in EBER expression is observed following 6 hours of treatment, after 24 and 48 hours, levels of EBER1 and EBER2 are both increased although levels of EBER1 are increased to a significantly greater extent than levels of EBER2. This result is consistent with shRNA data and is consistent with the observation that only EBER1 has an E-Box (c-Myc binding site) upstream of its transcriptional start site (Niller et al. 2003).

4.1.4 EBNA1 expression in Ad/AH-Puro-EBERs cell line

The data presented above confirm that EBNA1 is able to induce several factors involved in the regulation of EBER expression, however these experiments fail to illustrate definitively

Figure 4.35 - Dual luciferase reporter assay showing levels of c-Myc transcriptional activation activity in response to 4OHT treatment (250nM) of Ad/AH-neo-c-MycER-Puro-EBERs cells. Results are means of biological and technical triplicates, with error bars representative of the standard deviation of biological repeats.

Figure 4.36 – RT-PCR analysis of EBER1 and EBER2 levels in Ad/AH-neo-c-MycER-Puro-EBERs cells following treatment with 250nM 4OHT for 6, 24 and 48 hours. GAPDH is included as an internal control.

Figures 4.35 and 4.36

that EBNA1 increases EBER expression. To address this, the effect of expressing physiological amounts of EBNA1 in Ad/AH-Puro-EBERs cells was analysed by RT-PCR. Figure 4.37 shows analysis of EBNA1, EBER1 and EBER2 levels in Ad/AH-Puro-EBERs cells, following titration of EBNA1 expression vector pSG5-EBNA1, with RNA having been extracted for analysis at 8, 24, 48 and 72 hours post transfection. Between 1ng and 5ng of transfected plasmid DNA was required to attain levels of EBNA1 expression observed in Ad/AH-rEBV cells. At each time point, levels of EBER1 and EBER2 expression were significantly increased by each amount of EBNA1 expressed. Physiological levels of EBNA1 were sufficient to increase EBER expression, with increased amounts of EBNA1 expression not yielding any further over-expression of EBERs. The increase in levels of EBER expression can be attributed to EBNA1-mediated increases in levels of cellular EBER-associated transcription factors previously described in this chapter, as demonstrated by increases in TFIIIC-110 and ATF-2 mRNA, and $tRNA^{tyr}$ (Figure 4.38A). Densitometric analysis of EBER expression levels in these experiments (Figure 4.38B) revealed a 2 to 2.5-fold mediated increase in levels of EBER expression in response to EBNA1. Although levels of EBER expression are not increased to those seen in Ad/AH-rEBV cells, EBER expression is shown to be comparable to levels of expression seen in the Burkitt's Lymphoma cell line Namalwa (Figure 4.39).

4.1.5 Disruption of c-Myc regulatory region (X-box) upstream of EBER1

Previously published data had demonstrated c-Myc binding to E-boxes contained within an X-box region upstream of EBER1 (Niller et al. 2003). To confirm the importance of this site in the regulation of EBER expression, it was excised from pUC19-Puro-EBERs utilising molecular cloning techniques, before levels of EBER expression in subsequently established cell lines were analysed.

Figure 4.37 – RT-PCR analysis of EBER1 and EBER2 expression levels in Ad/AH-Puro-EBERs cells transiently transfected with pSG5-EBNA1 (titration from 1ng to 50ng) over a 72 hour time course. RNA was harvested and analysed at 8, 24, 48 and 72 hours post transfection. Levels of EBNA1 expression were also measured by RT-PCR with Ad/AH-rEBV RNA analysed (alongside 72 hour time-point data) as a positive control for EBER and EBNA1 expression. GAPDH is included as an internal control.

Figure 4.37

Figure 4.38 – (A) RT-PCR analysis of EBER-associated transcription factor mRNA levels in Ad/AH-Puro-EBERs cells following transient transfection with pSG5-EBNA1 (titration from 1ng to 50ng). Levels of ATF-2 mRNA, TFIIIC110 mRNA and cellular polIII target $tRNA^{tyr}$ were analysed using RNA harvested 48 hours post transfection with EBNA1. RT-PCR analysis of EBER1 and EBER2 is also shown along with levels of EBNA1 mRNA and GAPDH as an internal control. **(B)** Densitometric analysis of EBER expression in (A) represented as fold change from EBER expression in pSG5 control transfected cells. Error bars indicate the standard deviation between densitometric analyses of three biological repeats. RT-PCR images are included for comparison.

Figure 4.38

Figure 4.39 – RT-PCR analysis of EBER1 and EBER2 levels in Ad/AH, Ad/AH-rEBV, Namalwa BL cell lines and in Ad/AH-Puro-EBERs (Ad/AH-PE) cells that had been transiently transfected with a pSG5 control plasmid, or a pSG5-EBNA1 expression vector. Levels of EBNA1 were also assayed by RT-PCR with GAPDH included as an internal control.

Figure 4.39

Using online tools (AliBaba2.1), dry analysis of the effect on transcription factor binding of disrupting the wild type X-box sequence was conducted (Figure 4.40). E-box sequences were disrupted as previously described (Jones et al. 1996; Wang et al. 2004) (changed from CAGATG to CAGAGA, and CACGTG to CACGGA), leading to a clear reduction in predicted transcription factor binding, with c-Myc and associated transcription factors no longer predicted to bind to the sequence. This predicted reduction in transcription factor binding was tested empirically by EMSA analysis (Figure 4.41). Here, in a variety of Ad/AH and Akata BL cells lines, levels of transcription factor binding to the mutated X-box region are significantly reduced compared with binding to the wild-type X-box sequence. However, the c-Myc specificity of this reduction in transcription factor binding remains undetermined, as super-shift experiments conducted to confirm specificity were unsuccessful.

Attempts to generate the mutant sequence used in dry analysis and EMSA analysis were made using site-directed mutagenesis (of pUC19-Puro-EBERs). Despite considerable persistence attempts were not successful, and an alternative method of ablation of the E-boxes upstream of EBER1 was employed. Figure 4.42 gives details of endonuclease digestion of pUC19-Puro-EBERs and ligations to generate pUC19-Puro-EBERs-ΔX. Briefly, the X-box c-Myc binding site (containing both E-box regions) was excised from pUC19 EBERs plasmid using SacI and PmlI, excising bases -352 to -125 relative to the EBER1 transcriptional start site. Dry analysis of this novel sequence (Figure 4.43) predicted ablation of c-Myc binding.

pUC19-Puro-EBERs-ΔX was introduced into Ad/AH and Ad/AH-neo-c-MycER cells before puromycin drug treatment for two weeks to select a polyclonal population of cells, stably expressing the new expression vector. Subsequently, cells were screened by RT-PCR for EBER1 and EBER2 expression (Figures 4.44 and 4.45). Levels of EBER expression in Ad/AH-Puro-EBERs-ΔX and Ad/AH-neo-c-MycER-Puro-EBERs-ΔX were observed to be

Figure 4.40 – *In silico* analysis of transcription factor binding sites (using Alibaba 2.1 http://www.gene-regulation.com/pub/programs/alibaba2/index.html?) in wild-type X-box sequence and mutated X-box sequence.

Figure 4.40

Figure 4.41 – EMSA analysis of wild-type X-box sequence and mutated X-box sequence binding in Ad/AH, Ad/AH-rEBV, Ad/AH-EBNA1, Ad/AH serum starved Akata EBV-negative and Akata EBV-positive cells.

Figure 4.42 – Sequence (partial) analysis of the construction of pUC19-Puro-EBERs-ΔX. pUC19-Puro-EBERs plasmid DNA was cut with SacI and PmlI, followed by blunt-end filling and ligation, leading to the generation of pUC19-Puro-EBERs-ΔX, relevant areas of sequence are shown and annotated.

Figures 4.41 and 4.42

Figure 4.43 – *In silico* analysis of transcription factor binding sites (using Alibaba 2.1 http://www.gene-regulation.com/pub/programs/alibaba2/index.html?) in mutated X-box sequence of pUC19-Puro-EBERs-ΔX.

Figure 4.44 – RT-PCR analysis of the levels of stable EBER1 and EBER2 expression following generation of Ad/AH-Puro-EBERs-ΔX cell line in comparison with level of stable EBER expression observed in established pUC19-Puro-EBERs cell line. GAPDH is included as an internal control.

Figure 4.45 - RT-PCR analysis of the levels of stable EBER1 and EBER2 expression following generation of Ad/AH-neo c-MycER Puro-EBERs-ΔX cell line in comparison with level of stable EBER expression observed in established pUC19-Puro-EBERs cell line. GAPDH is included as an internal control.

Figures 4.43-4.45

equivalent to levels seen in Ad/AH-Puro-EBERs (albeit with a reduction in levels of EBER1 in Ad/AH-Puro-EBERs-ΔX cells).

The impact upon EBER expression of transient EBNA1 expression in Ad/AH-Puro-EBERs-ΔX cells was observed through transfection of pSG5-EBNA1 into the new cell line and, in parallel, Ad/AH-Puro-EBERs cells, where EBER induction by EBNA1 had previously been observed (Figure 4.37). Figure 4.46 confirms EBER induction in Ad/AH-Puro-EBERs cells upon expression of EBNA1, and that an induction of EBER1 and EBER2 expression is seen to a similar extent in Ad/AH-Puro-EBERs-ΔX cells, following transient expression of EBNA1.

Ad/AH-neo-c-MycER-Puro-EBERs-ΔX cells were treated with 4-OHT to functionally induce c-MycER before analysis of EBER expression by RT-PCR (Figure 4.47). Levels of EBER1 remain almost unchanged by c-MycER induction, with slight increases in levels of EBER2 observed after 6 and 24 hours. In comparison, in similar cells with the X-box upstream of EBER1 intact (Ad/AH-neo-c-MycER-Puro-EBERs) functional induction of c-MycER led to substantial induction of EBER1, and slight induction of EBER2 expression. Levels of EBER expression across the two cells lines following 24 hours of 4-OHT treatment are shown in Figure 4.48 for comparison. Such results suggest c-Myc influences EBER1 transcription through binding to upstream E-boxes, confirming the importance of these c-Myc binding sites in regulation of EBER expression.

4.1.6 Dominant-negative EBNA1 studies

As a converse of the experiments previously described (Figures 4.37 and 4.38), ablation of EBNA1 function through introduction and expression of dnEBNA1 (EBNA1 M1) in EBV-infected Ad/AH cells resulted in a titratable and robust decrease in levels of both EBER1 and EBER2 expression (Figure 4.49). Densitometric analysis revealed reductions of 2.1-fold in

Figure 4.46 - RT-PCR analysing changes in EBER1 and EBER2 expression levels in Ad/AH-Puro-EBERs cells, and Ad/AH-Puro-EBERs-ΔX cells following transient transfection of these cells with pSG5-EBNA1 (titration from 2ng to 200ng plasmid DNA). RNA was harvested and analysed 48 hours post-transfection. Levels of EBNA1 mRNA were also assessed by RT-PCR and GAPDH was included as an internal control.

Figure 4.47 - RT-PCR analysing levels of EBER1 and EBER2 expression in Ad/AH-neo-c-MycER Puro-EBERs-ΔX cells treated with 250nM 4OHT for 6, 24 and 48 hours. GAPDH is included as an internal control.

Figure 4.48 – RT-PCR comparing of levels of EBER1 and EBER2 in Ad/AH-neo-c-MycER-Puro-EBERs cells (A) and Ad/AH-neo-c-MycER-Puro-EBERs-ΔX cells (B). Cells were left untreated or treated with 250nM 4OHT for 24 hours. GAPDH is included as an internal control.

Figures 4.46-4.48

Figure 4.49 – RT-PCR analysis of EBER1 and EBER2 levels in Ad/AH-rEBV cells transiently transfected with an expression vector expressing a dominant negative (dn) EBNA1 (EBNA1 M1). A titration (from 1μg to 4μg) of dnEBNA1 is presented, along with a pSG5 control sample. RNA was harvested for analysis 24 hours post-transfection. GAPDH is included as an internal control.

Figure 4.50 – RT-PCR analysis of EBER1 and EBER2 expression in Ad/AH-Puro-EBERs cells transiently transfected with 10ng pSG5-EBNA1, and increasing amounts of dnEBNA1-M1 (ranging from 10ng to 50ng). RNA was harvested for analysis 24 hours post-transfection. GAPDH is included as an internal control.

Figures 4.49 and 4.50

EBER1 expression, and 2.6-fold in EBER2 expression, values which are consistent with the previously observed induction of EBER expression levels in response to EBNA1 (Figure 4.38B). Upon co-expression of EBNA1 and dnEBNA1 in Ad/AH-Puro-EBERs cells, it was possible to titrate out induction of EBER expression by EBNA1 with dnEBNA1, as demonstrated in Figure 4.50. These studies, combined with the induction of EBER expression seen following transient EBNA1 expression in Ad/AH-Puro-EBERs cells, confirm the significant enhancing effect of EBNA1 upon EBER expression.

4.2 Discussion

It has long been established that high levels of EBER expression are a feature of cells latently infected with EBV and in cells of EBV-associated malignancies (Arrand and Rymo 1982). The findings presented here provide evidence that EBNA1 plays a significant role in the regulation of EBER expression in epithelial cells. EBNA1 was shown to enhance levels of EBER expression, seemingly through induction of EBER-associated cellular transcription factors, illustrating its importance in the characteristic abundant expression of EBERs that is associated with EBV latent infection.

4.2.1 EBNA1 enhances cellular pol III transcription

Initial data (Figure 4.8) confirmed previous findings (Felton-Edkins et al. 2006) that like several other oncogenic viruses, EBV was able to increase the level of cellular pol III transcription, and that this increase was seen in both lymphoid and epithelial cells infected with EBV. Qualitative and quantitative data presented in Figures 4.9 to 4.13 reveal that EBNA1 is able selectively to affect TFIIIC subunit expression in epithelial cells, and that this may, at least in part, be responsible for the increase in expression of endogenous pol III products that is induced by EBV. The DNA sequences recognised by TFIIIC are the A- and B-block internal promoter elements found in most pol III-transcribed genes, including tRNA

and EBER genes, (Schramm and Hernandez 2002) and therefore the findings that EBNA1 induces TFIIIC and cellular pol III transcription are likely to be linked. The finding that EBNA1 induces TFIIIC is significant in the regulation of EBER expression, as *in vitro* transcription assays have revealed induction of EBER2 expression following the supplementation of cell fractions with TFIIIC, and ChIP assays have provided evidence that TFIIIC interacts with the EBER genes *in vivo* (Felton-Edkins et al. 2006). Elevation of TFIIIC expression following EBV infection has been identified as increasing occupancy of cellular target genes (Felton-Edkins et al. 2006), and the data presented in this chapter suggest a similar increase in occupancy of cellular target genes by TFIIIC would accompany the EBNA1-induced increase in TFIIIC expression.

It should be noted that although the most compelling data presented in this chapter were obtained using Ad/AH-EBNA1 cells (which express very high levels of EBNA1), other Ad/AH-EBNA1 clones were analysed in parallel (data not shown). Other clones which expressed lower levels of EBNA1 (closer to observed physiological levels) showed similar levels of induction, confirming that the EBNA1 clone used was representative, and that the results obtained are not attributable to over-expression of EBNA1.

mRNA levels of TFIIIB subunits TBP, Brf1 and Bdp1 were not consistently elevated in cell lines transfected with the EBNA1 expression vector (Figures 4.11 and 4.12). This finding was in contrast to *in vivo* studies conducted by co-workers which found NPC biopsies consistently to overexpress the mRNAs encoding TBP and Bdp1 (Dr JR. Arrand, personal communication). Induction of Bdp1 may contribute substantially to the high rates of pol III transcription that are triggered by EBV (Felton-Edkins et al. 2006) and it would be valuable to determine the mechanism(s) responsible for the increase in TBP and Bdp1 expression observed in NPC tumours, especially given *in vitro* transcription data revealing induction of EBER2 expression following supplementation of cell fractions with TFIIIB (Felton-Edkins et

al. 2006). It is possible that TFIIIB subunits are basally overexpressed in the cell lines that were examined, or that post-transcriptional regulation by EBNA1 occurs, which would explain the lack of induction of TFIIIB mRNAs seen in EBNA1-expressing cells. Alternatively, another EBV latent gene product may be responsible for the induction observed *in vivo*.

It is noticeable that although levels of TFIIIB subunit protein Bdp1have previously been demonstrated to be induced following EBV infection, no consistent increase in TFIIIB subunit mRNA was reported (Felton-Edkins et al. 2006). It would therefore be interesting to examine protein levels of TFIIIB subunits in EBNA1-expressing cells, and such studies were attempted in this project. However the antibodies utilised in immunoblot analysis were not sufficiently sensitive to detect adequate protein levels in cell lysates tested.

The significance of increased levels of cellular pol III transcription is not restricted to increased levels of viral transcripts such as the EBERs. It is well-established that pol III transcription is often deregulated in a wide range of malignant tumours and transformed cells (Chen et al. 1997; White 2005; Marshall et al. 2008; White 2008) and data suggest that increased pol III transcription is capable of promoting proliferation and oncogenic transformation in some cellular contexts (Johnson et al. 2008). In support of these findings, co-worker-conducted *in vivo* studies revealed induction of pol III specific transcription factors TFIIIB and TFIIIC at both the mRNA and protein level in NPC tumours (Dr JR. Arrand, personal communication). Given data revealing induction of TFIIIC subunits in EBNA1-expressing epithelial cells, and the association between EBV and NPC, it is tempting to speculate that increased TFIIIC subunit levels in NPC tumour cells could be mediated, in part, by EBNA1.

Following epithelial cell-based *in vitro* data presented here, and *in vivo* data derived by co-workers from epithelial cell carcinomas (Dr JR. Arrand, personal communication) it would be valuable to assess TFIIIC and TFIIIB levels, along with levels of pol III transcription in EBNA1-expressing lymphoid cell lines, and to examine levels of pol III-specific transcription factors in EBV-associated lymphomas. This analysis would reveal whether the results reported here, obtained in an epithelial cell background, are applicable to a broader range of cell types. Such a finding would be consistent with data showing increased cellular pol III transcription in EBV-positive Akata BL cells (when compared with their EBV-loss counterparts), which express a small complement of viral latent gene products, including EBNA1 (Figure 4.8 and Felton-Edkins et al. (2006)).

It may also prove valuable to assess the levels of the recently identified 35kd (Dumay-Odelot et al. 2007) subunit of TFIIIC in both EBV-infected and EBNA1-expressing epithelial and lymphoid cell lines.

4.2.2 EBNA1 influences typical pol II EBER-associated transcription factors ATF-2 and c-Myc

4.2.2.1 ATF-2

ATF-2 has been shown previously to be important for EBER expression, with deletion or mutation of the ATF-2 binding site upstream of EBER genes significantly impairing EBER expression (Howe and Shu 1989; 1993; Wensing et al. 2001). In agreement with such data, experiments using shRNA to ATF-2 (Figures 4.19 and 4.20) revealed levels of both EBER1 and EBER2 were substantially reduced following knock-down of ATF-2 using shRNA. These experiments were novel in their reduction of ATF-2 levels directly, rather than ablation of binding sites upstream of EBER genes before subsequent analysis of EBER expression. Additionally, ATF-2 has previously been demonstrated, through the use of ChIP assays, to

associate with EBER promoter regions and the promoter region of TFIIIC-220 (binding the CRE motifs) (Felton-Edkins et al. 2006), and in combination with data presented in this chapter and other published data, conclusive evidence exists for the importance of ATF-2 in the regulation of EBER expression.

Several previous studies have shown EBV-mediated regulation of ATF-2, though they conflict in their descriptions of the precise effect of EBV on ATF-2. Initial studies revealed that EBV triggers hyperphosphorylation of ATF-2 leading to increased activity (Kieser et al. 1997; Eliopoulos and Young 1998; Roberts and Cooper 1998; Adamson et al. 2000; Young and Rickinson 2004) with increased levels of mono-phosphorylated ATF-2 being observed in the absence of any increase in total levels of ATF-2. Recently published data were at odds with such observations, demonstrating that EBNA1 can induce an increase in total levels of ATF-2 (O'Neil et al. 2008). Data presented here support these recent data, with levels of ATF-2 mRNA shown to be increased in EBNA1-expressing Ad/AH, AGS and Hone-1 cells (Figure 4.15) and levels of total ATF-2 protein being induced in Ad/AH-EBNA1 and AGS-EBNA1 cells (Figure 4.16). Additionally, in Ad/AH-EBNA1 cells, increased levels of mono- and dual-phosphorylated ATF-2 were observed (Figures 4.17 and 4.18) along with increased levels of nuclear ATF-2 (Figure 4.21). These data suggest that EBNA1 acts to increase EBER expression both through induction of ATF-2 transcription and the resultant increase in levels of dual-phosphorylated and activated ATF-2. Further, RT-qPCR data (Figure 4.12) reveal statistically significant increases in levels of TFIIIC220 mRNA expression in EBNA1-expressing Ad/AH, AGS and Hone-1 cells. This induction may be, at least in part, ATF-2-mediated given the induction of ATF-2 in EBNA1-expressing cells, and previously published ChIP data demonstrating an association between ATF-2 and the TFIIIC220 promoter region (Felton-Edkins et al. 2006).

That EBNA1 alone is capable of inducing an increase in total- and activated-ATF-2 stands out as a novel and important finding, not only in terms of enhancing EBER expression, but also given the various significant roles ATF-2 is known to play in an assortment of cellular processes (Bhoumik and Ronai 2008).

4.2.2.2 c-Myc

The importance of c-Myc to expression of both EBER1 and EBER2 was examined in this chapter through a series of experiments involving the use of the inducible c-MycER fusion protein, and shRNA to c-Myc in established cell systems, and newly established EBER-expressing cell systems.

c-Myc directly interacts with EBER genes, through binding to E-Boxes upstream of EBER1 (Niller et al. 2003), and through its interaction with TFIIIB c-Myc can directly activate many pol III-transcribed genes (Gomez-Roman et al. 2003). This is consistent with the observed decrease in tRNA expression that accompanies c-Myc RNAi (Figure 4.33). However, EBER2 appears to be an exception, as in contrast to EBER1, EBER2 shows little response to RNAi or overexpression of c-Myc, in Ad/AH cells (Figures 4.33 and 4.38). This may reflect the unusual promoter arrangement and factor requirements of EBER genes, which differ from most cellular pol III promoters (Felton-Edkins et al. 2006). By excising the short region upstream of EBER1 containing the E-boxes to which c-Myc has been demonstrated to bind (Niller et al. 2003), this study reveals that these E-Boxes are required for induction of EBER1 by activated c-MycER (Figures 4.47 and 4.48). This contrasts with a previous report that this upstream region has little importance for EBER1 expression in 293 cells (Wensing et al. 2001). Differences between cell types may be responsible for the discrepancy. The data presented in this study suggest that the EBER genes show differential responsiveness to c-Myc due to E-box DNA motifs upstream of the EBER1 promoter.

Despite the demonstrated importance of the E-boxes for induction of EBER1 expression through the functional induction of the c-MycER fusion protein, this region was dispensable for induction of EBER expression by transient expression of EBNA1 (Figure 4.46). Further, basal levels of EBER expression in Ad/AH-Puro-EBERs, Ad/AH-neo-c-MycER-Puro-EBERs-ΔX and Ad/AH-Puro-EBERs-ΔX cell lines were roughly equivalent, again suggesting perhaps that although the E-boxes are critical in terms of c-Myc regulation of EBER expression, in the absence of such a regulatory mechanism other compensating mechanisms are present to allow high levels of EBER expression.

In addition to confirming the significance of c-Myc in the regulation of EBER expression, c-Myc levels and activity were analysed in EBNA1-expressing epithelial cells, to examine if EBNA1 exerted an effect on EBER expression through c-Myc. Consistent with previously published Affymetrix array data (Wood et al. 2007), induction of the levels of mRNA encoding c-Myc was observed in Ad/AH-EBNA1 cells (Figure 4.22). Growth regulated accumulation of c-myc mRNA has been widely reported previously (Kelly et al. 1983; Luscher and Eisenman 1990) however this mRNA induction was not observed in other EBNA1-expressing epithelial cells analysed. Further, levels of c-Myc and c-MycER protein were substantially reduced in EBNA1-expressing Ad/AH cells (Figures 4.23 and 4.27). This observation was in direct contrast to c-Myc protein levels reported in cells expressing LANA (KSHV's EBNA1 homologue), where stabilisation and activation of c-Myc is observed (Bubman et al. 2007; Liu et al. 2007).

Despite the observed reduction in levels of c-Myc protein, and no apparent change in the intracellular localisation of c-Myc (Figure 4.25), luciferase reporter assays revealed increased transcriptional activation activity of endogenous c-Myc and c-MycER in Ad/AH-EBNA1 cells (Figures 4.24 and 4.27). Although it is unclear how EBNA1 may mediate this induction of c-Myc activity, these data suggest that EBNA1 may influence c-Myc transcription – a

finding which as well as impacting upon EBER expression (in particular EBER1), could have a global impact upon cellular gene expression, given that c-Myc has been shown to be involved in the regulation of 15% of all cellular genes (Dang et al. 2006). Deregulation of c-Myc is also a common feature of a wide range of cancers, with up to 70% of human cancers showing deregulated expression of c-Myc (Kuttler and Mai 2006). c-Myc impacts upon a diverse range of pathways contributing to tumourigenesis (for a comprehensive review of c-Myc's cellular impact, see (Meyer and Penn 2008), and therefore by extrapolation, EBNA1 may play some part in c-Myc–mediated cellular changes. In addition to increased transcriptional activity of c-Myc in EBNA1-expressing cells having an impact upon cellular events, it should not be discounted that reduced levels of c-Myc in these cells may play a role in regulating cellular events dependent on protein:protein interactions between c-Myc and other crucial cellular factors.

Preliminary studies were conducted in an attempt to explain the reduced levels of c-Myc observed in EBNA1-expressing cells. Precise cellular regulation of c-Myc is crucial, with levels of c-Myc determining, at least in part, rates of cellular proliferation and differentiation. c-Myc has a short half-life of around 30 minutes (Hann and Eisenman 1984; Ramsay et al. 1986), allowing precise control of protein levels. Two key phosphorylation events regulate c-Myc stability: Ser62 is phosphorylated by extracellular-regulated kinase 1,2 (ERK), which stabilises c-Myc (Pulverer et al. 1994; Sears et al. 2000), and phosphorylation of Thr58 by GSK3 (an event dependent on prior phosphorylation of Ser62) promotes c-Myc degradation through the ubiquitin/proteosome pathway (Sears et al. 2000; Gregory et al. 2003). ERK and p-ERK levels were assessed both basally and following stimulation across an Ad/AH cell panel. Analysis was conducted post-stimulation due to very low levels of detectable p-ERK in unstimulated cells. Significantly reduced levels of p-ERK were seen in EBNA1-expressing cells following all cell stimulations, suggesting that decreased amounts of stabilised c-Myc

(phosphorylated at Ser62) may be present in EBNA1-expressing cells. Levels of total and phosphorylated (inactivated) GSK3β were also assessed. Total levels of GSK3β were increased in EBNA1-expressing cells. However, given the greater increase of the phosphorylated (inactivated) form of the protein (p-GSK3β) in these cells, it would seem that less phosphorylation at c-Myc Thr58 may occur in EBNA1-expressing cells. Such a reduction would result in a reduction of ubiquitin-mediated proteosomal degradation of c-Myc. Therefore, the reduced levels of c-Myc are seemingly not due to decreased protein stability in EBNA1-expressing cells, and initial protein half-life experiments seem to confirm this finding (Figure 4.31). However, this analysis is an indirect examination of the phosphorylation status of c-Myc in EBNA1-expressing cells, and it would be valuable to analyse levels of p-Ser62- and p-Thr58-c-Myc, especially in light of evidence that the KSHV encoded homologue of EBNA1, LANA, can act to regulate c-Myc stability (Bubman et al. 2007; Liu et al. 2007). In LANA-expressing cells, inactivation of nuclear GSK-3 was shown to reduce phosphorylation of c-Myc at Thr58, contributing to c-Myc stabilisation by decreasing c-Myc ubiquitination. Further, LANA was demonstrated to increase the levels of p-ERK and ERK phosphorylation of c-Myc on Ser62 (Liu et al. 2007).

Data presented in this chapter fail to provide elucidation of the mechanisms by which c-Myc protein levels are reduced in EBNA1-expressing Ad/AH cells. The reduction in protein level is observed despite an induction of c-Myc mRNA and no discernable negative influence upon protein stability. Despite the reduction in levels of c-Myc protein, transcriptional activity of c-Myc in Ad/AH-EBNA1 cells was increased. This increase is not explained by increased nuclear localisation of c-Myc, or increased levels of p-ERK which phosphorylates on c-Myc Ser62, a modification known to increase c-Myc transcriptional activity (Liu et al. 2007).

E-box binding (and transcriptional activation of reporter constructs) of c-Myc is dependent upon formation of dimers with co-factor Max (Dang 1999; Grandori et al. 2000). Max is ubiquitously and constitutively expressed in cells, but is also able to form dimers with cellular transcription factor Mad, and these heterodimers are able to form transcriptional repressors on the same E-box sequence elements, antagonising c-Myc function (Foley and Eisenman 1999). Both c-Myc and Mad expression is tightly regulated in relation to cell growth. c-Myc levels are high in cells with progressive cell cycles, but decrease as cells cease to proliferate and differentiate. Conversely Mad expression follows the opposite pattern, allowing precise regulation of levels of c-Myc/Max and Mad/Max heterodimers (Sears et al. 2000). Analysis of Max and Mad levels in EBNA1-expressing cells may prove crucial in determining mechanisms by which c-Myc transcription is elevated in EBNA1-expressing cells. Given the cellular importance of the fine balance of c-Myc levels and activity, it is no surprise that c-Myc regulation in EBNA1-expressing cells is complex. EBNA1 may be acting to increase levels and activity of c-Myc, possibly to increase levels of EBER expression, but changes in other cellular factors may be resulting in the discrepancies observed in the data. Such changes may be necessary in order to maintain the balance of levels and activity of this crucial cellular protein.

4.2.3 EBNA1 increases EBER expression

Experiments with cells expressing the pUC19-Puro-EBERs vector constitute an important part of the analysis of EBNA1's effect on EBER expression. It should be acknowledged that as the EBER genes in this vector lie downstream of the Puromycin resistance cassette and are transcribed in the same direction, it is possible that pol II transcripts could run through the EBER gene resulting in a long polycistronic RNA that would be detected by the PCR assay used for the EBERs. To ensure this does not occur, future analysis of this vector should

include PCR analysis using a forward primer designed in the Puromycin resistance cassette region in combination with the EBER1 reverse primer. A lack of product would demonstrate that no long, polycistronic RNA was produced, indicating that the EBERs were indeed being transcribed from their native promoters.

Although the data indicate that EBNA1, through a variety of mechanisms can induce EBER expression (Figure 4.38), the levels of expression in this model system are low when compared with those in Ad/AH cells stably infected with EBV (Figure 4.39). This may be attributable to the EBER expression plasmids in the model system being maintained in an integrated form. In this context it is notable that the Namalwa cell line, in which EBV is known to be integrated at low copy number (Henderson et al. 1983), also expresses the EBERs at low levels (Arrand and Rymo 1982; Arrand 2000), similar to those seen in this model system (Figure 4.39). In the context of whole virus infection, the EBV genome is usually maintained as a multi-copy episome. In this scenario, transcription factor binding access and kinetics may be very different, given that the EBER genes are adjacent to *OriP*, within the region of unusual chromatin structure (Wensing et al. 2001). The *OriP* region (absent from the Ad/AH-Puro-EBERs cell line) is also known to be a transcriptional enhancer region (Sugden and Warren 1989; Gahn and Sugden 1995) and has been previously demonstrated to increase EBER expression by 2- to 4-fold (Wensing et al. 2001). The number of copies of the EBER genes integrated into the Ad/AH-Puro-EBERs cell line generated is unknown, though it is unlikely to reach the number of viral episomes carried by EBV-infected Ad/AH cells.

Further, it is of note that EBNA1 does not seem to be sufficient to induce TFIIIB subunit expression and it is anticipated that pol III-transcribed genes (such as the EBERs) would be even more highly expressed in cells in which TFIIIB was induced in addition to TFIIIC, an environment which is observed in EBV-infected cells (Felton-Edkins et al. 2006).

Previous data have demonstrated that use of a dominant negative EBNA1 in LCLs carrying an integrated EBV genome led to little or no effect on cellular gene expression, or indeed gene expression from the integrated viral genome, with exception of a slight negative effect upon EBER expression (Kang et al. 2001). Such reports are in agreement with data presented in this study, with EBNA1 being able to have only a modest impact upon EBER expression where EBER genes are present in an integrated form.

Upon expressing a dominant negative EBNA1 in Ad/AH-rEBV cells, known to carry multiple EBV episomes, levels of EBER expression were robustly reduced (Figure 4.49). These experiments provide necessary converse data to complement experiments where EBNA1 was transiently supplied in trans, and further confirm the importance of EBNA1 in the mediation of EBER expression.

The data presented in this chapter provide compelling and extensive evidence that EBNA1 is capable of inducing EBER expression in epithelial cells through the induction of multiple cellular EBER-associated transcription factors, typical of factors involved in both pol II and pol III transcription. Cell systems have been developed allowing the examination of the effect of a trans-supplied EBNA1 upon EBER expression, and extensive studies demonstrate the significance of the typical pol II transcription factors in the mediation of EBER expression. The importance of the results presented stretches beyond the goals of this project, as the transcription factors shown to be induced in EBNA1-expressing epithelial cells are known to be important in a cellular context, with deregulation of nearly all transcription factors discussed here having a known involvement in cellular proliferation and oncogenesis.

Chapter 5

EBNA1 promoter binding studies

Chapter 5 – EBNA1 promoter binding studies

Every biological process relies upon the coordinated expression of genes, the products of which act cooperatively to mediate cellular function. Therefore, understanding the processes underpinning the control of cellular gene expression is essential to the comprehension of development and disease processes. Transcriptional regulation in higher eukaryotes is complex, and this is exemplified by the large number of proteins which control gene expression; there are more than 3,000 human transcription factors, a figure which represents approximately 10% of all human genes (Babu et al. 2004). Further, vast areas of the genome participate in transcription by acting as scaffolds on which regulatory complexes are able to assemble (Carroll et al. 2006).

In addition to cellular transcription factors, many virus-encoded proteins act to influence cellular gene expression through direct or indirect interaction with cellular promoter regions. Several oncogenic viruses have been shown to influence cellular transcription by such mechanisms, with the subsequent changes in cellular transcription contributing to the pathogenesis of the virus.

A recent study has identified deregulated direct targets of the HBV X protein, with 184 gene-targets shown to be directly deregulated (Sung et al. 2009). The roles of these target genes, and their relevance in cancer, was inferred through microarray database analysis, with six cellular pathways predicted to be significantly deregulated following HBV X protein binding to target-gene promoters.

HPV protein E2 binds to chromatin in association with the cellular bromodomain protein Brd4, with this interaction having been shown to be important for the transcriptional function of all papillomaviruses (Ilves et al. 2006; McPhillips et al. 2006; Schweiger et al. 2006).

Further, a study has demonstrated that a portion of bovine papillomavirus-1 E2 is bound to transcriptionally active chromatin (Kurg et al. 2005), with a more recent report finding that the E2 proteins bind to the chromatin of all active promoters, in association with the cellular Brd4 protein (Jang et al. 2009). However, the authors report that the association does not affect the transcriptional activity of these promoters and postulate that E2 associates with these regions in order to tether and maintain the viral genome in functionally active regions of the nucleus.

The adenovirus E1A protein has evolved to interact with key cellular transcription regulators and promoters to control cell cycle progression, cell differentiation and chromatin remodelling (Green et al. 2008), although there is a limited understanding of the molecular mechanisms and the precise roles of cellular regulatory factors involved in such viral processes. E1A is thought to repress cellular gene expression through interaction with two important cellular proteins: TATA-binding protein (TBP) and the multifunctional co-activator and histone acetyltransferase p300. E1A accesses transcriptional co-activators such as p300 on specific promoters before interacting with TBP to disrupt the TBP–TATA complex (Boyd et al. 2002; Green et al. 2008). In support of this, a basal core promoter activated by tethering p300 is repressible by E1A at the promoter level (Green et al. 2008).

HTLV-1 protein HBZ been shown to interact with other bZIP proteins, including the AP-1 transcription factors, resulting in the modulation of their transcriptional activity (Basbous et al. 2003; Thebault et al. 2004; Matsumoto et al. 2005). Further, HBZ in association with JunD has been shown to activate the hTERT promoter and HBZ and JunD have been demonstrated to coexist in the same DNA-protein complex at the proximal region of hTERT promoter (Kuhlmann et al. 2007).

Several members of the EBV latent protein complement are able to alter cellular transcription, as outlined in the introductory section of this thesis. Notably, EBNA2 and EBNA3C are known to regulate viral and cellular promoters through interactions with cellular transcription factors (Knight et al. 2003; Palermo et al. 2008), with EBNA1 also having been identified as binding to promoter regions of cellular genomic DNA in EBV-positive B-cells (Dresang et al. 2009). As EBNA1 is known to possess DNA-binding, protein-protein binding, and transcriptional activation activity, these findings seemingly have a broad cellular significance. Given the transcriptional induction of several EBER-associated cellular transcription factors described in Chapter 4, it was postulated that EBNA1 may be acting to induce cellular factors involved in EBER transcription through association with their promoter regions, most likely indirectly through cooperation with cellular transcription factors. In order to pursue this further, promoter binding experiments were performed, and form the basis this chapter.

The promoter binding field of study has developed into a widely used and rapidly changing area of transcription biology over recent years. Considerable effort has been made to identify cellular transcriptional networks and to map the regions of the genome that participate in the control of gene expression, with an accompanying evolution of experimental techniques that allow analysis of cellular transcription and promoter binding. Initial efforts to unravel the complex nature of regulation of cellular transcription utilised nuclease protection assays, and *in vitro* DNA-binding and reporter assays, with these methodologies allowing the identification of regulatory elements proximal to candidate genes and identification of direct targets of candidate transcription factors (Massie and Mills 2008). However, *in vitro* approaches to identify transcription factor-binding sites in the genome are hampered by both false negatives and false positives. The *in vivo* appearance of binding sites is further controlled by the packaging of genomic DNA in chromatin, which may mask some consensus

binding sites and reveal others. Therefore, alternative approaches were required to map which sites in cellular genomic DNA transcription factors are able to bind *in vivo*. Chromatin immunoprecipitation (ChIP) enables *in vivo* direct and indirect binding sites for specific transcription factors to be identified in the context of chromatin, therefore avoiding many of the problems associated with *in vitro* approaches (Solomon et al. 1988; Orlando and Paro 1993). ChIP can be used to investigate any target on chromatin against which it is possible to raise an antibody. Consequently, it has been successfully and widely utilised in the identification of regions of genomic DNA which associate with specific cellular transcription factors, cofactors, histone modifications and DNA methylation (Solomon et al. 1988; Orlando and Paro 1993; Weber et al. 2005). Importantly, ChIP has also been utilised in identifying the interaction of viral proteins with regions of cellular genomic DNA (Kuhlmann et al. 2007; Green et al. 2008; Jang et al. 2009; Sung et al. 2009).

ChIP was employed in this chapter to elucidate if EBNA1 was associated with the promoter region DNA of some EBER-associated cellular genes (typical of pol II transcription factors) which had been identified as being induced by EBNA1 in the previous chapter. In addition, ChIP analysis was used to demonstrate an EBNA1 association with the promoter regions of AP-1 transcription factors, which have previously been demonstrated to be induced at mRNA and functional levels in EBNA1-expressing epithelial cells (O'Neil et al. 2008). In addition, non-antibody based ChIP-like promoter binding (HaloCHIP) assays were used to establish which domains of EBNA1 may be responsible for any identified interactions with promoter region DNA, and to facilitate the expansion of ChIP-based promoter binding studies to an increased number of cellular targets, and a variety of epithelial cell lines. Further, *in silico* analysis of the promoter region DNA of transcriptionally induced genes was conducted, in parallel with *in vitro* studies of protein-protein interactions between EBNA1 and cellular

transcription factors, in an effort to establish the direct or indirect interaction of EBNA1 with promoter region DNA.

5.1 Results

5.1.1 Chromatin immunoprecipitation analysis of EBNA1 promoter binding

5.1.1.1 Validation of experimental conditions and PCR primers

To ensure specificity of downstream ChIP experimental analysis, sonication of genomic DNA into fragments of between 200bp and 1000bp was necessary. Figure 5.1 demonstrates that nine pulses of 10 seconds were sufficient to shear the majority of genomic DNA into fragments of the required size for downstream analysis, when using cell lysates of cell type and density used in subsequent ChIP experiments. It is notable that no smear of sheared DNA is observed in the absence of sonication, demonstrating a lack of DNA fragmentation prior to sonication. Cell lines used in ChIP experiments were screened by immunofluorescence staining for EBNA1 expression status (Figure 5.2) before experimental procedures were conducted.

To enable analysis of DNA associated with EBNA1, it was first necessary to ensure successful precipitation of EBNA1 protein with a specific antibody. Figure 5.3 shows immunoblotting for EBNA1, demonstrating that EBNA1 is specifically pulled down by the EBNA1 antibody chEBNA1, and not by an isotype control antibody (E-Cadherin).

Primers for the promoter regions of proposed EBNA1 target genes were designed using information from literature searches and online promoter databases, with all primer sets designed within 500bp of transcriptional start sites. Primers for the promoter region DNA of c-myc, ATF-2 (EBER-associated transcription factors) and c-jun (along with ATF-2, an AP-1 subunit upregulated in EBNA1-expressing cells), as well as primers for the EBV dyad-

Figure 5.1 – UV transilluminator image of an ethidium bromide stained agarose gel showing validation of sonication conditions for ChIP assays. 600µl of cross-linked Ad/AH-rEBV cell lysate (1 x 10^7 cells) was sonicated for an increasing number of 10 second pulses, with the sample kept on ice throughout and 30 second pauses between pulses. 20µl of sample was removed after each pulse, mixed with loading dye and subjected to gel electrophoresis. DNA size markers are loaded on the right-hand side of the gel, with the numbers at the top of the figure indicative of the number of 10 second pulses of sonication each sample was subjected to.

Figure 5.2 – Immunofluorescence staining for EBNA1 (R4 antibody) in Ad/AH (A), Ad/AH-rEBV (B), Ad/AH-neo (C) and Ad/AH-EBNA1 (D) cells. Images presented are at 400X magnification and the marker bar represents 10µM.

Figures 5.1 and 5.2

Figure 5.3 – Immunoblotting for EBNA1 following immunoprecipitation of Ad/AH-rEBV and -EBNA1 cell lysates with chEBNA1 antibody, or isotype control antibody E-Cadherin (E-Cad). Also included are cell lysates as positive controls, and input samples (5% of total sample), taken following pre-clearing of lysates.

Figure 5.4 – Validation of PCR primers designed for promoter regions of c-myc (A), ATF-2 (B), and c-jun (B). PCR primers designed for the EBV DS region are also validated (B). 50ng of Ad/AH-rEBV DNA was used per reaction as a template.

Figures 5.3 and 5.4

symmetry repeat (EBV DS) region (EBV genomic DNA, from the *OriP* region, constitutively bound directly by EBNA1), were optimised for annealing temperature (Figure 5.4A) and cycle number using Ad/AH-rEBV genomic DNA as template. Optimal conditions are defined as those that produce clean bands following agarose gel electrophoresis (Figure 5.4). Primers for the promoter region of GAPDH (negative control) were provided in the commercial ChIP kit used and did not require validation.

5.1.1.2 PCR analysis of ChIP DNA

Initial analysis of DNA from ChIP experiments was PCR based. GAPDH promoter DNA was successfully precipitated (Figure 5.5A) by an α-Histone antibody (positive control), demonstrating application of optimal ChIP experimental conditions. In the absence of EBNA1 (in Ad/AH and Ad/AH-neo lineages), analysis of chEBNA1 ChIP samples revealed no enrichment (relative to isotype control samples) for any promoter region DNA that was analysed (Figure 5.5B), demonstrating that the chEBNA1 antibody was not sufficient for promoter region DNA precipitation in the absence of EBNA1. Contrastingly, in Ad/AH-rEBV and Ad/AH-EBNA1 cells, enrichment was observed in some cases for c-jun, ATF-2 and c-myc promoter DNA in chEBNA1 samples, when compared with isotype control samples (Figure 5.5B). These data suggest that EBNA1 was associated with the promoter region DNA of these genes at the point of formaldehyde cross-linking. GAPDH promoter region DNA, in this instance serving as a negative control, was not enriched in the same experimental samples, demonstrating specificity of promoter DNA enrichment. EBV DS DNA levels were assessed for each sample (Figure 5.5B), with EBV DS DNA found to be present only in Ad/AH-rEBV samples (as expected). In these samples, a clear enrichment of EBV DS DNA was seen in chEBNA1 samples, acting as a specific positive control for the chEBNA1 antibody, as EBNA1 is known to bind directly to EBV DS DNA *in vivo* (Reisman et al. 1985; Gahn and Schildkraut 1989; Wysokenski and Yates 1989; Niller et al. 1995).

Figure 5.5A - PCR analysis of GAPDH promoter DNA performed on chromatin immunoprecipitated DNA from Ad/AH-rEBV cross-linked cell lysate. Rabbit IgG (negative control) and an α-Histone antibody (positive control) were used in the immunoprecipitation. Input represents 5% sample taken after pre-clearing and immediately prior to immunoprecipitation.

Figure 5.5B – PCR analysis of GAPDH promoter, c-jun promoter, ATF-2 promoter, c-myc promoter and EBV DS DNA performed on chromatin immunoprecipitated DNA from Ad/AH, Ad/AH-rEBV, Ad/AH-neo and Ad/AH-EBNA1 cross-linked cell lysates. E-Cadherin (E-Cad, isotype control) and chEBNA1 antibodies were used in the immunoprecipitation. Input represents 5% sample taken after pre-clearing and immediately prior to immunoprecipitation.

Figure 5.5

5.1.1.3 qPCR analysis of ChIP DNA

To allow accurate quantification of these data and to establish the statistical significance of the results, qPCR analysis of immunoprecipitated DNA was undertaken. qPCR primer/probe sets were designed in the same regions as PCR primer sets, with probe concentration for each primer probe set optimised for a five-fold increase in DNA concentration, as shown in Figure 5.6. To achieve this optimisation, Ad/AH-rEBV DNA was diluted to concentrations of 1ng/µl and 5ng/µl, with 5µl of each these diluted DNA solutions being used in experimental analysis. The amount of promoter region-specific probe was varied (constant primer concentration) and the fold change between samples of 5ng and 25ng DNA was determined (Figure 5.6). Probe concentrations that resulted in the most accurate fold change were subsequently utilised. Where large fluctuations in experimentally determined fold change were observed, the selected probe concentration was further tested to ensure reliability before use in analysis of ChIP samples.

Analysis of EBV DS DNA (Figure 5.7A) revealed an approximately 15-fold enrichment of DNA from isotype control to chEBNA1 samples, with EBV DS DNA being detectable only in Ad/AH-rEBV cells. No significant enrichment of GAPDH promoter DNA (from isotype control to chEBNA1 samples) was observed in any of the Ad/AH cell lines (Figure 5.7), these data again serving as an adequate negative control, demonstrating the specificity of the enrichment of promoter region DNA. Levels of enrichment for the promoter regions of EBER-associated transcription factors c-myc and ATF-2 were significantly increased (statistically) in Ad/AH-EBNA1 samples, compared with Ad/AH-neo samples (Figure 5.7B). ATF-2 promoter DNA was enriched by 7.5 fold, with c-myc promoter DNA enriched by 2.5 fold in Ad/AH-EBNA1 chEBNA1 samples. Given the transcriptional upregulation of these genes in EBNA1-expressing cells (as reported in Chapter 4), these data appear significant in explaining EBNA1's mechanism of EBER induction.

Figure 5.6 – qPCR analysis used in the optimisation of the concentration of qPCR probe to be used in subsequent experimental qPCR analysis of promoter regions of GAPDH, c-jun, junB, junD, c-fos, fosB, fra1, fra2 and ATF-2. The optimisation of the primer probe set for EBV DS repeat is also shown. Data are presented as calculated fold change from 5ng DNA samples, to 25ng DNA samples. Samples were analysed in technical triplicate, with error bars being representative of standard deviation between replicates. Also included for comparison is a bar illustrating an exact five-fold change.

Figure 5.6

Figure 5.6 contd

Figure 5.7 – qPCR analysis performed on chromatin immunoprecipitated DNA from (A) Ad/AH and Ad/AH-rEBV cross-linked cell lysates and , (B and C) Ad/AH-neo and Ad/AH-EBNA1 cross-linked cell lysates: (A) Analysis of EBV DS, and GAPDH promoter DNA; (B) Analysis of GAPDH, c-myc and ATF-2 promoter DNA; (C) Analysis of GAPDH promoter DNA, and promoter DNA of AP-1 subunits c-jun, junB, junD, c-fos, fosB, fra1, fra2 and ATF-2. Results represent qPCR values obtained from cross-linked genomic DNA immunoprecipitated using an EBNA1-specific antibody (chEBNA1) normalised to values obtained using an isotype control antibody (E-Cadherin). All experiments were conducted in biological and technical triplicate, with average values presented. Error bars are representative of standard deviation of biological replicates. Asterisks indicate that results differ significantly from the control: *, $P \leq 0.05$; **$\leq$ P,0.01.

Figure 5.7

In addition to promoter regions for which PCR analysis was carried out, qPCR analysis of the promoter region DNA of ATF-2 and c-jun's fellow AP-1 family member subunits was conducted (Figure 5.7C). This analysis, although not connected with EBNA1's effect upon EBER expression, was conducted following data being generated that revealed EBNA1 to induce AP-1 activity in NPC cells (O'Neil et al. 2008). Promoter region DNA of several AP-1 family subunit members was enriched in chEBNA1 samples (Figure 5.7C). However, the only statistically significant enrichments (in Ad/AH-EBNA1 samples compared with Ad/AH-neo samples) for ATF-2 (7.5-fold enrichment) and c-jun (5-fold enrichment) promoter region DNA.

5.1.2 HaloCHIP analysis of EBNA1 promoter binding

For analysis of the domain of EBNA1 responsible for promoter binding, antibody-based methods were deemed undesirable, due to the changes in antibody affinity for EBNA1 mutants lacking individual or multiple domains. To overcome this problem, vectors encoding EBNA1 mutants fused to a tag (HaloTag, from Promega UK) were generated, enabling the pull-down of these fusion proteins, in a covalent, non-antibody specific manner. Following the generation of the panel of expression vectors encoding these Halo-EBNA1 mutants using molecular biology techniques, HaloCHIP experiments were conducted following transient expression of the mutant fusion proteins. The transient, non-antibody-dependent nature of these experiments also afforded expansion of promoter binding studies to multiple cell lines, and the analysis of a larger variety of promoter region DNA targets.

5.1.2.1 Construction of Halo-EBNA1 mutant expression vectors

A panel of EBNA1 mutant expression vectors was obtained. Each EBNA1 mutant (ΔGly/Ala, Δ8-67, Δ61-83, Δ395-450, Δ41-376, Δ325-376) maintained on a lentivirus backbone. Functional details of each mutant are briefly outlined, having been more fully explained

previously in this thesis (Section 1.77): ΔGly/Ala-EBNA1 was used as a pseudo-wild type version of the protein, with only Gly/Ala repeats deleted. Studies have shown lack of Gly/Ala repeats does not affect EBNA1 DNA segregation, replication or transcriptional activation activities (Yates et al. 1985). The 325–376 region of EBNA1 mediates the interaction of EBNA1 with cellular chromatin and is necessary for the transcriptional activation function of EBNA1 (Kirchmaier and Sugden 1997; Shire et al. 1999; Ceccarelli and Frappier 2000; Wu et al. 2000; Wu et al. 2002). Δ395–450 mutation leaves an EBNA1 protein that is fully functional for all of the known functions of EBNA1 (replication, segregation and transcriptional activation), but which fails to bind the cellular USP7 protein (Holowaty et al. 2003). EBNA1 amino acids 8-67 have previously been shown to contribute to, though are not absolutely required for, EBNA1 replication, partitioning and transcriptional activation functions of EBNA1(Wu et al. 2002), with a Δ61-83 deletion of EBNA1residues having been demonstrated to lead to the elimination of transcriptional activation activity of EBNA1 (Wu et al. 2002). Δ41-376 EBNA1 is a gross mutant encompassing all other mutations within this EBNA1 mutant panel.

To each EBNA1 mutant-encoding sequence, it was necessary to add specific restriction endonuclease sites to each end of the EBNA1 mutant sequence, allowing cloning into the expression vector pFC14K. This was achieved through PCR amplification of EBNA1 fragments (shown in Figure 5.8) using specific primers which introduced a SgfI restriction site at the 5’ end of the EBNA1-encoding sequence, and a PmeI restriction site at the 3’ end of the EBNA1-encoding sequence. A schematic illustrating the workflow for the entire cloning procedure is shown in Figure 5.9, however variations from this procedure were necessary. Following PCR amplification of EBNA1 mutant sequences with specific restriction sites at 5’ and 3’ ends of the EBNA1 encoding sequence, despite considerable persistence, it was not possible to clone these products directly into the pFC14K vector

Figure 5.8 – PCR amplifications carried out with specific primers to introduce SgfI and PmlI restriction sites to products using a panel of EBNA1 mutants (ΔGly/Ala, Δ8-67, Δ61-83, Δ395-450, Δ41-376, Δ325-376) maintained on lentivirus backbones. Following optimisation of primer conditions (annealing temperature, extension time, etc.) successful amplification of the desired EBNA1 region was achieved (and is presented here). These PCR products possessed an SgfI binding site at the 5' end of the EBNA1-encoding sequence, and a PmeI binding site at the 3' end of the EBNA1-encoding sequence. Product sizes are given in brackets.

Figure 5.9 – Schematic (adapted from http://www.promega.com/tbs/tm254/tm254.pdf) illustrating the cloning workflow used to generate pFC14K-HaloΔEBNA1 mutants.

Figures 5.8 and 5.9

following digestion with appropriate endonucleases. This failure was possibly due to incomplete restriction of EBNA1 mutant PCR products, with only very small overhangs each side of the restriction sites. To facilitate transfer to the terminal vector, EBNA1 mutants (with SgfI and PmeI sites) were cloned into an intermediary pCR8-TOPO vector (Invitrogen, UK) using a topoisomerase enzyme. Diagnostic cuts with EcoRI (Figure 5.10) were conducted to demonstrate successful insertion of EBNA1 mutant sequences into this vector. Each EBNA1 mutant was subsequently fully sequenced in this vector, confirming that mutations had not been introduced in the PCR amplification step of cloning, and that SgfI and PmeI sites had been successfully installed at either end of the mutant sequence. Following PmeI and SgfI digestion of the pCR8-EBNA1 mutant constructs, each EBNA1-mutant insert was successfully cloned into the pFC14K expression vector (see Figure 5.11: plasmid map of pFC14K), in place of the lethal barnase gene between SgfI and EcoICRI sites (PmeI and EcoICRI both producing blunt ends), and in the same reading frame as the HaloTag protein, leading to expression of Halo-EBNA1 mutant proteins. These expression vectors were screened by diagnostic endonuclease digestion analysis (Figure 5.12), PCR for EBNA1 gene (Figure 5.13) and transient transfection of plasmid DNA into Ad/AH parental cells, to ensure expression of EBNA1 mutant fusion proteins (Figure 5.14). Each Halo-EBNA1 mutant expression vector was analysed in this way although, for brevity, data are shown for only Halo-ΔGly/Ala-EBNA1. Figure 5.15 shows immunoblot analysis of expression of each Halo-EBNA1 mutant protein following transient transfection of expression vectors into Ad/AH cells. HaloΔGly/Ala-EBNA1 shows very high levels of expression, with Halo-Δ395-450, -Δ41-376 and –Δ325-376 showing similar, lower levels of expression. Expression of Halo-Δ8-67 and –Δ61-83 is not observed, despite diagnostic endonuclease analysis and EBNA1 PCR analysis of plasmid DNA suggesting expression vector DNA should encode the desired proteins. Due to time constraints, further attempts to achieve expression of these mutants

Figure 5.10 – Diagnostic restriction digests of EBNA1 mutant PCR products in the pCR8 vector. (A) ΔGly/Ala; (B) Δ 8-67, Δ61-83 and Δ325-376; (C) Δ395-450 and Δ41-376. Miniprep DNA was digested with EcoRI to excise the insert from pCR8 vector.

Figure 5.10

Figure 5.11 – pFC14K plasmid map (can be accessed at http://www.promega.com/). TEV site refers to a TEV protease recognition sequence.

Figure 5.12 – Diagnostic restriction digest of ΔGly/Ala-EBNA1 in the pFC14K vector (pFC14K-HaloΔGly/Ala-EBNA1). Miniprep DNA was digested with NcoI. Where the insert is present, 2 NcoI sites result in excision of a 665bp fragment. Where the insert is absent, the vector is linearised.

Figures 5.11 and 5.12

Figure 5.13 – PCR analysis using EBNA1 primers conducted using miniprep DNA (pFC14K-HaloΔGly/Ala-EBNA1). Presence of product demonstrates successful insertion of fragment into vector.

Figure 5.14 – Immunoblot analysis of EBNA1 expression following transient expression of pFC14K-HaloΔGly/Ala-EBNA1 plasmid DNA in Ad/AH cells. A titration of expression vector DNA from 100ng to 2500ng was carried out. HaloTag-EBNA1 fusion protein is demonstrated to migrate at around 100kDa. Cell lysates were made 24 hours post-transfection. Ad/AH-EBNA1 cell lysate is included as a positive control for EBNA1 immunoblotting, and for comparison of protein size between wild-type EBNA1 and HaloTag-EBNA1 fusion protein.

Figures 5.13 and 5.14

Figure 5.15 – Immunoblot analysis of EBNA1 expression following transient expression of pFC14K-HaloΔGly/Ala-, HaloΔ8-67-, HaloΔ395-450-, HaloΔ61-83-, HaloΔ41-376- and HaloΔ325-376-EBNA1 plasmid DNA in Ad/AH parental cells. Note lack of expression of HaloΔ8-67- and HaloΔ61-85-EBNA1. In each instance, cell lysates were prepared 24 hours post-transfection with 1µg expression vector plasmid DNA.

Figure 5.16 – Diagnostic restriction digest (NotI digestion) confirming the insertion of oligonucleotide to put HaloTag in an open reading frame. The presence of a 1kb fragment illustrates oligonucleotide insertion, as the oligonucleotide possesses a NotI restriction site. The vector also possesses a single NotI site, and as such the plasmid would linearise if the oligonucleotide were not inserted.

Figure 5.17 – Immunoblot analysis of HaloTag protein expression, following transient transfection of Ad/AH parental cells with HaloTag-only miniprep DNA to confirm HaloTag protein expression following oligonucleotide insertion. The HaloTag protein migrates at ~32kDa. HaloEBNA1 transfected cell lysate is included as a positive control.

Figures 5.15-5.17

were abandoned, in favour of more extensive analysis of the successfully generated mutant panel.

The panel of Halo-EBNA1 mutants used in subsequent experiments therefore consisted of Halo-ΔGly/Ala, -Δ395-450, -Δ41-376 and -Δ325-376 EBNA1.

5.1.2.2 Construction and analysis of HaloTag

An expression vector encoding just the HaloTag element of Halo-EBNA1 mutants was generated to as a control to ensure that data obtained from Halo-EBNA1 mutant experiments were attributable to the EBNA1-mutant element of fusion proteins, and not the HaloTag. Briefly, an oligonucleotide was designed and inserted upstream of the HaloTag encoding sequence in pFC14K vector, in order to put the HaloTag protein in an open reading frame. The oligonucleotide insert also contained a NotI restriction site to allow detection of its insertion by endonuclease digestion analysis (Figure 5.16). Subsequently, prospective HaloTag expression vectors were transiently expressed in Ad/AH cells, with cell lysates being screened for HaloTag expression by immunoblotting using an anti-HaloTag antibody (Figure 5.17). Following immunoblot analysis of HaloTag pull-down with HaloLink resin (Figure 5.18), HaloTag was transiently expressed in Ad/AH cells before cross-linked cell lysates from these cells were utilised in HaloCHIP experiments. PCR analysis of DNA from these experiments is shown in Figure 5.19, with no enrichment for ATF-2 or GAPDH promoter DNA apparent in samples where HaloTag was specifically pulled down. qPCR analysis of DNA showed no enrichment of GAPDH, ATF-2, c-myc or c-jun promoter region DNA from control to experimental samples (Figure 5.20) confirming that the HaloTag portion of the Halo-EBNA1 fusion protein panel did not interact with promoter region DNA analysed.

Figure 5.18 – Immunoblotting for HaloTag to confirm pull down of HaloTag protein by HaloLink resin. Ad/AH cells were transiently transfected with 1μg plasmid DNA before lysates were made 24 hours post transfection. The sample was then treated as a HaloCHIP sample before being mixed with loading buffer and immunoblotting analysis. 'CON' refers to samples to which blocking ligand was added (preventing covalent binding of HaloTag to HaloLink resin), and 'EXP' refers to samples to which blocking ligand was not added (allowing covalent binding of HaloTag to resin).

Figure 5.19 – PCR analysis of GAPDH and ATF-2 promoter DNA performed on HaloLink resin-pulled down DNA from cross-linked cell lysates produced from Ad/AH cells transiently expressing HaloTag. 'CON' refers to samples to which blocking ligand was added, and 'EXP' refers to samples to which blocking ligand was not added. Input represents 5% of sample taken post sonication of lysate.

Figure 5.20 – qPCR analysis of GAPDH, c-jun, c-myc and ATF-2 promoter DNA performed on HaloLink resin-pulled down DNA from cross-linked cell lysates produced from Ad/AH cells transiently expressing HaloTag. Data are presented as fold increases from control (CON) to experimental (EXP) samples. All procedures were conducted in biological and technical triplicate, with average values presented. Error bars are representative of the standard deviations of biological replicates.

Figures 5.18-5.20

5.1.2.3 HaloChIP analysis of Halo-EBNA1 mutant panel

Prior to HaloCHIP experiments using the Halo-EBNA1 mutant panel, functional validation of Halo-ΔGly/Ala-EBNA1 (pseudo-wild type) was conducted. Following transient expression of Halo-ΔGly/Ala-EBNA1 in Ad/AH cells, RT-PCR analysis of ATF-2 levels and AP-1 luciferase reporter assays were conducted (Figure 5.21), revealing induction of ATF-2 mRNA and AP-1 reporter activity upon expression of Halo-ΔGly/Ala-EBNA1. These findings confirmed the functional activity of Halo-ΔGly/Ala-EBNA1. Immunoblot analysis of HaloLink resin pull-down of each Halo-EBNA1 mutant fusion protein (Figure 5.22) was also conducted prior to HaloCHIP experiments demonstrating that equivalent levels of each Halo-EBNA1 mutant were pulled down by HaloLink resin under experimental conditions.

Initial HaloCHIP experiments were conducted using Halo-ΔGly/Ala-EBNA1. PCR analysis of Halo-ΔGly/Ala-EBNA1-associated DNA (Figure 5.23) revealed substantial enrichment of ATF-2, c-myc and c-jun promoter region DNA in experimental samples (compared with control samples, where pull-down of Halo-ΔGly/Ala-EBNA1 was blocked). GAPDH promoter region DNA was included as a negative control, demonstrating experimental specificity of positive results. Enrichment for GAPDH promoter region DNA was not observed in experimental samples. These data did not provide any novel findings in terms of EBNA1 function, but are in agreement with results obtained using conventional ChIP analysis.

PCR analysis of HaloCHIP experiments conducted using each Halo-EBNA1 mutant is shown in Figure 5.24. For each mutant, no enrichment of GAPDH promoter region DNA was observed. Enrichment of ATF-2, c-jun and c-myc promoter DNA was observed in experimental samples for Halo-ΔGly/Ala and Halo-Δ395-450 EBNA1 experiments, indicating that the Δ395-450 mutation does not affect EBNA1's association with these

Figure 5.21 – Functional validation of HaloΔGly/Ala-EBNA1 in Ad/AH cells. Following transient transfection of Ad/AH cells with pFC14K-HaloΔGly/Ala-EBNA1: **(A)** RT-PCR was conducted analysing ATF-2 mRNA levels to confirm induction of ATF-2 transcription upon transient expression of 0.1µg and 0.5µg HaloΔGly/Ala-EBNA1 plasmid DNA. Levels of ATF-2 mRNA in Ad/AH-rEBV and Ad/AH-EBNA1 cells are included for comparison; **(B)** AP-1 dual luciferase reporter assays were conducted in Ad/AH cells transfected with empty vector control (pSG5) or HaloΔGly/Ala-EBNA1. Results are presented as a fold change in luminescence values from pSG5 control to HaloΔGly/Ala-EBNA1 samples.

Figure 5.22 – Immunoblotting for EBNA1 to confirm that all mutant Halo-EBNA1 fusion proteins are successfully pulled down by HaloLink Resin. Ad/AH cells were transiently transfected with 1µg plasmid DNA (with exception of pFC14K-HaloΔGly/Ala-EBNA1, where 0.5µg was used) before lysates were made 24 hours post transfection. Samples were then treated as HaloCHIP samples before being mixed with loading buffer and immunoblotting was carried out. 'CON' refers to samples to which blocking ligand was added, and 'EXP' refers to samples to which blocking ligand was not added.

Figure 5.23 – PCR analysis of HaloCHIP samples. HaloΔGlya/Ala-EBNA1 (0.5µg plasmid DNA transfected) was transiently expressed in Ad/AH cells which were cross-linked before harvest of lysates 24 hours post-transfection. PCR analysis was conducted using Halolink resin-pulled down DNA, with analysis of the promoter regions of GAPDH, ATF-2, c-myc and c-jun (as positive control) being conducted. Input sample is 5% of sample, taken post-sonication. 'CON' refers to samples to which blocking ligand was added, and 'EXP' refers to samples to which blocking ligand was not added.

Figures 5.21-5.23

Figure 5.24 – PCR analysis of HaloCHIP samples. HaloΔGlya/Ala-EBNA1 (0.5µg plasmid DNA transfected) and HaloΔ395-450 EBNA1, HaloΔ41-376 EBNA1, HaloΔ325-376 EBNA1 (1µg plasmid DNA transfected) were transiently expressed in Ad/AH cells which were cross-linked and harvested 24 hours post transfection. PCR analysis was conducted on Halolink resin-pulled down DNA for promoter regions of GAPDH, ATF-2, c-myc and c-jun (as positive control). Input sample is 5% of sample, taken post-sonication. 'CON' refers to samples to which blocking ligand was added, and 'EXP' refers to samples to which blocking ligand was not added.

Figure 5.25 – qPCR analysis of HaloCHIP samples following transient expression of Halo-EBNA1 mutants in Ad/AH cells (samples are as used in Figure 5.24). Data are presented as fold increases from control (CON) to experimental (EXP) samples. All procedures were conducted in biological and technical triplicate, with average values presented. Error bars represent the standard deviations of biological replicates. Asterisks (**) indicate that results are significantly different from the control (HaloTag only samples, figure 5.19), $P \leq 0.01$; § indicates that enrichment is significantly greater for this promoter region DNA than the observed enrichment for GAPDH promoter region DNA, $P \leq 0.05$.

Figures 5.24 and 5.25

promoter regions. In Halo-Δ41-376 experiments, no enrichment for promoter region DNA was observed, confirming that this gross deletion ablated EBNA1's association with promoter region DNA. Halo-Δ325-376 EBNA1 experiments revealed no enrichment of c-jun and c-myc promoter region DNA, although a slight enrichment of ATF-2 promoter DNA was observed. These data suggest that this region of EBNA1 is important for association with promoter regions of transcriptionally upregulated genes, although the slight enrichment of ATF-2 promoter region DNA suggests that other domains of EBNA1 may also be important in mediating the association of EBNA1 with this promoter region.

qPCR analysis of HaloCHIP experiments was conducted, allowing accurate quantification of results and determination of the statistical significance of data (Figure 5.25). Experimental samples from Halo-ΔGly/Ala-EBNA1 experiments show substantial enrichment for ATF-2, c-jun and c-myc promoter region DNA. Levels of enrichment were significantly different (statistically) from enrichment for GAPDH promoter DNA, and from enrichment for respective promoter region DNA in HaloTag experiments. Experimental samples from Halo-Δ395-450 EBNA1 experiments also show substantial enrichment for ATF-2, c-jun and c-myc promoter region DNA with levels of enrichment for each promoter region being significantly different (statistically) from enrichments for respective promoter regions in HaloTag experiments. Levels of enrichment for ATF-2 and c-jun promoter region DNA were also statistically significantly greater than the level of GAPDH promoter region DNA enrichment seen in Halo-Δ395-450 experiments. Enrichment for ATF-2, c-jun and c-myc promoter region DNA in experimental samples from Halo-Δ41-376 and –Δ325-376 experiments did not differ significantly (statistically) from GAPDH promoter region DNA enrichments, or levels of enrichments for respective promoter region DNA in HaloTag experiments. qPCR data obtained were consistent with previously described PCR analysis, providing compelling support for the findings based on PCR analysis.

5.1.2.4 Analysis of pol III transcription factor promoters

Following confirmation of conventional ChIP results in HaloCHIP experiments and analysis of Halo-EBNA1 mutants, HaloCHIP assays were used to analyse a larger variety of promoter region DNA targets. Having previously demonstrated EBNA1-mediated induction of TFIIIC subunits (Chapter 4), possible EBNA1 association with promoter regions of these subunits was analysed, along with EBNA1 association with the promoter regions of other pol III-related genes.

After relevant primer design and optimisation, analysis of TFIIIC and TFIIIB subunit promoter region DNA was conducted in Ad/AH cells using HaloCHIP experiments performed following Halo-ΔGly/Ala-EBNA1 expression. Enrichment of TFIIIC-220, -110, -102, and -90 promoter region DNA was observed in experimental samples, compared with control samples, indicating an association between EBNA1 and these promoter regions, although no apparent enrichment of TFIIIC-63 promoter region DNA (Figure 5.26) was observed. This is consistent with the previous finding that TFIIIC-63 was unique amongst the TFIIIC subunit genes in not responding to EBNA1 in Ad/AH cells. PCR analysis (using the same sample sets) of the promoter region DNA of TFIIIB subunits Brf1, Bdp1 and TBP revealed no enrichment in experimental samples (Figure 5.27), suggesting that EBNA1 does not associate with the promoter regions of these genes.

DNA for several cellular pol III-transcribed genes with internal promoter regions (5S rRNA, 7SL RNA and $tRNA^{tyr}$) was not enriched in experimental samples from Halo-ΔGly/Ala-EBNA1 experiments (Figure 5.28), indicating that EBNA1 is not present at these regions *in vivo*. As 7SL RNA has a hybrid promoter with an upstream promoter region in addition to an internal region, analysis of upstream promoter region DNA was also conducted, with no enrichment observed in experimental samples from Halo-ΔGly/Ala-EBNA1 experiments.

Figure 5.26 – PCR analysis of HaloΔGly/Ala-EBNA1 HaloCHIP samples in Ad/AH cells (samples are as used in Figure 5.24). The analysis was conducted for promoter region DNA of TFIIIC subunits TFIIIC-220, -110, -102, -90, -63 with GAPDH shown as negative control. Input sample is 5% of sample, taken post-sonication. 'CON' refers to samples to which blocking ligand was added, and 'EXP' refers to samples to which blocking ligand was not added.

Figure 5.27 – PCR analysis of HaloΔGly/Ala-EBNA1 HaloCHIP samples in Ad/AH cells (samples are as used in Figure 5.24). The analysis was conducted for promoter region DNA of TFIIIB subunits Brf1, Bdp1 and TBP with GAPDH shown as negative control. Input sample is 5% of sample, taken post-sonication. 'CON' refers to samples to which blocking ligand was added, and 'EXP' refers to samples to which blocking ligand was not added.

Figures 5.26 and 5.27

Figure 5.28 - PCR analysis of HaloΔGly/Ala-EBNA1 HaloCHIP samples in Ad/AH cells (samples are as used in Figure 5.24). Analysis conducted for 5S rRNA, 7SL RNA, and $tRNA^{tyr}$ internal promoter DNA along with 7SL RNA upstream promoter region DNA with GAPDH shown as negative control. Input sample is 5% of sample, taken post-sonication. 'CON' refers to samples to which blocking ligand was added, and 'EXP' refers to samples to which blocking ligand was not added.

Figure 5.29 - PCR analysis of HaloCHIP samples in AGS and Hone-1 cells. HaloΔGly/Ala-EBNA1 (0.5µg plasmid DNA transfected) was transiently expressed in AGS and Hone-1 cells which were cross-linked and harvested 24 hours post transfection. PCR analysis was conducted on Halolink resin-pulled down DNA for promoter regions of GAPDH and ATF-2. Input sample is 5% of sample, taken post-sonication. 'CON' refers to samples to which blocking ligand was added, and 'EXP' refers to samples to which blocking ligand was not added.

Figures 5.28 and 5.29

Combined, these data indicate that EBNA1 is present at the promoters of TFIIIC subunits upregulated in EBNA1-expressing epithelial cells, though it is absent from the promoter regions of cellular pol III-transcribed genes, or pol III-specific transcription factor subunits which are not upregulated in Ad/AH-EBNA1 cells. This analysis supports the hypothesis that EBNA1 can have a selective effect on expression of TFIIIC, and that this may be responsible (at least in part) for the increase in expression of endogenous pol III products that is induced by EBV.

5.1.2.5 HaloCHIP promoter binding analysis in AGS and Hone-1 cells

As all EBNA1 promoter binding studies thus far were conducted in Ad/AH cells, it was important to expand these studies to additional epithelial carcinoma cell models. The Halo-ΔGly/Ala-EBNA1 expression vector was transiently transfected into AGS and Hone-1 cells before HaloCHIP experiments were conducted and subsequent analysis of resultant DNA. PCR analysis (Figure 5.29) revealed no enrichment of GAPDH promoter region DNA (demonstrating experimental specificity in these cell lines) and modest enrichment of ATF-2 promoter region DNA. qPCR analysis allowed the quantification of these data, and direct comparison with results reported in Ad/AH cells. Figure 5.30 shows enrichment of ATF-2, c-jun and c-myc promoter region DNA in Ad/AH, AGS and Hone-1 cells, though levels of enrichment seen in AGS and Hone-1 cells are noticeably lower than those in Ad/AH cells. However, levels of enrichment for these promoter regions were significantly greater (statistically) than enrichment levels for GAPDH promoter region DNA in respective cell lines, confirming the presence of Halo-ΔGly/Ala-EBNA1 at the promoter regions of cellular genes upregulated in EBNA1-expressing epithelial cells.

Figure 5.30 - qPCR analysis of HaloCHIP samples following transient expression of HaloΔGly/Ala-EBNA1 in Ad/AH, AGS and Hone-1 cells (samples as used in Figure 5.29). Analysis was conducted for promoter region DNA of GAPDH, ATF-2, c-myc and c-jun genes. Asterisks indicate that enrichment for promoter DNA differs significantly from the enrichment of GAPDH promoter DNA for the same sample: *, $P \leq 0.05$; **, $P \leq 0.01$.

Figure 5.31 – Immunoblot analysis of immunoprecipitation using chEBNA1 and E-Cadherin (isotype control) antibodies in Ad/AH-rEBV and Ad/AH-EBNA1 cells. Immunoblotting was conducted for EBNA1 to confirm precipitation of EBNA1, and for ATF-2 to identify possible EBNA1-ATF-2 interactions. In addition to immunoprecipitated samples, also included are Ad/AH-rEBV and Ad/AH-EBNA1 cell lysates as positive controls, and input samples (5%), taken following pre-clearing of lysates.

Figures 5.30 and 5.31

5.1.3 Mechanism of EBNA1 promoter binding

Although ChIP and HaloCHIP experiments were successful in establishing an association between EBNA1 and the promoter regions of various transcriptionally upregulated genes, such experiments did not determine the nature of the interaction between EBNA1 and promoter region DNA. Given the pleiotropic nature of EBNA1 function, it was possible that EBNA1 could bind directly to DNA sequences, or that EBNA1 was interacting with other transcription factors present at the promoters of genes, thereby interacting indirectly with promoter region DNA. Sequence homology analysis of EBNA1-associated promoter regions revealed no significant regions of homology, suggesting that EBNA1 may be acting indirectly. Consistent with this, no known EBNA1 binding sites were identified in the promoter regions that were analysed.

To investigate possible protein-protein interactions between EBNA1 and cellular transcription factors, immunoprecipitation experiments were conducted, alongside equivalent experiments using Halo-ΔGlya/Ala-EBNA1. Figure 5.31 reveals a possible interaction between EBNA1 and ATF-2, although reciprocal immunoprecipitation experiments (using ATF-2 antibody in the immunoprecipitation) followed by immunblotting for EBNA1 were not successful in confirming the interaction. However when Halo-ΔGly/Ala-EBNA1 pull-down experiments were conducted (Figure 5.32A), along with a clear interaction between Halo-ΔGly/Ala-EBNA1 and USP7 (known to interact with EBNA1), an interaction between Halo-ΔGly/Ala-EBNA1 and ATF-2 was apparent. Such interactions between HaloTag and USP7 and ATF-2 were not detected (Figure 5.32B). These data suggest that EBNA1 does indeed interact with cellular transcription factor ATF-2, and such an interaction may be responsible, in some instances, for EBNA1-association with promoter regions of upregulated genes.

Figure 5.32 – Immunblot analysis of HaloLink resin-pull downs in Ad/AH cells transiently transfected with 5µg pFC14 K-HaloΔGly/Ala-EBNA1 (A), or 5µg pFC14K-HaloTag (B). Immunoblotting is conducted for ATF-2, USP7 and EBNA1. Input sample is 5% of sample, taken prior to HaloLink resin-pull down. 'CON' refers to samples to which blocking ligand was added, and 'EXP' refers to samples to which blocking ligand was not added.

Figure 5.32

5.2 Discussion

5.2.1 ChIP analysis

EBNA1 has previously been shown to bind to multiple sites within the human genome (Dresang et al. 2009) and is also known to have transcriptional regulatory properties on the viral Cp, Qp and LMP1 promoters (Sugden and Warren 1989; Sample et al. 1992; Gahn and Sugden 1995), leading to the hypothesis that EBNA1 may be associating with the promoter regions of genes transcriptionally induced in EBNA1-expressing cells. ChIP analysis provided significant mechanistic insight into EBNA1's induction of typical pol II, EBER-associated cellular transcription factors. Association of EBNA1 with promoter region DNA of both ATF-2 and c-myc (Figures 5.5 and 5.7B) was demonstrated, suggesting that EBNA1 may be influencing EBER expression by acting directly to transcriptionally induce EBER-associated transcription factors through association with their promoter regions.

It is noted that promoter occupancy by EBNA1 does not necessarily directly correlate with the magnitude of the resulting changes in gene expression. For example, levels of ATF-2 promoter DNA enrichment were three-fold greater than levels of c-Myc promoter DNA enrichment (Figure 5.7B), but corresponding variation in the magnitude of changes in gene expression were not observed (Chapter 4).

The AP-1 transcription factor (a dimer comprised of members of the Jun, Fos and ATF families) regulates a wide variety of cellular processes, including cell growth, death and survival, and differentiation (Shaulian and Karin 2002). AP-1 is often activated in a variety of viral infections (Tyler et al. 2001; Ludwig et al. 2003; Panteva et al. 2003) including EBV infection (Kieser et al. 1997; Eliopoulos and Young 1998). ChIP analysis revealed that EBNA1 was present at the promoters of at least two AP-1 subunit genes c-jun and ATF-2, two AP-1 subunits for which mRNA levels are induced in EBNA1-expressing epithelial cells

(O'Neil et al. 2008). It is proposed that this promoter binding is the mechanism by which EBNA1 enhances the transcription of these two AP-1 subunits, resulting in the elevated AP-1 activity reported in Ad/AH cells (O'Neil et al. 2008). This finding is significant given the variety of cellular processes in which AP-1 is involved (Shaulian and Karin 2002), and that AP-1 is implicated in a wide range of cancers where it impacts upon these tightly regulated processes and can therefore contribute to cellular transformation (Hess et al. 2004). As ChIP analysis revealed that JunB, JunD and FosB promoter DNA was not statistically significantly enriched in EBNA1-expressing cells (though there was a non-significant (statistically) four-fold enrichment of FosB promoter region DNA) it was considered that the regulation of these subunits was not mediated by EBNA1 promoter binding.

Controls included in ChIP experiments afford high levels of confidence in the specificity of results obtained. The lack of enrichment for GAPDH promoter region DNA confirmed that non-specific enrichment of DNA due to experimental techniques or reagents did not occur, and high levels of enrichment for EBV DS DNA confirmed that DNA known to be bound by EBNA1 *in vivo* (Reisman et al. 1985; Gahn and Schildkraut 1989; Wysokenski and Yates 1989; Niller et al. 1995) was precipitated under experimental conditions. It is interesting to note that levels of enrichment of promoter region DNA were similar in Ad/AH-rEBV and Ad/AH-EBNA1 samples (Figure 5.5, and qPCR data, not shown). Ad/AH-EBNA1 cells express much higher levels of EBNA1 than Ad/AH-rEBV cells (Figure 5.2) and these data suggest that overexpression of EBNA1 in Ad/AH cells does not increase the extent of association with promoter regions.

qPCR analysis of samples allowed accurate quantification of results, and increased sensitivity. Levels of enrichment for ATF-2 and c-myc promoter DNA appear similar when analysed by PCR (Figure 5.5), however upon quantitative analysis by qPCR, a three-fold

difference in levels of enrichment was observed. Similarly quantitative analysis of samples revealed enrichment for EBV DS DNA to be much greater than enrichment for any cellular promoter regions. These data suggest either a greater affinity of EBNA1 for EBV DS DNA, or differing modes of action for EBNA1 association with viral and cellular DNA.

Experimental analysis following this thesis should also include exploration of the possibility that EBNA1 may directly interact with promoters of the EBER genes. Such analysis is yet to be conducted, due to the proximity of *OriP* (to which EBNA1 is known to bind) to the EBER genes. However, the Ad/AH-Puro-EBERs cell system established in this thesis (Chapter 4) could be utilised, along with transient or stable expression of EBNA1, to enable ChIP analysis of the EBER promoters in assessment of a possible EBNA1 interaction.

5.2.2 HaloCHIP analysis

To elucidate the nature of EBNA1's interaction with cellular promoter region DNA and to map the domain(s) of EBNA1 involved in such interactions, it was necessary to employ a panel of EBNA1 mutants in promoter binding studies. Use of traditional ChIP assays was not suitable, given varying degrees of affinity of EBNA1 antibodies for different EBNA1 mutant proteins. The use of HaloTag-EBNA1 fusion proteins overcame this problem, enabling specific pull-down of EBNA1 mutants through covalent binding of the HaloTag to HaloLink resin. Not only did the use of tagged EBNA1 mutant fusion proteins allow analysis of the nature of previously established EBNA1 interactions with promoter region DNA in Ad/AH cells, the transient, non antibody-dependent nature of the experimental system facilitated analysis of EBNA1 promoter binding in several epithelial cell lines, and expansion of the range of target promoter region DNA that could be analysed.

Initial HaloCHIP experimental analysis centred on repetition of the results of standard ChIP assays using the Halo-ΔGly/Ala construct, termed pseudo wild-type as deletion of the

Gly/Ala repeat region of EBNA1 does not affect the DNA segregation, replication or transcriptional activation activities of EBNA1 (Yates et al. 1985). Consistent with this, Halo-ΔGly/Ala-EBNA1 showed functional similarity to EBNA1 in Ad/AH cells (Figure 5.21). HaloCHIP experiments showing enrichment for ATF-2, c-jun and c-myc promoter region DNA (Figures 5.23, 5.24 and 5.25) confirmed results obtained using standard ChIP methods, and although these data provided no additional insight into EBNA1 and its regulation of EBER expression, they afforded confidence in the reliability of subsequent HaloCHIP data.

Analysis of Halo-Δ395-450 EBNA1 HaloCHIP experiments revealed enrichments (that were statistically significant) similar to those observed in pseudo wild-type vector experiments (Figures 5.24 and 5.25) , confirming that the 395-450 region of EBNA1 is not required for association of EBNA1 with the promoter region DNA examined. This result is consistent with previous work, demonstrating Δ395-450 EBNA1 to be fully functional for all known functions of EBNA,1 with the exception of binding cellular protein USP7 (Holowaty et al. 2003) . Slight reductions in enrichment of c-myc promoter and c-jun promoter region DNA (in comparision to Halo-ΔGly/Ala-EBNA1 experiments) are attributed to conformational changes of EBNA1 associated with deletion of a region of protein.

Deletion of residues 41-376 of EBNA1 removes all functional regions of EBNA1, with the exception of the nuclear localisation signal (NLS) and the DNA binding and dimerisation domain. Despite the presence of the NLS, nuclear localisation of Δ41-376 EBNA1 mutant has been shown to be severely reduced (Wu et al. 2002). Given this large deletion of functional EBNA1 regions, it was not surprising that promoter binding of Halo-Δ41-376 EBNA1 was not observed following PCR and qPCR analysis of HaloCHIP experiments (Figures 5.24 and 5.25). These data, along with Tag only experiments (Figures 5.19 and 5.20) confirm that the EBNA1 section of fusion proteins, and not the HaloTag, is responsible for association with promoter region DNA in experiments where enrichment was observed.

Perhaps the most significant findings of Halo-EBNA1 mutant promoter binding experiments came from use of the Halo-Δ325-376 EBNA1 construct. PCR and qPCR analysis of DNA from these experiments revealed no enrichment for promoter region DNA of c-myc and c-jun genes, and only a slight (and not statistically significant) enrichment of ATF-2 promoter region DNA. Previously this deleted region of EBNA1 has been shown to be necessary for both transcriptional and chromosome segregation functions of EBNA1 (Kirchmaier and Sugden 1997; Shire et al. 1999; Ceccarelli and Frappier 2000; Wu et al. 2000; Wu et al. 2002), adding credence to the findings reported in this study. Data presented suggest that in this system, the Gly-Arg-rich sequence between amino acids 325 and 376 is necessary for the EBNA1 association with promoter region DNA of transcriptionally induced genes. The slight enrichment for ATF-2 promoter region DNA contrasts with the lack of enrichment for other promoter region DNA, and hints at possible variation in EBNA1's mode of action in its association with promoter regions.

Given these findings it would be valuable to expand the panel of Halo-EBNA1 mutants used in this study. Initial steps of the cloning procedure to allow analysis of Δ8-67 and Δ61-83 tagged EBNA1 mutants were successful (Figure 5.8), however upon transient expression of these vectors, Halo-Δ8-67 and –Δ61-83 EBNA1 were not detectable by immunoblotting (Figure 5.15). This could be due to lack of antibody recognition of the fusion proteins, although previous studies (using a different anti-EBNA1 antibody) were able to detect Δ8-67 and Δ61-83 EBNA1 mutants by immunoblotting, despite a reduction in expression levels of EBNA1 following these deletions (Wu et al. 2002).

Previous data (Wu et al. 2002) indicate that various EBNA1 functions have overlapping yet differing sequence requirements, with transcriptional activity dependent on residues 61 to 83 and 325 to 376, and being stimulated by residues 8 to 67. Partitioning requires residues 325 to 376 and is stimulated by residues 8 to 67, with replication involving redundant contributions

of both the 325 to 376, and 8 to 67 regions. As such, future analysis of the contribution of residues 6 to 67, and 61 to 83, to the association of EBNA1 with promoter region DNA of transcriptionally induced genes could prove significant.

HaloCHIP experiments afforded expansion of promoter binding studies, resulting in analysis of EBNA1 binding to a greater number of, and greater variety of, promoter regions of induced genes. Most notably, mechanistic analysis of the EBNA1-mediated induction of TFIIIC subunits and cellular pol III transcription (as reported in Chapter 4) was enabled. In findings similar to those observed for EBER-associated pol II cellular transcription factors ATF-2 and c-Myc, induction of TFIIIC subunits in EBNA1-expressing epithelial cells was accompanied by a clear association of EBNA1 with the promoter region DNA of these genes (Figure 5.26). Interestingly, promoter region DNA of each of the four TFIIIC subunits induced in Ad/AH-EBNA1 cells was enriched, whilst there was no enrichment of TFIIIC-63 promoter region DNA, TFIIIC-63 being the single TFIIIC subunit which was not found to be induced in Ad/AH-EBNA1 cells. These data seemingly reveal a clear correlation between EBNA1 promoter binding and transcriptional induction of (EBER-associated) genes. Further, no enrichment of TFIIIB subunit promoter region DNA was observed (Figure 5.27). These pol III specific transcription factor subunits were not consistently induced in EBNA1-expressing epithelial cells. Such data build upon the evidence presented in Chapter 4, suggesting that EBNA1 can have a selective effect on the expression of TFIIIC. Enrichment of cellular pol III-transcribed genes 5S rRNA, $tRNA^{Tyr}$ and 7SL RNA (with internal promoter regions) was not observed, nor was enrichment of the upstream promoter region of 7SL RNA (Figure 5.28). These data suggest that EBNA1 enhances cellular pol III transcription through selective induction of TFIIIC subunits (through interaction with their promoter regions) rather than a direct association with pol III-transcribed genes. Whether induction of the pol

III-transcribed EBERs is also through such an indirect mechanism, is yet to be determined. Analysis of EBNA1-association with EBER genes would be valuable in establishing if a direct interaction of EBNA1 with the EBER genes occurs. EBNA1 is known to associate with the EBV genome proximal to the EBER genes by binding of *OriP*, with a proximal *OriP* region having been demonstrated to enhance EBER expression (Wensing et al. 2001).

Promoter binding studies were expanded to two more epithelial cell lines (Figures 5.29 and 5.30), revealing statistically significant enrichments of ATF-2, c-myc and c-jun promoter region DNA in AGS and Hone-1 cells transfected with Halo-ΔGly/Ala-EBNA1. However, levels of enrichment were notably lower in AGS and Hone-1 cells, compared with Ad/AH cells, suggesting either differences in experimental efficacy or varying EBNA1 function in individual epithelial cell lines. Nevertheless, results obtained in Ad/AH cells were replicable in the additional epithelial cell lines analysed, affording confidence that other promoter binding data obtained in Ad/AH cells is applicable to a range of cell lineages. That c-myc promoter region DNA was enriched in HaloCHIP experiments conducted in AGS and Hone-1 cells is a surprising result, given the apparent lack of transcriptional induction of c-myc in EBNA1-expressing AGS and Hone-1 cells (Figure 4.21). However, although statistically significant, levels of enrichment were only around half of those observed in Ad/AH cells (Figure 5.30). Further, previous studies have indicated that promoter occupancy by EBNA1 does not necessarily lead to induction of gene transcription (Dresang et al. 2009). It would be valuable to expand the analysis of TFIIIC promoter binding by EBNA1 to AGS and Hone-1 cells, and examine whether a correlation existed in these cell lines between transcriptional induction of TFIIIC subunits and enrichment of promoter region DNA, as was observed in Ad/AH cells. Further, HaloCHIP analysis of the Halo-EBNA1 mutant panel across several epithelial cell lines would allow comparative analysis of EBNA1's mechanism of association with promoter regions in differing cell backgrounds.

In HaloCHIP experiments, levels of enrichment of promoter region DNA observed were often notably smaller than enrichment levels seen in conventional ChIP assays, especially for ATF-2 promoter region DNA (Figures 5.7 and 5.25). Levels of enrichment for differing promoter regions were more consistent in HaloCHIP experiments than ChIP assays, albeit generally at a lower level. This apparent reduction in enrichment levels may be attributable to several factors. Firstly, HaloCHIP experiments were carried out following transient expression of vectors, rather than in cell lines stably expressing EBNA1. Secondly, EBNA1-fusion proteins, by their very nature, were altered and possessed a 5' HaloTag. Although the HaloTag was shown not to be responsible for any interactions of the Halo-EBNA1 proteins (Figure 5.20) with promoter region DNA, it is possible that the HaloTag may have interfered (physically) with, and had a detrimental effect upon, EBNA1 promoter binding. It is also noted that even the pseudo-wild type Halo-EBNA1 (ΔGly/Ala) was not a complete EBNA1-fusion protein. Although previously shown not to affect EBNA1 function (Yates et al. 1985), it is possible that deletion of this region may change EBNA1 protein conformation in a manner detrimental to the novel promoter binding abilities reported here.

5.2.3 Mechanism of EBNA1 promoter binding

The presence of EBNA1 at promoters of genes induced in EBNA1-expressing cells affords a potential mechanistic insight into EBNA1's mode of action in enhancing expression of the EBERs. The nature of the interaction between EBNA1 and upregulated genes is, at present, undetermined. However lack of sequence homology, and the absence of any known EBNA1 DNA binding motifs (Baer et al. 1984; Ambinder et al. 1990; Kirchmaier and Sugden 1998; Dresang et al. 2009) in promoters with which EBNA1 association is shown suggests that direct binding of EBNA1 to promoter region DNA of induced genes is unlikely. Further, EBV DS DNA (a region to which EBNA1 is known to bind directly *in vivo* (Reisman et al.

1985; Gahn and Schildkraut 1989; Wysokenski and Yates 1989; Niller et al. 1995)) was enriched to a substantially greater extent than cellular promoter region DNA assayed, suggesting that EBNA1's mode of action in association with these regions of cellular DNA may vary from its DNA binding activity which enables direct binding to EBV DS region. It was therefore tempting to speculate that EBNA1's interaction with these regions may be more indirect, possibly through protein-protein interactions with other transcription factors and to investigate this possibility, immunprecipitations using chEBNA1 antibody (previously used in ChIP assays) were conducted, prior to immunoblotting for two selected cellular transcription factors, ATF-2 and c-Jun. These transcription factors were screened for an association with EBNA1 given their transcriptional induction in EBNA1-expressing cells and the self-regulatory nature of their transcription (Vlahopoulos et al. 2008). Additionally, AP-1 reporter activity is increased in EBNA1-expressing cells (Figure 5.21B, (O'Neil et al. 2008)), a phenomenon that in theory could be mediated, in part at least, by an interaction with EBNA1. Furthermore, *in silico* analysis revealed that each cellular transcription factor, reported (in Chapter 4) to be induced in EBNA1-expressing epithelial cells, contains at least one putative AP-1 binding site upstream of it transcriptional start site. Although no interaction between EBNA1 and c-Jun was detectable (data not shown), a possible interaction between EBNA1 and ATF-2 was identified (Figure 5.31), and despite reciprocal immunoprecipitation experiments proving unsuccessful, Halo-EBNA1-fusion protein pull-down experiments (Figure 5.32) confirmed the possible interaction between EBNA1 and ATF-2. Such data provide no evidence to support the hypothesis that any interaction between EBNA1 and ATF-2 occurs at the site of transcriptional activity of these proteins, however increased levels of nuclear ATF-2 in EBNA1-expressing cells (Figure 4.20) and the nuclear localisation of EBNA1 suggest that any direct interaction between these two proteins would be likely to occur in the nucleus. Analysis of a possible Halo-Δ325-376 EBNA1:ATF2

interaction could provide mechanistic insight into EBNA1's presence at the promoters of transcriptionally induced genes. If such an interaction was not identified, this would provide evidence that interaction of this Gly-Arg-rich region of EBNA1 with ATF-2 may be responsible for the reported association with promoter region DNA, given the lack of enrichment for promoter region DNA seen in HaloCHIP experiments conducted with this EBNA1 mutant fusion protein (Figure 5.25).

The concept of viral proteins interacting with cellular promoter region DNA through cooperation with cellular transcription factors, leading to changes in cellular transcription, has precedence. As described in the introduction to this chapter, proteins from HPV (Kurg et al. 2005), HTLV-1 (Basbous et al. 2003; Thebault et al. 2004; Matsumoto et al. 2005) and Adenoviruses (Boyd et al. 2002; Green et al. 2008) amongst others, are known to influence cellular transcription in such a manner. As such, although the hypothesis proposed here, that EBNA1 interacts with promoter region DNA of transcriptionally induced genes through interaction with cellular transcription factors, is in need of more supporting evidence, the data presented (in conjunction with the previous reports of viral proteins influencing cellular transcription in this manner) suggest that EBNA1 interacts with cellular promoter region DNA through interacting with cellular transcription factors. Further, given the specific association of EBNA1 with the promoter regions of genes induced in EBNA1-expressing cells, these interactions are suggested to influence cellular gene expression. EBNA1 then, seemingly acts to induce expression of EBERs through association with cellular promoter region DNA, thus influencing cellular factors connected with EBER transcription.

Chapter 6

Final Discussion and Future Work

Chapter 6 - General Discussion and Future Work

EBER1 and EBER2 are detected in all forms of EBV latency and are often used as a diagnostic marker for cellular infection by the virus. Although the EBERs are not required for the transformation of resting B-cells by EBV, they have been demonstrated to increase the efficiency of transformation by around 100-fold (Yajima et al. 2005). Further, expression of the EBERs is sufficient to maintain the tumourigenic potential of the EBV-associated B-cell malignancy from which the virus was first isolated, BL (Komano et al. 1999). The EBERs are abundantly transcribed by pol III in latently infected cells, with up to 10^7 copies of the EBERs present in each cell (Lerner et al. 1981; Arrand and Rymo 1982; Nanbo and Takada 2002).

Although classically a B-lymphotropic virus, EBV has the capacity to enter epithelial cells and shows a strong association with a number of epithelial malignancies. These malignancies include undifferentiated NPC, which shows a 100% association with EBV infection. The EBERs are frequently detected in the neoplastic cells of NPC together with EBNA1, LMP2A, LMP2B, the BARTs and variable levels of LMP1 although, in contrast to B-cells where the role of the EBERs is fairly well defined, the precise role of EBERs in epithelium and NPC tumourigenesis remains to be elucidated. However, high levels of EBER expression have been demonstrated to be crucial for oncogenic activity of EBERs in epithelial cells, with previously published data suggesting that high, but not low, levels of EBER expression could cause MDCK cells to form colonies in soft agar (Yoshizaki et al. 2007). The aim of this thesis was, therefore, to further elucidate the mechanisms by which EBV is able to achieve the high levels of EBER expression that are required for oncogenic activity in epithelial cells.

Given that EBV is maintained in epithelial and B-cells in a multi-copy episomal form, Chapter 3 explored the possibility that high levels of EBER expression were attributable to a

high copy number of the EBER genes. The hypothesis that EBV genomic copy number variation is directly responsible for fluctuations in levels of EBER expression between various cell lines was explored, with analysis conducted to establish if the expression of the EBERs increases monotonically with the average genome copy number across a panel of LCLs. Previous data, derived from plasmid-based experiments (Komano et al. 1999) and small-scale studies assessing the rate of EBER transcription in LCLs with varying copy number (Metzenberg 1989), had suggested that such a monotonic increase in levels of EBER expression with corresponding increases in average EBV genomic copy number may occur. However, the data presented provide convincing evidence that across the panel of LCLs analysed, no correlation between levels of EBER expression and average EBV genomic copy number was demonstrable. To confirm and expand upon these findings, it would be pertinent to conduct similar analysis across not only an extended panel of B-cells derived from several malignant backgrounds, but also across a panel of epithelial cells. Further, it would be interesting to extend the work of Metzenberg, analysing the rate of EBER transcription across a much larger panel of cells with varying copy number. Other pertinent experiments might assess the rate of EBER degradation across various cell lines to establish the consistency of this possible variable.

The findings presented in Chapter 3 are consistent with previous observations which suggest that the abundant expression of EBER genes requires EBV-induced changes to the cellular environment, and with previous studies suggesting a strong influence of trans-acting factors in controlling the transcription of the EBERs. Indeed, EBV-induced changes to the cellular environment that contribute to achieving high levels of EBER expression have recently been identified and described (Felton-Edkins et al. 2006). The possibility of EBV latent gene products influencing EBER expression has previously been suggested, not least because following B lymphocyte infection by EBV, the EBERs are temporally the last latent gene

product to be expressed (Rooney et al. 1989; Alfieri et al. 1991). Given that EBNA1 is expressed in all forms of viral latency (and is detectable in the vast majority of EBV-associated malignancies) and has previously been suggested to induce the transcription of EBER-associated cellular transcription factors ATF-2 and TFIIIC102 (Wood et al. 2007; O'Neil et al. 2008), the hypothesis that EBNA1 is able to influence cellular factors involved in the regulation of EBER expression was tested in Chapter 4. Several transcription factors, typical of pol II and pol III transcription, were found to be transcriptionally induced in EBNA1-expressing cells, seemingly confirming the hypothesis that EBNA1, at least in part, is responsible for mediating EBV-induced changes to the cellular environment that are conducive to high levels of EBER expression (Figure 6.1).

The EBER-associated cellular transcription factors shown to be induced by EBV-infection in this study have also been demonstrated to be induced by several other oncogenic viruses in disparate other studies, which are outlined in the introductory Chapter of this thesis. Given the variety of evolutionarily distinct viruses that are capable of influencing these cellular factors, it is likely that this influence confers a selective advantage to virus survival and/or replication. This raises the possibility that the increase in cellular pol III activity and induction of cellular transcription factors observed in EBV-positive and EBNA1-expressing cells has been selected for during the course of EBV evolution, rather than merely being a consequence of enhancing EBER expression. That pol III activation is a common response to the infection of cells by DNA tumour viruses, irrespective of whether such activation is required for viral gene expression (although activation is required for EBV expression of the EBERs, and adenovirus expression of VA RNAs), supports the idea that this activation has a selective benefit. Recent studies, which suggest that cellular pol III products including tRNA and 5S rRNA are needed in abundance for cells to grow and proliferate, concur with this notion (Johnson et al. 2008; Marshall and White 2008). However, the divergence and variety

Figure 6.1 – Simplified schematic summarizing findings of thesis chapters 4 and 5. EBNA1 is proposed to indirectly (possibly through protein:protein interactions with cellular transcription factors (TF)) interact with the promoter regions of c-myc, ATF-2 and TFIIIC genes in epithelial cells. This interaction has been demonstrated to be mediated by residues 325-376 of EBNA1 (not represented diagrammatically). The interaction of EBNA1 with promoter regions is proposed to enhance gene transcription, leading to increased levels of the EBER-associated cellular transcription factors c-myc, ATF-2 and TFIIIC. These transcription factors are known to interact with specific regulatory regions both upstream and downstream of the transcriptional start sites of EBER1 and EBER2, and have been demonstrated to be of significance in allowing high levels of EBER expression to occur. It is proposed that by enhancing levels of these EBER-associated cellular transcription factors, EBNA1 is able to increase levels of EBER expression. Further, EBNA1 may be directly interacting with the EBER genes, though this analysis was not carried out in this body of work.

Figure 6.1

of EBER-associated cellular transcription factors demonstrated to be induced by EBNA1 in Chapter 4 support the concept that EBV has specifically evolved multiple mechanisms to ensure abundant expression of the EBERs, and that the selective advantages produced may only have occurred as side-effects, albeit side-effects which are highly beneficial to virus survival.

Although general pol III-mediated transcription was demonstrated to be elevated in EBNA1-expressing cells, and EBNA1 was shown specifically to induce TFIIIC subunits in a range of cell lines, EBNA1's inability to induce levels of TFIIIB subunits, which are known to be over-expressed in NPC tumours (Dr JR. Arrand, personal communication), and limiting for transcription from type 2 pol III promoters (similar to EBER promoter regions), leaves the model of EBNA1's precise mode of action incomplete. Previous data have also revealed an individual TFIIIB subunit, Bdp1, to be induced in EBV-infected cells and limiting for pol III transcription (Felton-Edkins et al. 2006), a result at odds with the apparent lack of induction in EBNA1-expressing cells presented in Chapter 4. However, although very well characterised in the yeast *Saccharomyces cerevisiae*, the full picture of the multiple levels of regulation of pol III transcription is in the process of being fully defined in mammalian cells. For instance, in *S. cerevisiae*, Maf1 is an essential mediator of pol III repression in response to starvation and it has recently been shown that a Maf1 orthologue is also used to restrain pol III activity in mouse and human cells (Goodfellow et al. 2008). This study also revealed Maf1 to interact with pol III and associated transcription factor TFIIIB in mammalian cells, and, as in yeast, Maf1 was demonstrated to be phosphorylated in a serum-sensitive manner *in vivo*. This conservation of activity between yeast and mammals suggests a fundamental importance for the role of Maf1 in controlling pol III transcriptional activity. Given its role in regulation of TFIIIB, and the lack of increase in subunits of TFIIB in EBNA1-expressing

cells (despite an overall increase in levels of cellular pol III transcription), it is conceivable that EBNA1 may be acting on pol III activity through intermediaries such as Maf1.

Also presented in Chapter 4 are data revealing that EBNA1 acts to increase the transcriptional activation activity of c-Myc, despite a reduction in levels of c-Myc protein in EBNA1-expressing cells. These data hint at another possible method of EBNA1 acting to increase pol III transcription through an intermediary cellular factor, as c-Myc is known to directly activate pol III transcription (Oskarsson and Trumpp 2005). Indeed, endogenous c-Myc interacts with tRNA and 5S rRNA genes *in vivo*, and forms a stable association with endogenous TFIIIB (Felton-Edkins et al. 2003; Gomez-Roman et al. 2003). Moreover, scanning ChIP assays suggest that c-Myc co-localises with TFIIIB in the vicinity of transcriptional start sites, and has been demonstrated to recruit cellular cofactors TRRAP and GCN5 to tRNA and 5S rRNA genes leading to an increased gene occupancy by TFIIIB in response to c-Myc activity followed by recruitment of pol III (Kenneth et al. 2007). Such data provide possible mechanisms by which EBNA1 may be able to enhance the activity of TFIIIB to activate pol III transcription without inducing the expression of TFIIIB subunits, although it must be noted that c-Myc is not recruited to pol III genes by binding to E-box sites, and this recruitment forms the basis of the c-Myc transcriptional activation data in Chapter 4. Further, TFIIIB levels are known to be increased in tumours, suggesting that EBNA1 is only in part responsible for the increases seen in cellular pol III transcription in EBV-infected cells.

Nevertheless, EBNA1 is seemingly capable of overcoming the lack of TFIIIB induction, given the increase in transcription of cellular pol III transcripts and the EBERs in EBNA1-expressing cells. Other cellular regulators of pol III transcription are PTEN, which represses pol III activity by targeting TFIIIB (Woiwode et al. 2008), and p53, which inhibits pol III transcription by targeting TBP and inhibiting promoter occupancy by TFIIIB (Crighton et al.

2003). It is conceivable that EBNA1 may be able to reduce the inhibitory action of such cellular proteins on TFIIIB activity to compensate of the lack of induction of TFIIIB subunits, and studies of the effect of EBNA1 expression upon other cellular factors involved in the regulation of pol III transcription could prove significant.

Other interesting future analyses that may elucidate the extent of EBV and EBNA1 involvement in the regulation of pol III transcription, and the significance of this involvement in tumourigenesis, might include investigation of a possible role of EBV and EBNA1 in post-transcriptional regulation of pol III products. For example, the RNA methyltransferase Misu (NSUN2), which is a c-Myc target gene, has been demonstrated to methylate pol III products, and by doing so mediates Myc-induced cell proliferation and growth (Frye and Watt 2006). Given its upregulation in tumours, Misu would be another possible target gene for EBV and EBNA1-mediated oncogenesis, especially given Misu's status as a c-Myc target gene. The significance of Misu in regulating c-Myc-mediated cell cycle progression was confirmed recently, upon publication of data which suggest that via Misu, c-Myc promotes proliferation by stabilising the mitotic spindle in fast-dividing cells (Hussain et al. 2009).

The data presented in Chapter 5 offer a mechanistic insight into EBNA1's mode of action in inducing EBER-associated cellular transcription factors. Speculatively, it seems that EBNA1 is acting not through direct DNA-binding, but by interacting with other transcription factors present at promoter regions, possibly including ATF-2. Confirmation of this precise mode of action is essential in future studies, as is elucidation of a full range of transcription factors that associate with EBNA1, assuming that EBNA1 is interacting with promoter region DNA indirectly in this manner. To this end, ChIP-on-CHIP studies would be useful, not only in determining the possible broad range of cellular targets which EBNA1 may influence through interacting with promoter regions, but also in elucidating common themes in such promoter regions which may provide hints as to which transcription factors EBNA1 may be acting

through. A recently published study has carried out such ChIP-CHIP analysis on EBNA1 in an LCL (Dresang et al. 2009). The study identified 247 promoters in the human genome to be candidates for EBNA1 binding, although only 2 of these promoters contained the previously defined (Ambinder et al. 1990) EBNA1 DNA-binding sequence. Dresang and co-workers therefore generated a new EBNA1 DNA-binding consensus with increased degeneracy and found 54 of the 247 candidate promoters to contain this new degenerate sequence. However, EMSA analysis using an EBNA1 protein derivative of a subset of the 193 promoters not containing any consensus revealed a shift in all promoters tested, suggesting direct binding of DNA by EBNA1 whether a DNA-binding site for EBNA1 was predicted or not. However, the authors found that EBNA1 did not alter the expression of a reporter gene placed downstream of tested cellular promoters to which it binds, although the authors note that it is not clear if these data accurately reflect the ability of EBNA1 to regulate genes. Interestingly, the genes reported to be associated with the 247 candidate promoters identified (Dresang et al. 2009, supplementary information) do not include any identified in this thesis. However it should be noted that the ChIP analysis was conducted using B-cell nuclear lysates (rather than epithelial cell whole cell lysates) and was carried out using a different EBNA1 antibody. Promoter regions found to be associated with EBNA1 in this thesis do not contain an EBNA1 binding site, either the EBNA1 binding motif previously detailed (Ambinder et al. 1990), or the degenerate consensus proposed by Dresang and co-workers. Future ChIP-CHIP analysis under conditions used in this thesis would provide an interesting comparison with the analysis recently reported (Dresang et al. 2009), which does not seem to consider the possibility of EBNA1 acting upon promoter regions in an indirect manner.

Previous similar studies have been performed in analysis of other DNA tumour virus gene products. Notably, this year Sung and co-workers have been successful in identifying deregulated targets of the Hepatitis B virus (HBV) X protein through chip-based chromatin

immunoprecipitation (ChIP-CHIP) in combination with expression microarray profiling. 184 gene targets were identified as being directly deregulated by HBV X protein, and 144 transcription factors interacting with HBV X protein were computationally inferred, before experimental validation was conducted confirming that HBV X protein interacts with a selection of the predicted transcription factors and the promoters of the deregulated target genes of these transcription factors (Sung et al. 2009). A similar study to identify deregulated targets of EBNA1 could serve to confirm the findings presented here, identify more EBNA1 cellular targets, and uncover cellular transcription factors with which EBNA1 interacts to exert its cellular influence.

Experimental analysis following on from this thesis could also include exploration of the possibility that EBNA1 may directly interact with promoters of the EBER genes. Such analysis is yet to be conducted, possibly due to the proximity of *OriP* (to which EBNA1 is known to bind) to the EBER genes. However, the Ad/AH-Puro-EBERs cell system established in this thesis could be utilised, along with transient or stable expression of EBNA1, to enable ChIP analysis of the EBER promoters in assessment of a possible EBNA1 interaction. It would also be valuable to assess the expression of a wider range of cellular pol III transcripts in EBNA1-expressing cells, as although EBV was previously demonstrated to induce the expression of a variety of endogenous pol III transcripts, no type 3 promoter products previously examined (U6, 7SK, and MRP RNA) showed evidence of induction (Felton-Edkins et al. 2006). Analysis of such transcripts in EBNA1-expressing cells would allow determination of the selectivity of the stimulatory effect of EBNA1 on pol III-transcribed genes. As pol III-transcribed genes with type 3 promoters do not require TFIIIC for recruitment of the transcription complex (Schramm and Hernandez 2002), it is speculated that the expression of such transcripts would not be enhanced in EBNA1-expressing cells.

In summary, data presented in this thesis have shed new light onto the mechanisms of the regulation of EBER expression, which allow the EBERs to be expressed in such abundance. Data have confirmed that EBV-infection induces a change in the cellular environment, with the latent gene product EBNA1 acting at the promoters of cellular factors involved in EBER-expression to induce a cellular environment conducive to expression of the EBERs. Many of the cellular factors influenced by EBNA1 have oncogenic potential, increasing the significance of the findings presented beyond that of enhanced expression of virus-encoded oncogenic RNAs. As such, the data contribute to the growing weight of evidence that suggests that EBNA1 plays a role in EBV-mediated tumourigenesis.

Further, recently published data have suggested that the EBER promoters are able to drive the expression of shRNA fusion transcripts, with siRNAs processed from these fusion transcripts specifically and effectively able to inhibit expression of homologous reporter or endogenous genes in various types of cells (Choy et al. 2008). These findings suggest that the EBER promoters may be effective in driving the intracellular expression of shRNAs for effective silencing of target genes in mammalian cells and particularly, in EBV-infected cells. If such techniques are to be employed in the future, the data presented in this thesis would provide valuable insight into the regulation of EBER promoters, and may prove valuable in allowing maximum efficacy of possible therapeutic shRNAs.

REFERENCES

Adams, J. M., A. W. Harris, C. A. Pinkert, L. M. Corcoran, W. S. Alexander, S. Cory, R. D. Palmiter, and R. L. Brinster. (1985). The c-myc oncogene driven by immunoglobulin enhancers induces lymphoid malignancy in transgenic mice. Nature **318:**533-8.

Adamson, A. L., D. Darr, E. Holley-Guthrie, R. A. Johnson, A. Mauser, J. Swenson, and S. Kenney. (2000). Epstein-Barr virus immediate-early proteins BZLF1 and BRLF1 activate the ATF2 transcription factor by increasing the levels of phosphorylated p38 and c-Jun N-terminal kinases. J Virol **74:**1224-33.

Afar, D. E., A. Goga, J. McLaughlin, O. N. Witte, and C. L. Sawyers. (1994). Differential complementation of Bcr-Abl point mutants with c-Myc. Science **264:**424-6.

Alfieri, C., M. Birkenbach, and E. Kieff. (1991). Early events in Epstein-Barr virus infection of human B lymphocytes. Virology **181:**595-608.

Alland, L., R. Muhle, H. Hou, Jr., J. Potes, L. Chin, N. Schreiber-Agus, and R. A. DePinho. (1997). Role for N-CoR and histone deacetylase in Sin3-mediated transcriptional repression. Nature **387:**49-55.

Allday, M. J., and P. J. Farrell. (1994). Epstein-Barr virus nuclear antigen EBNA3C/6 expression maintains the level of latent membrane protein 1 in G1-arrested cells. J Virol **68:**3491-8.

Allen, M. D., L. S. Young, and C. W. Dawson. (2005). The Epstein-Barr virus-encoded LMP2A and LMP2B proteins promote epithelial cell spreading and motility. J Virol **79:**1789-802.

Alter, M. J. (1995). Epidemiology of hepatitis C in the West. Semin Liver Dis **15:**5-14.

Amati, B., M. W. Brooks, N. Levy, T. D. Littlewood, G. I. Evan, and H. Land. (1993). Oncogenic activity of the c-Myc protein requires dimerization with Max. Cell **72:**233-45.

Ambinder, R. F., W. A. Shah, D. R. Rawlins, G. S. Hayward, and S. D. Hayward. (1990). Definition of the sequence requirements for binding of the EBNA-1 protein to its palindromic target sites in Epstein-Barr virus DNA. J Virol **64:**2369-79.

Anderton, E., J. Yee, P. Smith, T. Crook, R. E. White, and M. J. Allday. (2008). Two Epstein-Barr virus (EBV) oncoproteins cooperate to repress expression of the proapoptotic tumour-suppressor Bim: clues to the pathogenesis of Burkitt's lymphoma. Oncogene **27:**421-33.

Aras, S., G. Singh, K. Johnston, T. Foster, and A. Aiyar. (2009). Zinc coordination is required for and regulates transcription activation by Epstein-Barr nuclear antigen 1. PLoS Pathog **5:**e1000469.

Araujo, I., H. D. Foss, A. Bittencourt, M. Hummel, G. Demel, N. Mendonca, H. Herbst, and H. Stein. (1996). Expression of Epstein-Barr virus-gene products in Burkitt's lymphoma in Northeast Brazil. Blood **87:**5279-86.

Araujo, I., H. D. Foss, M. Hummel, I. Anagnostopoulos, H. S. Barbosa, A. Bittencourt, and H. Stein. (1999). Frequent expansion of Epstein-Barr virus (EBV) infected cells in germinal centres of tonsils from an area with a high incidence of EBV-associated lymphoma. J Pathol **187:**326-30.

Arrand, J. R. 1998. Epstein-Barr Virus, p. 65-92. *In* D. R. Harper and J. R. Arrand (ed.), Viruses and Human Cancer. BIOS Scientific, Oxford.

Arrand, J. R., and L. Rymo. (1982). Characterization of the major Epstein-Barr virus-specific RNA in Burkitt lymphoma-derived cells. J Virol **41:**376-89.

Arrand, J. R., L. Rymo, J. E. Walsh, E. Bjorck, T. Lindahl, and B. E. Griffin. (1981). Molecular cloning of the complete Epstein-Barr virus genome as a set of overlapping restriction endonuclease fragments. Nucleic Acids Res **9:**2999-3014.

Arrand, J. R., L. S. Young, and J. D. Tugwood. (1989). Two families of sequences in the small RNA-encoding region of Epstein-Barr virus (EBV) correlate with EBV types A and B. J Virol **63:**983-6.

Artavanis-Tsakonas, S., K. Matsuno, and M. E. Fortini. (1995). Notch signaling. Science **268:**225-32.

Avolio-Hunter, T. M., P. N. Lewis, and L. Frappier. (2001). Epstein-Barr nuclear antigen 1 binds and destabilizes nucleosomes at the viral origin of latent DNA replication. Nucleic Acids Res **29:**3520-8.

Ayer, D. E., and R. N. Eisenman. (1993). A switch from Myc:Max to Mad:Max heterocomplexes accompanies monocyte/macrophage differentiation. Genes Dev **7:**2110-9.

Ayer, D. E., L. Kretzner, and R. N. Eisenman. (1993). Mad: a heterodimeric partner for Max that antagonizes Myc transcriptional activity. Cell **72:**211-22.

Ayer, D. E., Q. A. Lawrence, and R. N. Eisenman. (1995). Mad-Max transcriptional repression is mediated by ternary complex formation with mammalian homologs of yeast repressor Sin3. Cell **80:**767-76.

Babcock, G. J., L. L. Decker, R. B. Freeman, and D. A. Thorley-Lawson. (1999). Epstein-barr virus-infected resting memory B cells, not proliferating lymphoblasts, accumulate in the peripheral blood of immunosuppressed patients. J Exp Med **190:**567-76.

Babcock, G. J., L. L. Decker, M. Volk, and D. A. Thorley-Lawson. (1998). EBV persistence in memory B cells in vivo. Immunity **9:**395-404.

Babcock, G. J., D. Hochberg, and A. D. Thorley-Lawson. (2000). The expression pattern of Epstein-Barr virus latent genes in vivo is dependent upon the differentiation stage of the infected B cell. Immunity **13:**497-506.

Babu, M. M., N. M. Luscombe, L. Aravind, M. Gerstein, and S. A. Teichmann. (2004). Structure and evolution of transcriptional regulatory networks. Curr Opin Struct Biol **14:**283-91.

Baer, R., A. T. Bankier, M. D. Biggin, P. L. Deininger, P. J. Farrell, T. J. Gibson, G. Hatfull, G. S. Hudson, S. C. Satchwell, C. Seguin, and et al. (1984). DNA sequence and expression of the B95-8 Epstein-Barr virus genome. Nature **310:**207-11.

Bajaj, B. G., M. Murakami, Q. Cai, S. C. Verma, K. Lan, and E. S. Robertson. (2008). Epstein-Barr virus nuclear antigen 3C interacts with and enhances the stability of the c-Myc oncoprotein. J Virol **82:**4082-90.

Banati, F., A. Koroknai, D. Salamon, M. Takacs, S. Minarovits-Kormuta, H. Wolf, H. H. Niller, and J. Minarovits. (2008). CpG-methylation silences the activity of the RNA polymerase III transcribed EBER-1 promoter of Epstein-Barr virus. FEBS Lett **582:**705-9.

Barone, M. V., and S. A. Courtneidge. (1995). Myc but not Fos rescue of PDGF signalling block caused by kinase-inactive Src. Nature **378:**509-12.

Barth, S., T. Pfuhl, A. Mamiani, C. Ehses, K. Roemer, E. Kremmer, C. Jaker, J. Hock, G. Meister, and F. A. Grasser. (2008). Epstein-Barr virus-encoded microRNA miR-BART2 down-regulates the viral DNA polymerase BALF5. Nucleic Acids Res **36:**666-75.

Basbous, J., C. Arpin, G. Gaudray, M. Piechaczyk, C. Devaux, and J. M. Mesnard. (2003). The HBZ factor of human T-cell leukemia virus type I dimerizes with transcription factors JunB and c-Jun and modulates their transcriptional activity. J Biol Chem **278:**43620-7.

Baumforth, K. R., A. Birgersdotter, G. M. Reynolds, W. Wei, G. Kapatai, J. R. Flavell, E. Kalk, K. Piper, S. Lee, L. Machado, K. Hadley, A. Sundblad, J. Sjoberg, M. Bjorkholm, A. A. Porwit, L. F. Yap, S. Teo, R. G. Grundy, L. S. Young, I. Ernberg, C. B. Woodman, and P. G. Murray. (2008). Expression of the Epstein-Barr virus-

encoded Epstein-Barr virus nuclear antigen 1 in Hodgkin's lymphoma cells mediates Up-regulation of CCL20 and the migration of regulatory T cells. Am J Pathol **173:**195-204.

Baumforth, K. R., J. R. Flavell, G. M. Reynolds, G. Davies, T. R. Pettit, W. Wei, S. Morgan, T. Stankovic, Y. Kishi, H. Arai, M. Nowakova, G. Pratt, J. Aoki, M. J. Wakelam, L. S. Young, and P. G. Murray. (2005). Induction of autotaxin by the Epstein-Barr virus promotes the growth and survival of Hodgkin lymphoma cells. Blood **106:**2138-46.

Baumforth, K. R., L. S. Young, K. J. Flavell, C. Constandinou, and P. G. Murray. (1999). The Epstein-Barr virus and its association with human cancers. Mol Pathol **52:**307-22.

Becker, J. C., D. Schrama, and R. Houben. (2009). Merkel cell carcinoma. Cell Mol Life Sci **66:**1-8.

Beier, F., R. J. Lee, A. C. Taylor, R. G. Pestell, and P. LuValle. (1999). Identification of the cyclin D1 gene as a target of activating transcription factor 2 in chondrocytes. Proc Natl Acad Sci U S A **96:**1433-8.

Bell, M. J., R. Brennan, J. J. Miles, D. J. Moss, J. M. Burrows, and S. R. Burrows. (2008). Widespread sequence variation in Epstein-Barr virus nuclear antigen 1 influences the antiviral T cell response. J Infect Dis **197:**1594-7.

Berger, A. J., H. M. Kluger, N. Li, E. Kielhorn, R. Halaban, Z. Ronai, and D. L. Rimm. (2003). Subcellular localization of activating transcription factor 2 in melanoma specimens predicts patient survival. Cancer Res **63:**8103-7.

Bernstein, P. L., D. J. Herrick, R. D. Prokipcak, and J. Ross. (1992). Control of c-myc mRNA half-life in vitro by a protein capable of binding to a coding region stability determinant. Genes Dev **6:**642-54.

Bex, F., M. J. Yin, A. Burny, and R. B. Gaynor. (1998). Differential transcriptional activation by human T-cell leukemia virus type 1 Tax mutants is mediated by distinct interactions with CREB binding protein and p300. Mol Cell Biol **18:**2392-405.

Bhat, R. A., and B. Thimmappaya. (1985). Construction and analysis of additional adenovirus substitution mutants confirm the complementation of VAI RNA function by two small RNAs encoded by Epstein-Barr virus. J Virol **56:**750-6.

Bhat, R. A., and B. Thimmappaya. (1983). Two small RNAs encoded by Epstein-Barr virus can functionally substitute for the virus-associated RNAs in the lytic growth of adenovirus 5. Proc Natl Acad Sci U S A **80:**4789-93.

Bhatia, K., A. Raj, M. I. Guitierrez, J. G. Judde, G. Spangler, H. Venkatesh, and I. T. Magrath. (1996). Variation in the sequence of Epstein Barr virus nuclear antigen 1 in

normal peripheral blood lymphocytes and in Burkitt's lymphomas. Oncogene **13:**177-81.

Bhoumik, A., and Z. Ronai. (2008). ATF2: a transcription factor that elicits oncogenic or tumor suppressor activities. Cell Cycle **7:**2341-5.

Billin, A. N., and D. E. Ayer. (2006). The Mlx network: evidence for a parallel Max-like transcriptional network that regulates energy metabolism. Curr Top Microbiol Immunol **302:**255-78.

Bishop, J. M., and R. A. Weinberg. 1996. Molecular oncology. Scientific American, New York.

Blackwell, T. K., L. Kretzner, E. M. Blackwood, R. N. Eisenman, and H. Weintraub. (1990). Sequence-specific DNA binding by the c-Myc protein. Science **250:**1149-51.

Blackwood, E. M., and R. N. Eisenman. (1991). Max: a helix-loop-helix zipper protein that forms a sequence-specific DNA-binding complex with Myc. Science **251:**1211-7.

Blattner, W. A. (1999). Human retroviruses: their role in cancer. Proc Assoc Am Physicians **111:**563-72.

Bochkarev, A., J. A. Barwell, R. A. Pfuetzner, E. Bochkareva, L. Frappier, and A. M. Edwards. (1996). Crystal structure of the DNA-binding domain of the Epstein-Barr virus origin-binding protein, EBNA1, bound to DNA. Cell **84:**791-800.

Bornkamm, G. W. (2009). Epstein-Barr virus and the pathogenesis of Burkitt's lymphoma: more questions than answers. Int J Cancer **124:**1745-55.

Borza, C. M., and L. M. Hutt-Fletcher. (2002). Alternate replication in B cells and epithelial cells switches tropism of Epstein-Barr virus. Nat Med **8:**594-9.

Bose, S., L. F. Yap, M. Fung, J. Starzcynski, A. Saleh, S. Morgan, C. Dawson, M. B. Chukwuma, E. Maina, M. Buettner, W. Wei, J. Arrand, P. V. Lim, L. S. Young, S. H. Teo, T. Stankovic, C. B. Woodman, and P. G. Murray. (2009). The ATM tumour suppressor gene is down-regulated in EBV-associated nasopharyngeal carcinoma. J Pathol **217:**345-52.

Bouchard, C., O. Dittrich, A. Kiermaier, K. Dohmann, A. Menkel, M. Eilers, and B. Luscher. (2001). Regulation of cyclin D2 gene expression by the Myc/Max/Mad network: Myc-dependent TRRAP recruitment and histone acetylation at the cyclin D2 promoter. Genes Dev **15:**2042-7.

Boyd, J. M., P. M. Loewenstein, Q. Q. Tang Qq, L. Yu, and M. Green. (2002). Adenovirus E1A N-terminal amino acid sequence requirements for repression of transcription in vitro and in vivo correlate with those required for E1A interference with TBP-TATA complex

formation. J Virol **76:**1461-74.

Braithwaite, A. W., and C. L. Prives. (2006). p53: more research and more questions. Cell Death Differ **13:**877-80.

Brannon, A. R., J. A. Maresca, J. D. Boeke, M. A. Basrai, and A. A. McBride. (2005). Reconstitution of papillomavirus E2-mediated plasmid maintenance in Saccharomyces cerevisiae by the Brd4 bromodomain protein. Proc Natl Acad Sci U S A **102:**2998-3003.

Brauninger, A., T. Spieker, A. Mottok, A. S. Baur, R. Kuppers, and M. L. Hansmann. (2003). Epstein-Barr virus (EBV)-positive lymphoproliferations in post-transplant patients show immunoglobulin V gene mutation patterns suggesting interference of EBV with normal B cell differentiation processes. Eur J Immunol **33:**1593-602.

Brennan, B. (2006). Nasopharyngeal carcinoma. Orphanet J Rare Dis **1:**23.

Brenner, C., R. Deplus, C. Didelot, A. Loriot, E. Vire, C. De Smet, A. Gutierrez, D. Danovi, D. Bernard, T. Boon, P. G. Pelicci, B. Amati, T. Kouzarides, Y. de Launoit, L. Di Croce, and F. Fuks. (2005). Myc represses transcription through recruitment of DNA methyltransferase corepressor. Embo J **24:**336-46.

Brooks, J. M., D. S. Croom-Carter, A. M. Leese, R. J. Tierney, G. Habeshaw, and A. B. Rickinson. (2000). Cytotoxic T-lymphocyte responses to a polymorphic Epstein-Barr virus epitope identify healthy carriers with coresident viral strains. J Virol **74:**1801-9.

Bubman, D., I. Guasparri, and E. Cesarman. (2007). Deregulation of c-Myc in primary effusion lymphoma by Kaposi's sarcoma herpesvirus latency-associated nuclear antigen. Oncogene **26:**4979-86.

Burkitt, D. (1962). A children's cancer dependent on climatic factors. Nature **194:**232-4.

Burkitt, D. (1958). A sarcoma involving the jaws in African children. Br J Surg **46:**218-23.

Butel, J. S. (2000). Viral carcinogenesis: revelation of molecular mechanisms and etiology of human disease. Carcinogenesis **21:**405-26.

Cai, X., A. Schafer, S. Lu, J. P. Bilello, R. C. Desrosiers, R. Edwards, N. Raab-Traub, and B. R. Cullen. (2006). Epstein-Barr virus microRNAs are evolutionarily conserved and differentially expressed. PLoS Pathog **2:**e23.

Caldwell, R. G., R. C. Brown, and R. Longnecker. (2000). Epstein-Barr virus LMP2A-induced B-cell survival in two unique classes of EmuLMP2A transgenic mice. J Virol **74:**1101-13.

Caldwell, R. G., J. B. Wilson, S. J. Anderson, and R. Longnecker. (1998). Epstein-Barr virus

LMP2A drives B cell development and survival in the absence of normal B cell receptor signals. Immunity **9:**405-11.

Campisi, J., H. E. Gray, A. B. Pardee, M. Dean, and G. E. Sonenshein. (1984). Cell-cycle control of c-myc but not c-ras expression is lost following chemical transformation. Cell **36:**241-7.

Carroll, J. S., C. A. Meyer, J. Song, W. Li, T. R. Geistlinger, J. Eeckhoute, A. S. Brodsky, E. K. Keeton, K. C. Fertuck, G. F. Hall, Q. Wang, S. Bekiranov, V. Sementchenko, E. A. Fox, P. A. Silver, T. R. Gingeras, X. S. Liu, and M. Brown. (2006). Genome-wide analysis of estrogen receptor binding sites. Nat Genet **38:**1289-97.

Ceccarelli, D. F., and L. Frappier. (2000). Functional analyses of the EBNA1 origin DNA binding protein of Epstein-Barr virus. J Virol **74:**4939-48.

Cesarman, E., and E. A. Mesri. (1999). Virus-associated lymphomas. Curr Opin Oncol **11:**322-32.

Chaganti, S., A. I. Bell, N. B. Pastor, A. E. Milner, M. Drayson, J. Gordon, and A. B. Rickinson. (2005). Epstein-Barr virus infection in vitro can rescue germinal center B cells with inactivated immunoglobulin genes. Blood **106:**4249-52.

Chakraborty, A. A., and W. P. Tansey. (2009). Adenoviral E1A function through Myc. Cancer Res **69:**6-9.

Chan, A. S., K. F. To, K. W. Lo, M. Ding, X. Li, P. Johnson, and D. P. Huang. (2002). Frequent chromosome 9p losses in histologically normal nasopharyngeal epithelia from southern Chinese. Int J Cancer **102:**300-3.

Chan, A. S., K. F. To, K. W. Lo, K. F. Mak, W. Pak, B. Chiu, G. M. Tse, M. Ding, X. Li, J. C. Lee, and D. P. Huang. (2000). High frequency of chromosome 3p deletion in histologically normal nasopharyngeal epithelia from southern Chinese. Cancer Res **60:**5365-70.

Chan, A. T., Y. M. Lo, B. Zee, L. Y. Chan, B. B. Ma, S. F. Leung, F. Mo, M. Lai, S. Ho, D. P. Huang, and P. J. Johnson. (2002). Plasma Epstein-Barr virus DNA and residual disease after radiotherapy for undifferentiated nasopharyngeal carcinoma. J Natl Cancer Inst **94:**1614-9.

Chang, K. L., P. F. Albujar, Y. Y. Chen, R. M. Johnson, and L. M. Weiss. (1993). High prevalence of Epstein-Barr virus in the Reed-Sternberg cells of Hodgkin's disease occurring in Peru. Blood **81:**496-501.

Chang, T. C., D. Yu, Y. S. Lee, E. A. Wentzel, D. E. Arking, K. M. West, C. V. Dang, A. Thomas-Tikhonenko, and J. T. Mendell. (2008). Widespread microRNA repression by

Myc contributes to tumorigenesis. Nat Genet **40:**43-50.

Chaudhuri, B., H. Xu, I. Todorov, A. Dutta, and J. L. Yates. (2001). Human DNA replication initiation factors, ORC and MCM, associate with oriP of Epstein-Barr virus. Proc Natl Acad Sci U S A **98:**10085-9.

Chellappan, S., V. B. Kraus, B. Kroger, K. Munger, P. M. Howley, W. C. Phelps, and J. R. Nevins. (1992). Adenovirus E1A, simian virus 40 tumor antigen, and human papillomavirus E7 protein share the capacity to disrupt the interaction between transcription factor E2F and the retinoblastoma gene product. Proc Natl Acad Sci U S A **89:**4549-53.

Chen, F., L. F. Hu, I. Ernberg, G. Klein, and G. Winberg. (1995). Coupled transcription of Epstein-Barr virus latent membrane protein (LMP)-1 and LMP-2B genes in nasopharyngeal carcinomas. J Gen Virol **76 (Pt 1):**131-8.

Chen, H., P. Smith, R. F. Ambinder, and S. D. Hayward. (1999). Expression of Epstein-Barr virus BamHI-A rightward transcripts in latently infected B cells from peripheral blood. Blood **93:**3026-32.

Chen, P. C., C. C. Pan, A. H. Yang, L. S. Wang, and H. Chiang. (2002). Detection of Epstein-Barr virus genome within thymic epithelial tumours in Taiwanese patients by nested PCR, PCR in situ hybridization, and RNA in situ hybridization. J Pathol **197:**684-8.

Chen, S. Y., J. Lu, Y. C. Shih, and C. H. Tsai. (2002). Epstein-Barr virus latent membrane protein 2A regulates c-Jun protein through extracellular signal-regulated kinase. J Virol **76:**9556-61.

Chen, W., W. Bocker, J. Brosius, and H. Tiedge. (1997). Expression of neural BC200 RNA in human tumours. J Pathol **183:**345-51.

Chen, X., and J. Arrand. (2003). Establishment of a cell line producing a recombinant Epstein-Barr Virus expressing GFP. Chinese Journal of Microbiology and Immunology **23:**87-90.

Cheng, A. S., V. X. Jin, M. Fan, L. T. Smith, S. Liyanarachchi, P. S. Yan, Y. W. Leu, M. W. Chan, C. Plass, K. P. Nephew, R. V. Davuluri, and T. H. Huang. (2006). Combinatorial analysis of transcription factor partners reveals recruitment of c-MYC to estrogen receptor-alpha responsive promoters. Mol Cell **21:**393-404.

Cheng, S. W., K. P. Davies, E. Yung, R. J. Beltran, J. Yu, and G. V. Kalpana. (1999). c-MYC interacts with INI1/hSNF5 and requires the SWI/SNF complex for transactivation function. Nat Genet **22:**102-5.

Chesnokov, I., W. M. Chu, M. R. Botchan, and C. W. Schmid. (1996). p53 inhibits RNA

polymerase III-directed transcription in a promoter-dependent manner. Mol Cell Biol **16:**7084-8.

Cheung, A., and E. Kieff. (1982). Long internal direct repeat in Epstein-Barr virus DNA. J Virol **44:**286-94.

Cheung, R. K., and H. M. Dosch. (1991). The tyrosine kinase lck is critically involved in the growth transformation of human B lymphocytes. J Biol Chem **266:**8667-70.

Cho, Y. Y., A. M. Bode, H. Mizuno, B. Y. Choi, H. S. Choi, and Z. Dong. (2004). A novel role for mixed-lineage kinase-like mitogen-activated protein triple kinase alpha in neoplastic cell transformation and tumor development. Cancer Res **64:**3855-64.

Chow, L. S., K. W. Lo, J. Kwong, K. F. To, K. S. Tsang, C. W. Lam, R. Dammann, and D. P. Huang. (2004). RASSF1A is a target tumor suppressor from 3p21.3 in nasopharyngeal carcinoma. Int J Cancer **109:**839-47.

Choy, E. Y., K. H. Kok, S. W. Tsao, and D. Y. Jin. (2008). Utility of Epstein-Barr virus-encoded small RNA promoters for driving the expression of fusion transcripts harboring short hairpin RNAs. Gene Ther **15:**191-202.

Chu, Z. L., J. A. DiDonato, J. Hawiger, and D. W. Ballard. (1998). The tax oncoprotein of human T-cell leukemia virus type 1 associates with and persistently activates IkappaB kinases containing IKKalpha and IKKbeta. J Biol Chem **273:**15891-4.

Clarke, P. A., M. Schwemmle, J. Schickinger, K. Hilse, and M. J. Clemens. (1991). Binding of Epstein-Barr virus small RNA EBER-1 to the double-stranded RNA-activated protein kinase DAI. Nucleic Acids Res **19:**243-8.

Clarke, P. A., N. A. Sharp, and M. J. Clemens. (1992). Expression of genes for the Epstein-Barr virus small RNAs EBER-1 and EBER-2 in Daudi Burkitt's lymphoma cells: effects of interferon treatment. J Gen Virol **73 (Pt 12):**3169-75.

Cobbold, L. C., K. A. Spriggs, S. J. Haines, H. C. Dobbyn, C. Hayes, C. H. de Moor, K. S. Lilley, M. Bushell, and A. E. Willis. (2008). Identification of internal ribosome entry segment (IRES)-trans-acting factors for the Myc family of IRESs. Mol Cell Biol **28:**40-9.

Cohen, J. I., F. Wang, J. Mannick, and E. Kieff. (1989). Epstein-Barr virus nuclear protein 2 is a key determinant of lymphocyte transformation. Proc Natl Acad Sci U S A **86:**9558-62.

Crighton, D., A. Woiwode, C. Zhang, N. Mandavia, J. P. Morton, L. J. Warnock, J. Milner, R. J. White, and D. L. Johnson. (2003). p53 represses RNA polymerase III transcription by targeting TBP and inhibiting promoter occupancy by TFIIIB. Embo J **22:**2810-20.

Dadmanesh, F., J. L. Peterse, A. Sapino, A. Fonelli, and V. Eusebi. (2001). Lymphoepithelioma-like carcinoma of the breast: lack of evidence of Epstein-Barr virus infection. Histopathology **38:**54-61.

Dalla-Favera, R., M. Bregni, J. Erikson, D. Patterson, R. C. Gallo, and C. M. Croce. (1982). Human c-myc onc gene is located on the region of chromosome 8 that is translocated in Burkitt lymphoma cells. Proc Natl Acad Sci U S A **79:**7824-7.

Daly, N. L., D. A. Arvanitis, J. A. Fairley, N. Gomez-Roman, J. P. Morton, S. V. Graham, D. A. Spandidos, and R. J. White. (2005). Deregulation of RNA polymerase III transcription in cervical epithelium in response to high-risk human papillomavirus. Oncogene **24:**880-8.

Damania, B. (2007). DNA tumor viruses and human cancer. Trends Microbiol **15:**38-44.

Dang, C. V. (1999). c-Myc target genes involved in cell growth, apoptosis, and metabolism. Mol Cell Biol **19:**1-11.

Dang, C. V., M. McGuire, M. Buckmire, and W. M. Lee. (1989). Involvement of the 'leucine zipper' region in the oligomerization and transforming activity of human c-myc protein. Nature **337:**664-6.

Dang, C. V., K. A. O'Donnell, K. I. Zeller, T. Nguyen, R. C. Osthus, and F. Li. (2006). The c-Myc target gene network. Semin Cancer Biol **16:**253-64.

Dani, C., J. M. Blanchard, M. Piechaczyk, S. El Sabouty, L. Marty, and P. Jeanteur. (1984). Extreme instability of myc mRNA in normal and transformed human cells. Proc Natl Acad Sci U S A **81:**7046-50.

Davenport, M. G., and J. S. Pagano. (1999). Expression of EBNA-1 mRNA is regulated by cell cycle during Epstein-Barr virus type I latency. J Virol **73:**3154-61.

Davison, A. J., R. Eberle, B. Ehlers, G. S. Hayward, D. J. McGeoch, A. C. Minson, P. E. Pellett, B. Roizman, M. J. Studdert, and E. Thiry. (2009). The order Herpesvirales. Arch Virol **154:**171-7.

Dawson, C. W., G. Tramountanis, A. G. Eliopoulos, and L. S. Young. (2003). Epstein-Barr virus latent membrane protein 1 (LMP1) activates the phosphatidylinositol 3-kinase/Akt pathway to promote cell survival and induce actin filament remodeling. J Biol Chem **278:**3694-704.

De Cesare, D., D. Vallone, A. Caracciolo, P. Sassone-Corsi, C. Nerlov, and P. Verde. (1995). Heterodimerization of c-Jun with ATF-2 and c-Fos is required for positive and negative regulation of the human urokinase enhancer. Oncogene **11:**365-76.

de Jesus, O., P. R. Smith, L. C. Spender, C. Elgueta Karstegl, H. H. Niller, D. Huang, and P. J. Farrell. (2003). Updated Epstein-Barr virus (EBV) DNA sequence and analysis of a promoter for the BART (CST, BARF0) RNAs of EBV. J Gen Virol **84:**1443-50.

de Villiers, E. M., R. Schmidt, H. Delius, and H. zur Hausen. (2002). Heterogeneity of TT virus related sequences isolated from human tumour biopsy specimens. J Mol Med **80:**44-50.

Deacon, E. M., G. Pallesen, G. Niedobitek, J. Crocker, L. Brooks, A. B. Rickinson, and L. S. Young. (1993). Epstein-Barr virus and Hodgkin's disease: transcriptional analysis of virus latency in the malignant cells. J Exp Med **177:**339-49.

Dean, M., R. A. Levine, W. Ran, M. S. Kindy, G. E. Sonenshein, and J. Campisi. (1986). Regulation of c-myc transcription and mRNA abundance by serum growth factors and cell contact. J Biol Chem **261:**9161-6.

DeCaprio, J. A., J. W. Ludlow, J. Figge, J. Y. Shew, C. M. Huang, W. H. Lee, E. Marsilio, E. Paucha, and D. M. Livingston. (1988). SV40 large tumor antigen forms a specific complex with the product of the retinoblastoma susceptibility gene. Cell **54:**275-83.

Delecluse, H. J., S. Bartnizke, W. Hammerschmidt, J. Bullerdiek, and G. W. Bornkamm. (1993). Episomal and integrated copies of Epstein-Barr virus coexist in Burkitt lymphoma cell lines. J Virol **67:**1292-9.

Deng, Z., C. Atanasiu, J. S. Burg, D. Broccoli, and P. M. Lieberman. (2003). Telomere repeat binding factors TRF1, TRF2, and hRAP1 modulate replication of Epstein-Barr virus OriP. J Virol **77:**11992-2001.

Deng, Z., L. Lezina, C. J. Chen, S. Shtivelband, W. So, and P. M. Lieberman. (2002). Telomeric proteins regulate episomal maintenance of Epstein-Barr virus origin of plasmid replication. Mol Cell **9:**493-503.

Dews, M., A. Homayouni, D. Yu, D. Murphy, C. Sevignani, E. Wentzel, E. E. Furth, W. M. Lee, G. H. Enders, J. T. Mendell, and A. Thomas-Tikhonenko. (2006). Augmentation of tumor angiogenesis by a Myc-activated microRNA cluster. Nat Genet **38:**1060-5.

Dhar, S. K., K. Yoshida, Y. Machida, P. Khaira, B. Chaudhuri, J. A. Wohlschlegel, M. Leffak, J. Yates, and A. Dutta. (2001). Replication from oriP of Epstein-Barr virus requires human ORC and is inhibited by geminin. Cell **106:**287-96.

Diamandopoulos, G. T. (1996). Cancer: an historical perspective. Anticancer Res **16:**1595-602.

Dieci, G., G. Fiorino, M. Castelnuovo, M. Teichmann, and A. Pagano. (2007). The expanding RNA polymerase III transcriptome. Trends Genet **23:**614-22.

Dillner, J., B. Kallin, G. Klein, H. Jornvall, H. Alexander, and R. Lerner. (1985). Antibodies against synthetic peptides react with the second Epstein-Barr virus-associated nuclear antigen. Embo J **4:**1813-8.

Dirmeier, U., R. Hoffmann, E. Kilger, U. Schultheiss, C. Briseno, O. Gires, A. Kieser, D. Eick, B. Sugden, and W. Hammerschmidt. (2005). Latent membrane protein 1 of Epstein-Barr virus coordinately regulates proliferation with control of apoptosis. Oncogene **24:**1711-7.

Dotti, G., R. Fiocchi, T. Motta, A. Gamba, E. Gotti, B. Gridelli, G. Borleri, C. Manzoni, P. Viero, G. Remuzzi, T. Barbui, and A. Rambaldi. (2000). Epstein-Barr virus-negative lymphoproliferate disorders in long-term survivors after heart, kidney, and liver transplant. Transplantation **69:**827-33.

Dresang, L. R., D. T. Vereide, and B. Sugden. (2009). Identifying sites bound by Epstein-Barr virus nuclear antigen 1 (EBNA1) in the human genome: defining a position-weighted matrix to predict sites bound by EBNA1 in viral genomes. J Virol **83:**2930-40.

Duellman, S. J., K. L. Thompson, J. J. Coon, and R. R. Burgess. (2009). Phosphorylation sites of Epstein-Barr virus EBNA1 regulate its function. J Gen Virol.

Dumay-Odelot, H., C. Marck, S. Durrieu-Gaillard, O. Lefebvre, S. Jourdain, M. Prochazkova, A. Pflieger, and M. Teichmann. (2007). Identification, molecular cloning, and characterization of the sixth subunit of human transcription factor TFIIIC. J Biol Chem **282:**17179-89.

Dutton, A., C. B. Woodman, M. B. Chukwuma, J. I. Last, W. Wei, M. Vockerodt, K. R. Baumforth, J. R. Flavell, M. Rowe, A. M. Taylor, L. S. Young, and P. G. Murray. (2007). Bmi-1 is induced by the Epstein-Barr virus oncogene LMP1 and regulates the expression of viral target genes in Hodgkin lymphoma cells. Blood **109:**2597-603.

Dyson, N., P. M. Howley, K. Munger, and E. Harlow. (1989). The human papilloma virus-16 E7 oncoprotein is able to bind to the retinoblastoma gene product. Science **243:**934-7.

Eberhardy, S. R., and P. J. Farnham. (2002). Myc recruits P-TEFb to mediate the final step in the transcriptional activation of the cad promoter. J Biol Chem **277:**40156-62.

Echendu, C. W., and P. D. Ling. (2008). Regulation of Sp100A subnuclear localization and transcriptional function by EBNA-LP and interferon. J Interferon Cytokine Res **28:**667-78.

Edwards, R. H., A. R. Marquitz, and N. Raab-Traub. (2008). Epstein-Barr virus BART microRNAs are produced from a large intron prior to splicing. J Virol **82:**9094-106.

Eilebrecht, S., F. X. Pellay, P. Odenwalder, G. Brysbaert, B. J. Benecke, and A. Benecke.

(2008). EBER2 RNA-induced transcriptome changes identify cellular processes likely targeted during Epstein Barr Virus infection. BMC Res Notes **1:**100.

Eliopoulos, A. G., N. J. Gallagher, S. M. Blake, C. W. Dawson, and L. S. Young. (1999). Activation of the p38 mitogen-activated protein kinase pathway by Epstein-Barr virus-encoded latent membrane protein 1 coregulates interleukin-6 and interleukin-8 production. J Biol Chem **274:**16085-96.

Eliopoulos, A. G., M. Stack, C. W. Dawson, K. M. Kaye, L. Hodgkin, S. Sihota, M. Rowe, and L. S. Young. (1997). Epstein-Barr virus-encoded LMP1 and CD40 mediate IL-6 production in epithelial cells via an NF-kappaB pathway involving TNF receptor-associated factors. Oncogene **14:**2899-916.

Eliopoulos, A. G., and L. S. Young. (1998). Activation of the cJun N-terminal kinase (JNK) pathway by the Epstein-Barr virus-encoded latent membrane protein 1 (LMP1). Oncogene **16:**1731-42.

Epstein, M. A. (2001). Historical background. Philos Trans R Soc Lond B Biol Sci **356:**413-20.

Epstein, M. A., G. Henle, B. G. Achong, and Y. M. Barr. (1965). Morphological and Biological Studies on a Virus in Cultured Lymphoblasts from Burkitt's Lymphoma. J Exp Med **121:**761-70.

Fattovich, G., T. Stroffolini, I. Zagni, and F. Donato. (2004). Hepatocellular carcinoma in cirrhosis: incidence and risk factors. Gastroenterology **127:**S35-50.

Faumont, N., S. Durand-Panteix, M. Schlee, S. Gromminger, M. Schuhmacher, M. Holzel, G. Laux, R. Mailhammer, A. Rosenwald, L. M. Staudt, G. W. Bornkamm, and J. Feuillard. (2009). c-Myc and Rel/NF-kappaB are the two master transcriptional systems activated in the latency III program of Epstein-Barr virus-immortalized B cells. J Virol **83:**5014-27.

Faumont, N., C. Le Clorennec, P. Teira, G. Goormachtigh, J. Coll, Y. Canitrot, C. Cazaux, J. S. Hoffmann, P. Brousset, G. Delsol, J. Feuillard, and F. Meggetto. (2009). Regulation of DNA Polymerase {beta} by the LMP1 Oncoprotein of EBV through the Nuclear Factor-{kappa}B Pathway. Cancer Res.

Feederle, R., M. Kost, M. Baumann, A. Janz, E. Drouet, W. Hammerschmidt, and H. J. Delecluse. (2000). The Epstein-Barr virus lytic program is controlled by the co-operative functions of two transactivators. Embo J **19:**3080-9.

Felton-Edkins, Z. A., J. A. Fairley, E. L. Graham, I. M. Johnston, R. J. White, and P. H. Scott. (2003). The mitogen-activated protein (MAP) kinase ERK induces tRNA synthesis by phosphorylating TFIIIB. Embo J **22:**2422-32.

Felton-Edkins, Z. A., A. Kondrashov, D. Karali, J. A. Fairley, C. W. Dawson, J. R. Arrand, L. S. Young, and R. J. White. (2006). Epstein-Barr virus induces cellular transcription factors to allow active expression of EBER genes by RNA polymerase III. J Biol Chem **281:**33871-80.

Felton-Edkins, Z. A., and R. J. White. (2002). Multiple mechanisms contribute to the activation of RNA polymerase III transcription in cells transformed by papovaviruses. J Biol Chem **277:**48182-91.

Fernandez, P. C., S. R. Frank, L. Wang, M. Schroeder, S. Liu, J. Greene, A. Cocito, and B. Amati. (2003). Genomic targets of the human c-Myc protein. Genes Dev **17:**1115-29.

Fischer, N., E. Kremmer, G. Lautscham, N. Mueller-Lantzsch, and F. A. Grasser. (1997). Epstein-Barr virus nuclear antigen 1 forms a complex with the nuclear transporter karyopherin alpha2. J Biol Chem **272:**3999-4005.

Flavell, J. R., K. R. Baumforth, V. H. Wood, G. L. Davies, W. Wei, G. M. Reynolds, S. Morgan, A. Boyce, G. L. Kelly, L. S. Young, and P. G. Murray. (2008). Down-regulation of the TGF-beta target gene, PTPRK, by the Epstein-Barr virus encoded EBNA1 contributes to the growth and survival of Hodgkin lymphoma cells. Blood **111:**292-301.

Fok, V., K. Friend, and J. A. Steitz. (2006). Epstein-Barr virus noncoding RNAs are confined to the nucleus, whereas their partner, the human La protein, undergoes nucleocytoplasmic shuttling. J Cell Biol **173:**319-25.

Fok, V., R. M. Mitton-Fry, A. Grech, and J. A. Steitz. (2006). Multiple domains of EBER 1, an Epstein-Barr virus noncoding RNA, recruit human ribosomal protein L22. Rna **12:**872-82.

Foley, K. P., and R. N. Eisenman. (1999). Two MAD tails: what the recent knockouts of Mad1 and Mxi1 tell us about the MYC/MAX/MAD network. Biochim Biophys Acta **1423:**M37-47.

Franklin, A. A., M. F. Kubik, M. N. Uittenbogaard, A. Brauweiler, P. Utaisincharoen, M. A. Matthews, W. S. Dynan, J. P. Hoeffler, and J. K. Nyborg. (1993). Transactivation by the human T-cell leukemia virus Tax protein is mediated through enhanced binding of activating transcription factor-2 (ATF-2) ATF-2 response and cAMP element-binding protein (CREB). J Biol Chem **268:**21225-31.

Frappier, L., and M. O'Donnell. (1991). Overproduction, purification, and characterization of EBNA1, the origin binding protein of Epstein-Barr virus. J Biol Chem **266:**7819-26.

Friend, S. H., R. Bernards, S. Rogelj, R. A. Weinberg, J. M. Rapaport, D. M. Albert, and T. P. Dryja. (1986). A human DNA segment with properties of the gene that predisposes to

retinoblastoma and osteosarcoma. Nature **323:**643-6.

Fruehling, S., and R. Longnecker. (1997). The immunoreceptor tyrosine-based activation motif of Epstein-Barr virus LMP2A is essential for blocking BCR-mediated signal transduction. Virology **235:**241-51.

Fruehling, S., R. Swart, K. M. Dolwick, E. Kremmer, and R. Longnecker. (1998). Tyrosine 112 of latent membrane protein 2A is essential for protein tyrosine kinase loading and regulation of Epstein-Barr virus latency. J Virol **72:**7796-806.

Frye, M., and F. M. Watt. (2006). The RNA methyltransferase Misu (NSun2) mediates Myc-induced proliferation and is upregulated in tumors. Curr Biol **16:**971-81.

Fujii, T., T. Kawai, K. Saito, K. Fukushima, T. Hasegawa, M. Tokunaga, and T. Yokoyama. (1993). EBER-1 expression in thymic carcinoma. Acta Pathol Jpn **43:**107-10.

Fukayama, M., Y. Hayashi, Y. Iwasaki, J. Chong, T. Ooba, T. Takizawa, M. Koike, S. Mizutani, M. Miyaki, and K. Hirai. (1994). Epstein-Barr virus-associated gastric carcinoma and Epstein-Barr virus infection of the stomach. Lab Invest **71:**73-81.

Fukayama, M., R. Hino, and H. Uozaki. (2008). Epstein-Barr virus and gastric carcinoma: virus-host interactions leading to carcinoma. Cancer Sci **99:**1726-33.

Fukuda, M., and R. Longnecker. (2005). Epstein-Barr virus (EBV) latent membrane protein 2A regulates B-cell receptor-induced apoptosis and EBV reactivation through tyrosine phosphorylation. J Virol **79:**8655-60.

Fukuda, M., and R. Longnecker. (2004). Latent membrane protein 2A inhibits transforming growth factor-beta 1-induced apoptosis through the phosphatidylinositol 3-kinase/Akt pathway. J Virol **78:**1697-705.

Gahn, T. A., and C. L. Schildkraut. (1989). The Epstein-Barr virus origin of plasmid replication, oriP, contains both the initiation and termination sites of DNA replication. Cell **58:**527-35.

Gahn, T. A., and B. Sugden. (1995). An EBNA-1-dependent enhancer acts from a distance of 10 kilobase pairs to increase expression of the Epstein-Barr virus LMP gene. J Virol **69:**2633-6.

Gan, Y. J., B. I. Razzouk, T. Su, and J. W. Sixbey. (2002). A defective, rearranged Epstein-Barr virus genome in EBER-negative and EBER-positive Hodgkin's disease. Am J Pathol **160:**781-6.

Gatto, G., A. Rossi, D. Rossi, S. Kroening, S. Bonatti, and M. Mallardo. (2008). Epstein-Barr

virus latent membrane protein 1 trans-activates miR-155 transcription through the NF-kappaB pathway. Nucleic Acids Res **36:**6608-19.

Ghadge, G. D., P. Malhotra, M. R. Furtado, R. Dhar, and B. Thimmapaya. (1994). In vitro analysis of virus-associated RNA I (VAI RNA): inhibition of the double-stranded RNA-activated protein kinase PKR by VAI RNA mutants correlates with the in vivo phenotype and the structural integrity of the central domain. J Virol **68:**4137-51.

Gilligan, K., P. Rajadurai, L. Resnick, and N. Raab-Traub. (1990). Epstein-Barr virus small nuclear RNAs are not expressed in permissively infected cells in AIDS-associated leukoplakia. Proc Natl Acad Sci U S A **87:**8790-4.

Gilligan, K., H. Sato, P. Rajadurai, P. Busson, L. Young, A. Rickinson, T. Tursz, and N. Raab-Traub. (1990). Novel transcription from the Epstein-Barr virus terminal EcoRI fragment, DIJhet, in a nasopharyngeal carcinoma. J Virol **64:**4948-56.

Gilligan, K. J., P. Rajadurai, J. C. Lin, P. Busson, M. Abdel-Hamid, U. Prasad, T. Tursz, and N. Raab-Traub. (1991). Expression of the Epstein-Barr virus BamHI A fragment in nasopharyngeal carcinoma: evidence for a viral protein expressed in vivo. J Virol **65:**6252-9.

Gires, O., F. Kohlhuber, E. Kilger, M. Baumann, A. Kieser, C. Kaiser, R. Zeidler, B. Scheffer, M. Ueffing, and W. Hammerschmidt. (1999). Latent membrane protein 1 of Epstein-Barr virus interacts with JAK3 and activates STAT proteins. Embo J **18:**3064-73.

Gires, O., U. Zimber-Strobl, R. Gonnella, M. Ueffing, G. Marschall, R. Zeidler, D. Pich, and W. Hammerschmidt. (1997). Latent membrane protein 1 of Epstein-Barr virus mimics a constitutively active receptor molecule. Embo J **16:**6131-40.

Gomez-Roman, N., C. Grandori, R. N. Eisenman, and R. J. White. (2003). Direct activation of RNA polymerase III transcription by c-Myc. Nature **421:**290-4.

Gonda, T. J., and D. Metcalf. (1984). Expression of myb, myc and fos proto-oncogenes during the differentiation of a murine myeloid leukaemia. Nature **310:**249-51.

Goodfellow, S. J., E. L. Graham, T. Kantidakis, L. Marshall, B. A. Coppins, D. Oficjalska-Pham, M. Gerard, O. Lefebvre, and R. J. White. (2008). Regulation of RNA polymerase III transcription by Maf1 in mammalian cells. J Mol Biol **378:**481-91.

Gordon, J., L. Walker, G. Guy, G. Brown, M. Rowe, and A. Rickinson. (1986). Control of human B-lymphocyte replication. II. Transforming Epstein-Barr virus exploits three distinct viral signals to undermine three separate control points in B-cell growth. Immunology **58:**591-5.

Gottesfeld, J. M., D. L. Johnson, and J. K. Nyborg. (1996). Transcriptional activation of RNA

polymerase III-dependent genes by the human T-cell leukemia virus type 1 tax protein. Mol Cell Biol **16:**1777-85.

Grandori, C., S. M. Cowley, L. P. James, and R. N. Eisenman. (2000). The Myc/Max/Mad network and the transcriptional control of cell behavior. Annu Rev Cell Dev Biol **16:**653-99.

Gratama, J. W., M. A. Oosterveer, G. Klein, and I. Ernberg. (1990). EBNA size polymorphism can be used to trace Epstein-Barr virus spread within families. J Virol **64:**4703-8.

Green, M., N. K. Panesar, and P. M. Loewenstein. (2008). The transcription-repression domain of the adenovirus E1A oncoprotein targets p300 at the promoter. Oncogene **27:**4446-55.

Greenspan, J. S., D. Greenspan, E. T. Lennette, D. I. Abrams, M. A. Conant, V. Petersen, and U. K. Freese. (1985). Replication of Epstein-Barr virus within the epithelial cells of oral "hairy" leukoplakia, an AIDS-associated lesion. N Engl J Med **313:**1564-71.

Gregory, M. A., Y. Qi, and S. R. Hann. (2003). Phosphorylation by glycogen synthase kinase-3 controls c-myc proteolysis and subnuclear localization. J Biol Chem **278:**51606-12.

Greifenegger, N., M. Jager, L. A. Kunz-Schughart, H. Wolf, and F. Schwarzmann. (1998). Epstein-Barr virus small RNA (EBER) genes: differential regulation during lytic viral replication. J Virol **72:**9323-8.

Grinstein, S., M. V. Preciado, P. Gattuso, P. A. Chabay, W. H. Warren, E. De Matteo, and V. E. Gould. (2002). Demonstration of Epstein-Barr virus in carcinomas of various sites. Cancer Res **62:**4876-8.

Grogan, E. A., W. P. Summers, S. Dowling, D. Shedd, L. Gradoville, and G. Miller. (1983). Two Epstein-Barr viral nuclear neoantigens distinguished by gene transfer, serology, and chromosome binding. Proc Natl Acad Sci U S A **80:**7650-3.

Grossman, S. R., E. Johannsen, X. Tong, R. Yalamanchili, and E. Kieff. (1994). The Epstein-Barr virus nuclear antigen 2 transactivator is directed to response elements by the J kappa recombination signal binding protein. Proc Natl Acad Sci U S A **91:**7568-72.

Grundhoff, A., C. S. Sullivan, and D. Ganem. (2006). A combined computational and microarray-based approach identifies novel microRNAs encoded by human gamma-herpesviruses. Rna **12:**733-50.

Guan, H., J. Jiao, and R. P. Ricciardi. (2008). Tumorigenic adenovirus type 12 E1A inhibits phosphorylation of NF-kappaB by PKAc, causing loss of DNA binding and transactivation. J Virol **82:**40-8.

Guasparri, I., D. Bubman, and E. Cesarman. (2008). EBV LMP2A affects LMP1-mediated NF-kappaB signaling and survival of lymphoma cells by regulating TRAF2 expression. Blood **111:**3813-20.

Gulley, M. L. (2001). Molecular diagnosis of Epstein-Barr virus-related diseases. J Mol Diagn **3:**1-10.

Gulley, M. L., and W. Tang. (2008). Laboratory assays for Epstein-Barr virus-related disease. J Mol Diagn **10:**279-92.

Gupta, S., D. Campbell, B. Derijard, and R. J. Davis. (1995). Transcription factor ATF2 regulation by the JNK signal transduction pathway. Science **267:**389-93.

Gutierrez, M. I., A. Raj, G. Spangler, A. Sharma, A. Hussain, J. G. Judde, S. W. Tsao, P. W. Yuen, I. Joab, I. T. Magrath, and K. Bhatia. (1997). Sequence variations in EBNA-1 may dictate restriction of tissue distribution of Epstein-Barr virus in normal and tumour cells. J Gen Virol **78 (Pt 7):**1663-70.

Habeshaw, G., Q. Y. Yao, A. I. Bell, D. Morton, and A. B. Rickinson. (1999). Epstein-barr virus nuclear antigen 1 sequences in endemic and sporadic Burkitt's lymphoma reflect virus strains prevalent in different geographic areas. J Virol **73:**965-75.

Hagmeyer, B. M., P. Angel, and H. van Dam. (1995). Modulation of AP-1/ATF transcription factor activity by the adenovirus-E1A oncogene products. Bioessays **17:**621-9.

Hai, T., and M. G. Hartman. (2001). The molecular biology and nomenclature of the activating transcription factor/cAMP responsive element binding family of transcription factors: activating transcription factor proteins and homeostasis. Gene **273:**1-11.

Hai, T. W., F. Liu, W. J. Coukos, and M. R. Green. (1989). Transcription factor ATF cDNA clones: an extensive family of leucine zipper proteins able to selectively form DNA-binding heterodimers. Genes Dev **3:**2083-90.

Hammerschmidt, W., and B. Sugden. (1989). Genetic analysis of immortalizing functions of Epstein-Barr virus in human B lymphocytes. Nature **340:**393-7.

Hammerschmidt, W., and B. Sugden. (1988). Identification and characterization of oriLyt, a lytic origin of DNA replication of Epstein-Barr virus. Cell **55:**427-33.

Hanahan, D., and R. A. Weinberg. (2000). The hallmarks of cancer. Cell **100:**57-70.

Hann, S. R. (2006). Role of post-translational modifications in regulating c-Myc proteolysis, transcriptional activity and biological function. Semin Cancer Biol **16:**288-302.

Hann, S. R., and R. N. Eisenman. (1984). Proteins encoded by the human c-myc oncogene: differential expression in neoplastic cells. Mol Cell Biol **4:**2486-97.

Harabuchi, Y., S. Imai, J. Wakashima, M. Hirao, A. Kataura, T. Osato, and S. Kon. (1996). Nasal T-cell lymphoma causally associated with Epstein-Barr virus: clinicopathologic, phenotypic, and genotypic studies. Cancer **77:**2137-49.

Harabuchi, Y., N. Yamanaka, A. Kataura, S. Imai, T. Kinoshita, F. Mizuno, and T. Osato. (1990). Epstein-Barr virus in nasal T-cell lymphomas in patients with lethal midline granuloma. Lancet **335:**128-30.

Harris, A., B. D. Young, and B. E. Griffin. (1985). Random association of Epstein-Barr virus genomes with host cell metaphase chromosomes in Burkitt's lymphoma-derived cell lines. J Virol **56:**328-32.

Harrod, R., Y. Tang, C. Nicot, H. S. Lu, A. Vassilev, Y. Nakatani, and C. Z. Giam. (1998). An exposed KID-like domain in human T-cell lymphotropic virus type 1 Tax is responsible for the recruitment of coactivators CBP/p300. Mol Cell Biol **18:**5052-61.

Hassan, M., D. Selimovic, H. Ghozlan, and O. Abdel-kader. (2009). Hepatitis C virus core protein triggers hepatic angiogenesis by a mechanism including multiple pathways. Hepatology **49:**1469-82.

Hateboer, G., H. T. Timmers, A. K. Rustgi, M. Billaud, L. J. van 't Veer, and R. Bernards. (1993). TATA-binding protein and the retinoblastoma gene product bind to overlapping epitopes on c-Myc and adenovirus E1A protein. Proc Natl Acad Sci U S A **90:**8489-93.

He, N., N. S. Jahchan, E. Hong, Q. Li, M. A. Bayfield, R. J. Maraia, K. Luo, and Q. Zhou. (2008). A La-related protein modulates 7SK snRNP integrity to suppress P-TEFb-dependent transcriptional elongation and tumorigenesis. Mol Cell **29:**588-99.

He, T. C., A. B. Sparks, C. Rago, H. Hermeking, L. Zawel, L. T. da Costa, P. J. Morin, B. Vogelstein, and K. W. Kinzler. (1998). Identification of c-MYC as a target of the APC pathway. Science **281:**1509-12.

Hearing, J., Y. Mulhaupt, and S. Harper. (1992). Interaction of Epstein-Barr virus nuclear antigen 1 with the viral latent origin of replication. J Virol **66:**694-705.

Henderson, S., M. Rowe, C. Gregory, D. Croom-Carter, F. Wang, R. Longnecker, E. Kieff, and A. Rickinson. (1991). Induction of bcl-2 expression by Epstein-Barr virus latent membrane protein 1 protects infected B cells from programmed cell death. Cell **65:**1107-15.

Henle, G., and W. Henle. (1966). Immunofluorescence in cells derived from Burkitt's lymphoma. J Bacteriol **91:**1248-56.

Henle, G., W. Henle, and V. Diehl. (1968). Relation of Burkitt's tumor-associated herpes-ytpe virus to infectious mononucleosis. Proc Natl Acad Sci U S A **59:**94-101.

Henle, W., V. Diehl, G. Kohn, H. Zur Hausen, and G. Henle. (1967). Herpes-type virus and chromosome marker in normal leukocytes after growth with irradiated Burkitt cells. Science **157:**1064-5.

Henle, W., and G. Henle. (1970). Evidence for a relation of Epstein-Barr virus to Burkitt's lymphoma and nasopharyngeal carcinoma. Bibl Haematol**:**706-13.

Hennessy, K., and E. Kieff. (1985). A second nuclear protein is encoded by Epstein-Barr virus in latent infection. Science **227:**1238-40.

Hernandez-Ramon, E. E., J. E. Burns, W. Zhang, H. F. Walker, S. Allen, A. A. Antson, and N. J. Maitland. (2008). Dimerization of the human papillomavirus type 16 E2 N terminus results in DNA looping within the upstream regulatory region. J Virol **82:**4853-61.

Herrmann, K., P. Frangou, J. Middeldorp, and G. Niedobitek. (2002). Epstein-Barr virus replication in tongue epithelial cells. J Gen Virol **83:**2995-8.

Hess, J., P. Angel, and M. Schorpp-Kistner. (2004). AP-1 subunits: quarrel and harmony among siblings. J Cell Sci **117:**5965-73.

Hildesheim, A., L. M. Anderson, C. J. Chen, Y. J. Cheng, L. A. Brinton, A. K. Daly, C. D. Reed, I. H. Chen, N. E. Caporaso, M. M. Hsu, J. Y. Chen, J. R. Idle, R. N. Hoover, C. S. Yang, and S. K. Chhabra. (1997). CYP2E1 genetic polymorphisms and risk of nasopharyngeal carcinoma in Taiwan. J Natl Cancer Inst **89:**1207-12.

Hildesheim, A., C. J. Chen, N. E. Caporaso, Y. J. Cheng, R. N. Hoover, M. M. Hsu, P. H. Levine, I. H. Chen, J. Y. Chen, C. S. Yang, and et al. (1995). Cytochrome P4502E1 genetic polymorphisms and risk of nasopharyngeal carcinoma: results from a case-control study conducted in Taiwan. Cancer Epidemiol Biomarkers Prev **4:**607-10.

Hirai, K., and M. Shirakata. (2001). Replication licensing of the EBV oriP minichromosome. Curr Top Microbiol Immunol **258:**13-33.

Hirsch, H. A., G. W. Jawdekar, K. A. Lee, L. Gu, and R. W. Henry. (2004). Distinct mechanisms for repression of RNA polymerase III transcription by the retinoblastoma tumor suppressor protein. Mol Cell Biol **24:**5989-99.

Hitt, M. M., M. J. Allday, T. Hara, L. Karran, M. D. Jones, P. Busson, T. Tursz, I. Ernberg, and B. E. Griffin. (1989). EBV gene expression in an NPC-related tumour. Embo J **8:**2639-51.

Hoeffler, W. K., R. Kovelman, and R. G. Roeder. (1988). Activation of transcription factor IIIC by the adenovirus E1A protein. Cell **53:**907-20.

Hofelmayr, H., L. J. Strobl, G. Marschall, G. W. Bornkamm, and U. Zimber-Strobl. (2001). Activated Notch1 can transiently substitute for EBNA2 in the maintenance of proliferation of LMP1-expressing immortalized B cells. J Virol **75:**2033-40.

Hofelmayr, H., L. J. Strobl, C. Stein, G. Laux, G. Marschall, G. W. Bornkamm, and U. Zimber-Strobl. (1999). Activated mouse Notch1 transactivates Epstein-Barr virus nuclear antigen 2-regulated viral promoters. J Virol **73:**2770-80.

Holowaty, M. N., Y. Sheng, T. Nguyen, C. Arrowsmith, and L. Frappier. (2003). Protein interaction domains of the ubiquitin-specific protease, USP7/HAUSP. J Biol Chem **278:**47753-61.

Holowaty, M. N., M. Zeghouf, H. Wu, J. Tellam, V. Athanasopoulos, J. Greenblatt, and L. Frappier. (2003). Protein profiling with Epstein-Barr nuclear antigen-1 reveals an interaction with the herpesvirus-associated ubiquitin-specific protease HAUSP/USP7. J Biol Chem **278:**29987-94.

Horner, D., M. Lewis, and P. J. Farrell. (1995). Novel hypotheses for the roles of EBNA-1 and BHRF1 in EBV-related cancers. Intervirology **38:**195-205.

Hovanessian, A. G. (1989). The double stranded RNA-activated protein kinase induced by interferon: dsRNA-PK. J Interferon Res **9:**641-7.

Howe, J. G., and M. D. Shu. (1989). Epstein-Barr virus small RNA (EBER) genes: unique transcription units that combine RNA polymerase II and III promoter elements. Cell **57:**825-34.

Howe, J. G., and M. D. Shu. (1993). Upstream basal promoter element important for exclusive RNA polymerase III transcription of the EBER 2 gene. Mol Cell Biol **13:**2655-65.

Howe, J. G., and J. A. Steitz. (1986). Localization of Epstein-Barr virus-encoded small RNAs by in situ hybridization. Proc Natl Acad Sci U S A **83:**9006-10.

Huang, D. P., J. H. Ho, D. Saw, and T. B. Teoh. (1978). Carcinoma of the nasal and paranasal regions in rats fed Cantonese salted marine fish. IARC Sci Publ**:**315-28.

Huang, S., J. Chen, H. Wang, B. Sun, H. Wang, Z. Zhang, X. Zhang, and Z. Chen. (2009). Influenza A virus matrix protein 1 interacts with hTFIIIC102-s, a short isoform of the polypeptide 3 subunit of human general transcription factor IIIC. Arch Virol **154:**1101-10.

Hudnall, S. D., Y. Ge, L. Wei, N. P. Yang, H. Q. Wang, and T. Chen. (2005). Distribution and phenotype of Epstein-Barr virus-infected cells in human pharyngeal tonsils. Mod Pathol **18:**519-27.

Huen, D. S., S. A. Henderson, D. Croom-Carter, and M. Rowe. (1995). The Epstein-Barr virus latent membrane protein-1 (LMP1) mediates activation of NF-kappa B and cell surface phenotype via two effector regions in its carboxy-terminal cytoplasmic domain. Oncogene **10:**549-60.

Hui, A. B., K. W. Lo, S. F. Leung, P. Teo, M. K. Fung, K. F. To, N. Wong, P. H. Choi, J. C. Lee, and D. P. Huang. (1999). Detection of recurrent chromosomal gains and losses in primary nasopharyngeal carcinoma by comparative genomic hybridisation. Int J Cancer **82:**498-503.

Hui, A. B., K. W. Lo, P. M. Teo, K. F. To, and D. P. Huang. (2002). Genome wide detection of oncogene amplifications in nasopharyngeal carcinoma by array based comparative genomic hybridization. Int J Oncol **20:**467-73.

Hume, A. J., and R. F. Kalejta. (2009). Regulation of the retinoblastoma proteins by the human herpesviruses. Cell Div **4:**1.

Humme, S., G. Reisbach, R. Feederle, H. J. Delecluse, K. Bousset, W. Hammerschmidt, and A. Schepers. (2003). The EBV nuclear antigen 1 (EBNA1) enhances B cell immortalization several thousandfold. Proc Natl Acad Sci U S A **100:**10989-94.

Hung, S. C., M. S. Kang, and E. Kieff. (2001). Maintenance of Epstein-Barr virus (EBV) oriP-based episomes requires EBV-encoded nuclear antigen-1 chromosome-binding domains, which can be replaced by high-mobility group-I or histone H1. Proc Natl Acad Sci U S A **98:**1865-70.

Hussain, S., S. B. Benavente, E. Nascimento, I. Dragoni, A. Kurowski, A. Gillich, P. Humphreys, and M. Frye. (2009). The nucleolar RNA methyltransferase Misu (NSun2) is required for mitotic spindle stability. J Cell Biol **186:**27-40.

Ikeda, M., A. Ikeda, L. C. Longan, and R. Longnecker. (2000). The Epstein-Barr virus latent membrane protein 2A PY motif recruits WW domain-containing ubiquitin-protein ligases. Virology **268:**178-91.

Ikuta, K., Y. Satoh, Y. Hoshikawa, and T. Sairenji. (2000). Detection of Epstein-Barr virus in salivas and throat washings in healthy adults and children. Microbes Infect **2:**115-20.

Ilves, I., K. Maemets, T. Silla, K. Janikson, and M. Ustav. (2006). Brd4 is involved in multiple processes of the bovine papillomavirus type 1 life cycle. J Virol **80:**3660-5.

Imai, S., S. Koizumi, M. Sugiura, M. Tokunaga, Y. Uemura, N. Yamamoto, S. Tanaka, E.

Sato, and T. Osato. (1994). Gastric carcinoma: monoclonal epithelial malignant cells expressing Epstein-Barr virus latent infection protein. Proc Natl Acad Sci U S A **91:**9131-5.

Iwai, K., N. Mori, M. Oie, N. Yamamoto, and M. Fujii. (2001). Human T-cell leukemia virus type 1 tax protein activates transcription through AP-1 site by inducing DNA binding activity in T cells. Virology **279:**38-46.

Iwakiri, D., Y. Eizuru, M. Tokunaga, and K. Takada. (2003). Autocrine growth of Epstein-Barr virus-positive gastric carcinoma cells mediated by an Epstein-Barr virus-encoded small RNA. Cancer Res **63:**7062-7.

Iwakiri, D., M. Samanta, and K. Takada. (2006). [Mechanisms of EBV-mediated oncogenesis]. Uirusu **56:**201-8.

Iwakiri, D., T. S. Sheen, J. Y. Chen, D. P. Huang, and K. Takada. (2005). Epstein-Barr virus-encoded small RNA induces insulin-like growth factor 1 and supports growth of nasopharyngeal carcinoma-derived cell lines. Oncogene **24:**1767-73.

Izumi, K. M., E. D. Cahir McFarland, E. A. Riley, D. Rizzo, Y. Chen, and E. Kieff. (1999). The residues between the two transformation effector sites of Epstein-Barr virus latent membrane protein 1 are not critical for B-lymphocyte growth transformation. J Virol **73:**9908-16.

Jackson, P., I. Mastrangelo, M. Reed, P. Tegtmeyer, G. Yardley, and J. Barrett. (1998). Synergistic transcriptional activation of the MCK promoter by p53: tetramers link separated DNA response elements by DNA looping. Oncogene **16:**283-92.

Jang, M. K., D. Kwon, and A. A. McBride. (2009). Papillomavirus E2 proteins and the host BRD4 protein associate with transcriptionally active cellular chromatin. J Virol **83:**2592-600.

Jat, P., and J. R. Arrand. (1982). In vitro transcription of two Epstein-Barr virus specified small RNA molecules. Nucleic Acids Res **10:**3407-25.

Javier, R. T., and J. S. Butel. (2008). The history of tumor virology. Cancer Res **68:**7693-706.

Jeon, J. P., H. Y. Nam, S. M. Shim, and B. G. Han. (2009). Sustained viral activity of epstein-Barr virus contributes to cellular immortalization of lymphoblastoid cell lines. Mol Cells **27:**143-8.

Johannessen, I., M. Asghar, and D. H. Crawford. (2000). Essential role for T cells in human B-cell lymphoproliferative disease development in severe combined immunodeficient mice. Br J Haematol **109:**600-10.

Johannsen, E., C. L. Miller, S. R. Grossman, and E. Kieff. (1996). EBNA-2 and EBNA-3C extensively and mutually exclusively associate with RBPJkappa in Epstein-Barr virus-transformed B lymphocytes. J Virol **70:**4179-83.

Johnson, S. A., L. Dubeau, and D. L. Johnson. (2008). Enhanced RNA polymerase III-dependent transcription is required for oncogenic transformation. J Biol Chem **283:**19184-91.

Johnson, S. A., L. Dubeau, M. Kawalek, A. Dervan, A. H. Schonthal, C. V. Dang, and D. L. Johnson. (2003). Increased expression of TATA-binding protein, the central transcription factor, can contribute to oncogenesis. Mol Cell Biol **23:**3043-51.

Johnson, S. S., C. Zhang, J. Fromm, I. M. Willis, and D. L. Johnson. (2007). Mammalian Maf1 is a negative regulator of transcription by all three nuclear RNA polymerases. Mol Cell **26:**367-79.

Jones, J. F., S. Shurin, C. Abramowsky, R. R. Tubbs, C. G. Sciotto, R. Wahl, J. Sands, D. Gottman, B. Z. Katz, and J. Sklar. (1988). T-cell lymphomas containing Epstein-Barr viral DNA in patients with chronic Epstein-Barr virus infections. N Engl J Med **318:**733-41.

Jones, R. M., J. Branda, K. A. Johnston, M. Polymenis, M. Gadd, A. Rustgi, L. Callanan, and E. V. Schmidt. (1996). An essential E box in the promoter of the gene encoding the mRNA cap-binding protein (eukaryotic initiation factor 4E) is a target for activation by c-myc. Mol Cell Biol **16:**4754-64.

Jones, T. R., and M. D. Cole. (1987). Rapid cytoplasmic turnover of c-myc mRNA: requirement of the 3' untranslated sequences. Mol Cell Biol **7:**4513-21.

Juven-Gershon, T., J. Y. Hsu, J. W. Theisen, and J. T. Kadonaga. (2008). The RNA polymerase II core promoter - the gateway to transcription. Curr Opin Cell Biol **20:**253-9.

Kaiser, C., G. Laux, D. Eick, N. Jochner, G. W. Bornkamm, and B. Kempkes. (1999). The proto-oncogene c-myc is a direct target gene of Epstein-Barr virus nuclear antigen 2. J Virol **73:**4481-4.

Kanavaros, P., M. C. Lescs, J. Briere, M. Divine, F. Galateau, I. Joab, J. Bosq, J. P. Farcet, F. Reyes, and P. Gaulard. (1993). Nasal T-cell lymphoma: a clinicopathologic entity associated with peculiar phenotype and with Epstein-Barr virus. Blood **81:**2688-95.

Kanazawa, S., L. Soucek, G. Evan, T. Okamoto, and B. M. Peterlin. (2003). c-Myc recruits P-TEFb for transcription, cellular proliferation and apoptosis. Oncogene **22:**5707-11.

Kanda, T., M. Otter, and G. M. Wahl. (2001). Coupling of mitotic chromosome tethering and

replication competence in epstein-barr virus-based plasmids. Mol Cell Biol **21:**3576-88.

Kanegane, H., K. Nomura, T. Miyawaki, and G. Tosato. (2002). Biological aspects of Epstein-Barr virus (EBV)-infected lymphocytes in chronic active EBV infection and associated malignancies. Crit Rev Oncol Hematol **44:**239-49.

Kang, M. S., S. C. Hung, and E. Kieff. (2001). Epstein-Barr virus nuclear antigen 1 activates transcription from episomal but not integrated DNA and does not alter lymphocyte growth. Proc Natl Acad Sci U S A **98:**15233-8.

Kang, M. S., H. Lu, T. Yasui, A. Sharpe, H. Warren, E. Cahir-McFarland, R. Bronson, S. C. Hung, and E. Kieff. (2005). Epstein-Barr virus nuclear antigen 1 does not induce lymphoma in transgenic FVB mice. Proc Natl Acad Sci U S A **102:**820-5.

Kang, M. S., V. Soni, R. Bronson, and E. Kieff. (2008). Epstein-Barr virus nuclear antigen 1 does not cause lymphoma in C57BL/6J mice. J Virol **82:**4180-3.

Kapatai, G., and P. Murray. (2007). Contribution of the Epstein Barr virus to the molecular pathogenesis of Hodgkin lymphoma. J Clin Pathol **60:**1342-9.

Kapoor, P., and L. Frappier. (2003). EBNA1 partitions Epstein-Barr virus plasmids in yeast cells by attaching to human EBNA1-binding protein 2 on mitotic chromosomes. J Virol **77:**6946-56.

Kapoor, P., B. D. Lavoie, and L. Frappier. (2005). EBP2 plays a key role in Epstein-Barr virus mitotic segregation and is regulated by aurora family kinases. Mol Cell Biol **25:**4934-45.

Kapoor, P., K. Shire, and L. Frappier. (2001). Reconstitution of Epstein-Barr virus-based plasmid partitioning in budding yeast. Embo J **20:**222-30.

Karajannis, M. A., M. Hummel, I. Anagnostopoulos, and H. Stein. (1997). Strict lymphotropism of Epstein-Barr virus during acute infectious mononucleosis in nonimmunocompromised individuals. Blood **89:**2856-62.

Kardinal, C. G., and J. W. Yarbro. (1979). A conceptual history of cancer. Semin Oncol **6:**396-408.

Kato, G. J., J. Barrett, M. Villa-Garcia, and C. V. Dang. (1990). An amino-terminal c-myc domain required for neoplastic transformation activates transcription. Mol Cell Biol **10:**5914-20.

Kaye, K. M., K. M. Izumi, and E. Kieff. (1993). Epstein-Barr virus latent membrane protein 1 is essential for B-lymphocyte growth transformation. Proc Natl Acad Sci U S A **90:**9150-4.

Kelly, G., A. Bell, and A. Rickinson. (2002). Epstein-Barr virus-associated Burkitt lymphomagenesis selects for downregulation of the nuclear antigen EBNA2. Nat Med **8:**1098-104.

Kelly, G. L., H. M. Long, J. Stylianou, W. A. Thomas, A. Leese, A. I. Bell, G. W. Bornkamm, J. Mautner, A. B. Rickinson, and M. Rowe. (2009). An Epstein-Barr virus anti-apoptotic protein constitutively expressed in transformed cells and implicated in burkitt lymphomagenesis: the Wp/BHRF1 link. PLoS Pathog **5:**e1000341.

Kelly, K., B. H. Cochran, C. D. Stiles, and P. Leder. (1983). Cell-specific regulation of the c-myc gene by lymphocyte mitogens and platelet-derived growth factor. Cell **35:**603-10.

Kennedy, G., J. Komano, and B. Sugden. (2003). Epstein-Barr virus provides a survival factor to Burkitt's lymphomas. Proc Natl Acad Sci U S A **100:**14269-74.

Kenneth, N. S., L. Marshall, and R. J. White. (2008). Recruitment of RNA polymerase III in vivo. Nucleic Acids Res **36:**3757-64.

Kenneth, N. S., B. A. Ramsbottom, N. Gomez-Roman, L. Marshall, P. A. Cole, and R. J. White. (2007). TRRAP and GCN5 are used by c-Myc to activate RNA polymerase III transcription. Proc Natl Acad Sci U S A **104:**14917-22.

Kenneth, N. S., and R. J. White. (2009). Regulation by c-Myc of ncRNA expression. Curr Opin Genet Dev **19:**38-43.

Kieff, E., and A. Rickinson. 2001. Epstein-Barr Virus, p. 2511–2574. *In* D. M. Knipe, P. M. Howley, D. E. Griffin, and B. N. Fields (ed.), Fields virology. Lippincott Williams & Wilkins, Philadelphia.

Kienzle, N., M. Buck, S. Greco, K. Krauer, and T. B. Sculley. (1999). Epstein-Barr virus-encoded RK-BARF0 protein expression. J Virol **73:**8902-6.

Kieser, A., E. Kilger, O. Gires, M. Ueffing, W. Kolch, and W. Hammerschmidt. (1997). Epstein-Barr virus latent membrane protein-1 triggers AP-1 activity via the c-Jun N-terminal kinase cascade. Embo J **16:**6478-85.

Kikuta, H., Y. Taguchi, K. Tomizawa, K. Kojima, N. Kawamura, A. Ishizaka, Y. Sakiyama, S. Matsumoto, S. Imai, T. Kinoshita, and et al. (1988). Epstein-Barr virus genome-positive T lymphocytes in a boy with chronic active EBV infection associated with Kawasaki-like disease. Nature **333:**455-7.

Kilger, E., A. Kieser, M. Baumann, and W. Hammerschmidt. (1998). Epstein-Barr virus-mediated B-cell proliferation is dependent upon latent membrane protein 1, which simulates an activated CD40 receptor. Embo J **17:**1700-9.

Kim, A. L., M. Maher, J. B. Hayman, J. Ozer, D. Zerby, J. L. Yates, and P. M. Lieberman. (1997). An imperfect correlation between DNA replication activity of Epstein-Barr virus nuclear antigen 1 (EBNA1) and binding to the nuclear import receptor, Rch1/importin alpha. Virology **239:**340-51.

Kirchmaier, A. L., and B. Sugden. (1997). Dominant-negative inhibitors of EBNA-1 of Epstein-Barr virus. J Virol **71:**1766-75.

Kiss, C., J. Nishikawa, K. Takada, P. Trivedi, G. Klein, and L. Szekely. (2003). T cell leukemia I oncogene expression depends on the presence of Epstein-Barr virus in the virus-carrying Burkitt lymphoma lines. Proc Natl Acad Sci U S A **100:**4813-8.

Kitagawa, N., M. Goto, K. Kurozumi, S. Maruo, M. Fukayama, T. Naoe, M. Yasukawa, K. Hino, T. Suzuki, S. Todo, and K. Takada. (2000). Epstein-Barr virus-encoded poly(A)(-) RNA supports Burkitt's lymphoma growth through interleukin-10 induction. Embo J **19:**6742-50.

Klein, E., L. L. Kis, and G. Klein. (2007). Epstein-Barr virus infection in humans: from harmless to life endangering virus-lymphocyte interactions. Oncogene **26:**1297-305.

Kleinert, H., A. Gladen, M. Geisler, and B. J. Benecke. (1988). Differential regulation of transcription of human 7 S K and 7 S L RNA genes. J Biol Chem **263:**11511-5.

Knight, J. S., K. Lan, C. Subramanian, and E. S. Robertson. (2003). Epstein-Barr virus nuclear antigen 3C recruits histone deacetylase activity and associates with the corepressors mSin3A and NCoR in human B-cell lines. J Virol **77:**4261-72.

Knox, P. G., Q. X. Li, A. B. Rickinson, and L. S. Young. (1996). In vitro production of stable Epstein-Barr virus-positive epithelial cell clones which resemble the virus:cell interaction observed in nasopharyngeal carcinoma. Virology **215:**40-50.

Kohlhof, H., F. Hampel, R. Hoffmann, H. Burtscher, U. H. Weidle, M. Holzel, D. Eick, U. Zimber-Strobl, and L. J. Strobl. (2009). Notch1, Notch2, and Epstein-Barr virus-encoded nuclear antigen 2 signaling differentially affects proliferation and survival of Epstein-Barr virus-infected B cells. Blood **113:**5506-15.

Komano, J., S. Maruo, K. Kurozumi, T. Oda, and K. Takada. (1999). Oncogenic role of Epstein-Barr virus-encoded RNAs in Burkitt's lymphoma cell line Akata. J Virol **73:**9827-31.

Komano, J., M. Sugiura, and K. Takada. (1998). Epstein-Barr virus contributes to the malignant phenotype and to apoptosis resistance in Burkitt's lymphoma cell line Akata. J Virol **72:**9150-6.

Korabecna, M., M. Ludvikova, and A. Skalova. (2003). Molecular diagnosis of Epstein-Barr

virus in paraffin-embedded tissues of tumors with abundant lymphoid infiltration. Neoplasma **50:**8-12.

Kovalchuk, A. L., C. F. Qi, T. A. Torrey, L. Taddesse-Heath, L. Feigenbaum, S. S. Park, A. Gerbitz, G. Klobeck, K. Hoertnagel, A. Polack, G. W. Bornkamm, S. Janz, and H. C. Morse, 3rd. (2000). Burkitt lymphoma in the mouse. J Exp Med **192:**1183-90.

Kripalani-Joshi, S., and H. Y. Law. (1994). Identification of integrated Epstein-Barr virus in nasopharyngeal carcinoma using pulse field gel electrophoresis. Int J Cancer **56:**187-92.

Krithivas, A., M. Fujimuro, M. Weidner, D. B. Young, and S. D. Hayward. (2002). Protein interactions targeting the latency-associated nuclear antigen of Kaposi's sarcoma-associated herpesvirus to cell chromosomes. J Virol **76:**11596-604.

Krysan, P. J., S. B. Haase, and M. P. Calos. (1989). Isolation of human sequences that replicate autonomously in human cells. Mol Cell Biol **9:**1026-33.

Kuhlmann, A. S., J. Villaudy, L. Gazzolo, M. Castellazzi, J. M. Mesnard, and M. Duc Dodon. (2007). HTLV-1 HBZ cooperates with JunD to enhance transcription of the human telomerase reverse transcriptase gene (hTERT). Retrovirology **4:**92.

Kuppers, R. (2002). Molecular biology of Hodgkin's lymphoma. Adv Cancer Res **84:**277-312.

Kurg, R., K. Sild, A. Ilves, M. Sepp, and M. Ustav. (2005). Association of bovine papillomavirus E2 protein with nuclear structures in vivo. J Virol **79:**10528-39.

Kurth, J., T. Spieker, J. Wustrow, G. J. Strickler, L. M. Hansmann, K. Rajewsky, and R. Kuppers. (2000). EBV-infected B cells in infectious mononucleosis: viral strategies for spreading in the B cell compartment and establishing latency. Immunity **13:**485-95.

Kuttler, F., and S. Mai. (2006). c-Myc, Genomic Instability and Disease. Genome Dyn **1:**171-90.

Kwok, R. P., M. E. Laurance, J. R. Lundblad, P. S. Goldman, H. Shih, L. M. Connor, S. J. Marriott, and R. H. Goodman. (1996). Control of cAMP-regulated enhancers by the viral transactivator Tax through CREB and the co-activator CBP. Nature **380:**642-6.

Lachman, H. M., and A. I. Skoultchi. (1984). Expression of c-myc changes during differentiation of mouse erythroleukaemia cells. Nature **310:**592-4.

Laherty, C. D., H. M. Hu, A. W. Opipari, F. Wang, and V. M. Dixit. (1992). The Epstein-Barr virus LMP1 gene product induces A20 zinc finger protein expression by activating nuclear factor kappa B. J Biol Chem **267:**24157-60.

Laichalk, L. L., D. Hochberg, G. J. Babcock, R. B. Freeman, and D. A. Thorley-Lawson.

(2002). The dispersal of mucosal memory B cells: evidence from persistent EBV infection. Immunity **16:**745-54.

Laichalk, L. L., and D. A. Thorley-Lawson. (2005). Terminal differentiation into plasma cells initiates the replicative cycle of Epstein-Barr virus in vivo. J Virol **79:**1296-307.

Laing, K. G., A. Elia, I. Jeffrey, V. Matys, V. J. Tilleray, B. Souberbielle, and M. J. Clemens. (2002). In vivo effects of the Epstein-Barr virus small RNA EBER-1 on protein synthesis and cell growth regulation. Virology **297:**253-69.

Laing, K. G., V. Matys, and M. J. Clemens. (1995). Effects of expression of the Epstein-Barr virus small RNA EBER-1 in heterologous cells on protein synthesis and cell growth. Biochem Soc Trans **23:**311S.

Landschulz, W. H., P. F. Johnson, and S. L. McKnight. (1988). The leucine zipper: a hypothetical structure common to a new class of DNA binding proteins. Science **240:**1759-64.

Lane, D. P., and L. V. Crawford. (1979). T antigen is bound to a host protein in SV40-transformed cells. Nature **278:**261-3.

Larminie, C. G., J. E. Sutcliffe, K. Tosh, A. G. Winter, Z. A. Felton-Edkins, and R. J. White. (1999). Activation of RNA polymerase III transcription in cells transformed by simian virus 40. Mol Cell Biol **19:**4927-34.

Lauer, G. M., and B. D. Walker. (2001). Hepatitis C virus infection. N Engl J Med **345:**41-52.

Lauritzen, A. F., U. Hording, and H. W. Nielsen. (1994). Epstein-Barr virus and Hodgkin's disease: a comparative immunological, in situ hybridization, and polymerase chain reaction study. Apmis **102:**495-500.

Lawrence, J. B., C. A. Villnave, and R. H. Singer. (1988). Sensitive, high-resolution chromatin and chromosome mapping in situ: presence and orientation of two closely integrated copies of EBV in a lymphoma line. Cell **52:**51-61.

Leder, A., P. K. Pattengale, A. Kuo, T. A. Stewart, and P. Leder. (1986). Consequences of widespread deregulation of the c-myc gene in transgenic mice: multiple neoplasms and normal development. Cell **45:**485-95.

Leder, P., J. Battey, G. Lenoir, C. Moulding, W. Murphy, H. Potter, T. Stewart, and R. Taub. (1983). Translocations among antibody genes in human cancer. Science **222:**765-71.

Lee, H. S., M. S. Chang, H. K. Yang, B. L. Lee, and W. H. Kim. (2004). Epstein-barr virus-positive gastric carcinoma has a distinct protein expression profile in comparison with

epstein-barr virus-negative carcinoma. Clin Cancer Res **10:**1698-705.

Lee, M. A., M. E. Diamond, and J. L. Yates. (1999). Genetic evidence that EBNA-1 is needed for efficient, stable latent infection by Epstein-Barr virus. J Virol **73:**2974-82.

Lee, W. H., R. Bookstein, F. Hong, L. J. Young, J. Y. Shew, and E. Y. Lee. (1987). Human retinoblastoma susceptibility gene: cloning, identification, and sequence. Science **235:**1394-9.

Leight, E. R., and B. Sugden. (2000). EBNA-1: a protein pivotal to latent infection by Epstein-Barr virus. Rev Med Virol **10:**83-100.

Leong, I. T., B. J. Fernandes, and D. Mock. (2001). Epstein-Barr virus detection in non-Hodgkin's lymphoma of the oral cavity: an immunocytochemical and in situ hybridization study. Oral Surg Oral Med Oral Pathol Oral Radiol Endod **92:**184-93.

Lerner, M. R., N. C. Andrews, G. Miller, and J. A. Steitz. (1981). Two small RNAs encoded by Epstein-Barr virus and complexed with protein are precipitated by antibodies from patients with systemic lupus erythematosus. Proc Natl Acad Sci U S A **78:**805-9.

Lerner, M. R., J. A. Boyle, J. A. Hardin, and J. A. Steitz. (1981). Two novel classes of small ribonucleoproteins detected by antibodies associated with lupus erythematosus. Science **211:**400-2.

Levens, D. (2008). How the c-myc promoter works and why it sometimes does not. J Natl Cancer Inst Monogr**:**41-3.

Levine, A. J. 1991. Viruses. Scientific American Library, New York.

Levitskaya, J., A. Sharipo, A. Leonchiks, A. Ciechanover, and M. G. Masucci. (1997). Inhibition of ubiquitin/proteasome-dependent protein degradation by the Gly-Ala repeat domain of the Epstein-Barr virus nuclear antigen 1. Proc Natl Acad Sci U S A **94:**12616-21.

Li, M., D. Chen, A. Shiloh, J. Luo, A. Y. Nikolaev, J. Qin, and W. Gu. (2002). Deubiquitination of p53 by HAUSP is an important pathway for p53 stabilization. Nature **416:**648-53.

Li, Q. X., L. S. Young, G. Niedobitek, C. W. Dawson, M. Birkenbach, F. Wang, and A. B. Rickinson. (1992). Epstein-Barr virus infection and replication in a human epithelial cell system. Nature **356:**347-50.

Li, X. Y., and M. R. Green. (1996). Intramolecular inhibition of activating transcription factor-2 function by its DNA-binding domain. Genes Dev **10:**517-27.

Liang, C. L., C. N. Tsai, P. J. Chung, J. L. Chen, C. M. Sun, R. H. Chen, J. H. Hong, and Y. S. Chang. (2000). Transcription of Epstein-Barr virus-encoded nuclear antigen 1 promoter Qp is repressed by transforming growth factor-beta via Smad4 binding element in human BL cells. Virology **277:**184-92.

Lin, A., S. Wang, T. Nguyen, K. Shire, and L. Frappier. (2008). The EBNA1 protein of Epstein-Barr virus functionally interacts with Brd4. J Virol **82:**12009-19.

Lindstrom, M. S., and K. G. Wiman. (2002). Role of genetic and epigenetic changes in Burkitt lymphoma. Semin Cancer Biol **12:**381-7.

Ling, P. D., J. Tan, and R. Peng. (2009). Nuclear-cytoplasmic shuttling is not required for EBV EBNA-LP transcriptional coactivation function. J Virol.

Linzer, D. I., and A. J. Levine. (1979). Characterization of a 54K dalton cellular SV40 tumor antigen present in SV40-transformed cells and uninfected embryonal carcinoma cells. Cell **17:**43-52.

Littlewood, T. D., D. C. Hancock, P. S. Danielian, M. G. Parker, and G. I. Evan. (1995). A modified oestrogen receptor ligand-binding domain as an improved switch for the regulation of heterologous proteins. Nucleic Acids Res **23:**1686-90.

Liu, J., H. J. Martin, G. Liao, and S. D. Hayward. (2007). The Kaposi's sarcoma-associated herpesvirus LANA protein stabilizes and activates c-Myc. J Virol **81:**10451-9.

Livak, K. J., and T. D. Schmittgen. (2001). Analysis of relative gene expression data using real-time quantitative PCR and the 2(-Delta Delta C(T)) Method. Methods **25:**402-8.

Livingstone, C., G. Patel, and N. Jones. (1995). ATF-2 contains a phosphorylation-dependent transcriptional activation domain. Embo J **14:**1785-97.

Lo, A. K., K. F. To, K. W. Lo, R. W. Lung, J. W. Hui, G. Liao, and S. D. Hayward. (2007). Modulation of LMP1 protein expression by EBV-encoded microRNAs. Proc Natl Acad Sci U S A **104:**16164-9.

Lo, K. W., S. T. Cheung, S. F. Leung, A. van Hasselt, Y. S. Tsang, K. F. Mak, Y. F. Chung, J. K. Woo, J. C. Lee, and D. P. Huang. (1996). Hypermethylation of the p16 gene in nasopharyngeal carcinoma. Cancer Res **56:**2721-5.

Lo, K. W., and D. P. Huang. (2002). Genetic and epigenetic changes in nasopharyngeal carcinoma. Semin Cancer Biol **12:**451-62.

Lo, K. W., J. Kwong, A. B. Hui, S. Y. Chan, K. F. To, A. S. Chan, L. S. Chow, P. M. Teo, P. J. Johnson, and D. P. Huang. (2001). High frequency of promoter hypermethylation of RASSF1A in nasopharyngeal carcinoma. Cancer Res **61:**3877-81.

Lo, K. W., K. F. To, and D. P. Huang. (2004). Focus on nasopharyngeal carcinoma. Cancer Cell **5:**423-8.

Longan, L., and R. Longnecker. (2000). Epstein-Barr virus latent membrane protein 2A has no growth-altering effects when expressed in differentiating epithelia. J Gen Virol **81:**2245-52.

Longnecker, R. (2000). Epstein-Barr virus latency: LMP2, a regulator or means for Epstein-Barr virus persistence? Adv Cancer Res **79:**175-200.

Longnecker, R., and E. Kieff. (1990). A second Epstein-Barr virus membrane protein (LMP2) is expressed in latent infection and colocalizes with LMP1. J Virol **64:**2319-26.

Lubyova, B., M. J. Kellum, J. A. Frisancho, and P. M. Pitha. (2007). Stimulation of c-Myc transcriptional activity by vIRF-3 of Kaposi sarcoma-associated herpesvirus. J Biol Chem **282:**31944-53.

Lucchesi, W., G. Brady, O. Dittrich-Breiholz, M. Kracht, R. Russ, and P. J. Farrell. (2008). Differential gene regulation by Epstein-Barr virus type 1 and type 2 EBNA2. J Virol **82:**7456-66.

Ludwig, S., O. Planz, S. Pleschka, and T. Wolff. (2003). Influenza-virus-induced signaling cascades: targets for antiviral therapy? Trends Mol Med **9:**46-52.

Lupton, S., and A. J. Levine. (1985). Mapping genetic elements of Epstein-Barr virus that facilitate extrachromosomal persistence of Epstein-Barr virus-derived plasmids in human cells. Mol Cell Biol **5:**2533-42.

Luscher, B., and R. N. Eisenman. (1990). New light on Myc and Myb. Part I. Myc. Genes Dev **4:**2025-35.

Ma, H. C., T. W. Lin, H. Li, S. M. Iguchi-Ariga, H. Ariga, Y. L. Chuang, J. H. Ou, and S. Y. Lo. (2008). Hepatitis C virus ARFP/F protein interacts with cellular MM-1 protein and enhances the gene trans-activation activity of c-Myc. J Biomed Sci **15:**417-25.

Ma, Q., X. Li, D. Vale-Cruz, M. L. Brown, F. Beier, and P. LuValle. (2007). Activating transcription factor 2 controls Bcl-2 promoter activity in growth plate chondrocytes. J Cell Biochem **101:**477-87.

Mackey, D., T. Middleton, and B. Sugden. (1995). Multiple regions within EBNA1 can link DNAs. J Virol **69:**6199-208.

Mackey, D., and B. Sugden. (1999). The linking regions of EBNA1 are essential for its support of replication and transcription. Mol Cell Biol **19:**3349-59.

Maekawa, T., T. Shinagawa, Y. Sano, T. Sakuma, S. Nomura, K. Nagasaki, Y. Miki, F. Saito-Ohara, J. Inazawa, T. Kohno, J. Yokota, and S. Ishii. (2007). Reduced levels of ATF-2 predispose mice to mammary tumors. Mol Cell Biol **27:**1730-44.

Mainou, B. A., and N. Raab-Traub. (2006). LMP1 strain variants: biological and molecular properties. J Virol **80:**6458-68.

Marcu, K. B., S. A. Bossone, and A. J. Patel. (1992). myc function and regulation. Annu Rev Biochem **61:**809-60.

Marechal, V., A. Dehee, R. Chikhi-Brachet, T. Piolot, M. Coppey-Moisan, and J. C. Nicolas. (1999). Mapping EBNA-1 domains involved in binding to metaphase chromosomes. J Virol **73:**4385-92.

Marks, J. E., J. L. Phillips, and H. R. Menck. (1998). The National Cancer Data Base report on the relationship of race and national origin to the histology of nasopharyngeal carcinoma. Cancer **83:**582-8.

Marshall, L., N. S. Kenneth, and R. J. White. (2008). Elevated tRNA(iMet) synthesis can drive cell proliferation and oncogenic transformation. Cell **133:**78-89.

Marshall, L., and R. J. White. (2008). Non-coding RNA production by RNA polymerase III is implicated in cancer. Nat Rev Cancer **8:**911-4.

Marshall, N. A., L. E. Christie, L. R. Munro, D. J. Culligan, P. W. Johnston, R. N. Barker, and M. A. Vickers. (2004). Immunosuppressive regulatory T cells are abundant in the reactive lymphocytes of Hodgkin lymphoma. Blood **103:**1755-62.

Massie, C. E., and I. G. Mills. (2008). ChIPping away at gene regulation. EMBO Rep **9:**337-43.

Matsumoto, J., T. Ohshima, O. Isono, and K. Shimotohno. (2005). HTLV-1 HBZ suppresses AP-1 activity by impairing both the DNA-binding ability and the stability of c-Jun protein. Oncogene **24:**1001-10.

Matsuoka, M., and K. T. Jeang. (2007). Human T-cell leukaemia virus type 1 (HTLV-1) infectivity and cellular transformation. Nat Rev Cancer **7:**270-80.

McCann, E. M., G. L. Kelly, A. B. Rickinson, and A. I. Bell. (2001). Genetic analysis of the Epstein-Barr virus-coded leader protein EBNA-LP as a co-activator of EBNA2 function. J Gen Virol **82:**3067-79.

McClain, K. L., C. T. Leach, H. B. Jenson, V. V. Joshi, B. H. Pollock, R. T. Parmley, F. J. DiCarlo, E. G. Chadwick, and S. B. Murphy. (1995). Association of Epstein-Barr virus with leiomyosarcomas in children with AIDS. N Engl J Med **332:**12-8.

McLaughlin-Drubin, M. E., and K. Munger. (2008). Viruses associated with human cancer. Biochim Biophys Acta **1782:**127-50.

McMahon, S. B., H. A. Van Buskirk, K. A. Dugan, T. D. Copeland, and M. D. Cole. (1998). The novel ATM-related protein TRRAP is an essential cofactor for the c-Myc and E2F oncoproteins. Cell **94:**363-74.

McMurray, H. R., and D. J. McCance. (2003). Human papillomavirus type 16 E6 activates TERT gene transcription through induction of c-Myc and release of USF-mediated repression. J Virol **77:**9852-61.

McPhillips, M. G., J. G. Oliveira, J. E. Spindler, R. Mitra, and A. A. McBride. (2006). Brd4 is required for e2-mediated transcriptional activation but not genome partitioning of all papillomaviruses. J Virol **80:**9530-43.

McPhillips, M. G., K. Ozato, and A. A. McBride. (2005). Interaction of bovine papillomavirus E2 protein with Brd4 stabilizes its association with chromatin. J Virol **79:**8920-32.

Metzenberg, S. (1990). Levels of Epstein-Barr virus DNA in lymphoblastoid cell lines are correlated with frequencies of spontaneous lytic growth but not with levels of expression of EBNA-1, EBNA-2, or latent membrane protein. J Virol **64:**437-44.

Metzenberg, S. (1989). Relative rates of RNA synthesis across the genome of Epstein-Barr virus are highest near oriP and oriLyt. J Virol **63:**4938-44.

Meyer, N., and L. Z. Penn. (2008). Reflecting on 25 years with MYC. Nat Rev Cancer **8:**976-90.

Miethe, J., C. Schwartz, K. Wottrich, D. Wenning, and K. H. Klempnauer. (2001). Crosstalk between Myc and activating transcription factor 2 (ATF2): Myc prolongs the half-life and induces phosphorylation of ATF2. Oncogene **20:**8116-24.

Miller, C. L., A. L. Burkhardt, J. H. Lee, B. Stealey, R. Longnecker, J. B. Bolen, and E. Kieff. (1995). Integral membrane protein 2 of Epstein-Barr virus regulates reactivation from latency through dominant negative effects on protein-tyrosine kinases. Immunity **2:**155-66.

Minarovits, J., L. F. Hu, Z. Marcsek, S. Minarovits-Kormuta, G. Klein, and I. Ernberg. (1992). RNA polymerase III-transcribed EBER 1 and 2 transcription units are expressed and hypomethylated in the major Epstein-Barr virus-carrying cell types. J Gen Virol **73 (Pt 7):**1687-92.

Morris, M. A., C. W. Dawson, W. Wei, J. D. O'Neil, S. E. Stewart, J. Jia, A. I. Bell, L. S. Young, and J. R. Arrand. (2008). Epstein-Barr virus-encoded LMP1 induces a

hyperproliferative and inflammatory gene expression programme in cultured keratinocytes. J Gen Virol **89:**2806-20.

Morton, J. P., T. Kantidakis, and R. J. White. (2007). RNA polymerase III transcription is repressed in response to the tumour suppressor ARF. Nucleic Acids Res **35:**3046-52.

Mrazek, J., S. B. Kreutmayer, F. A. Grasser, N. Polacek, and A. Huttenhofer. (2007). Subtractive hybridization identifies novel differentially expressed ncRNA species in EBV-infected human B cells. Nucleic Acids Res **35:**e73.

Mueller-Lantzsch, N., G. M. Lenoir, M. Sauter, K. Takaki, J. M. Bechet, C. Kuklik-Roos, D. Wunderlich, and G. W. Bornkamm. (1985). Identification of the coding region for a second Epstein-Barr virus nuclear antigen (EBNA 2) by transfection of cloned DNA fragments. Embo J **4:**1805-11.

Muller, J., and B. J. Benecke. (1999). Analysis of transcription factors binding to the human 7SL RNA gene promoter. Biochem Cell Biol **77:**431-8.

Murakami, M., K. Lan, C. Subramanian, and E. S. Robertson. (2005). Epstein-Barr virus nuclear antigen 1 interacts with Nm23-H1 in lymphoblastoid cell lines and inhibits its ability to suppress cell migration. J Virol **79:**1559-68.

Murray, P. G., and L. S. Young. (2002). The Role of the Epstein-Barr virus in human disease. Front Biosci **7:**d519-40.

Murre, C., P. S. McCaw, and D. Baltimore. (1989). A new DNA binding and dimerization motif in immunoglobulin enhancer binding, daughterless, MyoD, and myc proteins. Cell **56:**777-83.

Nair, S. K., and S. K. Burley. (2006). Structural aspects of interactions within the Myc/Max/Mad network. Curr Top Microbiol Immunol **302:**123-43.

Nanbo, A., K. Inoue, K. Adachi-Takasawa, and K. Takada. (2002). Epstein-Barr virus RNA confers resistance to interferon-alpha-induced apoptosis in Burkitt's lymphoma. Embo J **21:**954-65.

Nanbo, A., A. Sugden, and B. Sugden. (2007). The coupling of synthesis and partitioning of EBV's plasmid replicon is revealed in live cells. Embo J **26:**4252-62.

Nanbo, A., and K. Takada. (2002). The role of Epstein-Barr virus-encoded small RNAs (EBERs) in oncogenesis. Rev Med Virol **12:**321-6.

Nanbo, A., H. Yoshiyama, and K. Takada. (2005). Epstein-Barr virus-encoded poly(A)- RNA confers resistance to apoptosis mediated through Fas by blocking the PKR pathway in human epithelial intestine 407 cells. J Virol **79:**12280-5.

Nelson, B. P., M. A. Nalesnik, D. W. Bahler, J. Locker, J. J. Fung, and S. H. Swerdlow. (2000). Epstein-Barr virus-negative post-transplant lymphoproliferative disorders: a distinct entity? Am J Surg Pathol **24:**375-85.

Nemerow, G. R., C. Mold, V. K. Schwend, V. Tollefson, and N. R. Cooper. (1987). Identification of gp350 as the viral glycoprotein mediating attachment of Epstein-Barr virus (EBV) to the EBV/C3d receptor of B cells: sequence homology of gp350 and C3 complement fragment C3d. J Virol **61:**1416-20.

Neri, A., F. Barriga, G. Inghirami, D. M. Knowles, J. Neequaye, I. T. Magrath, and R. Dalla-Favera. (1991). Epstein-Barr virus infection precedes clonal expansion in Burkitt's and acquired immunodeficiency syndrome-associated lymphoma. Blood **77:**1092-5.

Nesbit, C. E., J. M. Tersak, and E. V. Prochownik. (1999). MYC oncogenes and human neoplastic disease. Oncogene **18:**3004-16.

Niedobitek, G., A. Agathanggelou, P. Barber, L. A. Smallman, E. L. Jones, and L. S. Young. (1993). P53 overexpression and Epstein-Barr virus infection in undifferentiated and squamous cell nasopharyngeal carcinomas. J Pathol **170:**457-61.

Niedobitek, G., A. Agathanggelou, H. Herbst, L. Whitehead, D. H. Wright, and L. S. Young. (1997). Epstein-Barr virus (EBV) infection in infectious mononucleosis: virus latency, replication and phenotype of EBV-infected cells. J Pathol **182:**151-9.

Niedobitek, G., L. S. Young, C. K. Sam, L. Brooks, U. Prasad, and A. B. Rickinson. (1992). Expression of Epstein-Barr virus genes and of lymphocyte activation molecules in undifferentiated nasopharyngeal carcinomas. Am J Pathol **140:**879-87.

Niller, H. H., G. Glaser, R. Knuchel, and H. Wolf. (1995). Nucleoprotein complexes and DNA 5'-ends at oriP of Epstein-Barr virus. J Biol Chem **270:**12864-8.

Niller, H. H., D. Salamon, K. Ilg, A. Koroknai, F. Banati, G. Bauml, O. Rucker, F. Schwarzmann, H. Wolf, and J. Minarovits. (2003). The in vivo binding site for oncoprotein c-Myc in the promoter for Epstein-Barr virus (EBV) encoding RNA (EBER) 1 suggests a specific role for EBV in lymphomagenesis. Med Sci Monit **9:**HY1-9.

Nitsche, F., A. Bell, and A. Rickinson. (1997). Epstein-Barr virus leader protein enhances EBNA-2-mediated transactivation of latent membrane protein 1 expression: a role for the W1W2 repeat domain. J Virol **71:**6619-28.

Nonkwelo, C., J. Skinner, A. Bell, A. Rickinson, and J. Sample. (1996). Transcription start sites downstream of the Epstein-Barr virus (EBV) Fp promoter in early-passage Burkitt lymphoma cells define a fourth promoter for expression of the EBV EBNA-1 protein. J Virol **70:**623-7.

Nonoyama, M., and J. S. Pagano. (1972). Separation of Epstein-Barr virus DNA from large chromosomal DNA in non-virus-producing cells. Nat New Biol **238:**169-71.

O'Connell, B. C., A. F. Cheung, C. P. Simkevich, W. Tam, X. Ren, M. K. Mateyak, and J. M. Sedivy. (2003). A large scale genetic analysis of c-Myc-regulated gene expression patterns. J Biol Chem **278:**12563-73.

O'Donnell, K. A., E. A. Wentzel, K. I. Zeller, C. V. Dang, and J. T. Mendell. (2005). c-Myc-regulated microRNAs modulate E2F1 expression. Nature **435:**839-43.

O'Neil, J. D., T. J. Owen, V. H. Wood, K. L. Date, R. Valentine, M. B. Chukwuma, J. R. Arrand, C. W. Dawson, and L. S. Young. (2008). Epstein-Barr virus-encoded EBNA1 modulates the AP-1 transcription factor pathway in nasopharyngeal carcinoma cells and enhances angiogenesis in vitro. J Gen Virol **89:**2833-42.

Orian, A., B. van Steensel, J. Delrow, H. J. Bussemaker, L. Li, T. Sawado, E. Williams, L. W. Loo, S. M. Cowley, C. Yost, S. Pierce, B. A. Edgar, S. M. Parkhurst, and R. N. Eisenman. (2003). Genomic binding by the Drosophila Myc, Max, Mad/Mnt transcription factor network. Genes Dev **17:**1101-14.

Orlando, V., and R. Paro. (1993). Mapping Polycomb-repressed domains in the bithorax complex using in vivo formaldehyde cross-linked chromatin. Cell **75:**1187-98.

Orphanides, G., T. Lagrange, and D. Reinberg. (1996). The general transcription factors of RNA polymerase II. Genes Dev **10:**2657-83.

Oskarsson, T., and A. Trumpp. (2005). The Myc trilogy: lord of RNA polymerases. Nat Cell Biol **7:**215-7.

Oster, S. K., C. S. Ho, E. L. Soucie, and L. Z. Penn. (2002). The myc oncogene: MarvelouslY Complex. Adv Cancer Res **84:**81-154.

Ouwens, D. M., N. D. de Ruiter, G. C. van der Zon, A. P. Carter, J. Schouten, C. van der Burgt, K. Kooistra, J. L. Bos, J. A. Maassen, and H. van Dam. (2002). Growth factors can activate ATF2 via a two-step mechanism: phosphorylation of Thr71 through the Ras-MEK-ERK pathway and of Thr69 through RalGDS-Src-p38. Embo J **21:**3782-93.

Pagano, J. S., M. Blaser, M. A. Buendia, B. Damania, K. Khalili, N. Raab-Traub, and B. Roizman. (2004). Infectious agents and cancer: criteria for a causal relation. Semin Cancer Biol **14:**453-71.

Pajic, A., M. S. Staege, D. Dudziak, M. Schuhmacher, D. Spitkovsky, G. Eissner, M. Brielmeier, A. Polack, and G. W. Bornkamm. (2001). Antagonistic effects of c-myc and Epstein-Barr virus latent genes on the phenotype of human B cells. Int J Cancer

93:810-6.

Palefsky, J. M., J. Berline, D. Greenspan, and J. S. Greenspan. (2002). Evidence for trafficking of Epstein-Barr virus strains between hairy leukoplakia and peripheral blood lymphocytes. J Gen Virol **83:**317-21.

Palermo, R. D., H. M. Webb, A. Gunnell, and M. J. West. (2008). Regulation of transcription by the Epstein-Barr virus nuclear antigen EBNA 2. Biochem Soc Trans **36:**625-8.

Pang, R., E. Tse, and R. T. Poon. (2006). Molecular pathways in hepatocellular carcinoma. Cancer Lett **240:**157-69.

Panousis, C. G., and D. T. Rowe. (1997). Epstein-Barr virus latent membrane protein 2 associates with and is a substrate for mitogen-activated protein kinase. J Virol **71:**4752-60.

Panteva, M., H. Korkaya, and S. Jameel. (2003). Hepatitis viruses and the MAPK pathway: is this a survival strategy? Virus Res **92:**131-40.

Parker, G. A., T. Crook, M. Bain, E. A. Sara, P. J. Farrell, and M. J. Allday. (1996). Epstein-Barr virus nuclear antigen (EBNA)3C is an immortalizing oncoprotein with similar properties to adenovirus E1A and papillomavirus E7. Oncogene **13:**2541-9.

Patel, J. H., A. P. Loboda, M. K. Showe, L. C. Showe, and S. B. McMahon. (2004). Analysis of genomic targets reveals complex functions of MYC. Nat Rev Cancer **4:**562-8.

Pathmanathan, R., U. Prasad, G. Chandrika, R. Sadler, K. Flynn, and N. Raab-Traub. (1995). Undifferentiated, nonkeratinizing, and squamous cell carcinoma of the nasopharynx. Variants of Epstein-Barr virus-infected neoplasia. Am J Pathol **146:**1355-67.

Pawlotsky, J. M. (2004). Pathophysiology of hepatitis C virus infection and related liver disease. Trends Microbiol **12:**96-102.

Pegtel, D. M., J. Middeldorp, and D. A. Thorley-Lawson. (2004). Epstein-Barr virus infection in ex vivo tonsil epithelial cell cultures of asymptomatic carriers. J Virol **78:**12613-24.

Peloponese, J. M., Jr., and K. T. Jeang. (2006). Role for Akt/protein kinase B and activator protein-1 in cellular proliferation induced by the human T-cell leukemia virus type 1 tax oncoprotein. J Biol Chem **281:**8927-38.

Peng, R., S. C. Moses, J. Tan, E. Kremmer, and P. D. Ling. (2005). The Epstein-Barr virus EBNA-LP protein preferentially coactivates EBNA2-mediated stimulation of latent membrane proteins expressed from the viral divergent promoter. J Virol **79:**4492-505.

Petti, L., C. Sample, and E. Kieff. (1990). Subnuclear localization and phosphorylation of Epstein-Barr virus latent infection nuclear proteins. Virology **176:**563-74.

Pfeffer, S., M. Zavolan, F. A. Grasser, M. Chien, J. J. Russo, J. Ju, B. John, A. J. Enright, D. Marks, C. Sander, and T. Tuschl. (2004). Identification of virus-encoded microRNAs. Science **304:**734-6.

Poiesz, B. J., F. W. Ruscetti, A. F. Gazdar, P. A. Bunn, J. D. Minna, and R. C. Gallo. (1980). Detection and isolation of type C retrovirus particles from fresh and cultured lymphocytes of a patient with cutaneous T-cell lymphoma. Proc Natl Acad Sci U S A **77:**7415-9.

Polack, A., K. Hortnagel, A. Pajic, B. Christoph, B. Baier, M. Falk, J. Mautner, C. Geltinger, G. W. Bornkamm, and B. Kempkes. (1996). c-myc activation renders proliferation of Epstein-Barr virus (EBV)-transformed cells independent of EBV nuclear antigen 2 and latent membrane protein 1. Proc Natl Acad Sci U S A **93:**10411-6.

Pope, J. H., M. K. Horne, and W. Scott. (1968). Transformation of foetal human keukocytes in vitro by filtrates of a human leukaemic cell line containing herpes-like virus. Int J Cancer **3:**857-66.

Portal, D., A. Rosendorff, and E. Kieff. (2006). Epstein-Barr nuclear antigen leader protein coactivates transcription through interaction with histone deacetylase 4. Proc Natl Acad Sci U S A **103:**19278-83.

Poynard, T., M. F. Yuen, V. Ratziu, and C. L. Lai. (2003). Viral hepatitis C. Lancet **362:**2095-100.

Prendergast, G. C., and E. B. Ziff. (1991). Methylation-sensitive sequence-specific DNA binding by the c-Myc basic region. Science **251:**186-9.

Puglielli, M. T., N. Desai, and S. H. Speck. (1997). Regulation of EBNA gene transcription in lymphoblastoid cell lines: characterization of sequences downstream of BCR2 (Cp). J Virol **71:**120-8.

Pulverer, B. J., C. Fisher, K. Vousden, T. Littlewood, G. Evan, and J. R. Woodgett. (1994). Site-specific modulation of c-Myc cotransformation by residues phosphorylated in vivo. Oncogene **9:**59-70.

Raab-Traub, N. (2002). Epstein-Barr virus in the pathogenesis of NPC. Semin Cancer Biol **12:**431-41.

Raab-Traub, N., and K. Flynn. (1986). The structure of the termini of the Epstein-Barr virus as a marker of clonal cellular proliferation. Cell **47:**883-9.

Raab-Traub, N., K. Flynn, G. Pearson, A. Huang, P. Levine, A. Lanier, and J. Pagano. (1987). The differentiated form of nasopharyngeal carcinoma contains Epstein-Barr virus DNA. Int J Cancer **39:**25-9.

Raab-Traub, N., P. Rajadurai, K. Flynn, and A. P. Lanier. (1991). Epstein-Barr virus infection in carcinoma of the salivary gland. J Virol **65:**7032-6.

Rabson, M., L. Gradoville, L. Heston, and G. Miller. (1982). Non-immortalizing P3J-HR-1 Epstein-Barr virus: a deletion mutant of its transforming parent, Jijoye. J Virol **44:**834-44.

Radkov, S. A., M. Bain, P. J. Farrell, M. West, M. Rowe, and M. J. Allday. (1997). Epstein-Barr virus EBNA3C represses Cp, the major promoter for EBNA expression, but has no effect on the promoter of the cell gene CD21. J Virol **71:**8552-62.

Radkov, S. A., R. Touitou, A. Brehm, M. Rowe, M. West, T. Kouzarides, and M. J. Allday. (1999). Epstein-Barr virus nuclear antigen 3C interacts with histone deacetylase to repress transcription. J Virol **73:**5688-97.

Ramsay, G., L. Stanton, M. Schwab, and J. M. Bishop. (1986). Human proto-oncogene N-myc encodes nuclear proteins that bind DNA. Mol Cell Biol **6:**4450-7.

Read, M. A., M. Z. Whitley, S. Gupta, J. W. Pierce, J. Best, R. J. Davis, and T. Collins. (1997). Tumor necrosis factor alpha-induced E-selectin expression is activated by the nuclear factor-kappaB and c-JUN N-terminal kinase/p38 mitogen-activated protein kinase pathways. J Biol Chem **272:**2753-61.

Reichart, P. A., A. Langford, H. R. Gelderblom, H. D. Pohle, J. Becker, and H. Wolf. (1989). Oral hairy leukoplakia: observations in 95 cases and review of the literature. J Oral Pathol Med **18:**410-5.

Reisman, D., and B. Sugden. (1986). trans activation of an Epstein-Barr viral transcriptional enhancer by the Epstein-Barr viral nuclear antigen 1. Mol Cell Biol **6:**3838-46.

Reisman, D., J. Yates, and B. Sugden. (1985). A putative origin of replication of plasmids derived from Epstein-Barr virus is composed of two cis-acting components. Mol Cell Biol **5:**1822-32.

Rickinson, A. B., L. S. Young, and M. Rowe. (1987). Influence of the Epstein-Barr virus nuclear antigen EBNA 2 on the growth phenotype of virus-transformed B cells. J Virol **61:**1310-7.

Ricote, M., I. Garcia-Tunon, F. Bethencourt, B. Fraile, P. Onsurbe, R. Paniagua, and M. Royuela. (2006). The p38 transduction pathway in prostatic neoplasia. J Pathol **208:**401-7.

Roberts, M. L., and N. R. Cooper. (1998). Activation of a ras-MAPK-dependent pathway by Epstein-Barr virus latent membrane protein 1 is essential for cellular transformation. Virology **240:**93-9.

Robertson, E. S., J. Lin, and E. Kieff. (1996). The amino-terminal domains of Epstein-Barr virus nuclear proteins 3A, 3B, and 3C interact with RBPJ(kappa). J Virol **70:**3068-74.

Roizman, B., and P. Pellett. 2001. *Herpesviridae*, p. 2381-2397. *In* B. N. Fields, D. M. Knipe, P. M. Howley, and D. E. Griffin (ed.), Fields Virology, 4th ed. Lippincott Williams & Wilkins, Philadelphia ; London.

Rooney, C., J. G. Howe, S. H. Speck, and G. Miller. (1989). Influence of Burkitt's lymphoma and primary B cells on latent gene expression by the nonimmortalizing P3J-HR-1 strain of Epstein-Barr virus. J Virol **63:**1531-9.

Rosa, M. D., E. Gottlieb, M. R. Lerner, and J. A. Steitz. (1981). Striking similarities are exhibited by two small Epstein-Barr virus-encoded ribonucleic acids and the adenovirus-associated ribonucleic acids VAI and VAII. Mol Cell Biol **1:**785-96.

Roussel, M. F., J. L. Cleveland, S. A. Shurtleff, and C. J. Sherr. (1991). Myc rescue of a mutant CSF-1 receptor impaired in mitogenic signalling. Nature **353:**361-3.

Rovedo, M., and R. Longnecker. (2008). Epstein-Barr virus latent membrane protein 2A preferentially signals through the Src family kinase Lyn. J Virol **82:**8520-8.

Rovedo, M., and R. Longnecker. (2007). Epstein-barr virus latent membrane protein 2B (LMP2B) modulates LMP2A activity. J Virol **81:**84-94.

Rowe, D. T. (1999). Epstein-Barr virus immortalization and latency. Front Biosci **4:**D346-71.

Rowe, M., A. L. Lear, D. Croom-Carter, A. H. Davies, and A. B. Rickinson. (1992). Three pathways of Epstein-Barr virus gene activation from EBNA1-positive latency in B lymphocytes. J Virol **66:**122-31.

Rowe, M., D. T. Rowe, C. D. Gregory, L. S. Young, P. J. Farrell, H. Rupani, and A. B. Rickinson. (1987). Differences in B cell growth phenotype reflect novel patterns of Epstein-Barr virus latent gene expression in Burkitt's lymphoma cells. Embo J **6:**2743-51.

Ruf, I. K., K. A. Lackey, S. Warudkar, and J. T. Sample. (2005). Protection from interferon-induced apoptosis by Epstein-Barr virus small RNAs is not mediated by inhibition of PKR. J Virol **79:**14562-9.

Ruf, I. K., P. W. Rhyne, C. Yang, J. L. Cleveland, and J. T. Sample. (2000). Epstein-Barr virus small RNAs potentiate tumorigenicity of Burkitt lymphoma cells independently of

an effect on apoptosis. J Virol **74:**10223-8.

Ruf, I. K., P. W. Rhyne, H. Yang, C. M. Borza, L. M. Hutt-Fletcher, J. L. Cleveland, and J. T. Sample. (1999). Epstein-barr virus regulates c-MYC, apoptosis, and tumorigenicity in Burkitt lymphoma. Mol Cell Biol **19:**1651-60.

Ryan, J. L., D. R. Morgan, R. L. Dominguez, L. B. Thorne, S. H. Elmore, M. Mino-Kenudson, G. Y. Lauwers, J. K. Booker, and M. L. Gulley. (2009). High levels of Epstein-Barr virus DNA in latently infected gastric adenocarcinoma. Lab Invest **89:**80-90.

Rymo, L., G. Klein, and A. Ricksten. (1985). Expression of a second Epstein-Barr virus-determined nuclear antigen in mouse cells after gene transfer with a cloned fragment of the viral genome. Proc Natl Acad Sci U S A **82:**3435-9.

Saito, I., T. Miyamura, A. Ohbayashi, H. Harada, T. Katayama, S. Kikuchi, Y. Watanabe, S. Koi, M. Onji, Y. Ohta, and et al. (1990). Hepatitis C virus infection is associated with the development of hepatocellular carcinoma. Proc Natl Acad Sci U S A **87:**6547-9.

Sakai, T., Y. Taniguchi, K. Tamura, S. Minoguchi, T. Fukuhara, L. J. Strobl, U. Zimber-Strobl, G. W. Bornkamm, and T. Honjo. (1998). Functional replacement of the intracellular region of the Notch1 receptor by Epstein-Barr virus nuclear antigen 2. J Virol **72:**6034-9.

Samanta, M., D. Iwakiri, T. Kanda, T. Imaizumi, and K. Takada. (2006). EB virus-encoded RNAs are recognized by RIG-I and activate signaling to induce type I IFN. Embo J **25:**4207-14.

Samanta, M., D. Iwakiri, and K. Takada. (2008). Epstein-Barr virus-encoded small RNA induces IL-10 through RIG-I-mediated IRF-3 signaling. Oncogene **27:**4150-60.

Sample, J., L. Brooks, C. Sample, L. Young, M. Rowe, C. Gregory, A. Rickinson, and E. Kieff. (1991). Restricted Epstein-Barr virus protein expression in Burkitt lymphoma is due to a different Epstein-Barr nuclear antigen 1 transcriptional initiation site. Proc Natl Acad Sci U S A **88:**6343-7.

Sample, J., E. B. Henson, and C. Sample. (1992). The Epstein-Barr virus nuclear protein 1 promoter active in type I latency is autoregulated. J Virol **66:**4654-61.

Sample, J., L. Young, B. Martin, T. Chatman, E. Kieff, A. Rickinson, and E. Kieff. (1990). Epstein-Barr virus types 1 and 2 differ in their EBNA-3A, EBNA-3B, and EBNA-3C genes. J Virol **64:**4084-92.

Sandvej, K., J. W. Gratama, M. Munch, X. G. Zhou, R. L. Bolhuis, B. S. Andresen, N. Gregersen, and S. Hamilton-Dutoit. (1997). Sequence analysis of the Epstein-Barr

virus (EBV) latent membrane protein-1 gene and promoter region: identification of four variants among wild-type EBV isolates. Blood **90:**323-30.

Sandvej, K., L. Krenacs, S. J. Hamilton-Dutoit, J. L. Rindum, J. J. Pindborg, and G. Pallesen. (1992). Epstein-Barr virus latent and replicative gene expression in oral hairy leukoplakia. Histopathology **20:**387-95.

Saridakis, V., Y. Sheng, F. Sarkari, M. N. Holowaty, K. Shire, T. Nguyen, R. G. Zhang, J. Liao, W. Lee, A. M. Edwards, C. H. Arrowsmith, and L. Frappier. (2005). Structure of the p53 binding domain of HAUSP/USP7 bound to Epstein-Barr nuclear antigen 1 implications for EBV-mediated immortalization. Mol Cell **18:**25-36.

Schaefer, B. C., J. L. Strominger, and S. H. Speck. (1995). The Epstein-Barr virus BamHI F promoter is an early lytic promoter: lack of correlation with EBNA 1 gene transcription in group 1 Burkitt's lymphoma cell lines. J Virol **69:**5039-47.

Schaefer, B. C., J. L. Strominger, and S. H. Speck. (1997). Host-cell-determined methylation of specific Epstein-Barr virus promoters regulates the choice between distinct viral latency programs. Mol Cell Biol **17:**364-77.

Schaefer, B. C., J. L. Strominger, and S. H. Speck. (1996). A simple reverse transcriptase PCR assay to distinguish EBNA1 gene transcripts associated with type I and II latency from those arising during induction of the viral lytic cycle. J Virol **70:**8204-8.

Schaefer, B. C., M. Woisetschlaeger, J. L. Strominger, and S. H. Speck. (1991). Exclusive expression of Epstein-Barr virus nuclear antigen 1 in Burkitt lymphoma arises from a third promoter, distinct from the promoters used in latently infected lymphocytes. Proc Natl Acad Sci U S A **88:**6550-4.

Schepers, A., M. Ritzi, K. Bousset, E. Kremmer, J. L. Yates, J. Harwood, J. F. Diffley, and W. Hammerschmidt. (2001). Human origin recognition complex binds to the region of the latent origin of DNA replication of Epstein-Barr virus. Embo J **20:**4588-602.

Schneider, B. G., M. L. Gulley, P. Eagan, J. C. Bravo, R. Mera, and J. Geradts. (2000). Loss of p16/CDKN2A tumor suppressor protein in gastric adenocarcinoma is associated with Epstein-Barr virus and anatomic location in the body of the stomach. Hum Pathol **31:**45-50.

Scholle, F., K. M. Bendt, and N. Raab-Traub. (2000). Epstein-Barr virus LMP2A transforms epithelial cells, inhibits cell differentiation, and activates Akt. J Virol **74:**10681-9.

Scholle, F., R. Longnecker, and N. Raab-Traub. (1999). Epithelial cell adhesion to extracellular matrix proteins induces tyrosine phosphorylation of the Epstein-Barr virus latent membrane protein 2: a role for C-terminal Src kinase. J Virol **73:**4767-75.

Schramm, L., and N. Hernandez. (2002). Recruitment of RNA polymerase III to its target promoters. Genes Dev **16:**2593-620.

Schwartz, L. B., V. E. Sklar, J. A. Jaehning, R. Weinmann, and R. G. Roeder. (1974). Isolation and partial characterization of the multiple forms of deoxyribonucleic acid-dependent ribonucleic acid polymerase in the mouse myeloma, MOPC 315. J Biol Chem **249:**5889-97.

Schweiger, M. R., J. You, and P. M. Howley. (2006). Bromodomain protein 4 mediates the papillomavirus E2 transcriptional activation function. J Virol **80:**4276-85.

Schwemmle, M., M. J. Clemens, K. Hilse, K. Pfeifer, H. Troster, W. E. Muller, and M. Bachmann. (1992). Localization of Epstein-Barr virus-encoded RNAs EBER-1 and EBER-2 in interphase and mitotic Burkitt lymphoma cells. Proc Natl Acad Sci U S A **89:**10292-6.

Scoggin, K. E., A. Ulloa, and J. K. Nyborg. (2001). The oncoprotein Tax binds the SRC-1-interacting domain of CBP/p300 to mediate transcriptional activation. Mol Cell Biol **21:**5520-30.

Scott, P. H., C. A. Cairns, J. E. Sutcliffe, H. M. Alzuherri, A. McLees, A. G. Winter, and R. J. White. (2001). Regulation of RNA polymerase III transcription during cell cycle entry. J Biol Chem **276:**1005-14.

Sears, J., M. Ujihara, S. Wong, C. Ott, J. Middeldorp, and A. Aiyar. (2004). The amino terminus of Epstein-Barr Virus (EBV) nuclear antigen 1 contains AT hooks that facilitate the replication and partitioning of latent EBV genomes by tethering them to cellular chromosomes. J Virol **78:**11487-505.

Sears, R., F. Nuckolls, E. Haura, Y. Taya, K. Tamai, and J. R. Nevins. (2000). Multiple Ras-dependent phosphorylation pathways regulate Myc protein stability. Genes Dev **14:**2501-14.

Shanmugaratnam, K. (1978). Histological typing of nasopharyngeal carcinoma. IARC Sci Publ**:**3-12.

Shannon-Lowe, C., E. Adland, A. I. Bell, H. J. Delecluse, A. B. Rickinson, and M. Rowe. (2009). Features distinguishing Epstein Barr virus infections of epithelial cells and B cells: Viral genome expression, genome maintenance, and genome amplification. J Virol.

Shannon-Lowe, C., G. Baldwin, R. Feederle, A. Bell, A. Rickinson, and H. J. Delecluse. (2005). Epstein-Barr virus-induced B-cell transformation: quantitating events from virus binding to cell outgrowth. J Gen Virol **86:**3009-19.

Sharipo, A., M. Imreh, A. Leonchiks, S. Imreh, and M. G. Masucci. (1998). A minimal

glycine-alanine repeat prevents the interaction of ubiquitinated I kappaB alpha with the proteasome: a new mechanism for selective inhibition of proteolysis. Nat Med **4:**939-44.

Sharma-Walia, N., H. H. Krishnan, P. P. Naranatt, L. Zeng, M. S. Smith, and B. Chandran. (2005). ERK1/2 and MEK1/2 induced by Kaposi's sarcoma-associated herpesvirus (human herpesvirus 8) early during infection of target cells are essential for expression of viral genes and for establishment of infection. J Virol **79:**10308-29.

Shaulian, E., and M. Karin. (2002). AP-1 as a regulator of cell life and death. Nat Cell Biol **4:**E131-6.

Sheu, L. F., A. Chen, C. L. Meng, K. C. Ho, W. H. Lee, F. J. Leu, and C. F. Chao. (1996). Enhanced malignant progression of nasopharyngeal carcinoma cells mediated by the expression of Epstein-Barr nuclear antigen 1 in vivo. J Pathol **180:**243-8.

Shibata, D., and L. M. Weiss. (1992). Epstein-Barr virus-associated gastric adenocarcinoma. Am J Pathol **140:**769-74.

Shimizu, N., A. Tanabe-Tochikura, Y. Kuroiwa, and K. Takada. (1994). Isolation of Epstein-Barr virus (EBV)-negative cell clones from the EBV-positive Burkitt's lymphoma (BL) line Akata: malignant phenotypes of BL cells are dependent on EBV. J Virol **68:**6069-73.

Shimizu, N., H. Yoshiyama, and K. Takada. (1996). Clonal propagation of Epstein-Barr virus (EBV) recombinants in EBV-negative Akata cells. J Virol **70:**7260-3.

Shire, K., D. F. Ceccarelli, T. M. Avolio-Hunter, and L. Frappier. (1999). EBP2, a human protein that interacts with sequences of the Epstein-Barr virus nuclear antigen 1 important for plasmid maintenance. J Virol **73:**2587-95.

Shire, K., P. Kapoor, K. Jiang, M. N. Hing, N. Sivachandran, T. Nguyen, and L. Frappier. (2006). Regulation of the EBNA1 Epstein-Barr virus protein by serine phosphorylation and arginine methylation. J Virol **80:**5261-72.

Shu, C. H., Y. S. Chang, C. L. Liang, S. T. Liu, C. Z. Lin, and P. Chang. (1992). Distribution of type A and type B EBV in normal individuals and patients with head and neck carcinomas in Taiwan. J Virol Methods **38:**123-30.

Silins, S. L., and T. B. Sculley. (1994). Modulation of vimentin, the CD40 activation antigen and Burkitt's lymphoma antigen (CD77) by the Epstein-Barr virus nuclear antigen EBNA-4. Virology **202:**16-24.

Simpson, K., A. McGuigan, and C. Huxley. (1996). Stable episomal maintenance of yeast artificial chromosomes in human cells. Mol Cell Biol **16:**5117-26.

Sinclair, A. J., I. Palmero, G. Peters, and P. J. Farrell. (1994). EBNA-2 and EBNA-LP cooperate to cause G0 to G1 transition during immortalization of resting human B lymphocytes by Epstein-Barr virus. Embo J **13:**3321-8.

Singh, G., S. Aras, A. H. Zea, S. Koochekpour, and A. Aiyar. (2009). Optimal transactivation by Epstein-Barr nuclear antigen 1 requires the UR1 and ATH1 domains. J Virol **83:**4227-35.

Sivachandran, N., F. Sarkari, and L. Frappier. (2008). Epstein-Barr nuclear antigen 1 contributes to nasopharyngeal carcinoma through disruption of PML nuclear bodies. PLoS Pathog **4:**e1000170.

Sixbey, J. W., J. G. Nedrud, N. Raab-Traub, R. A. Hanes, and J. S. Pagano. (1984). Epstein-Barr virus replication in oropharyngeal epithelial cells. N Engl J Med **310:**1225-30.

Slots, J., I. Saygun, M. Sabeti, and A. Kubar. (2006). Epstein-Barr virus in oral diseases. J Periodontal Res **41:**235-44.

Smirnova, I. S., N. D. Aksenov, E. V. Kashuba, P. Payakurel, V. V. Grabovetsky, A. D. Zaberezhny, M. S. Vonsky, L. Buchinska, P. Biberfeld, J. Hinkula, and M. G. Isaguliants. (2006). Hepatitis C virus core protein transforms murine fibroblasts by promoting genomic instability. Cell Oncol **28:**177-90.

Smith, P. R., O. de Jesus, D. Turner, M. Hollyoake, C. E. Karstegl, B. E. Griffin, L. Karran, Y. Wang, S. D. Hayward, and P. J. Farrell. (2000). Structure and coding content of CST (BART) family RNAs of Epstein-Barr virus. J Virol **74:**3082-92.

Snudden, D. K., P. R. Smith, D. Lai, M. H. Ng, and B. E. Griffin. (1995). Alterations in the structure of the EBV nuclear antigen, EBNA1, in epithelial cell tumours. Oncogene **10:**1545-52.

Solomon, M. J., P. L. Larsen, and A. Varshavsky. (1988). Mapping protein-DNA interactions in vivo with formaldehyde: evidence that histone H4 is retained on a highly transcribed gene. Cell **53:**937-47.

Song, H., S. H. Ki, S. G. Kim, and A. Moon. (2006). Activating transcription factor 2 mediates matrix metalloproteinase-2 transcriptional activation induced by p38 in breast epithelial cells. Cancer Res **66:**10487-96.

Spano, J. P., P. Busson, D. Atlan, J. Bourhis, J. P. Pignon, C. Esteban, and J. P. Armand. (2003). Nasopharyngeal carcinomas: an update. Eur J Cancer **39:**2121-35.

Spotts, G. D., S. V. Patel, Q. Xiao, and S. R. Hann. (1997). Identification of downstream-initiated c-Myc proteins which are dominant-negative inhibitors of transactivation by full-length c-Myc proteins. Mol Cell Biol **17:**1459-68.

Srinivas, S. K., and J. W. Sixbey. (1995). Epstein-Barr virus induction of recombinase-activating genes RAG1 and RAG2. J Virol **69:**8155-8.

Staudt, L. M. (2000). The molecular and cellular origins of Hodgkin's disease. J Exp Med **191:**207-12.

Steiger, D., M. Furrer, D. Schwinkendorf, and P. Gallant. (2008). Max-independent functions of Myc in Drosophila melanogaster. Nat Genet **40:**1084-91.

Stein, T., D. Crighton, J. M. Boyle, J. M. Varley, and R. J. White. (2002). RNA polymerase III transcription can be derepressed by oncogenes or mutations that compromise p53 function in tumours and Li-Fraumeni syndrome. Oncogene **21:**2961-70.

Sternas, L., T. Middleton, and B. Sugden. (1990). The average number of molecules of Epstein-Barr nuclear antigen 1 per cell does not correlate with the average number of Epstein-Barr virus (EBV) DNA molecules per cell among different clones of EBV-immortalized cells. J Virol **64:**2407-10.

Stewart, S., C. W. Dawson, K. Takada, J. Curnow, C. A. Moody, J. W. Sixbey, and L. S. Young. (2004). Epstein-Barr virus-encoded LMP2A regulates viral and cellular gene expression by modulation of the NF-kappaB transcription factor pathway. Proc Natl Acad Sci U S A **101:**15730-5.

Stone, J., T. de Lange, G. Ramsay, E. Jakobovits, J. M. Bishop, H. Varmus, and W. Lee. (1987). Definition of regions in human c-myc that are involved in transformation and nuclear localization. Mol Cell Biol **7:**1697-709.

Strobl, L. J., H. Hofelmayr, G. Marschall, M. Brielmeier, G. W. Bornkamm, and U. Zimber-Strobl. (2000). Activated Notch1 modulates gene expression in B cells similarly to Epstein-Barr viral nuclear antigen 2. J Virol **74:**1727-35.

Suankratay, C., S. Shuangshoti, A. Mutirangura, V. Prasanthai, S. Lerdlum, S. Shuangshoti, J. Pintong, and H. Wilde. (2005). Epstein-Barr virus infection-associated smooth-muscle tumors in patients with AIDS. Clin Infect Dis **40:**1521-8.

Sugawara, Y., Y. Mizugaki, T. Uchida, T. Torii, S. Imai, M. Makuuchi, and K. Takada. (1999). Detection of Epstein-Barr virus (EBV) in hepatocellular carcinoma tissue: a novel EBV latency characterized by the absence of EBV-encoded small RNA expression. Virology **256:**196-202.

Sugden, B., and N. Warren. (1989). A promoter of Epstein-Barr virus that can function during latent infection can be transactivated by EBNA-1, a viral protein required for viral DNA replication during latent infection. J Virol **63:**2644-9.

Sugiura, M., S. Imai, M. Tokunaga, S. Koizumi, M. Uchizawa, K. Okamoto, and T. Osato. (1996). Transcriptional analysis of Epstein-Barr virus gene expression in EBV-positive gastric carcinoma: unique viral latency in the tumour cells. Br J Cancer **74:**625-31.

Summers, H., J. A. Barwell, R. A. Pfuetzner, A. M. Edwards, and L. Frappier. (1996). Cooperative assembly of EBNA1 on the Epstein-Barr virus latent origin of replication. J Virol **70:**1228-31.

Sun, S. C., and D. W. Ballard. (1999). Persistent activation of NF-kappaB by the tax transforming protein of HTLV-1: hijacking cellular IkappaB kinases. Oncogene **18:**6948-58.

Sung, N. S., S. Kenney, D. Gutsch, and J. S. Pagano. (1991). EBNA-2 transactivates a lymphoid-specific enhancer in the BamHI C promoter of Epstein-Barr virus. J Virol **65:**2164-9.

Sung, N. S., J. Wilson, M. Davenport, N. D. Sista, and J. S. Pagano. (1994). Reciprocal regulation of the Epstein-Barr virus BamHI-F promoter by EBNA-1 and an E2F transcription factor. Mol Cell Biol **14:**7144-52.

Sung, W. K., Y. Lu, C. W. Lee, D. Zhang, M. Ronaghi, and C. G. Lee. (2009). Deregulated direct targets of the hepatitis B viral (HBV) protein, HBx, identified through chromatin immunoprecipitation and expression microarray profiling. J Biol Chem.

Sutcliffe, J. E., T. R. Brown, S. J. Allison, P. H. Scott, and R. J. White. (2000). Retinoblastoma protein disrupts interactions required for RNA polymerase III transcription. Mol Cell Biol **20:**9192-202.

Sutcliffe, J. E., C. A. Cairns, A. McLees, S. J. Allison, K. Tosh, and R. J. White. (1999). RNA polymerase III transcription factor IIIB is a target for repression by pocket proteins p107 and p130. Mol Cell Biol **19:**4255-61.

Swaminathan, S. (2008). Noncoding RNAs produced by oncogenic human herpesviruses. J Cell Physiol **216:**321-6.

Swaminathan, S., B. Tomkinson, and E. Kieff. (1991). Recombinant Epstein-Barr virus with small RNA (EBER) genes deleted transforms lymphocytes and replicates in vitro. Proc Natl Acad Sci U S A **88:**1546-50.

Szekely, L., G. Selivanova, K. P. Magnusson, G. Klein, and K. G. Wiman. (1993). EBNA-5, an Epstein-Barr virus-encoded nuclear antigen, binds to the retinoblastoma and p53 proteins. Proc Natl Acad Sci U S A **90:**5455-9.

Takada, K., and A. Nanbo. (2001). The role of EBERs in oncogenesis. Semin Cancer Biol **11:**461-7.

Tanner, J., J. Weis, D. Fearon, Y. Whang, and E. Kieff. (1987). Epstein-Barr virus gp350/220 binding to the B lymphocyte C3d receptor mediates adsorption, capping, and endocytosis. Cell **50:**203-13.

Tanner, J. E., C. Alfieri, T. A. Chatila, and F. Diaz-Mitoma. (1996). Induction of interleukin-6 after stimulation of human B-cell CD21 by Epstein-Barr virus glycoproteins gp350 and gp220. J Virol **70:**570-5.

Tao, Q., K. D. Robertson, A. Manns, A. Hildesheim, and R. F. Ambinder. (1998). Epstein-Barr virus (EBV) in endemic Burkitt's lymphoma: molecular analysis of primary tumor tissue. Blood **91:**1373-81.

Taub, R., I. Kirsch, C. Morton, G. Lenoir, D. Swan, S. Tronick, S. Aaronson, and P. Leder. (1982). Translocation of the c-myc gene into the immunoglobulin heavy chain locus in human Burkitt lymphoma and murine plasmacytoma cells. Proc Natl Acad Sci U S A **79:**7837-41.

Teramoto, N., L. Szekely, and G. Klein. (1998). Differential expression and localization of EBER-1 and EBER-2 in Epstein-Barr virus-carrying cells. J Hum Virol **1:**307-13.

Thebault, S., J. Basbous, P. Hivin, C. Devaux, and J. M. Mesnard. (2004). HBZ interacts with JunD and stimulates its transcriptional activity. FEBS Lett **562:**165-70.

Thompson, M. P., and R. Kurzrock. (2004). Epstein-Barr virus and cancer. Clin Cancer Res **10:**803-21.

Thorley-Lawson, D. A. (2005). EBV the prototypical human tumor virus--just how bad is it? J Allergy Clin Immunol **116:**251-61; quiz 262.

Thorley-Lawson, D. A. (2001). Epstein-Barr virus: exploiting the immune system. Nat Rev Immunol **1:**75-82.

Thorley-Lawson, D. A., and A. Gross. (2004). Persistence of the Epstein-Barr virus and the origins of associated lymphomas. N Engl J Med **350:**1328-37.

Timms, J. M., A. Bell, J. R. Flavell, P. G. Murray, A. B. Rickinson, A. Traverse-Glehen, F. Berger, and H. J. Delecluse. (2003). Target cells of Epstein-Barr-virus (EBV)-positive post-transplant lymphoproliferative disease: similarities to EBV-positive Hodgkin's lymphoma. Lancet **361:**217-23.

Tindberg, N., M. Porsmyr-Palmertz, and A. Simi. (2000). Contribution of MAP kinase pathways to the activation of ATF-2 in human neuroblastoma cells. Neurochem Res **25:**527-31.

Toczyski, D. P., A. G. Matera, D. C. Ward, and J. A. Steitz. (1994). The Epstein-Barr virus (EBV) small RNA EBER1 binds and relocalizes ribosomal protein L22 in EBV-infected human B lymphocytes. Proc Natl Acad Sci U S A **91:**3463-7.

Toczyski, D. P., and J. A. Steitz. (1991). EAP, a highly conserved cellular protein associated with Epstein-Barr virus small RNAs (EBERs). Embo J **10:**459-66.

Tokunaga, M., C. E. Land, Y. Uemura, T. Tokudome, S. Tanaka, and E. Sato. (1993). Epstein-Barr virus in gastric carcinoma. Am J Pathol **143:**1250-4.

Tomkinson, B., and E. Kieff. (1992). Second-site homologous recombination in Epstein-Barr virus: insertion of type 1 EBNA 3 genes in place of type 2 has no effect on in vitro infection. J Virol **66:**780-9.

Tomkinson, B., E. Robertson, and E. Kieff. (1993). Epstein-Barr virus nuclear proteins EBNA-3A and EBNA-3C are essential for B-lymphocyte growth transformation. J Virol **67:**2014-25.

Trivedi, P., L. F. Hu, F. Chen, B. Christensson, M. G. Masucci, G. Klein, and G. Winberg. (1994). Epstein-Barr virus (EBV)-encoded membrane protein LMP1 from a nasopharyngeal carcinoma is non-immunogenic in a murine model system, in contrast to a B cell-derived homologue. Eur J Cancer **30A:**84-8.

Tsai, C. N., S. T. Liu, and Y. S. Chang. (1995). Identification of a novel promoter located within the Bam HI Q region of the Epstein-Barr virus genome for the EBNA 1 gene. DNA Cell Biol **14:**767-76.

Tsao, S. W., G. Tramoutanis, C. W. Dawson, A. K. Lo, and D. P. Huang. (2002). The significance of LMP1 expression in nasopharyngeal carcinoma. Semin Cancer Biol **12:**473-87.

Tyler, K. L., P. Clarke, R. L. DeBiasi, D. Kominsky, and G. J. Poggioli. (2001). Reoviruses and the host cell. Trends Microbiol **9:**560-4.

Uccini, S., F. Monardo, A. Stoppacciaro, A. Gradilone, A. M. Agliano, A. Faggioni, V. Manzari, L. Vago, G. Costanzi, L. P. Ruco, and et al. (1990). High frequency of Epstein-Barr virus genome detection in Hodgkin's disease of HIV-positive patients. Int J Cancer **46:**581-5.

Uchida, J., T. Yasui, Y. Takaoka-Shichijo, M. Muraoka, W. Kulwichit, N. Raab-Traub, and H. Kikutani. (1999). Mimicry of CD40 signals by Epstein-Barr virus LMP1 in B lymphocyte responses. Science **286:**300-3.

Ullu, E., and A. M. Weiner. (1985). Upstream sequences modulate the internal promoter of the human 7SL RNA gene. Nature **318:**371-4.

Uozaki, H., and M. Fukayama. (2008). Epstein-Barr Virus and Gastric Carcinoma - Viral Carcinogenesis through Epigenetic Mechanisms. Int J Clin Exp Pathol **1:**198-216.

Urisman, A., R. J. Molinaro, N. Fischer, S. J. Plummer, G. Casey, E. A. Klein, K. Malathi, C. Magi-Galluzzi, R. R. Tubbs, D. Ganem, R. H. Silverman, and J. L. DeRisi. (2006). Identification of a novel Gammaretrovirus in prostate tumors of patients homozygous for R462Q RNASEL variant. PLoS Pathog **2:**e25.

Van Scoy, S., I. Watakabe, A. R. Krainer, and J. Hearing. (2000). Human p32: a coactivator for Epstein-Barr virus nuclear antigen-1-mediated transcriptional activation and possible role in viral latent cycle DNA replication. Virology **275:**145-57.

Vasef, M. A., A. Ferlito, and L. M. Weiss. (1997). Nasopharyngeal carcinoma, with emphasis on its relationship to Epstein-Barr virus. Ann Otol Rhinol Laryngol **106:**348-56.

Vervoorts, J., J. Luscher-Firzlaff, and B. Luscher. (2006). The ins and outs of MYC regulation by posttranslational mechanisms. J Biol Chem **281:**34725-9.

Vlahopoulos, S. A., S. Logotheti, D. Mikas, A. Giarika, V. Gorgoulis, and V. Zoumpourlis. (2008). The role of ATF-2 in oncogenesis. Bioessays **30:**314-27.

Vo, Q. N., J. Geradts, M. L. Gulley, D. A. Boudreau, J. C. Bravo, and B. G. Schneider. (2002). Epstein-Barr virus in gastric adenocarcinomas: association with ethnicity and CDKN2A promoter methylation. J Clin Pathol **55:**669-75.

Wahlstrom, T., and M. Henriksson. (2007). Mnt takes control as key regulator of the myc/max/mxd network. Adv Cancer Res **97:**61-80.

Walling, D. M., C. M. Flaitz, and C. M. Nichols. (2003). Epstein-Barr virus replication in oral hairy leukoplakia: response, persistence, and resistance to treatment with valacyclovir. J Infect Dis **188:**883-90.

Walling, D. M., P. D. Ling, A. V. Gordadze, M. Montes-Walters, C. M. Flaitz, and C. M. Nichols. (2004). Expression of Epstein-Barr virus latent genes in oral epithelium: determinants of the pathogenesis of oral hairy leukoplakia. J Infect Dis **190:**396-9.

Walling, D. M., and N. Raab-Traub. (1994). Epstein-Barr virus intrastrain recombination in oral hairy leukoplakia. J Virol **68:**7909-17.

Wang, D., D. Liebowitz, and E. Kieff. (1985). An EBV membrane protein expressed in immortalized lymphocytes transforms established rodent cells. Cell **43:**831-40.

Wang, F., C. Gregory, C. Sample, M. Rowe, D. Liebowitz, R. Murray, A. Rickinson, and E. Kieff. (1990). Epstein-Barr virus latent membrane protein (LMP1) and nuclear proteins 2

and 3C are effectors of phenotypic changes in B lymphocytes: EBNA-2 and LMP1 cooperatively induce CD23. J Virol **64:**2309-18.

Wang, G. L., K. W. Lo, K. S. Tsang, N. Y. Chung, Y. S. Tsang, S. T. Cheung, J. C. Lee, and D. P. Huang. (1999). Inhibiting tumorigenic potential by restoration of p16 in nasopharyngeal carcinoma. Br J Cancer **81:**1122-6.

Wang, H. D., A. Trivedi, and D. L. Johnson. (1997). Hepatitis B virus X protein induces RNA polymerase III-dependent gene transcription and increases cellular TATA-binding protein by activating the Ras signaling pathway. Mol Cell Biol **17:**6838-46.

Wang, H. D., C. H. Yuh, C. V. Dang, and D. L. Johnson. (1995). The hepatitis B virus X protein increases the cellular level of TATA-binding protein, which mediates transactivation of RNA polymerase III genes. Mol Cell Biol **15:**6720-8.

Wang, L., D. P. Dittmer, C. C. Tomlinson, F. D. Fakhari, and B. Damania. (2006). Immortalization of primary endothelial cells by the K1 protein of Kaposi's sarcoma-associated herpesvirus. Cancer Res **66:**3658-66.

Wang, Q., H. Salman, M. Danilenko, and G. P. Studzinski. (2005). Cooperation between antioxidants and 1,25-dihydroxyvitamin D3 in induction of leukemia HL60 cell differentiation through the JNK/AP-1/Egr-1 pathway. J Cell Physiol **204:**964-74.

Wang, S., J. Skorczewski, X. Feng, L. Mei, and J. E. Murphy-Ullrich. (2004). Glucose up-regulates thrombospondin 1 gene transcription and transforming growth factor-beta activity through antagonism of cGMP-dependent protein kinase repression via upstream stimulatory factor 2. J Biol Chem **279:**34311-22.

Wang, Y., J. E. Finan, J. M. Middeldorp, and S. D. Hayward. (1997). P32/TAP, a cellular protein that interacts with EBNA-1 of Epstein-Barr virus. Virology **236:**18-29.

Wang, Y., S. A. Xue, G. Hallden, J. Francis, M. Yuan, B. E. Griffin, and N. R. Lemoine. (2005). Virus-associated RNA I-deleted adenovirus, a potential oncolytic agent targeting EBV-associated tumors. Cancer Res **65:**1523-31.

Wang, Y. W., H. S. Chang, C. H. Lin, and W. C. Yu. (2007). HPV-18 E7 conjugates to c-Myc and mediates its transcriptional activity. Int J Biochem Cell Biol **39:**402-12.

Wanzel, M., S. Herold, and M. Eilers. (2003). Transcriptional repression by Myc. Trends Cell Biol **13:**146-50.

Weber, M., J. J. Davies, D. Wittig, E. J. Oakeley, M. Haase, W. L. Lam, and D. Schubeler. (2005). Chromosome-wide and promoter-specific analyses identify sites of differential DNA methylation in normal and transformed human cells. Nat Genet **37:**853-62.

Webster-Cyriaque, J., J. Middeldorp, and N. Raab-Traub. (2000). Hairy leukoplakia: an unusual combination of transforming and permissive Epstein-Barr virus infections. J Virol **74:**7610-8.

Webster-Cyriaque, J., and N. Raab-Traub. (1998). Transcription of Epstein-Barr virus latent cycle genes in oral hairy leukoplakia. Virology **248:**53-65.

Weinberg, R. A. (1995). The retinoblastoma protein and cell cycle control. Cell **81:**323-30.

Weinreb, M., P. J. Day, F. Niggli, E. K. Green, A. O. Nyong'o, N. A. Othieno-Abinya, M. S. Riyat, F. Raafat, and J. R. Mann. (1996). The consistent association between Epstein-Barr virus and Hodgkin's disease in children in Kenya. Blood **87:**3828-36.

Weng, A. P., J. M. Millholland, Y. Yashiro-Ohtani, M. L. Arcangeli, A. Lau, C. Wai, C. Del Bianco, C. G. Rodriguez, H. Sai, J. Tobias, Y. Li, M. S. Wolfe, C. Shachaf, D. Felsher, S. C. Blacklow, W. S. Pear, and J. C. Aster. (2006). c-Myc is an important direct target of Notch1 in T-cell acute lymphoblastic leukemia/lymphoma. Genes Dev **20:**2096-109.

Wensing, B., A. Stuhler, P. Jenkins, M. Hollyoake, C. E. Karstegl, and P. J. Farrell. (2001). Variant chromatin structure of the oriP region of Epstein-Barr virus and regulation of EBER1 expression by upstream sequences and oriP. J Virol **75:**6235-41.

White, R. J. (2004). RNA polymerase III transcription and cancer. Oncogene **23:**3208-16.

White, R. J. (2005). RNA polymerases I and III, growth control and cancer. Nat Rev Mol Cell Biol **6:**69-78.

White, R. J. (2008). RNA polymerases I and III, non-coding RNAs and cancer. Trends Genet **24:**622-9.

Whitley, R. J. 2006. Herpesviruses (Human), in *Encyclopedia of Life Sciences*. Chichester: John Wiley and Sons Ltd (www.els.net).

Whyte, P., K. J. Buchkovich, J. M. Horowitz, S. H. Friend, M. Raybuck, R. A. Weinberg, and E. Harlow. (1988). Association between an oncogene and an anti-oncogene: the adenovirus E1A proteins bind to the retinoblastoma gene product. Nature **334:**124-9.

Wierstra, I., and J. Alves. (2008). The c-myc promoter: still MysterY and challenge. Adv Cancer Res **99:**113-333.

Willis, I. M., and R. D. Moir. (2007). Integration of nutritional and stress signaling pathways by Maf1. Trends Biochem Sci **32:**51-3.

Wilson, J. B., J. L. Bell, and A. J. Levine. (1996). Expression of Epstein-Barr virus nuclear

antigen-1 induces B cell neoplasia in transgenic mice. Embo J **15:**3117-26.

Winter, A. G., G. Sourvinos, S. J. Allison, K. Tosh, P. H. Scott, D. A. Spandidos, and R. J. White. (2000). RNA polymerase III transcription factor TFIIIC2 is overexpressed in ovarian tumors. Proc Natl Acad Sci U S A **97:**12619-24.

Woiwode, A., S. A. Johnson, S. Zhong, C. Zhang, R. G. Roeder, M. Teichmann, and D. L. Johnson. (2008). PTEN represses RNA polymerase III-dependent transcription by targeting the TFIIIB complex. Mol Cell Biol **28:**4204-14.

Wong, H. L., X. Wang, R. C. Chang, D. Y. Jin, H. Feng, Q. Wang, K. W. Lo, D. P. Huang, P. W. Yuen, K. Takada, Y. C. Wong, and S. W. Tsao. (2005). Stable expression of EBERs in immortalized nasopharyngeal epithelial cells confers resistance to apoptotic stress. Mol Carcinog **44:**92-101.

Wong, N., A. B. Hui, B. Fan, K. W. Lo, E. Pang, S. F. Leung, D. P. Huang, and P. J. Johnson. (2003). Molecular cytogenetic characterization of nasopharyngeal carcinoma cell lines and xenografts by comparative genomic hybridization and spectral karyotyping. Cancer Genet Cytogenet **140:**124-32.

Woo, I. S., T. Kohno, K. Inoue, S. Ishii, and J. Yokota. (2002). Infrequent mutations of the activating transcription factor-2 gene in human lung cancer, neuroblastoma and breast cancer. Int J Oncol **20:**527-31.

Wood, V. H., J. D. O'Neil, W. Wei, S. E. Stewart, C. W. Dawson, and L. S. Young. (2007). Epstein-Barr virus-encoded EBNA1 regulates cellular gene transcription and modulates the STAT1 and TGFbeta signaling pathways. Oncogene **26:**4135-47.

Woychik, N. A., and M. Hampsey. (2002). The RNA polymerase II machinery: structure illuminates function. Cell **108:**453-63.

Wrightham, M. N., J. P. Stewart, N. J. Janjua, S. D. Pepper, C. Sample, C. M. Rooney, and J. R. Arrand. (1995). Antigenic and sequence variation in the C-terminal unique domain of the Epstein-Barr virus nuclear antigen EBNA-1. Virology **208:**521-30.

Wu, H., D. F. Ceccarelli, and L. Frappier. (2000). The DNA segregation mechanism of Epstein-Barr virus nuclear antigen 1. EMBO Rep **1:**140-4.

Wu, H., P. Kapoor, and L. Frappier. (2002). Separation of the DNA replication, segregation, and transcriptional activation functions of Epstein-Barr nuclear antigen 1. J Virol **76:**2480-90.

Wu, J., H. Suzuki, A. A. Akhand, Y. W. Zhou, K. Hossain, and I. Nakashima. (2002). Modes of activation of mitogen-activated protein kinases and their roles in cepharanthine-induced apoptosis in human leukemia cells. Cell Signal **14:**509-15.

Wu, S., C. Cetinkaya, M. J. Munoz-Alonso, N. von der Lehr, F. Bahram, V. Beuger, M. Eilers, J. Leon, and L. G. Larsson. (2003). Myc represses differentiation-induced p21CIP1 expression via Miz-1-dependent interaction with the p21 core promoter. Oncogene **22:**351-60.

Wu, Y., S. Maruo, M. Yajima, T. Kanda, and K. Takada. (2007). Epstein-Barr virus (EBV)-encoded RNA 2 (EBER2) but not EBER1 plays a critical role in EBV-induced B-cell growth transformation. J Virol **81:**11236-45.

Wysokenski, D. A., and J. L. Yates. (1989). Multiple EBNA1-binding sites are required to form an EBNA1-dependent enhancer and to activate a minimal replicative origin within oriP of Epstein-Barr virus. J Virol **63:**2657-66.

Xing, L., and E. Kieff. (2007). Epstein-Barr virus BHRF1 micro- and stable RNAs during latency III and after induction of replication. J Virol **81:**9967-75.

Xu, D., N. Popov, M. Hou, Q. Wang, M. Bjorkholm, A. Gruber, A. R. Menkel, and M. Henriksson. (2001). Switch from Myc/Max to Mad1/Max binding and decrease in histone acetylation at the telomerase reverse transcriptase promoter during differentiation of HL60 cells. Proc Natl Acad Sci U S A **98:**3826-31.

Yajima, M., T. Kanda, and K. Takada. (2005). Critical role of Epstein-Barr Virus (EBV)-encoded RNA in efficient EBV-induced B-lymphocyte growth transformation. J Virol **79:**4298-307.

Yamamoto, N., T. Takizawa, Y. Iwanaga, N. Shimizu, and N. Yamamoto. (2000). Malignant transformation of B lymphoma cell line BJAB by Epstein-Barr virus-encoded small RNAs. FEBS Lett **484:**153-8.

Yang, L., K. Aozasa, K. Oshimi, and K. Takada. (2004). Epstein-Barr virus (EBV)-encoded RNA promotes growth of EBV-infected T cells through interleukin-9 induction. Cancer Res **64:**5332-7.

Yang, L., J. He, L. Chen, and G. Wang. (2008). Hepatitis B virus X protein upregulates expression of SMYD3 and C-MYC in HepG2 cells. Med Oncol.

Yates, J., N. Warren, D. Reisman, and B. Sugden. (1984). A cis-acting element from the Epstein-Barr viral genome that permits stable replication of recombinant plasmids in latently infected cells. Proc Natl Acad Sci U S A **81:**3806-10.

Yates, J. L., and S. M. Camiolo. (1988). Dissection of DNA replication and enhancer functions of Epstein-Barr virus nuclear antigen 1 Cancer Cells **6:**197-205.

Yates, J. L., S. M. Camiolo, and J. M. Bashaw. (2000). The minimal replicator of Epstein-Barr

virus oriP. J Virol **74:**4512-22.

Yates, J. L., N. Warren, and B. Sugden. (1985). Stable replication of plasmids derived from Epstein-Barr virus in various mammalian cells. Nature **313:**812-5.

Yeh, E., M. Cunningham, H. Arnold, D. Chasse, T. Monteith, G. Ivaldi, W. C. Hahn, P. T. Stukenberg, S. Shenolikar, T. Uchida, C. M. Counter, J. R. Nevins, A. R. Means, and R. Sears. (2004). A signalling pathway controlling c-Myc degradation that impacts oncogenic transformation of human cells. Nat Cell Biol **6:**308-18.

Yoo, L. I., M. Mooney, M. T. Puglielli, and S. H. Speck. (1997). B-cell lines immortalized with an Epstein-Barr virus mutant lacking the Cp EBNA2 enhancer are biased toward utilization of the oriP-proximal EBNA gene promoter Wp1. J Virol **71:**9134-42.

Yoshizaki, T., K. Endo, Q. Ren, N. Wakisaka, S. Murono, S. Kondo, H. Sato, and M. Furukawa. (2007). Oncogenic role of Epstein-Barr virus-encoded small RNAs (EBERs) in nasopharyngeal carcinoma. Auris Nasus Larynx **34:**73-8.

You, J., J. L. Croyle, A. Nishimura, K. Ozato, and P. M. Howley. (2004). Interaction of the bovine papillomavirus E2 protein with Brd4 tethers the viral DNA to host mitotic chromosomes. Cell **117:**349-60.

You, J., V. Srinivasan, G. V. Denis, W. J. Harrington, Jr., M. E. Ballestas, K. M. Kaye, and P. M. Howley. (2006). Kaposi's sarcoma-associated herpesvirus latency-associated nuclear antigen interacts with bromodomain protein Brd4 on host mitotic chromosomes. J Virol **80:**8909-19.

Young, L., C. Alfieri, K. Hennessy, H. Evans, C. O'Hara, K. C. Anderson, J. Ritz, R. S. Shapiro, A. Rickinson, E. Kieff, and et al. (1989). Expression of Epstein-Barr virus transformation-associated genes in tissues of patients with EBV lymphoproliferative disease. N Engl J Med **321:**1080-5.

Young, L. S., C. W. Dawson, D. Clark, H. Rupani, P. Busson, T. Tursz, A. Johnson, and A. B. Rickinson. (1988). Epstein-Barr virus gene expression in nasopharyngeal carcinoma. J Gen Virol **69 (Pt 5):**1051-65.

Young, L. S., and P. G. Murray. (2003). Epstein-Barr virus and oncogenesis: from latent genes to tumours. Oncogene **22:**5108-21.

Young, L. S., and A. B. Rickinson. (2004). Epstein-Barr virus: 40 years on. Nat Rev Cancer **4:**757-68.

Yu, M. C., J. H. Ho, S. H. Lai, and B. E. Henderson. (1986). Cantonese-style salted fish as a cause of nasopharyngeal carcinoma: report of a case-control study in Hong Kong. Cancer Res **46:**956-61.

Yu, M. C., and J. M. Yuan. (2002). Epidemiology of nasopharyngeal carcinoma. Semin Cancer Biol **12:**421-9.

Zeuthen, J. (1983). Epstein-Barr virus (EBV), lymphocytes and transformation. J Cancer Res Clin Oncol **106:**1-11.

Zhang, D., L. Frappier, E. Gibbs, J. Hurwitz, and M. O'Donnell. (1998). Human RPA (hSSB) interacts with EBNA1, the latent origin binding protein of Epstein-Barr virus. Nucleic Acids Res **26:**631-7.

Zhang, J., H. Chen, G. Weinmaster, and S. D. Hayward. (2001). Epstein-Barr virus BamHi-a rightward transcript-encoded RPMS protein interacts with the CBF1-associated corepressor CIR to negatively regulate the activity of EBNA2 and NotchIC. J Virol **75:**2946-56.

Zhang, L., and J. S. Pagano. (1999). Interferon regulatory factor 2 represses the Epstein-Barr virus BamHI Q latency promoter in type III latency. Mol Cell Biol **19:**3216-23.

Zhang, L., and J. S. Pagano. (2000). Interferon regulatory factor 7 is induced by Epstein-Barr virus latent membrane protein 1. J Virol **74:**1061-8.

Zhang, X., H. Zhang, and L. Ye. (2006). Effects of hepatitis B virus X protein on the development of liver cancer. J Lab Clin Med **147:**58-66.

Zhang, Y., J. H. Ohyashiki, T. Takaku, N. Shimizu, and K. Ohyashiki. (2006). Transcriptional profiling of Epstein-Barr virus (EBV) genes and host cellular genes in nasal NK/T-cell lymphoma and chronic active EBV infection. Br J Cancer **94:**599-608.

Zhao, L. J., and C. Z. Giam. (1992). Human T-cell lymphotropic virus type I (HTLV-I) transcriptional activator, Tax, enhances CREB binding to HTLV-I 21-base-pair repeats by protein-protein interaction. Proc Natl Acad Sci U S A **89:**7070-4.

Zhao, L. J., L. Wang, H. Ren, J. Cao, L. Li, J. S. Ke, and Z. T. Qi. (2005). Hepatitis C virus E2 protein promotes human hepatoma cell proliferation through the MAPK/ERK signaling pathway via cellular receptors. Exp Cell Res **305:**23-32.

Zimber-Strobl, U., L. Strobl, H. Hofelmayr, B. Kempkes, M. S. Staege, G. Laux, B. Christoph, A. Polack, and G. W. Bornkamm. (1999). EBNA2 and c-myc in B cell immortalization by Epstein-Barr virus and in the pathogenesis of Burkitt's lymphoma. Curr Top Microbiol Immunol **246:**315-20; discussion 321.

Zur Hausen, A., B. P. van Rees, J. van Beek, M. E. Craanen, E. Bloemena, G. J. Offerhaus, C. J. Meijer, and A. J. van den Brule. (2004). Epstein-Barr virus in gastric carcinomas and gastric stump carcinomas: a late event in gastric carcinogenesis. J Clin Pathol

57:487-91.

zur Hausen, H., H. Schulte-Holthausen, G. Klein, W. Henle, G. Henle, P. Clifford, and L. Santesson. (1970). EBV DNA in biopsies of Burkitt tumours and anaplastic carcinomas of the nasopharynx. Nature **228:**1056-8.

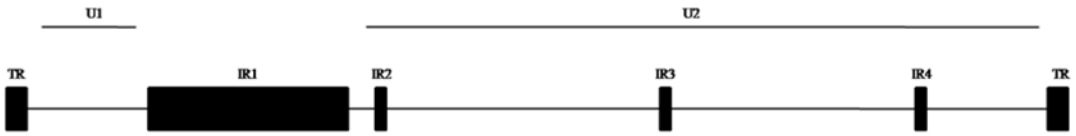

A Adapted from Arrand (1998)

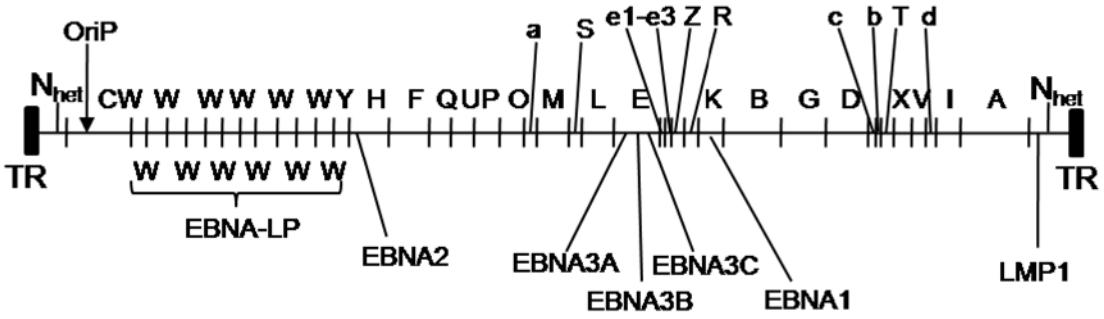

B Adapted from Young and Rickinson (2004)

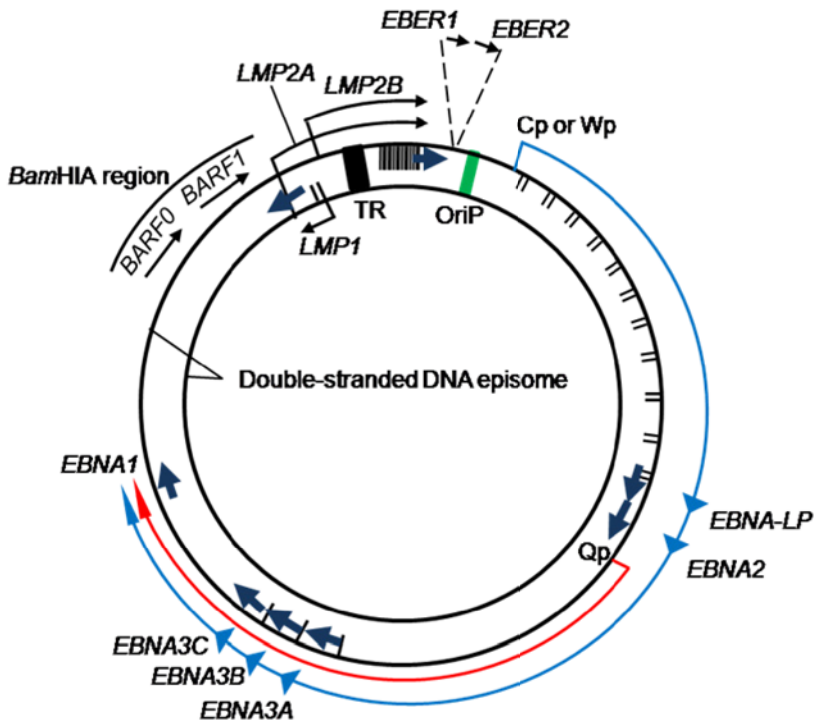

C Adapted from Young and Rickinson (2004)

Figure 1.1

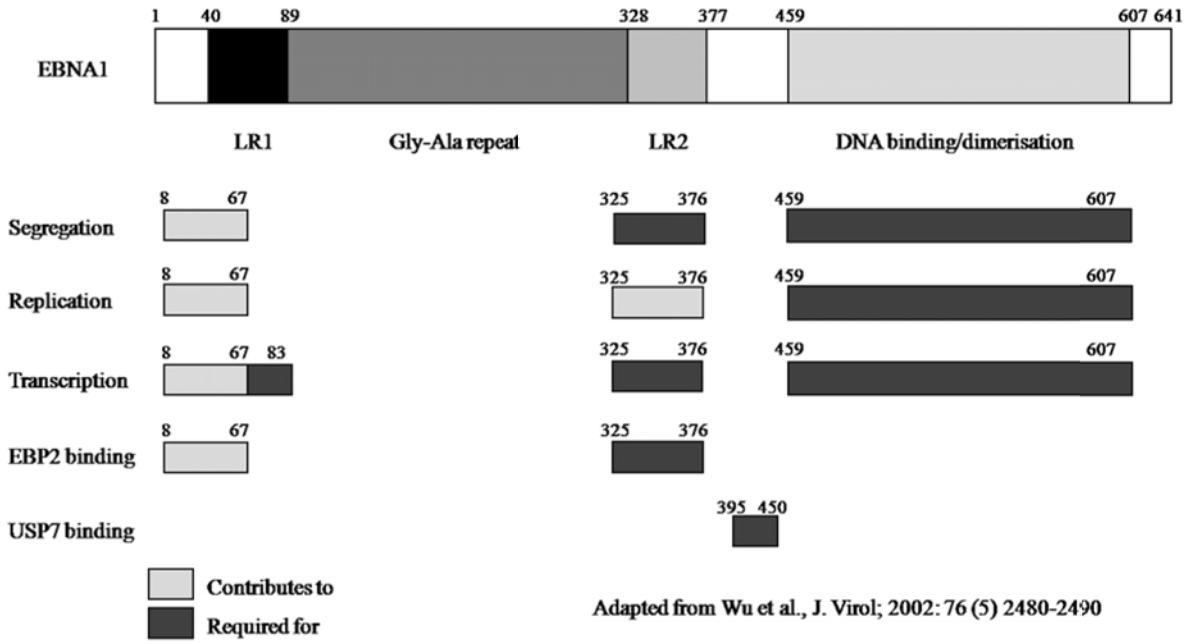
1
40
89
328
377
459
607 641
EBNA1
LR1
Gly-Ala repeat
LR2
DNA binding/dimerisation
Segregation
Replication
Transcription
EBP2 binding
USP7 binding
8
67
83
325
376
395 450
459
607
Contributes to
Required for
Adapted from Wu et al., J. Virol; 2002: 76 (5) 2480-2490

Figure 1.2

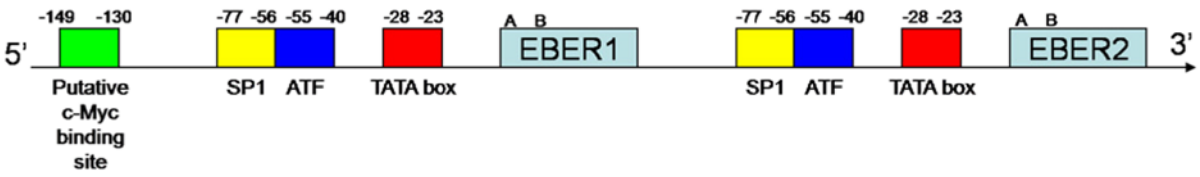
-149 -130
-77 -56 -55 -40
-28 -23
A B
EBER1
-77 -56 -55 -40
-28 -23
A B
EBER2
5'
3'
Putative c-Myc binding site
SP1
ATF
TATA box
SP1
ATF
TATA box

Figure 1.3

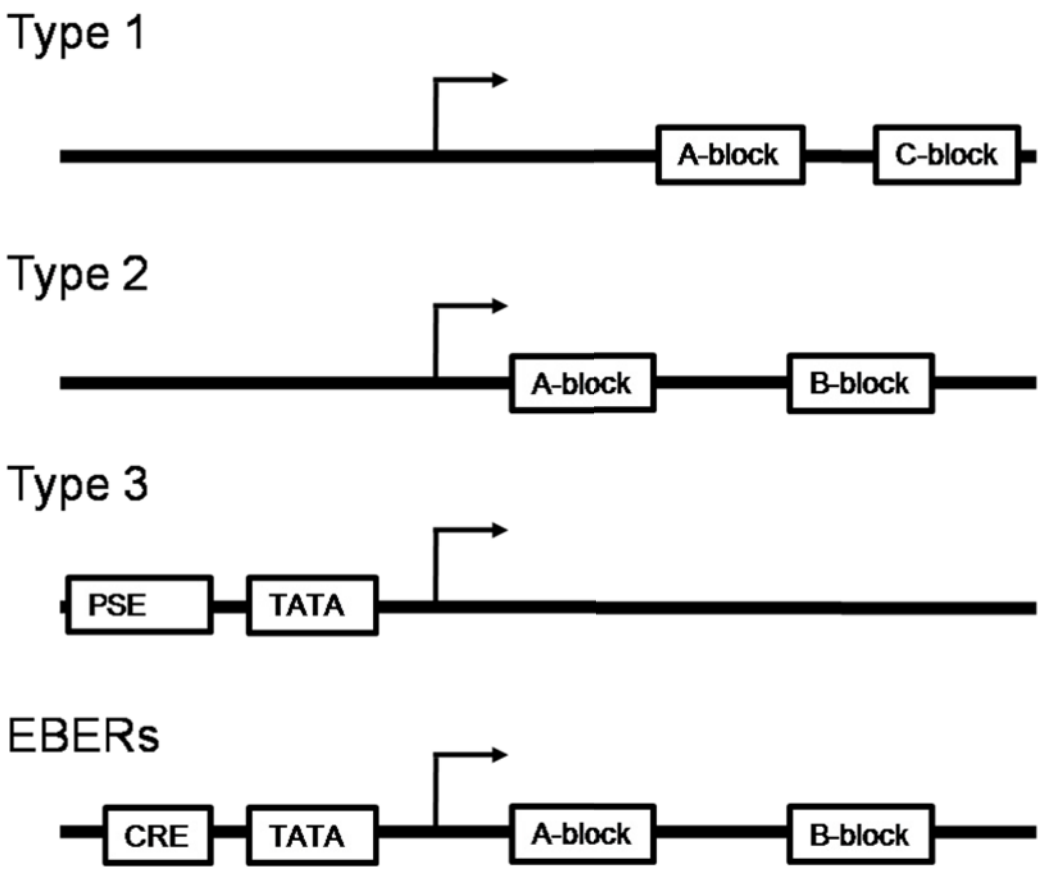

Adapted from Felton-Edkins et al, (2006)

Figure 1.4

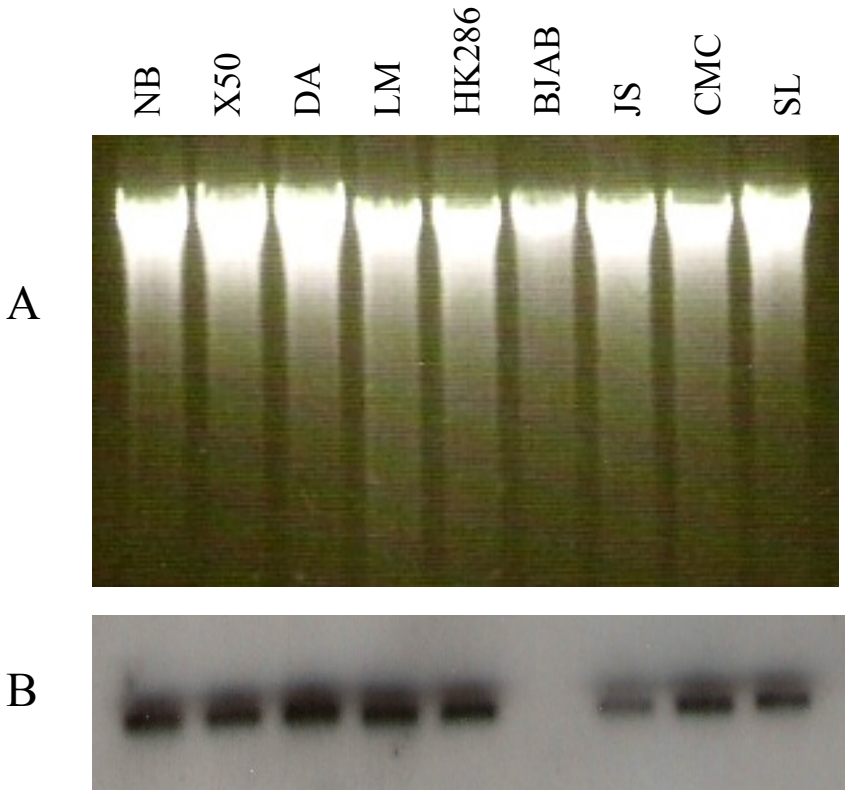

Figure 3.1

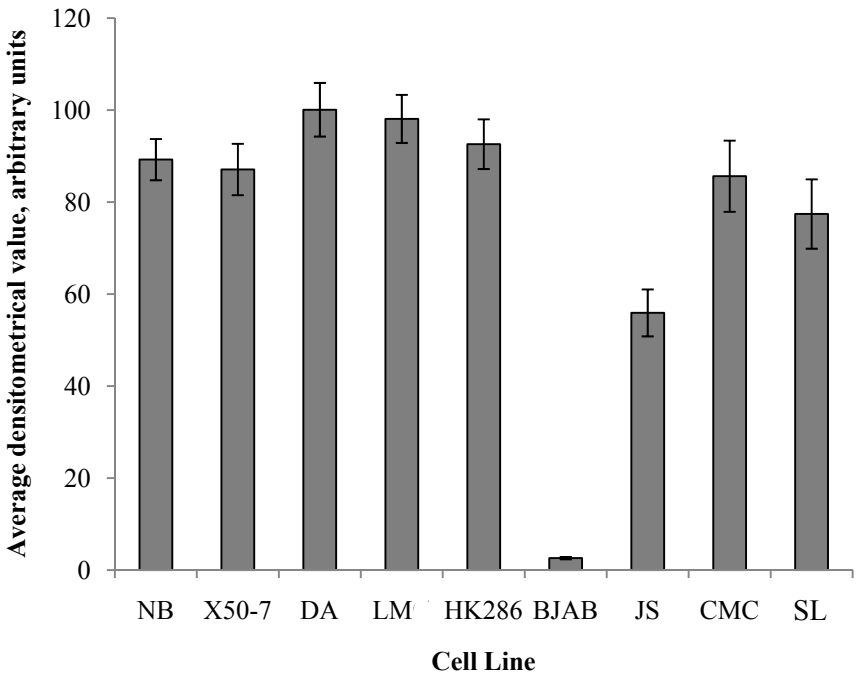

Figure 3.2

A

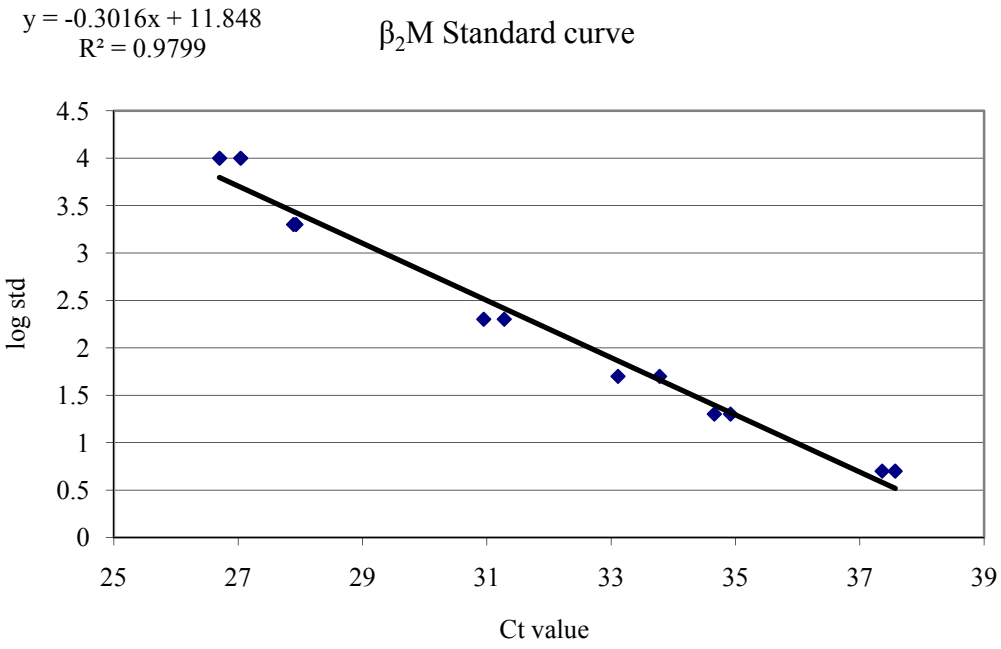
y = -0.3016x + 11.848
R² = 0.9799
β2M Standard curve
log std
Ct value
4.5
4
3.5
3
2.5
2
1.5
1
0.5
0
25
27
29
31
33
35
37
39

B

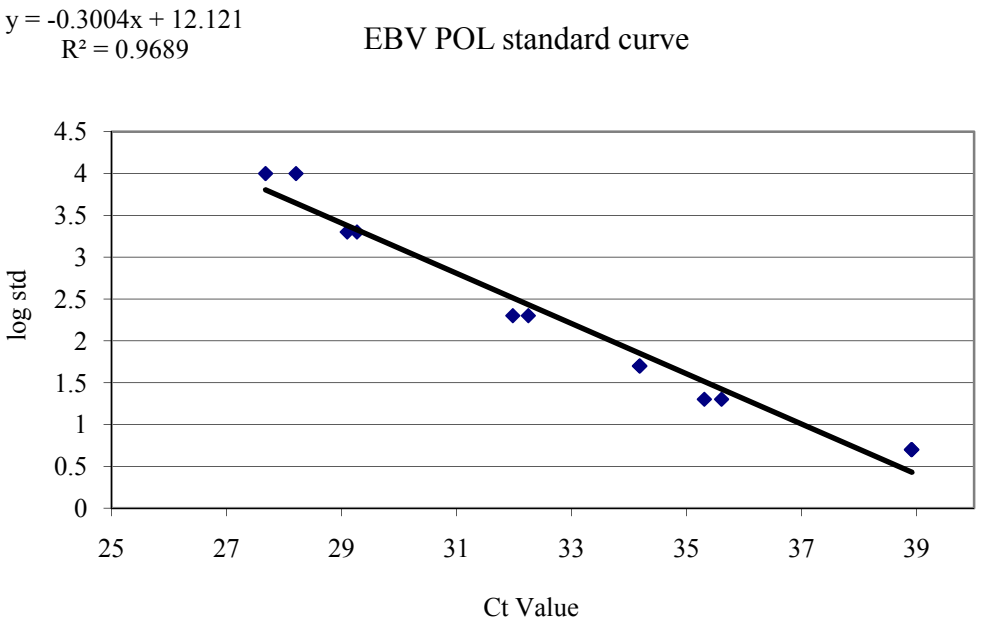
y = -0.3004x + 12.121
R² = 0.9689
EBV POL standard curve
log std
Ct Value
4.5
4
3.5
3
2.5
2
1.5
1
0.5
0
25
27
29
31
33
35
37
39

Figure 3.3

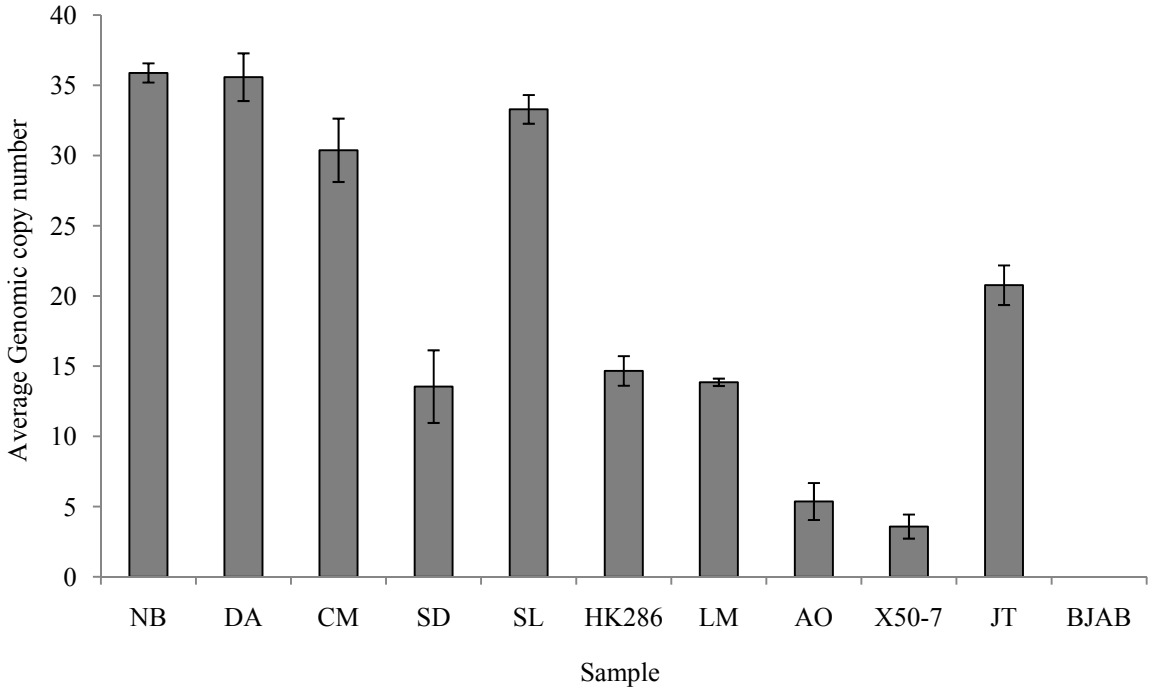

Figure 3.4

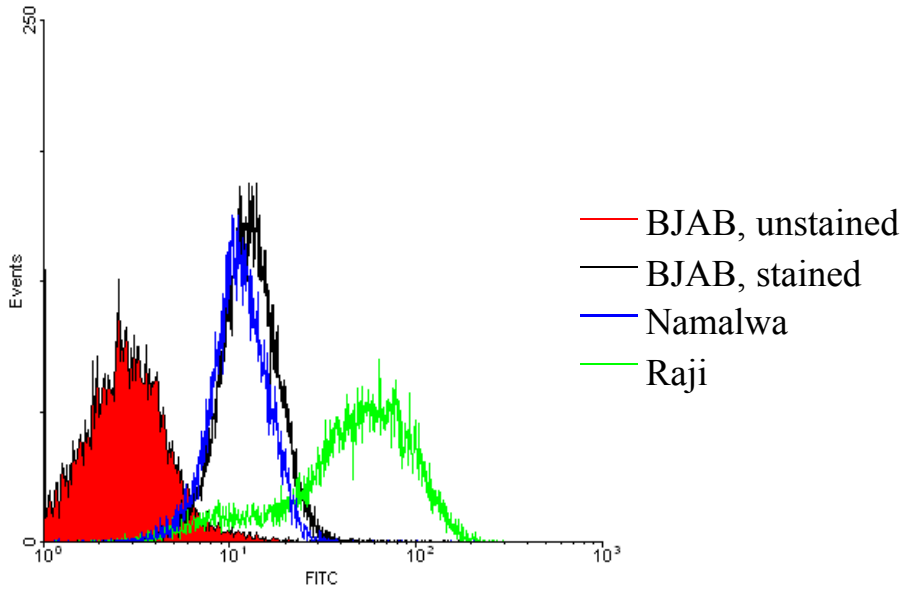

Figure 3.5

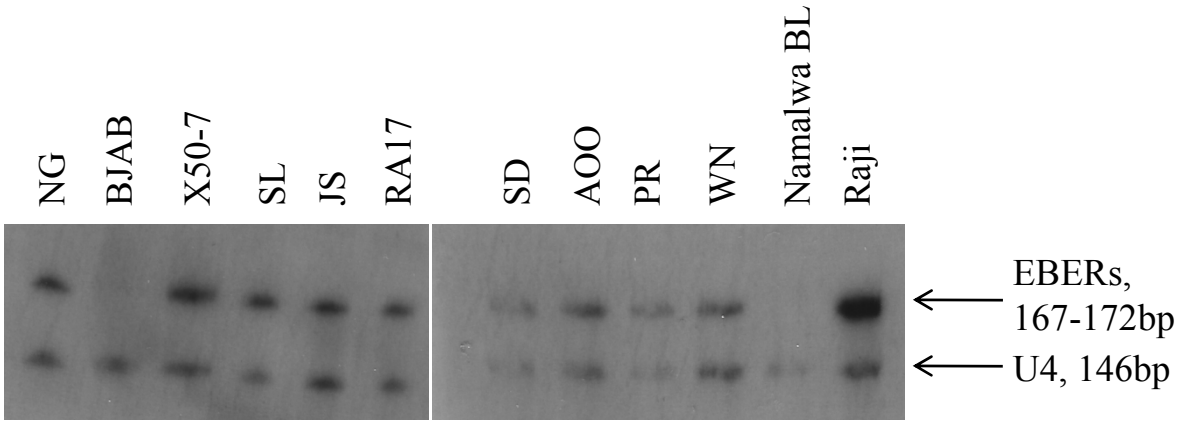

Figure 3.6

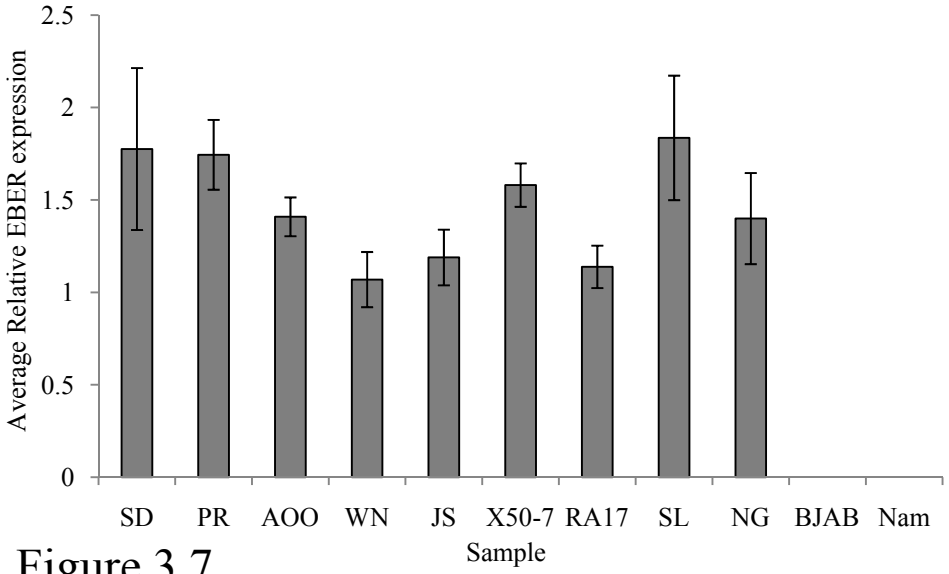

Figure 3.7

A

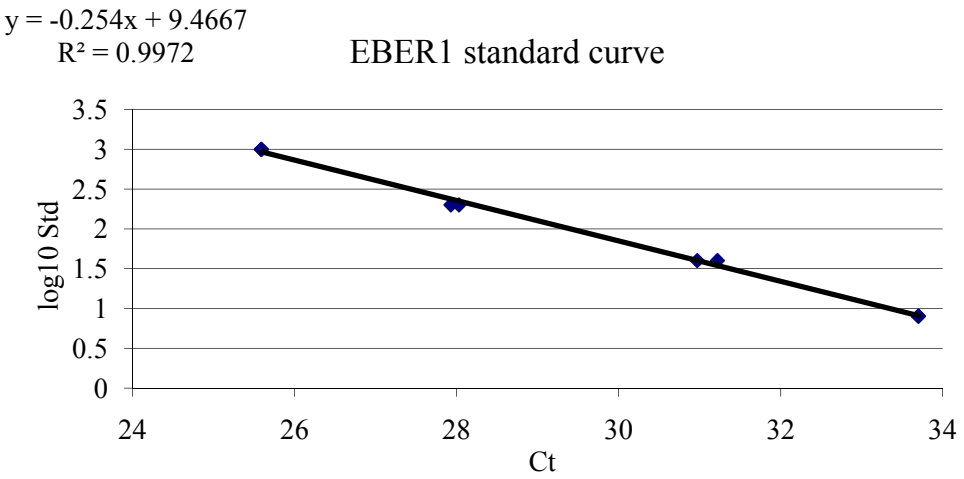

B

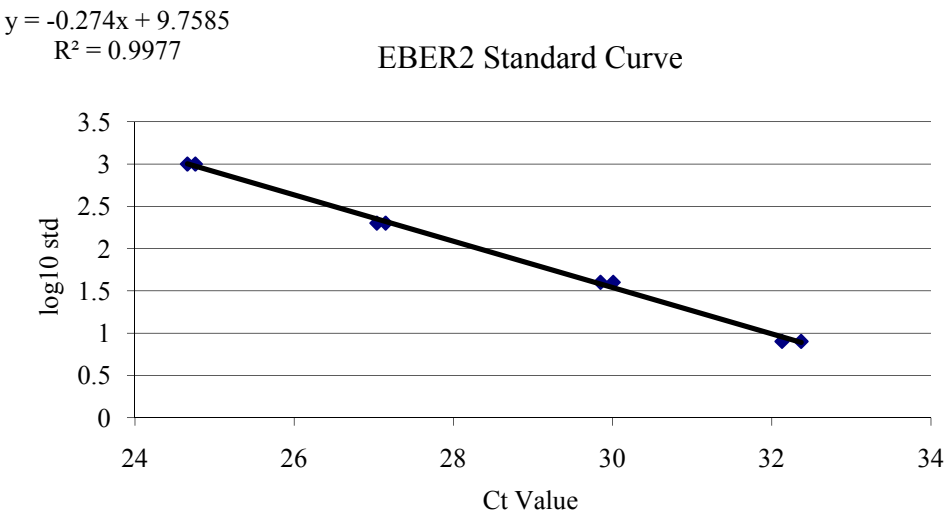

Figure 3.8

A

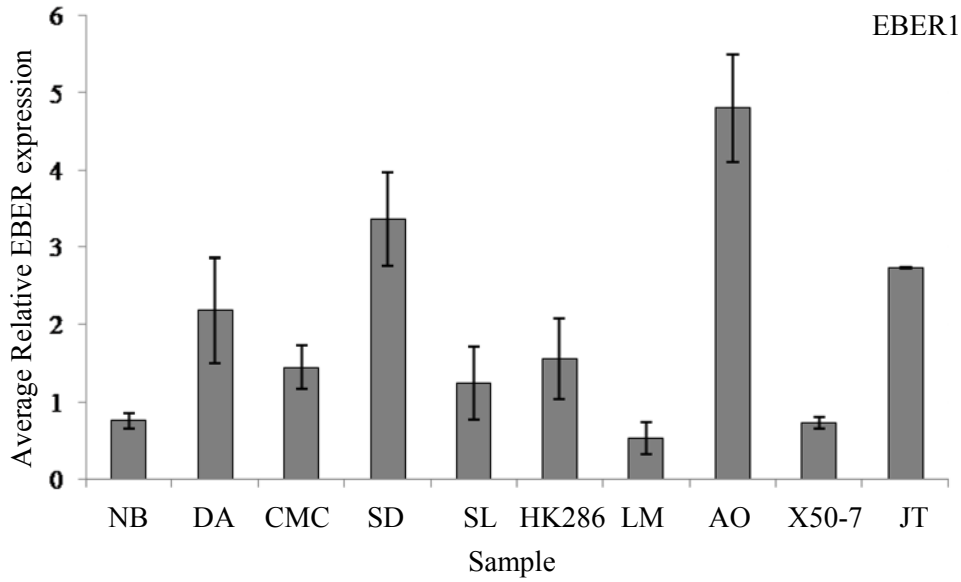

B

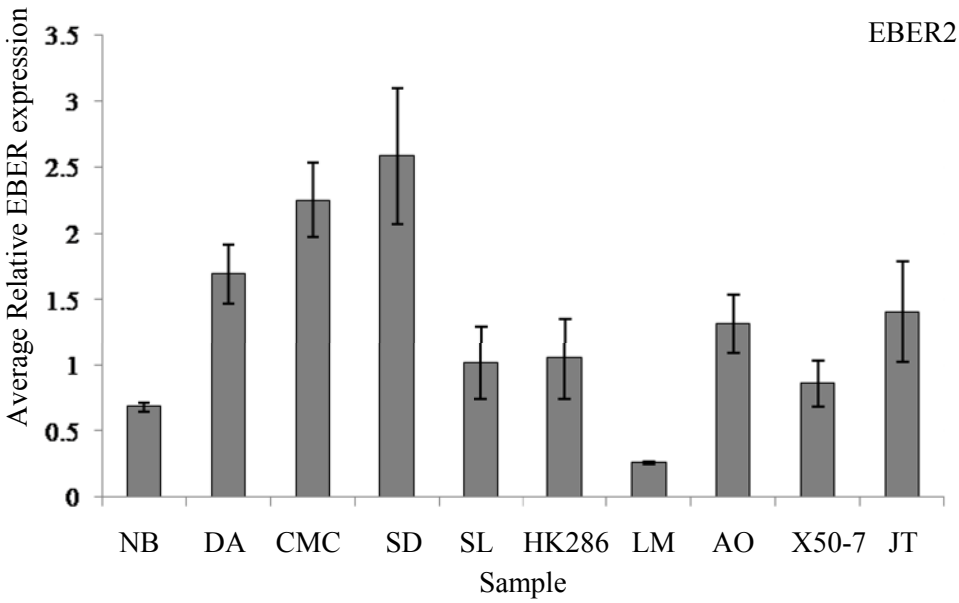

C

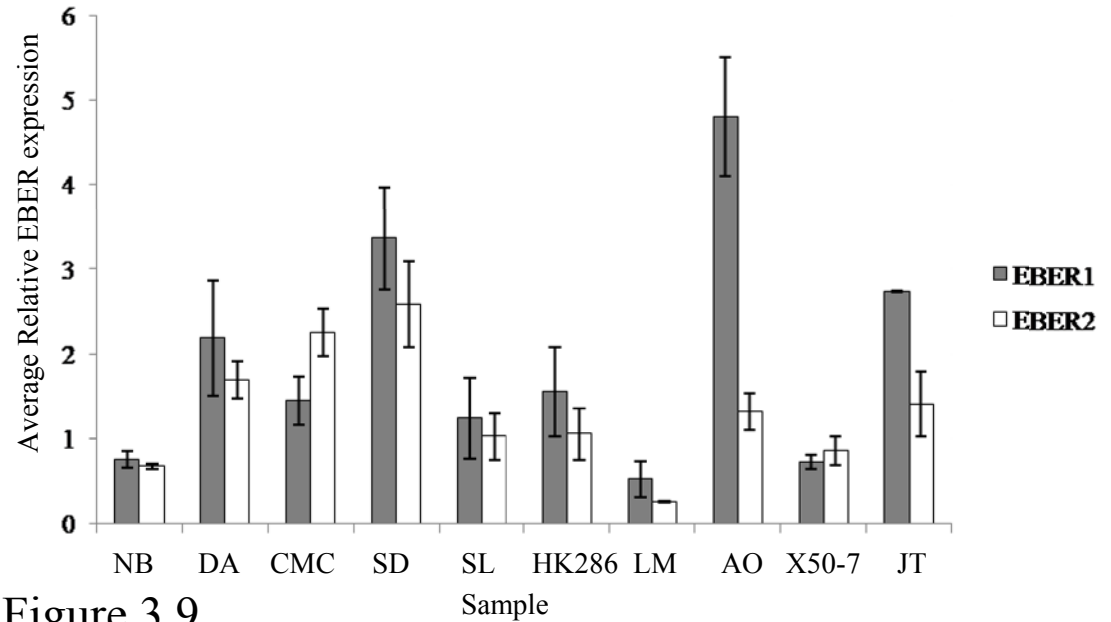

Figure 3.9

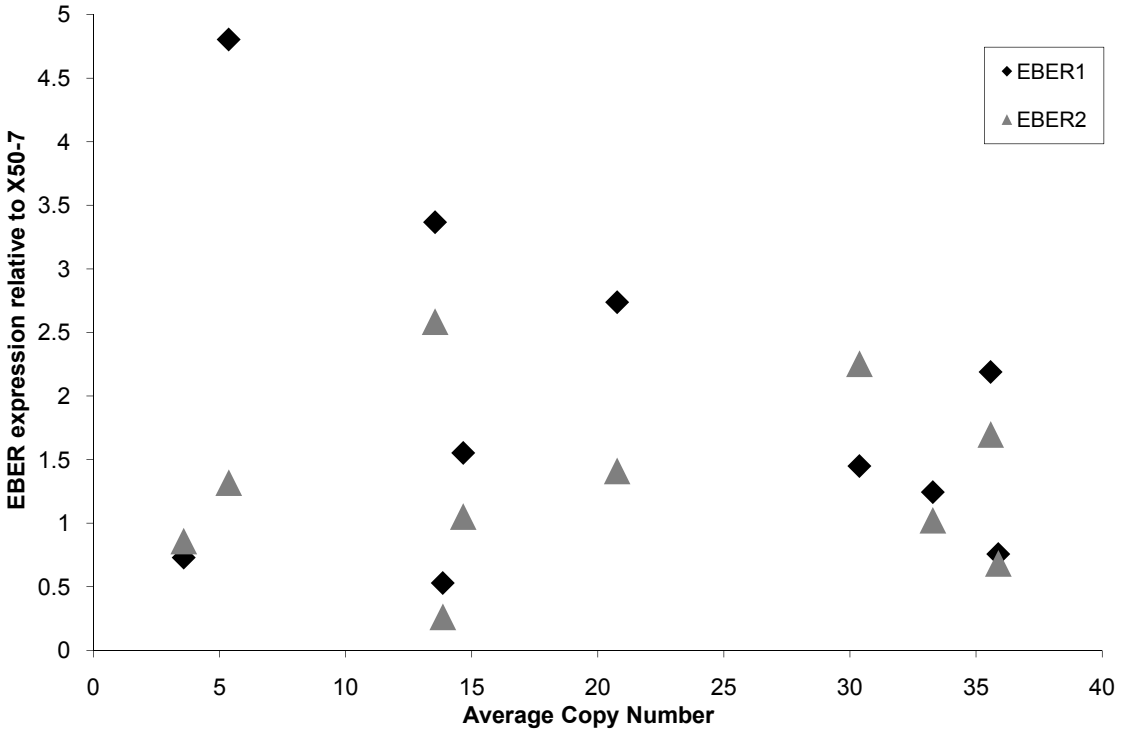
EBER expression relative to X50-7
Average Copy Number
EBER1
EBER2
0
0.5
1
1.5
2
2.5
3
3.5
4
4.5
5
0
5
10
15
20
25
30
35
40

Figure 3.10

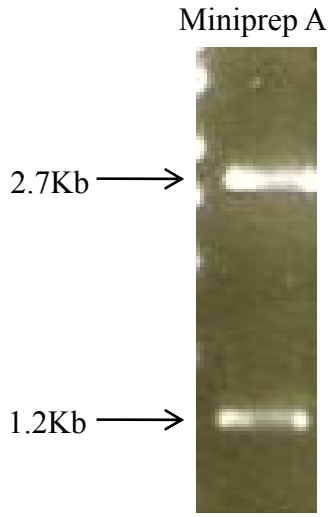

Figure 4.1

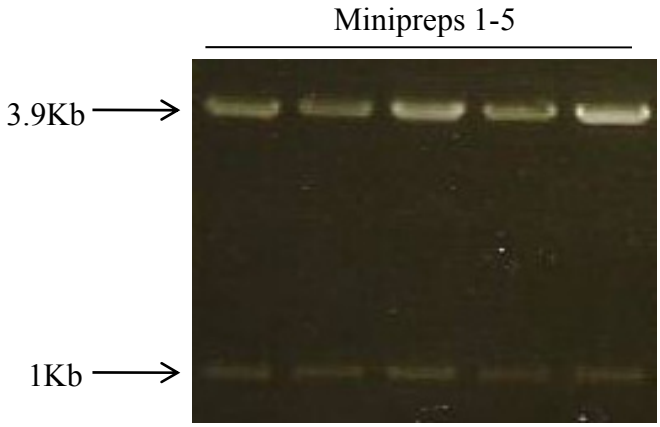

Figure 4.2

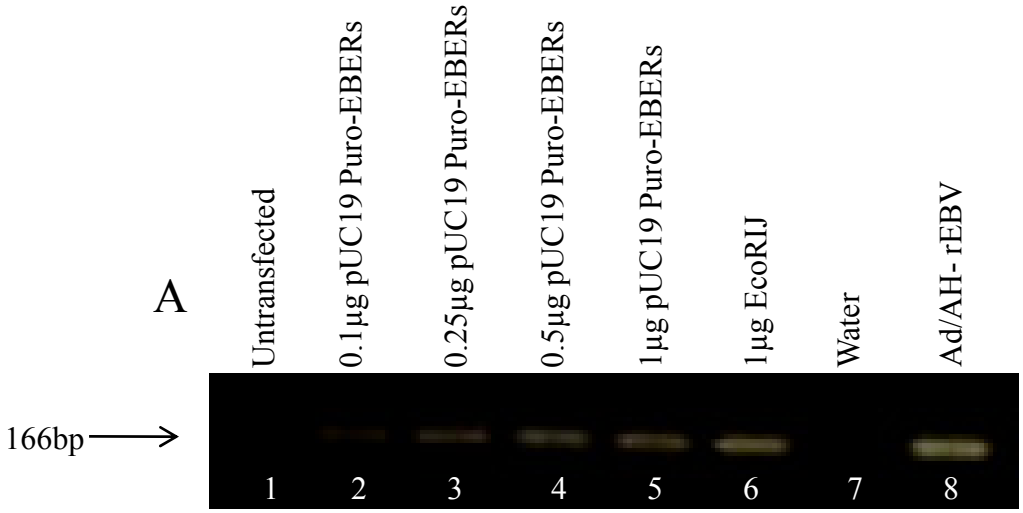

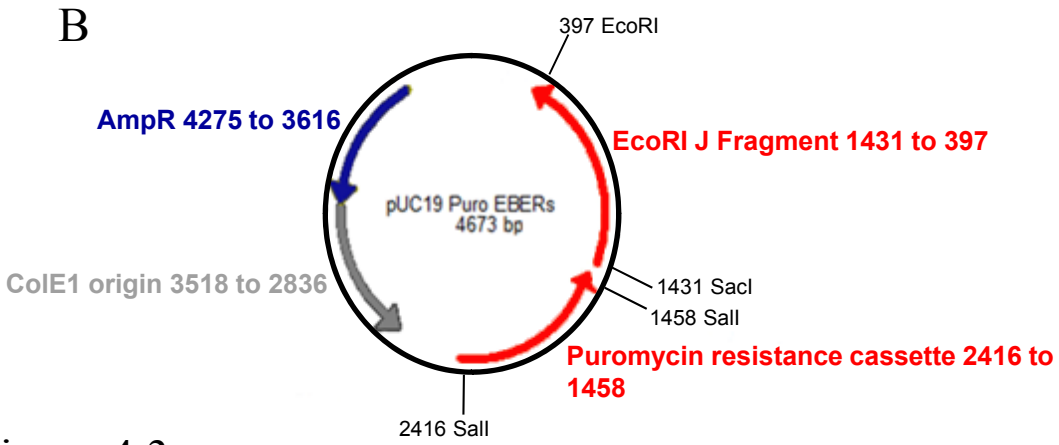

Figure 4.3

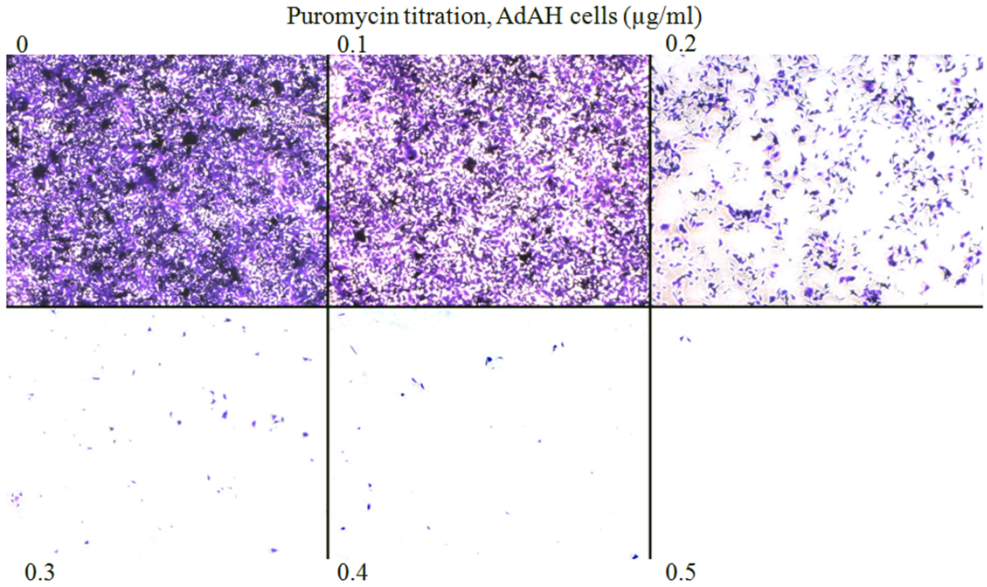

Figure 4.4

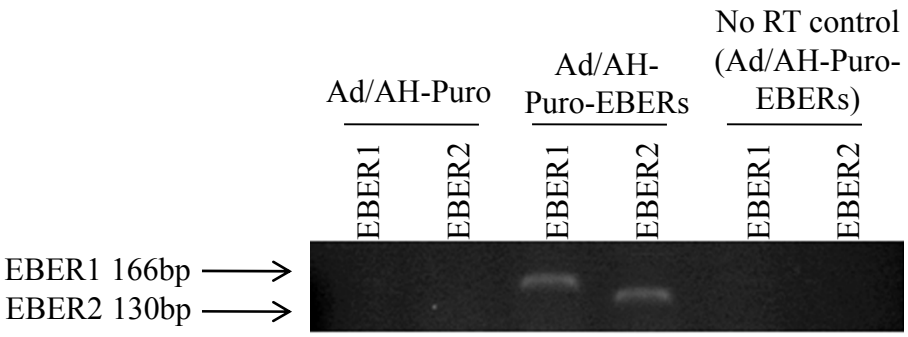

Figure 4.5

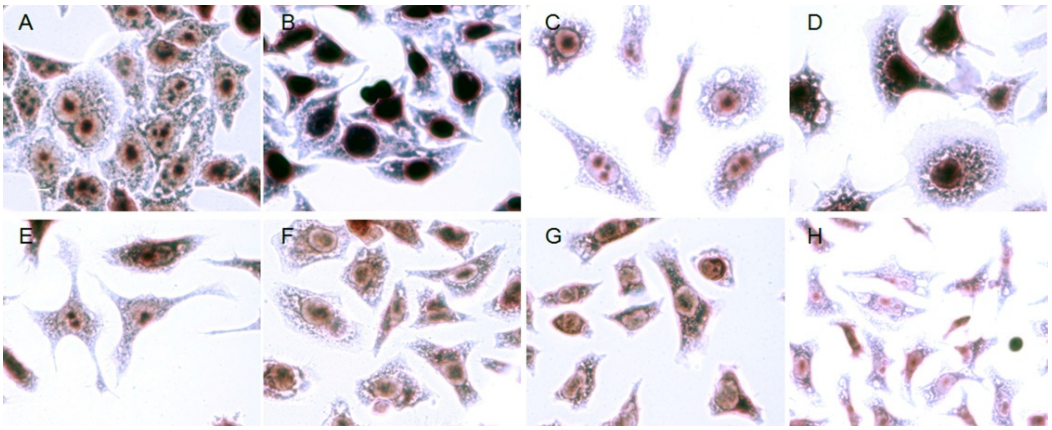

Figure 4.6

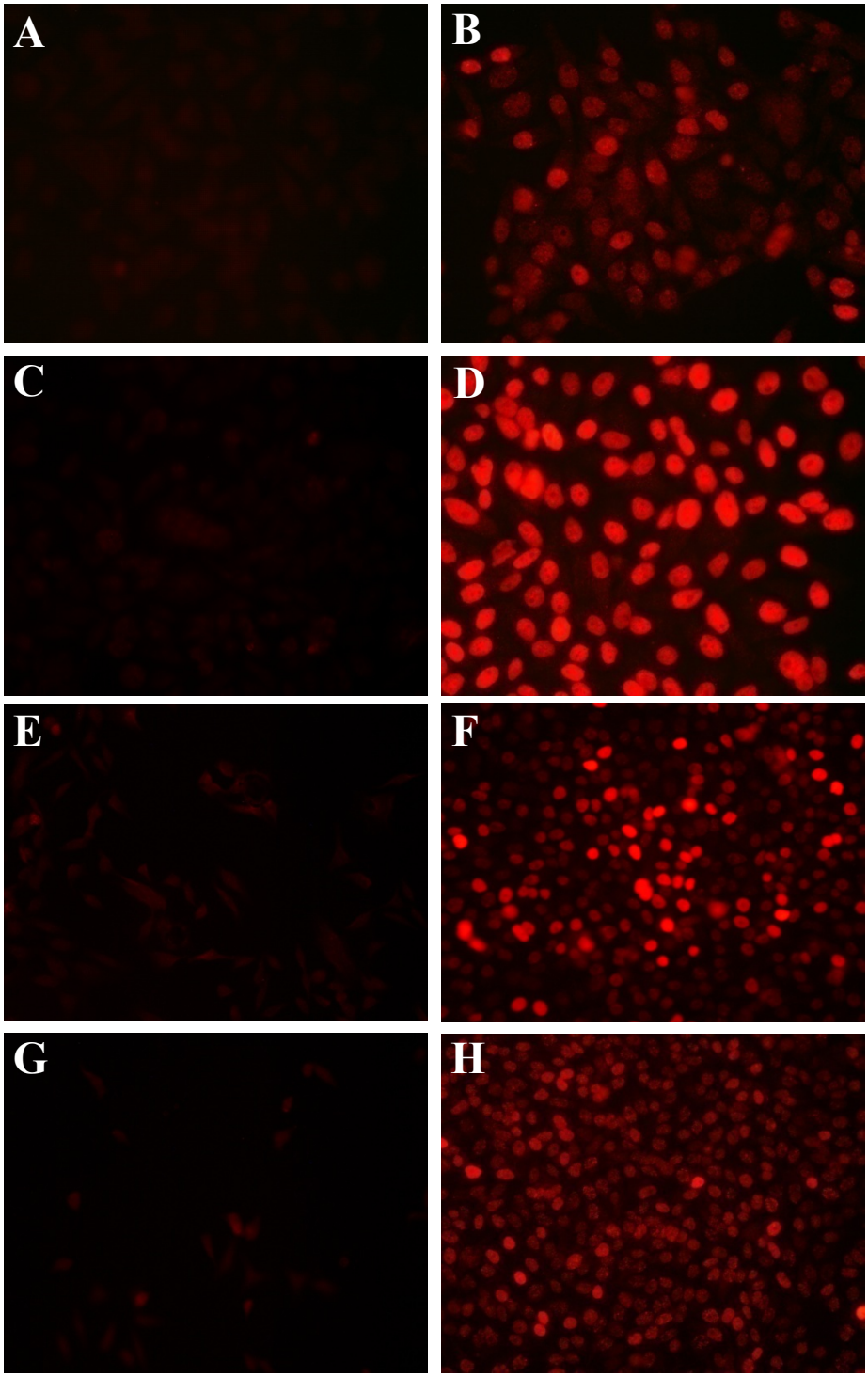

Figure 4.7

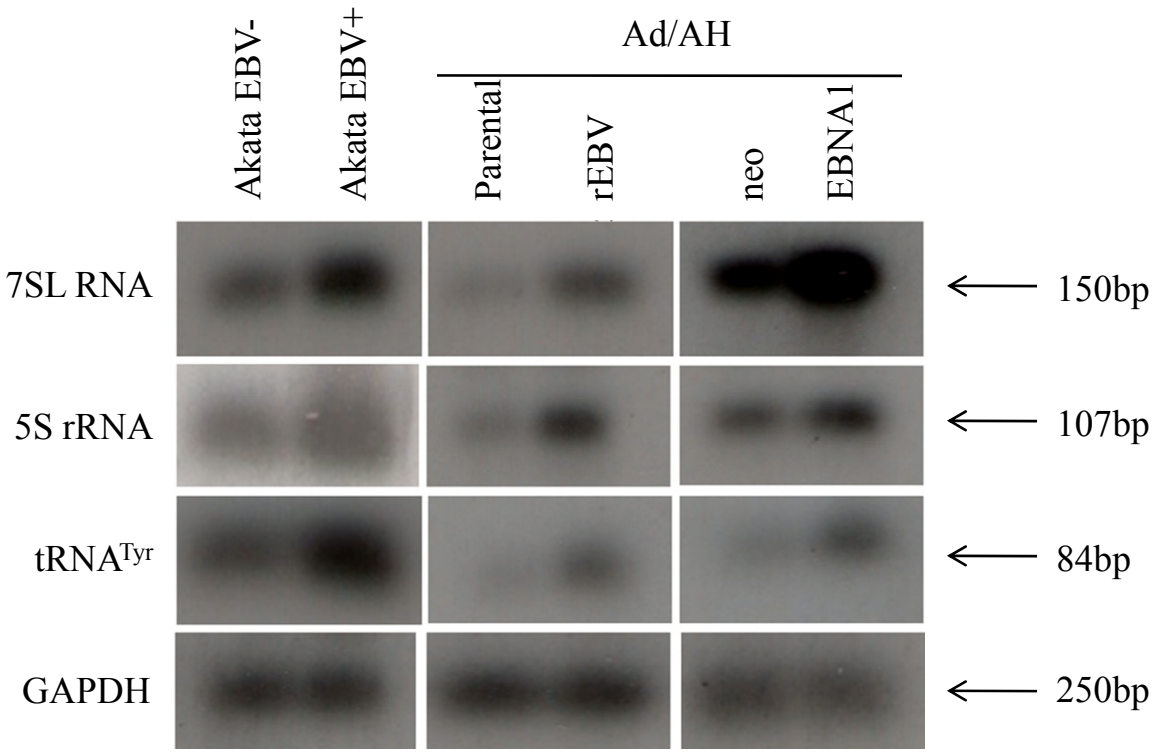

Figure 4.8

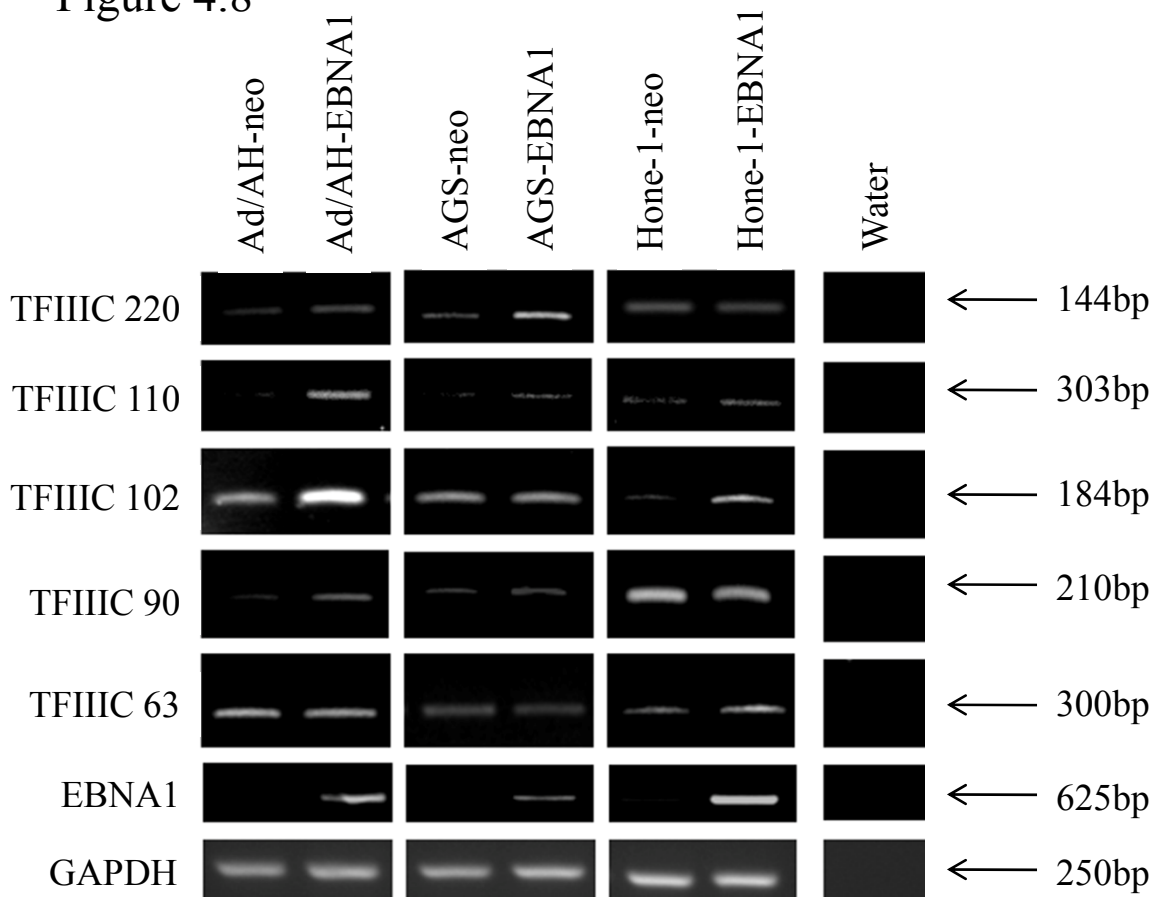

Figure 4.9

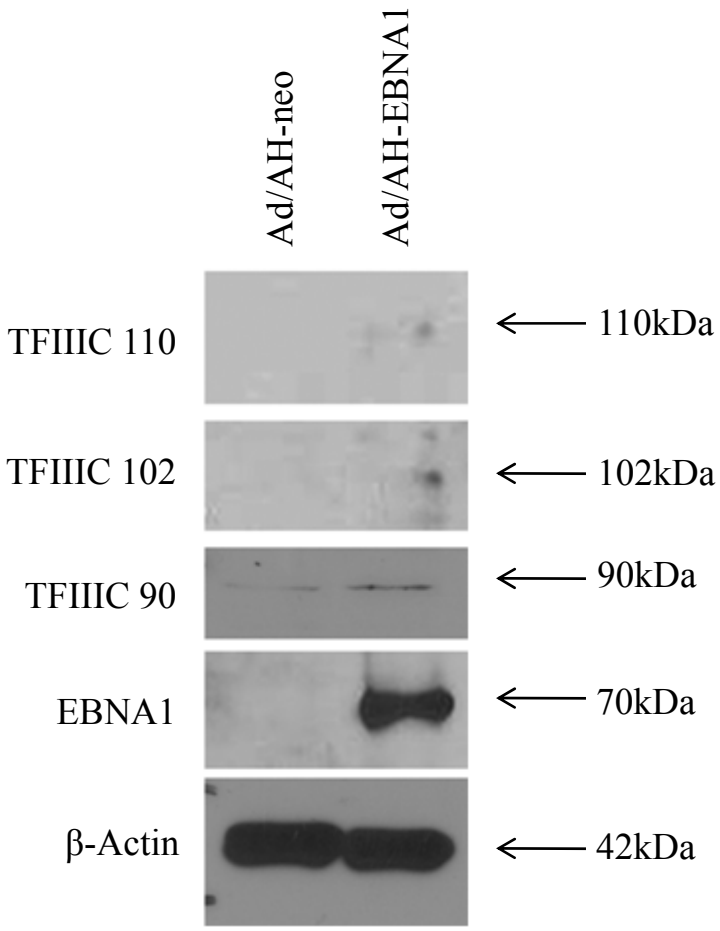

Figure 4.10

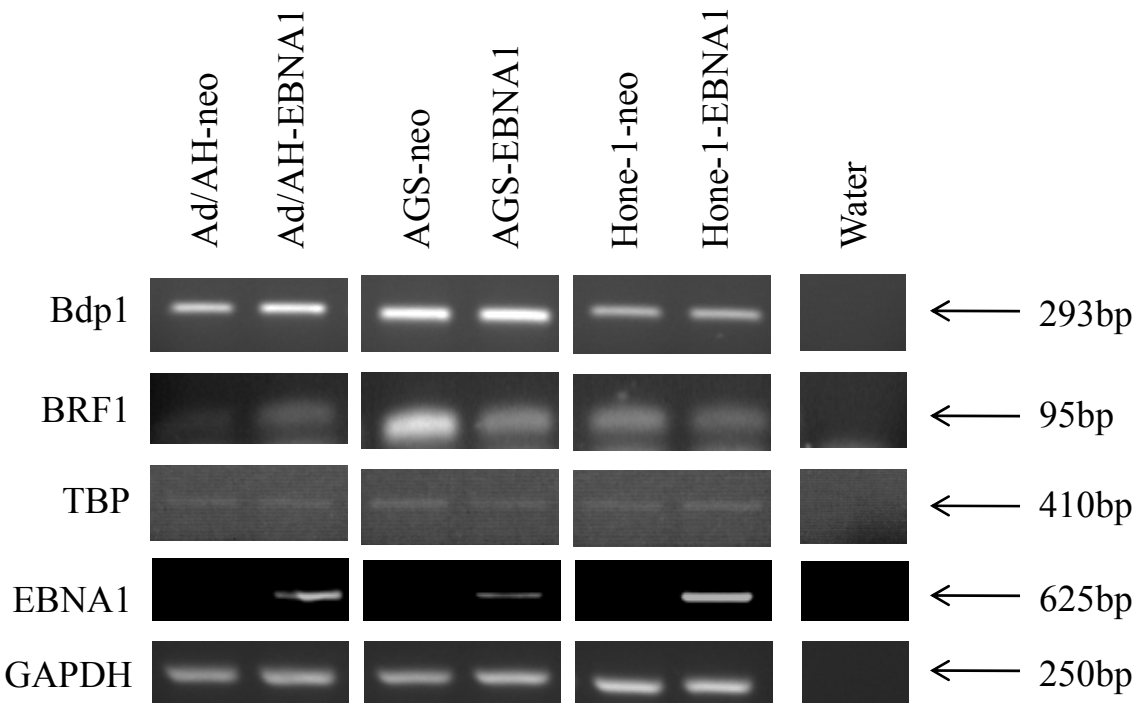

Figure 4.11

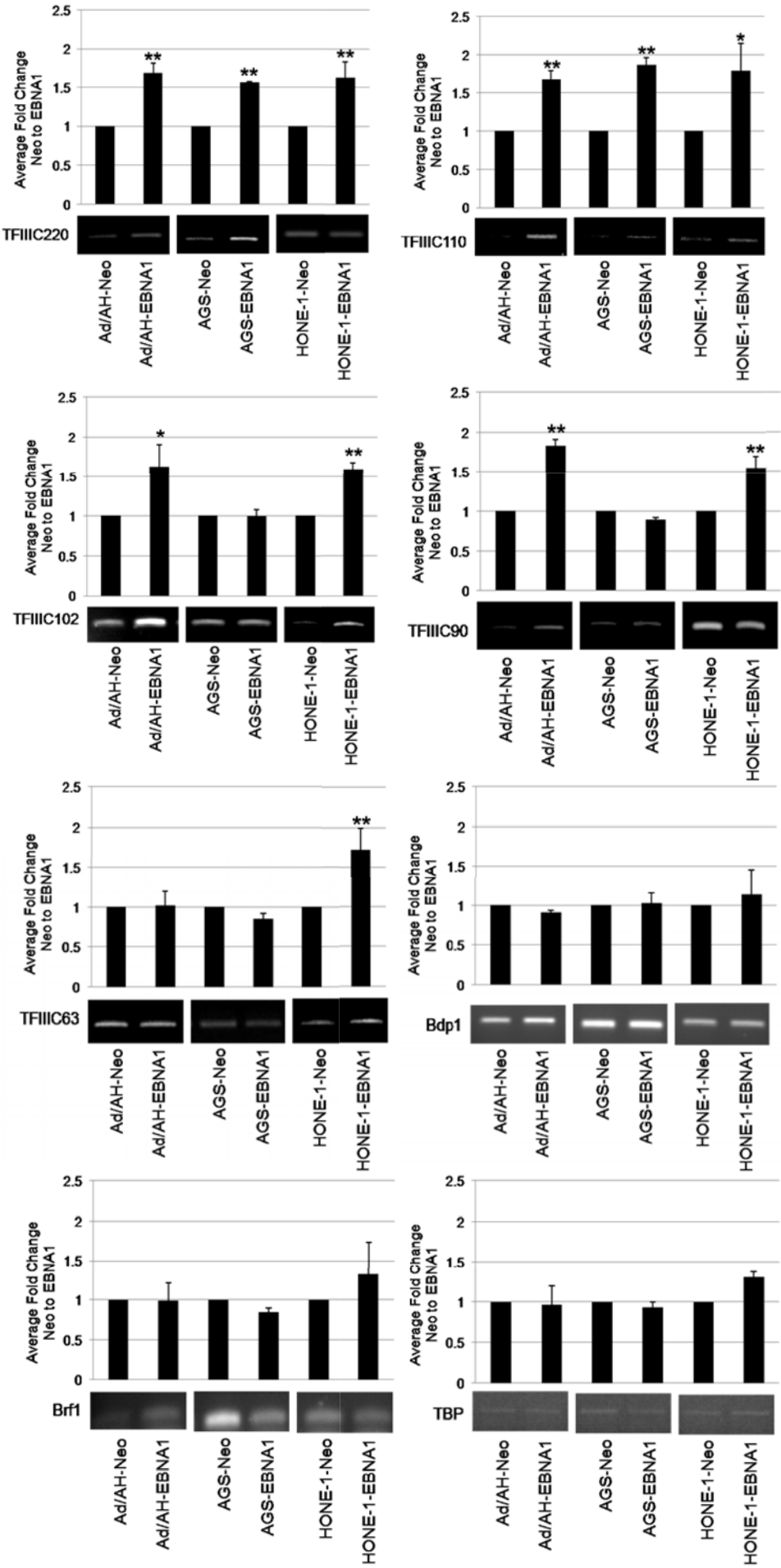
Average Fold Change Neo to EBNA1
TFIIIC220
TFIIIC110
TFIIIC102
TFIIIC90
TFIIIC63
Bdp1
Brf1
TBP
Ad/AH-Neo
Ad/AH-EBNA1
AGS-Neo
AGS-EBNA1
HONE-1-Neo
HONE-1-EBNA1

Figure 4.12

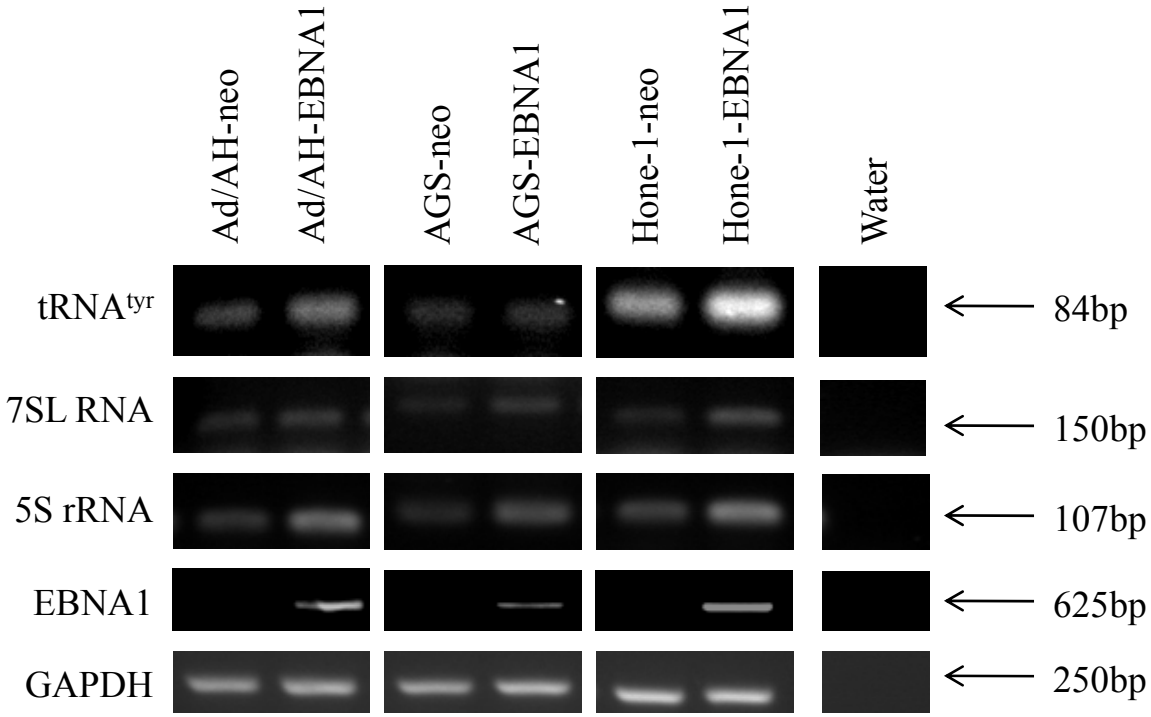

Figure 4.13

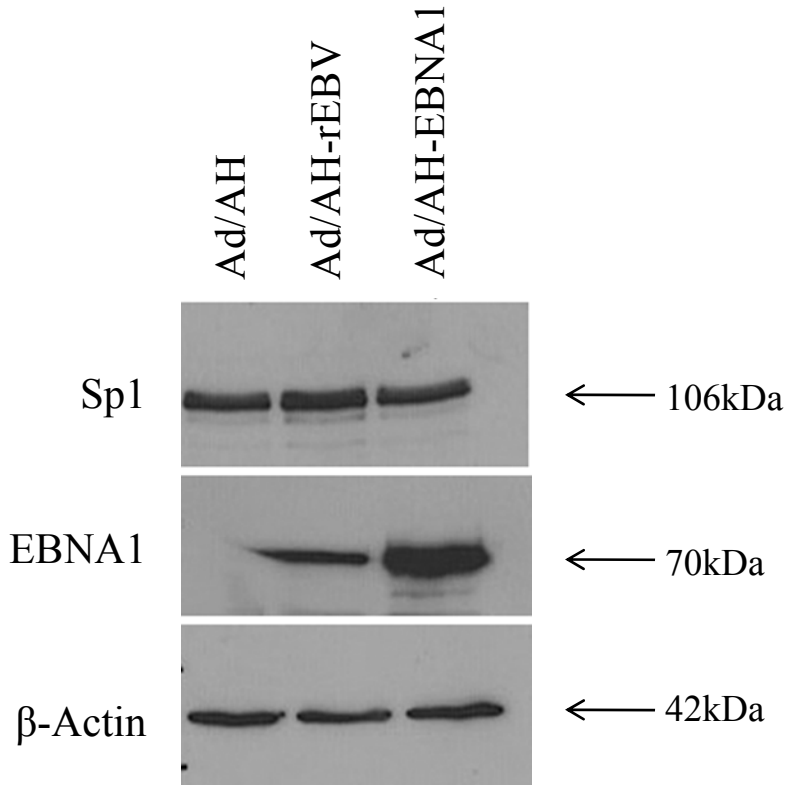

Figure 4.14

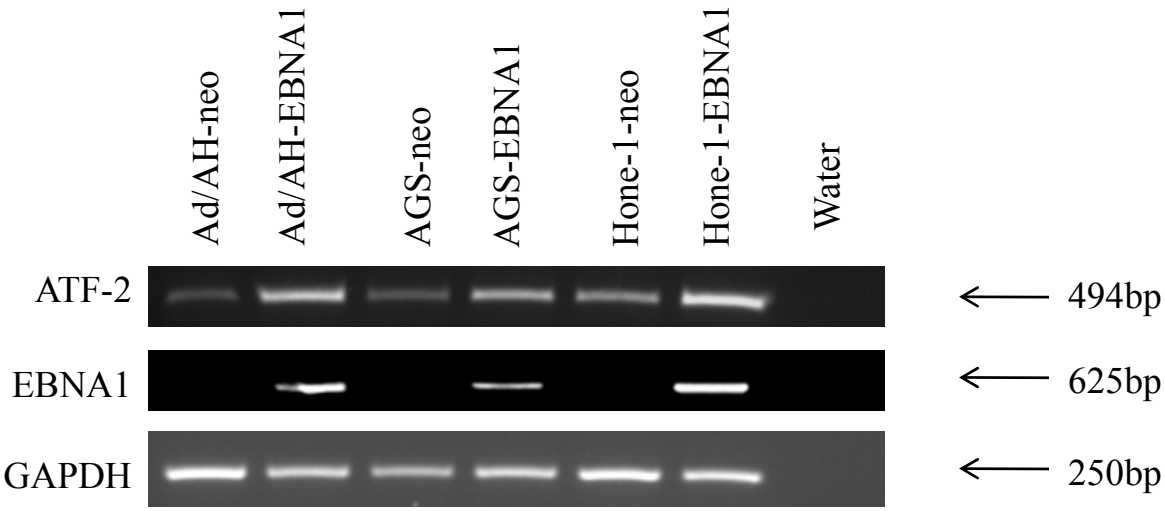

Figure 4.15

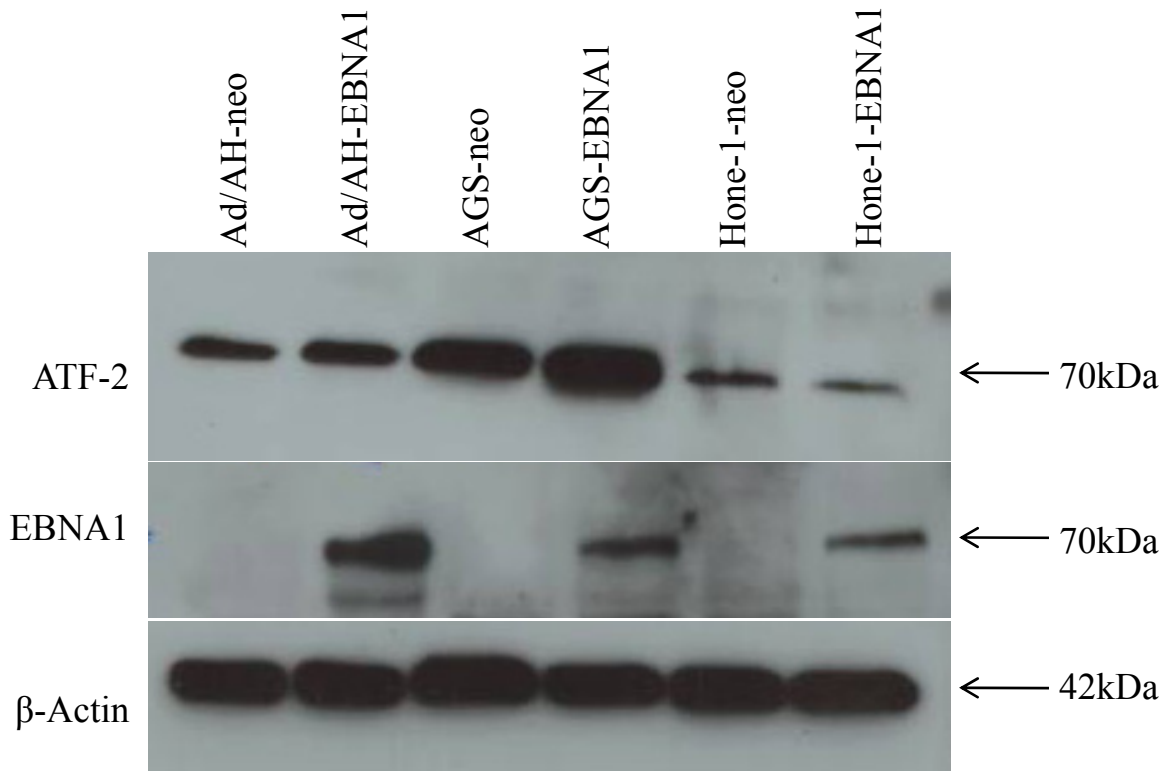

Figure 4.16

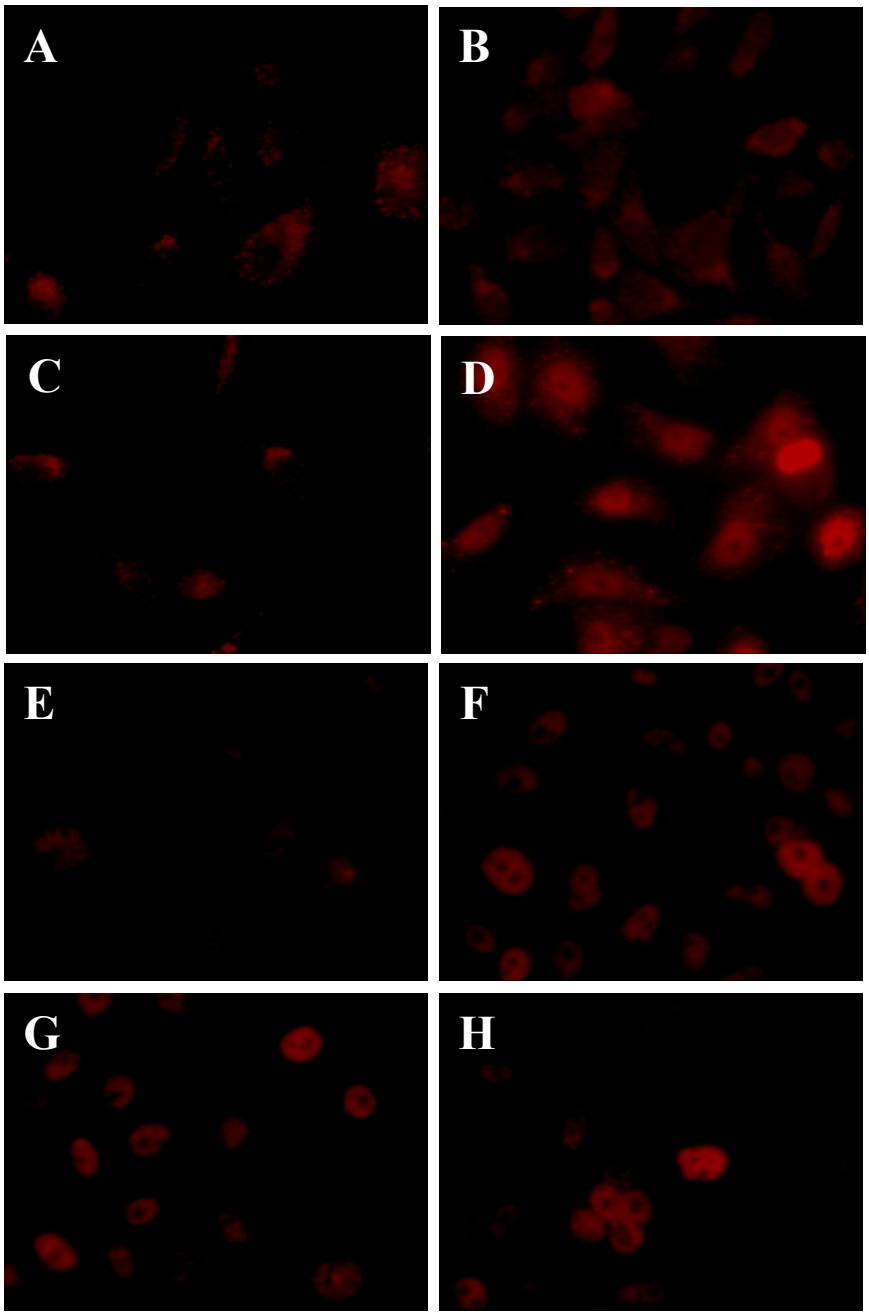

Figure 4.17

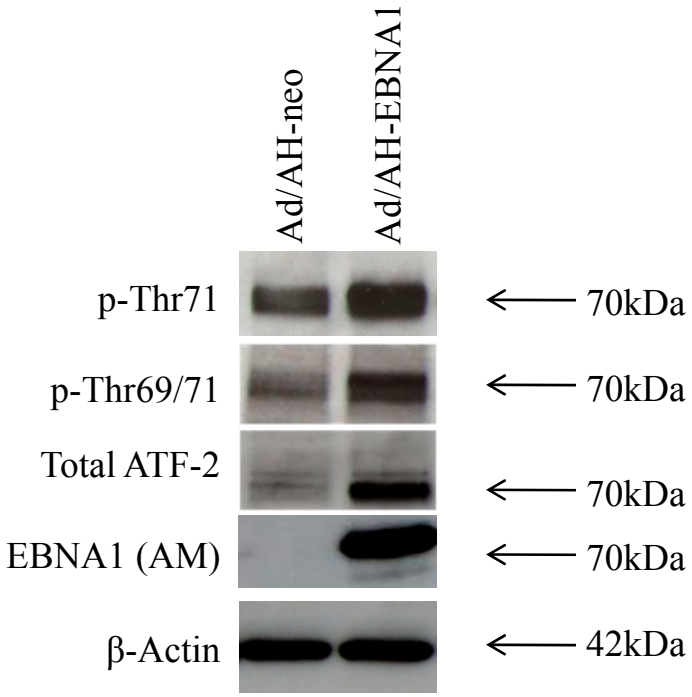

Figure 4.18

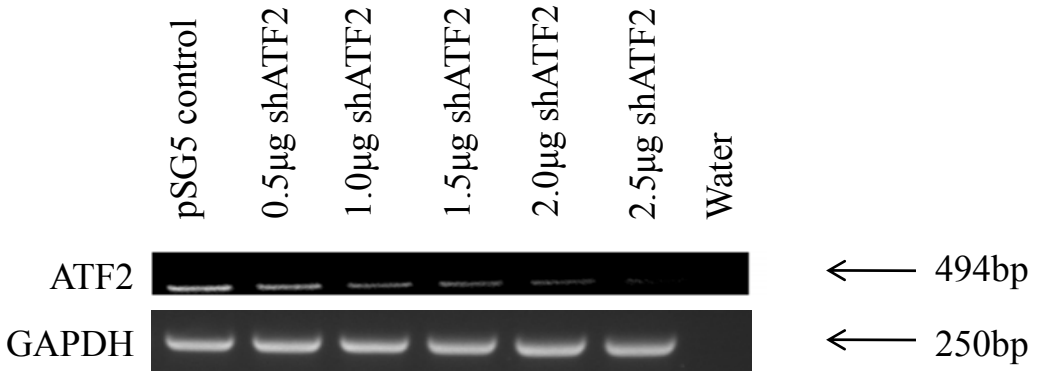

Figure 4.19

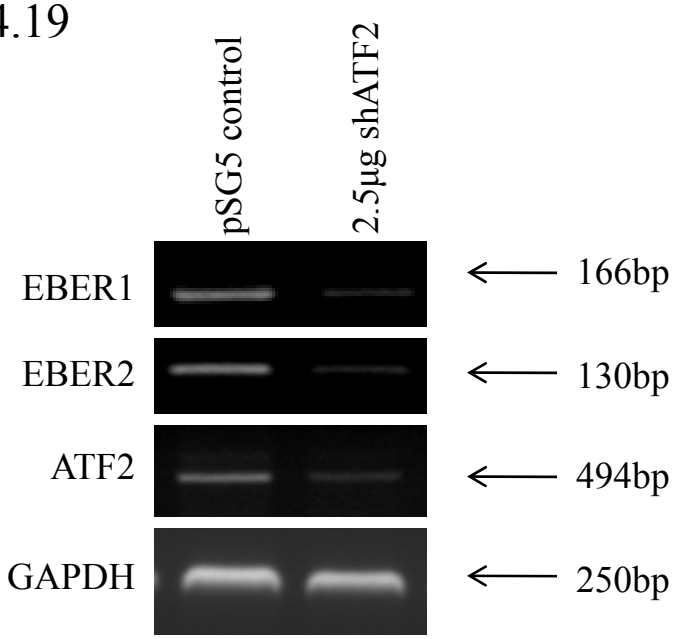

Figure 4.20

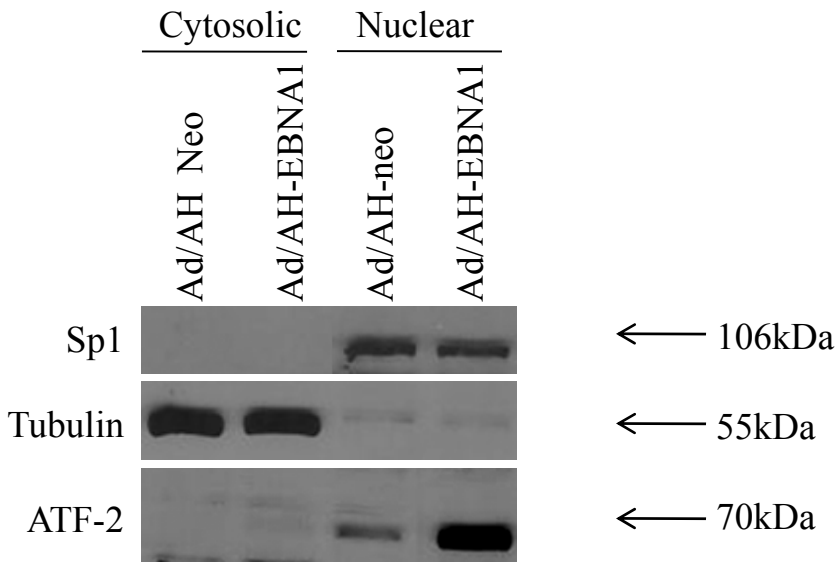

Figure 4.21

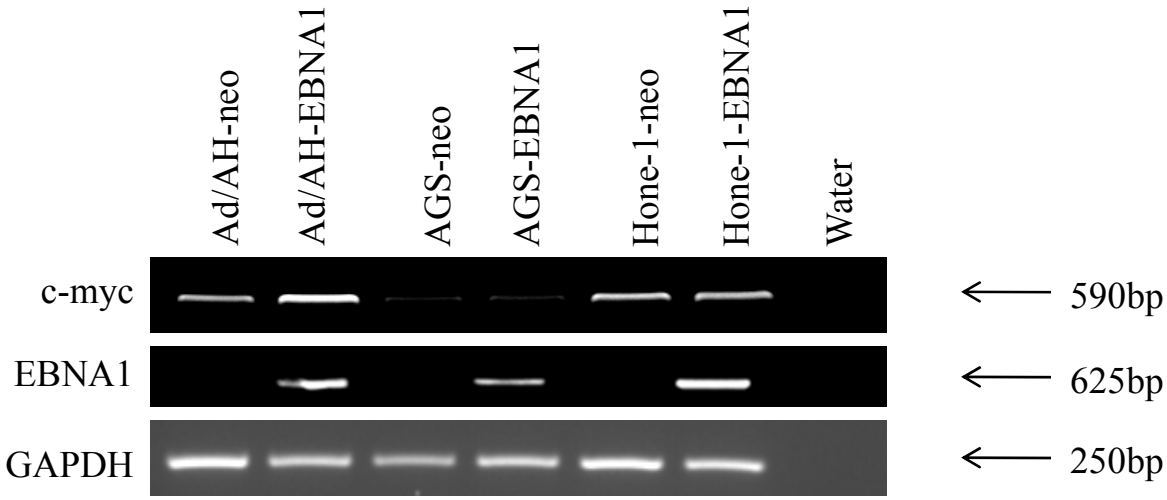

Figure 4.22

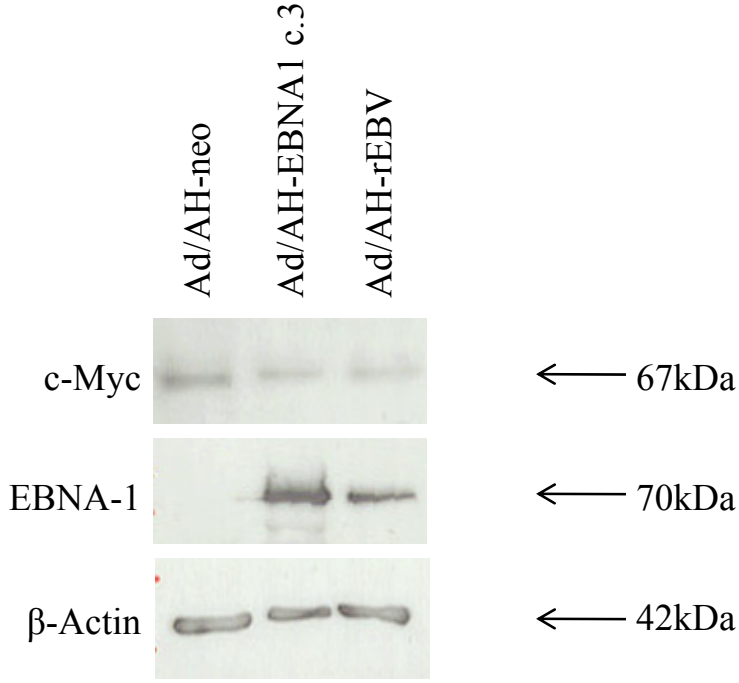

Figure 4.23

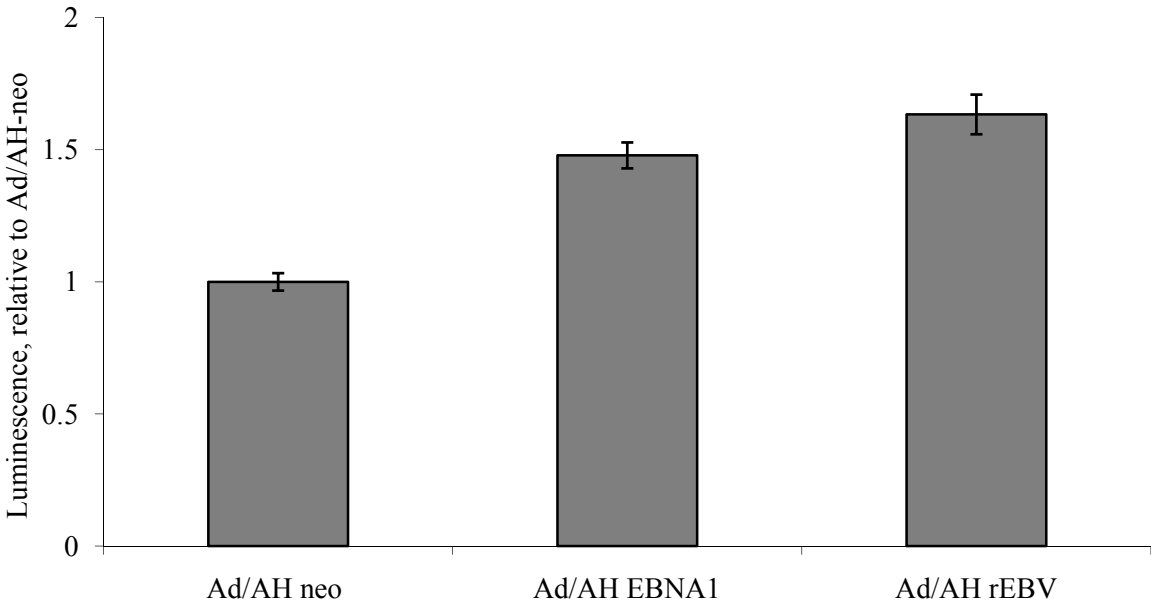

Figure 4.24

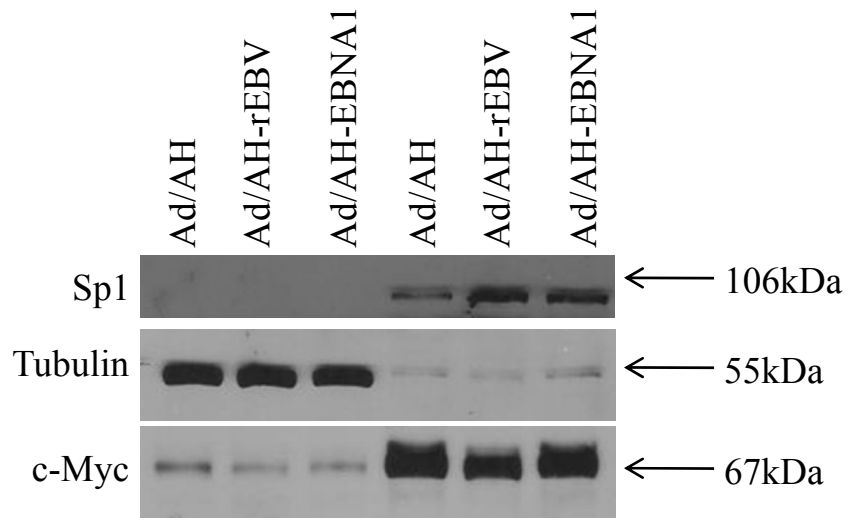

Figure 4.25

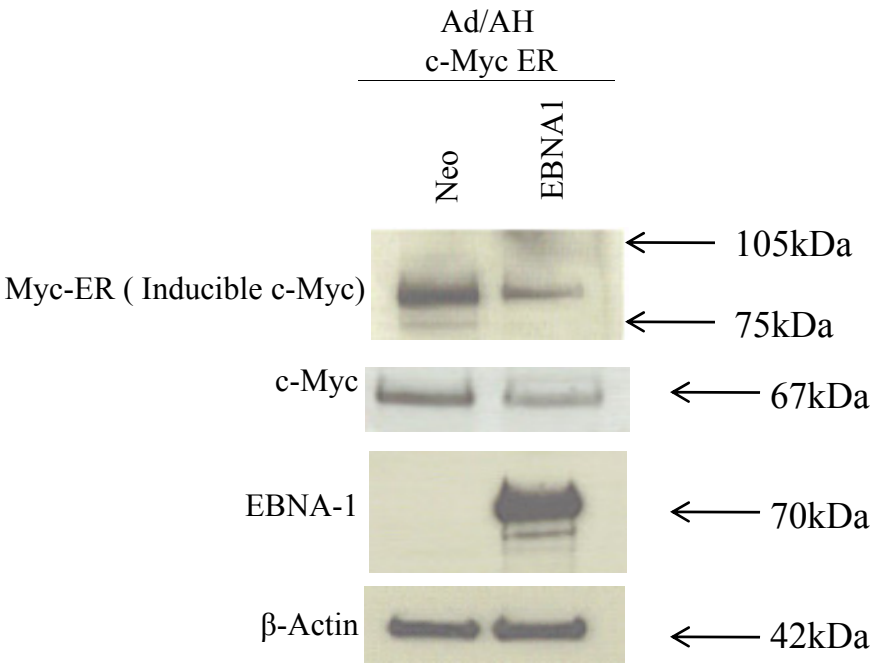

Figure 4.26

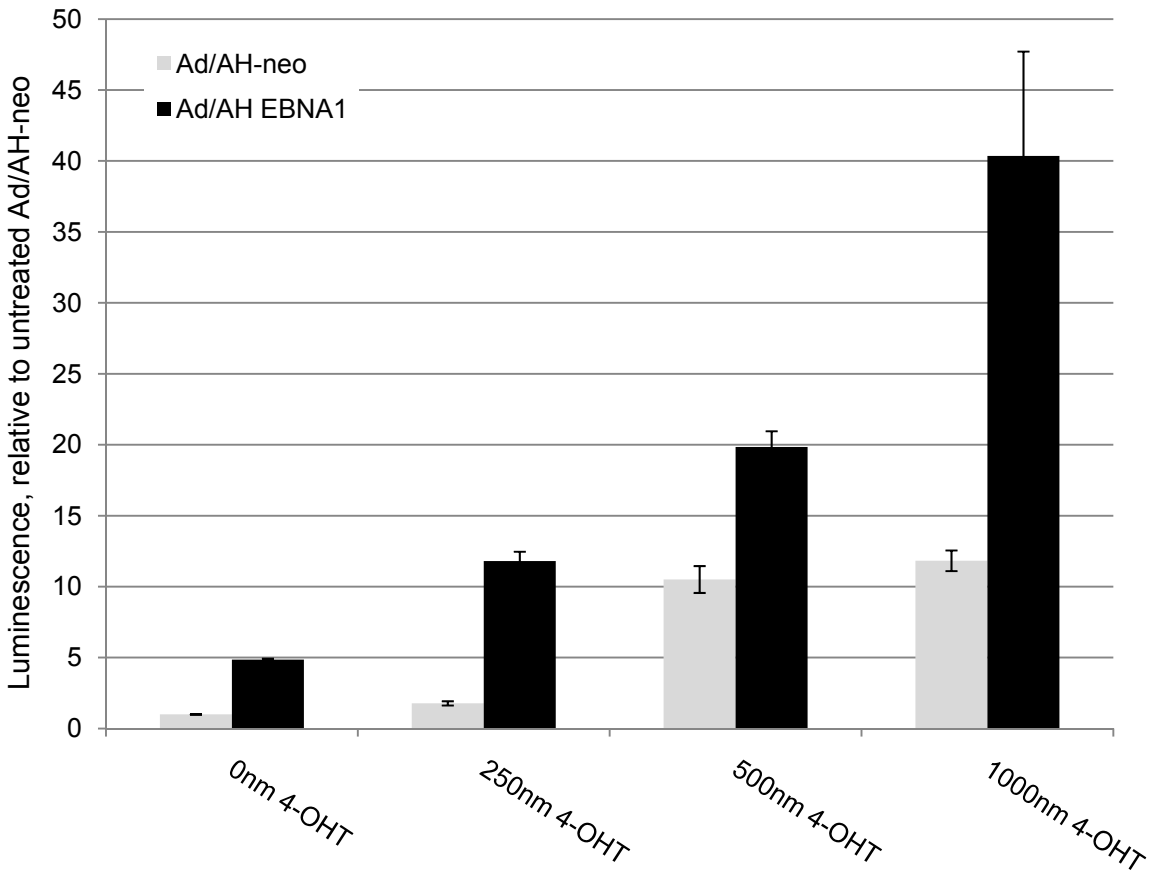

Figure 4.27

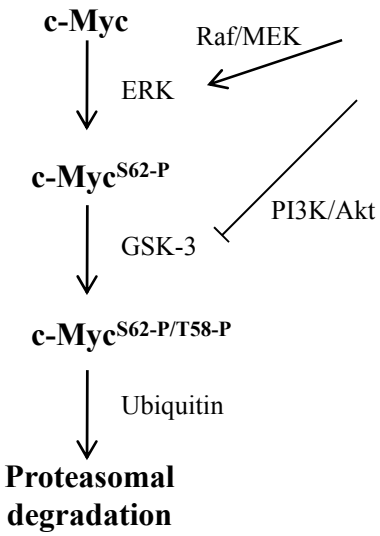

Figure 4.28

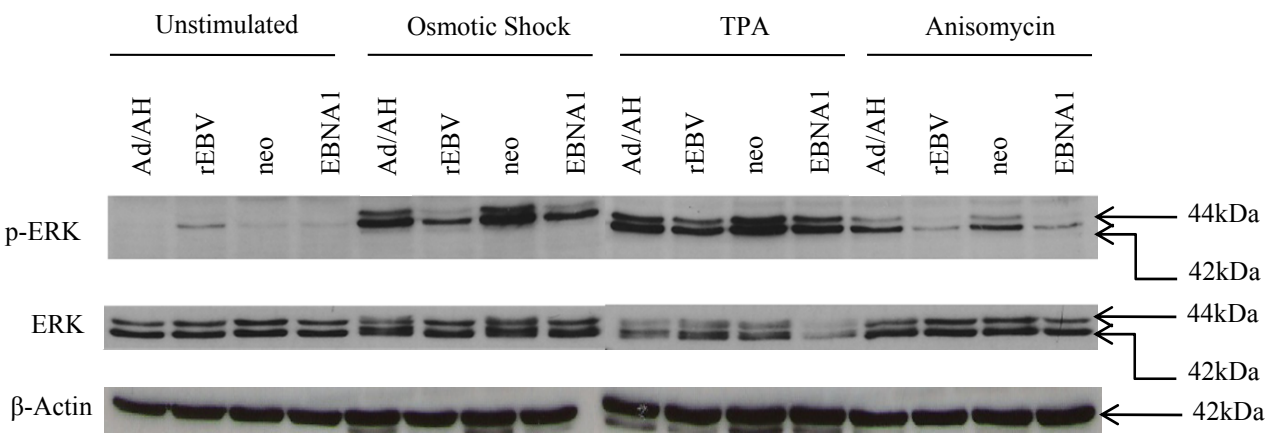

Figure 4.29

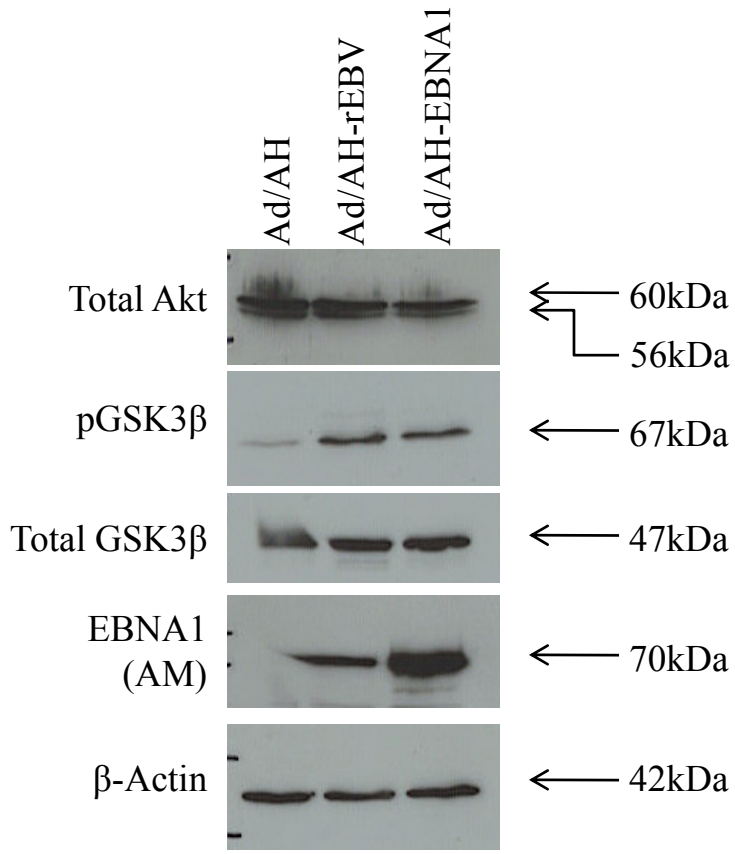

Figure 4.30

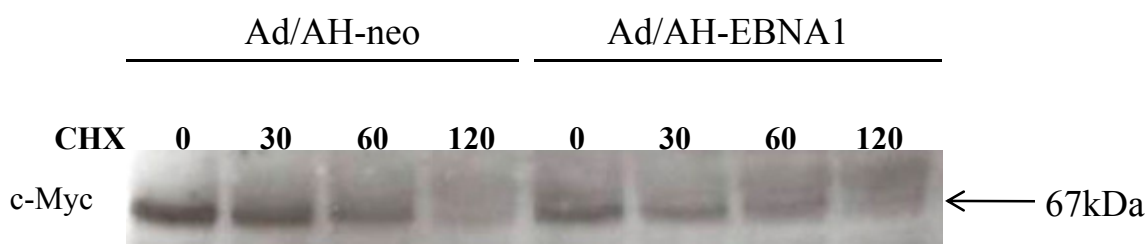

Figure 4.31

Figure 4.32

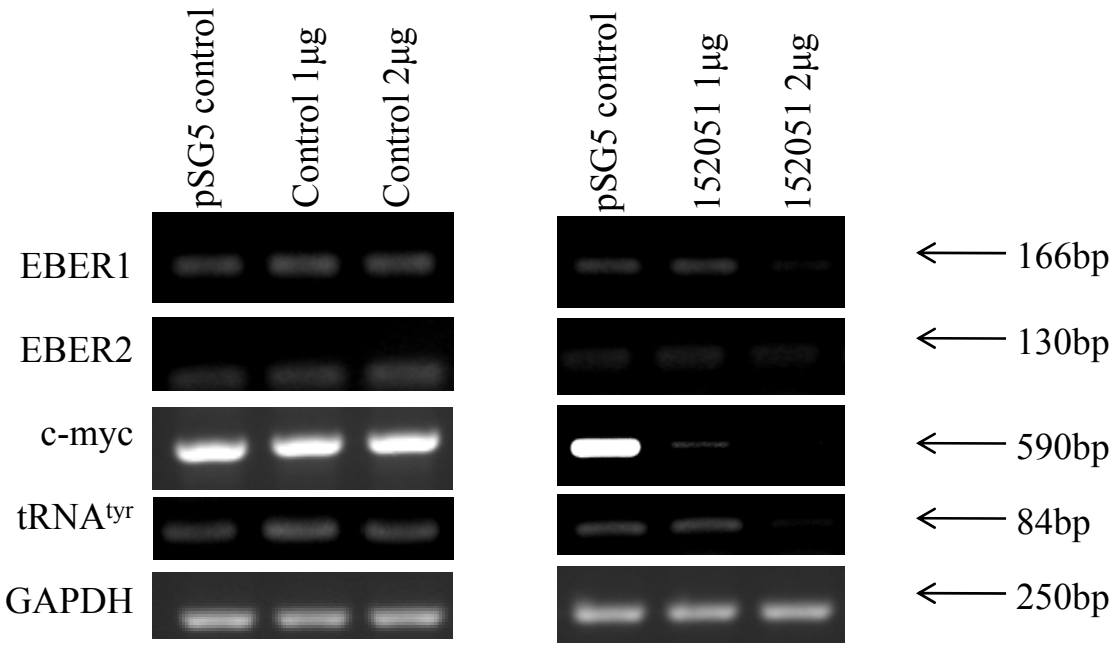

Figure 4.33

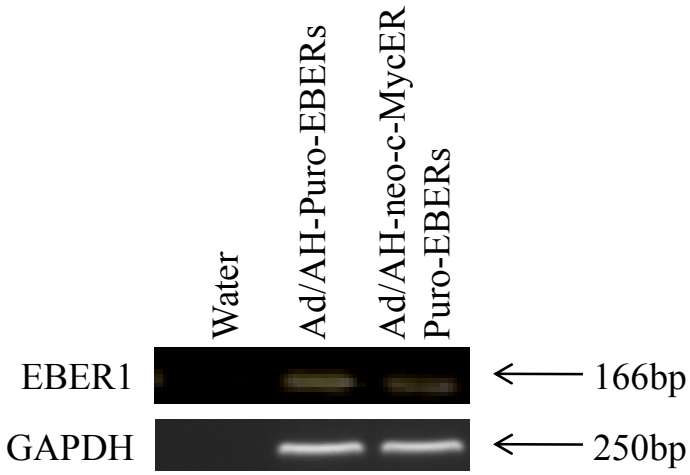

Figure 4.34

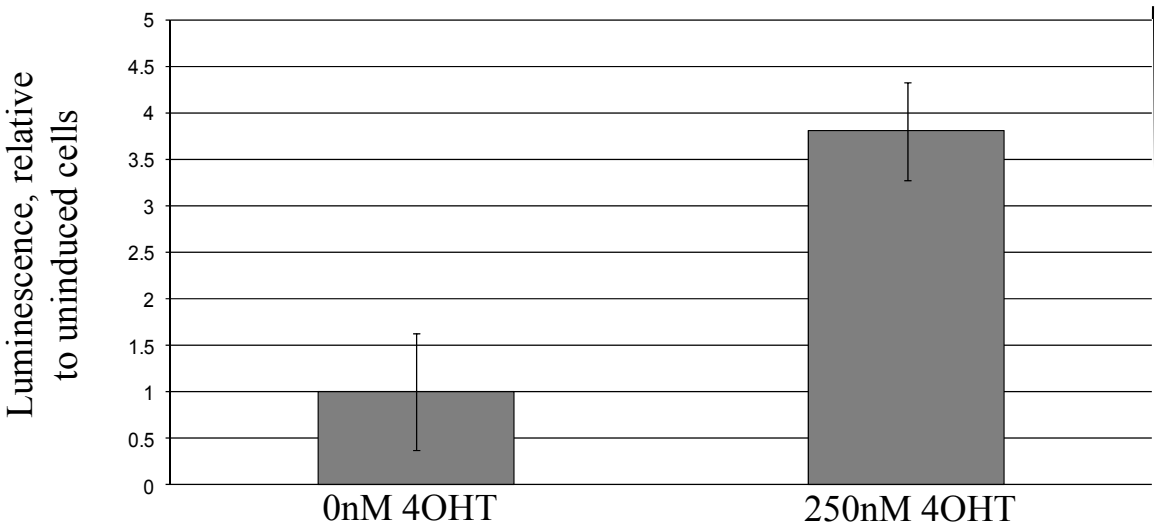

Figure 4.35

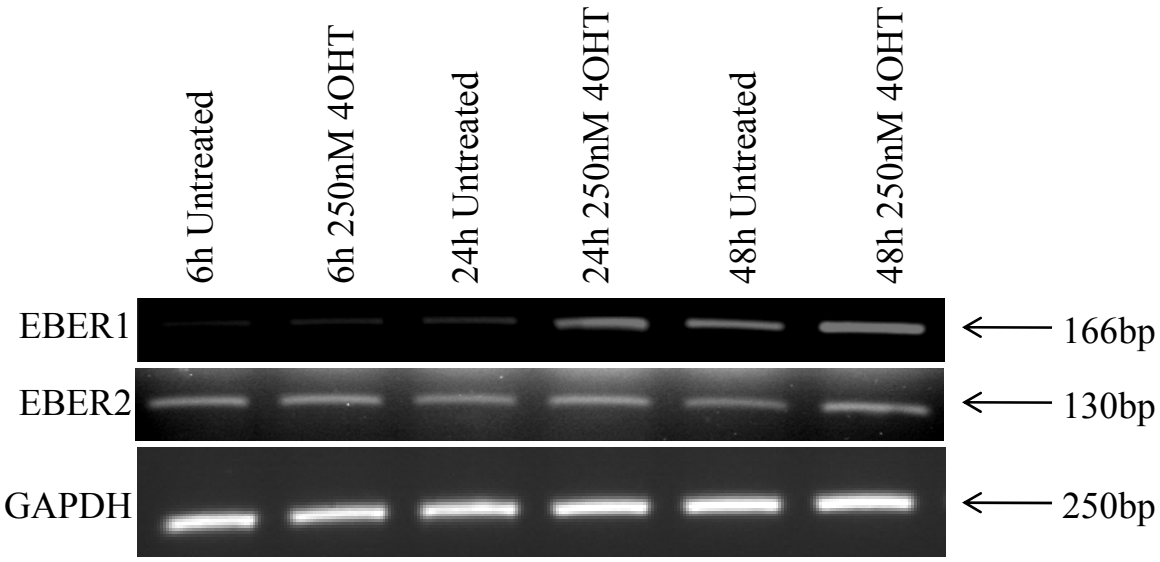

Figure 4.36

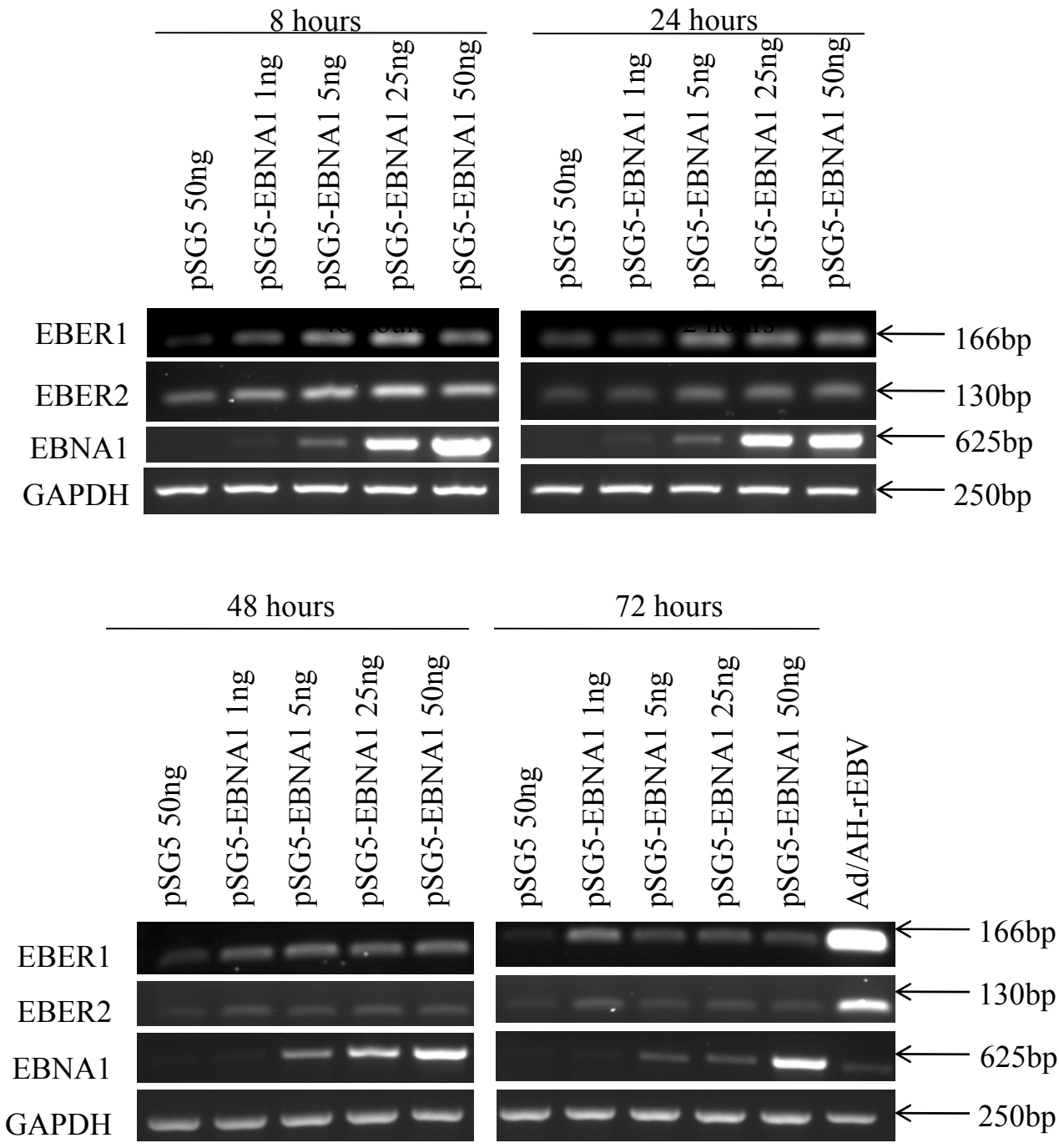
8 hours
24 hours
pSG5 50ng
pSG5-EBNA1 1ng
pSG5-EBNA1 5ng
pSG5-EBNA1 25ng
pSG5-EBNA1 50ng
EBER1
EBER2
EBNA1
GAPDH
166bp
130bp
625bp
250bp
48 hours
72 hours
Ad/AH-rEBV

Figure 4.37

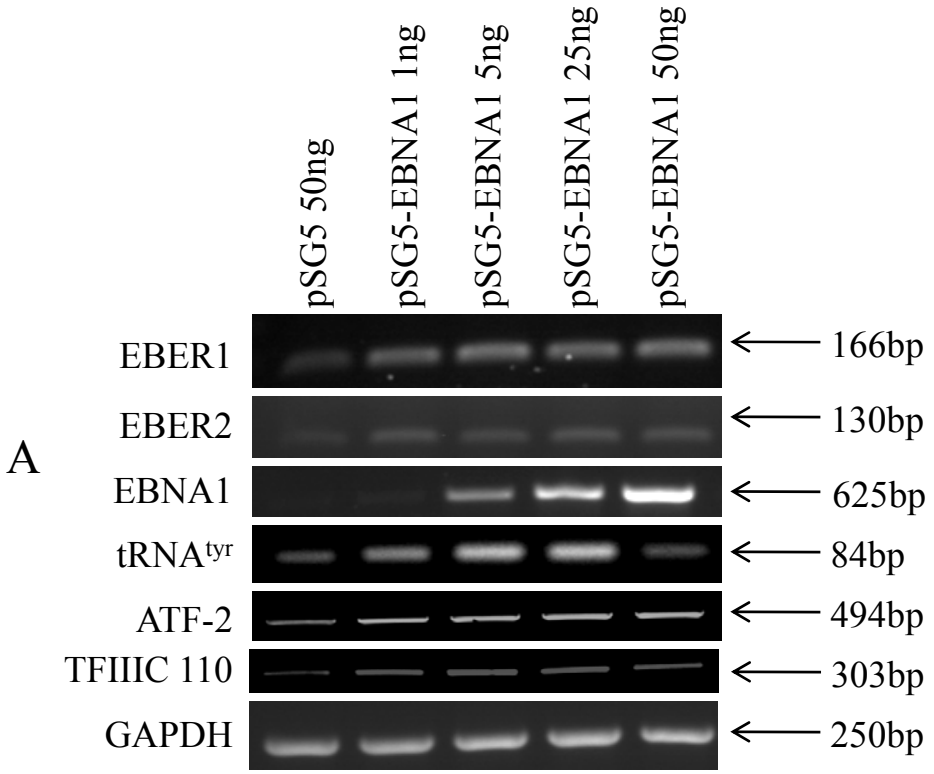
A
pSG5 50ng
pSG5-EBNA1 1ng
pSG5-EBNA1 5ng
pSG5-EBNA1 25ng
pSG5-EBNA1 50ng
EBER1
EBER2
EBNA1
tRNA^tyr
ATF-2
TFIIIC 110
GAPDH
166bp
130bp
625bp
84bp
494bp
303bp
250bp

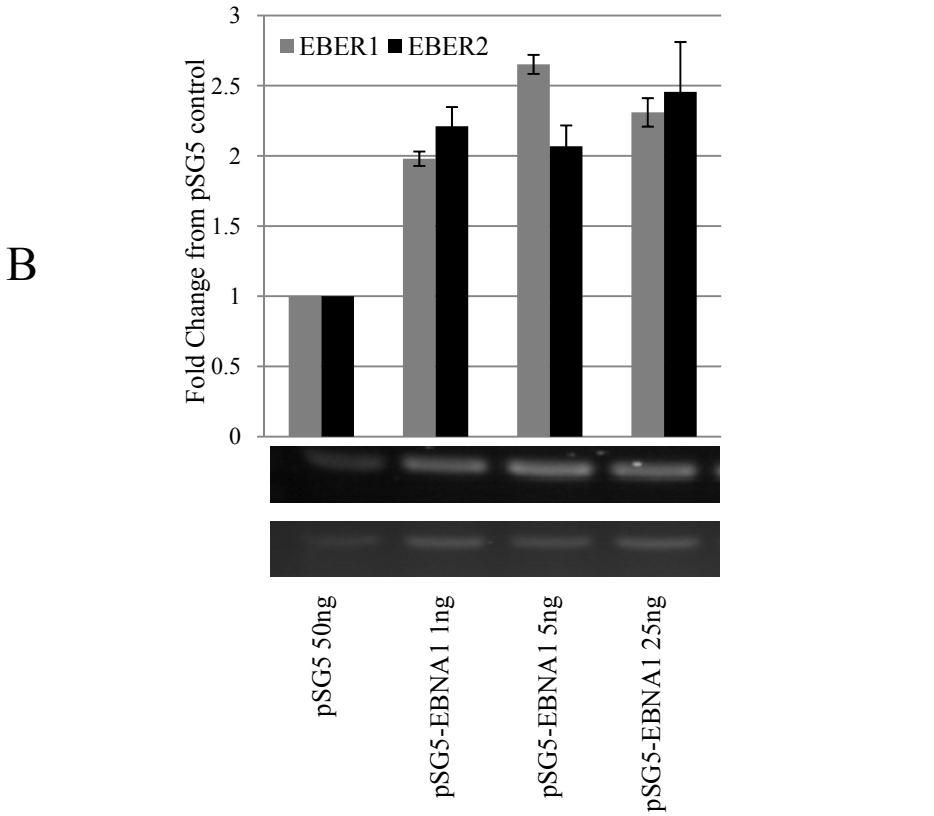
B
EBER1
EBER2
Fold Change from pSG5 control
0
0.5
1
1.5
2
2.5
3
pSG5 50ng
pSG5-EBNA1 1ng
pSG5-EBNA1 5ng
pSG5-EBNA1 25ng

Figure 4.38

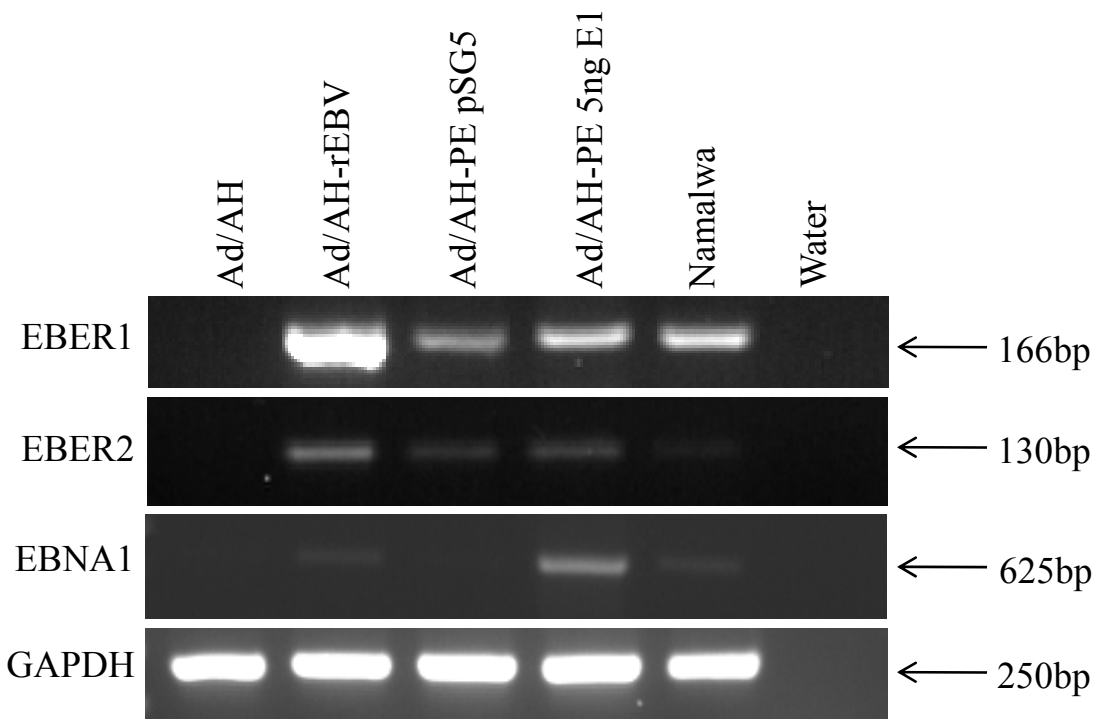
Ad/AH
Ad/AH-rEBV
Ad/AH-PE pSG5
Ad/AH-PE 5ng E1
Namalwa
Water
EBER1
EBER2
EBNA1
GAPDH
166bp
130bp
625bp
250bp

Figure 4.39

AliBaba2.1 predicts the following sites in your sequence

Sequence seq_247

Wild-type X-Box sequence

```
seq(    0..   59)    cgaccgcgccaccagatggcacacgtgggggaaat
Segments:
1.3.2.1     18   27                        ===c-Myc==
1.3.2.2     18   27                       ====Max1==
1.3.1.2     19   28                        ====USF===
2.3.1.0     21   30                          ====Sp1===
4.1.1.0     27   37                                =====D1====
9.9.590     27   37                                ==NF-kappaB
2.3.4.0     28   37                                 =MBP-1 (1)
9.9.213     28   37                                 ===EBP-1==

8 segments in this sequence identified as potential binding sites
```

AliBaba2.1 predicts the following sites in your sequence

Sequence seq_246

Mutant X-Box sequence

```
seq(    0..   59)    cgaccgcgccaccagagagcacacggaggggaaat
Segments:
9.9.590     27   37                                ==NF-kappaB
2.3.4.0     28   37                                 ==AGIE-BP1
4.1.1.0     28   37                                 =NF-kappaB
9.9.213     28   37                                 ===EBP-1==

4 segments in this sequence identified as potential binding sites
```

Figure 4.40

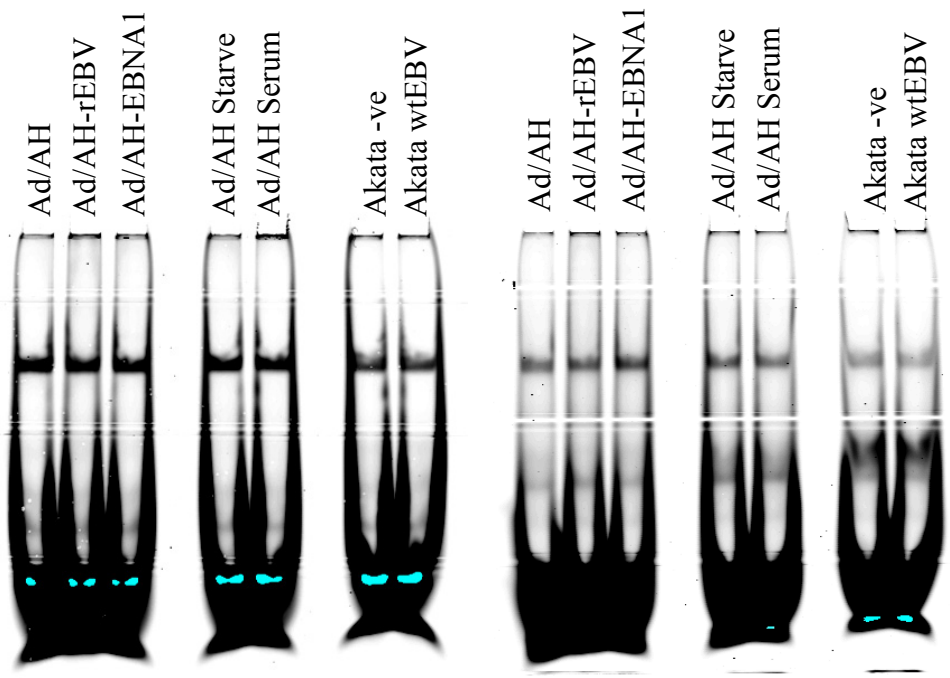

Figure 4.41

Figure 4.42

AliBaba2.1 predicts the following sites in your sequence

Sequence seq_196

==========

seq(0.. 59) cggggtctcggagctgtgggggaaatgagg

Segments:

2.3.1.0	12	21	====Sp1===
3.5.2.0	18	27	===Elf-1==
2.2.1.1	22	31	===GATA-1=

3 segments in this sequence identified as potential binding sites

---

3 segments in complete file identified as potential binding sites

Figure 4.43

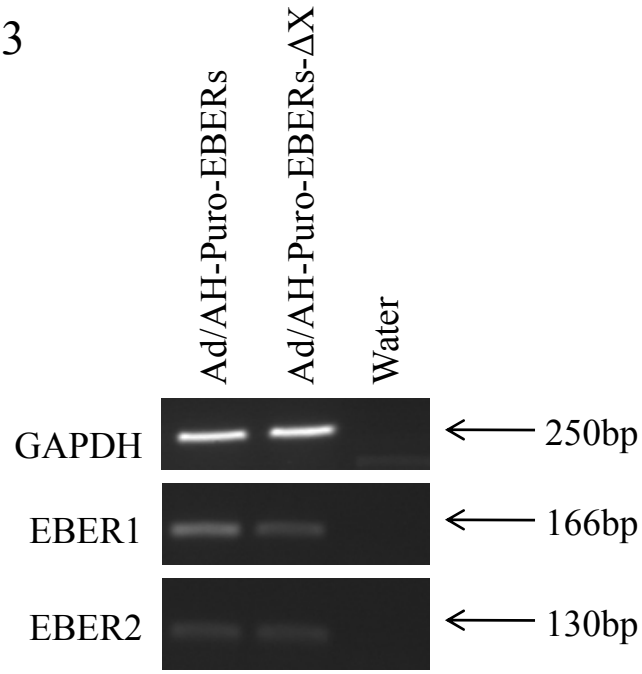

Figure 4.44

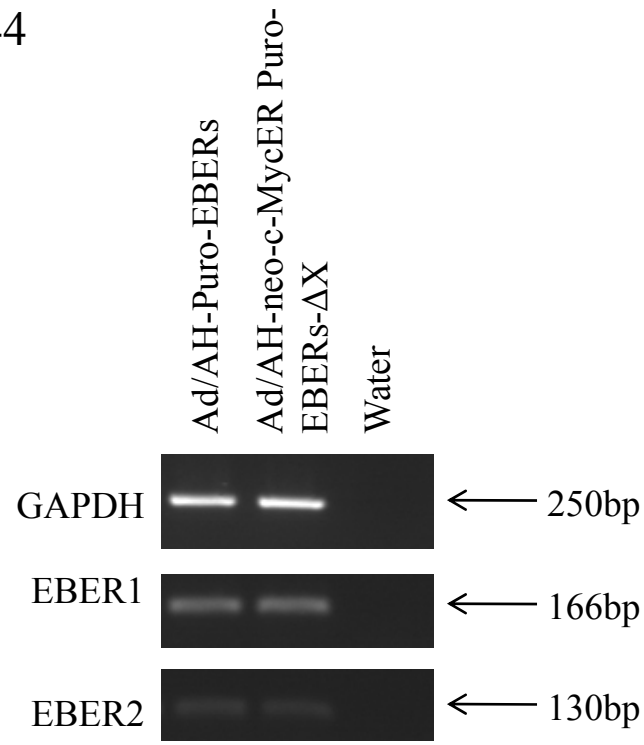

Figure 4.45

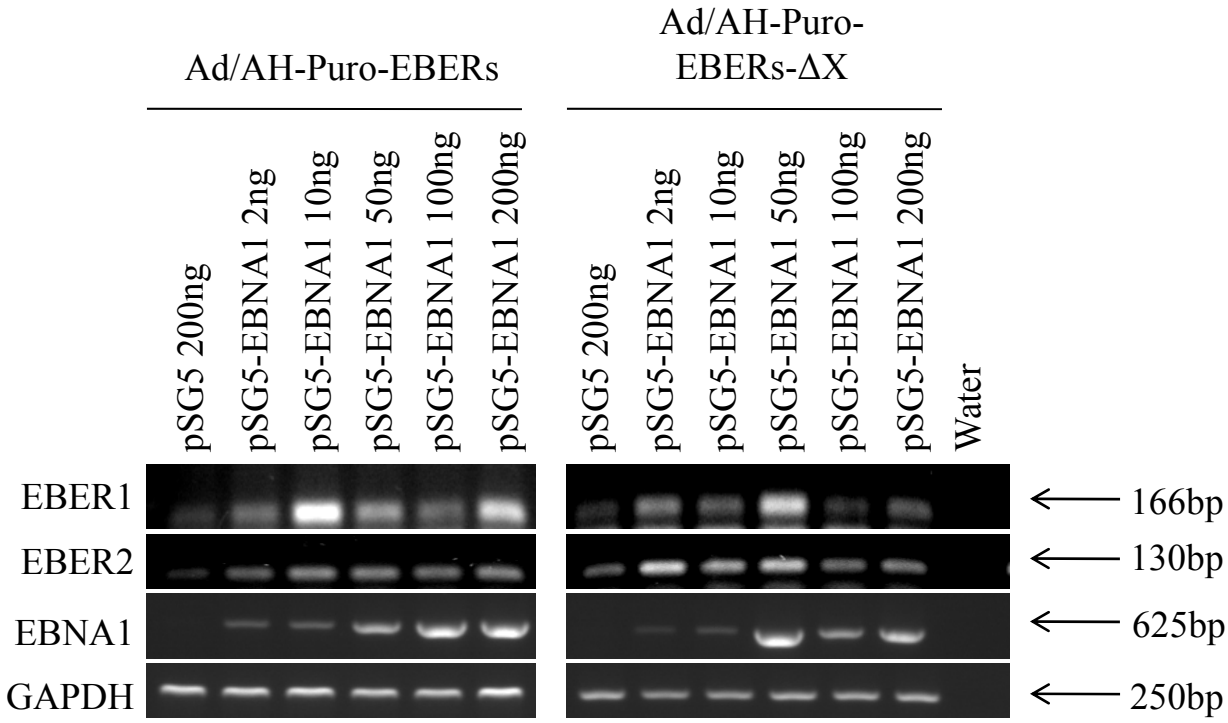

Figure 4.46

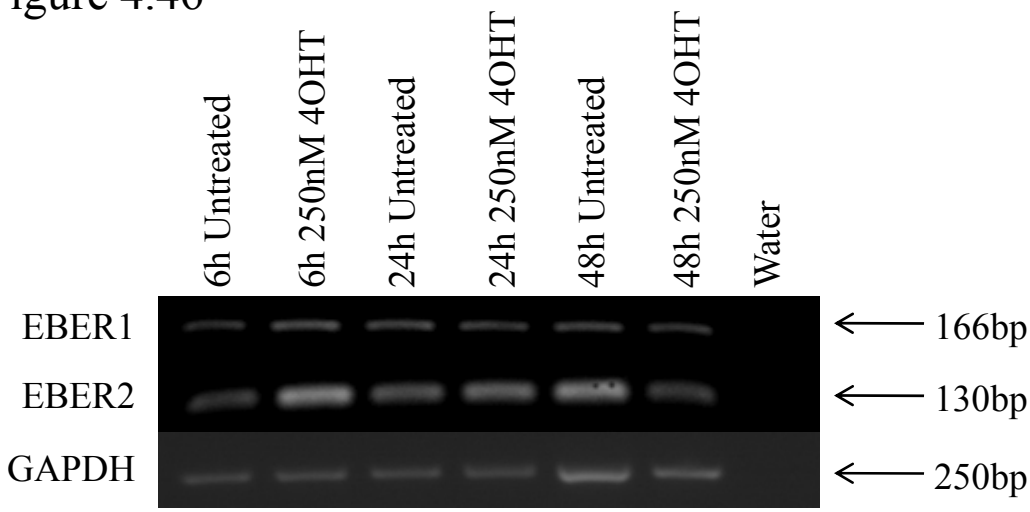

Figure 4.47

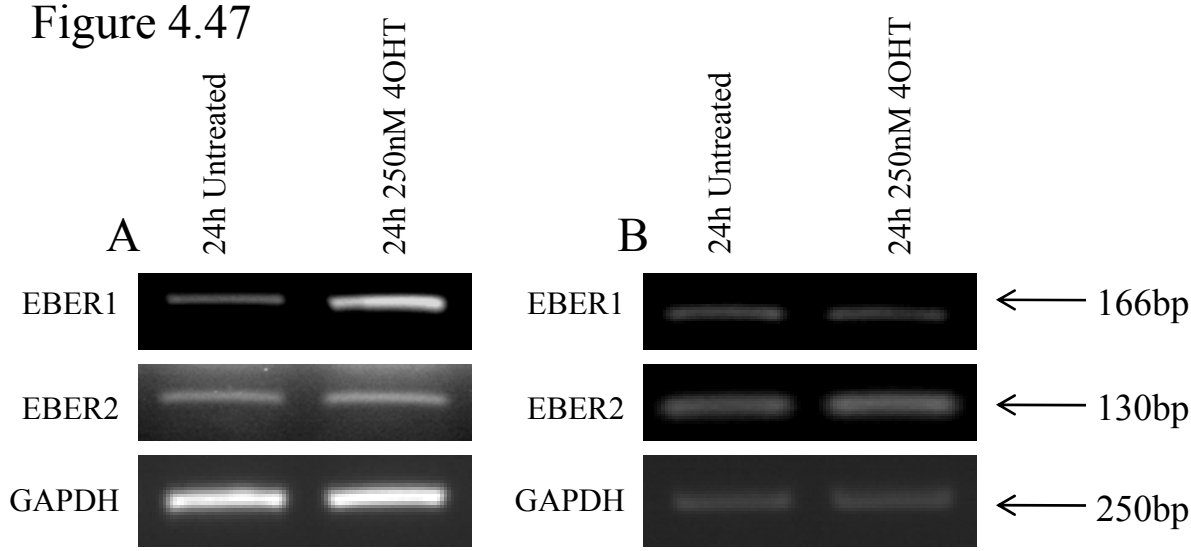

Figure 4.48

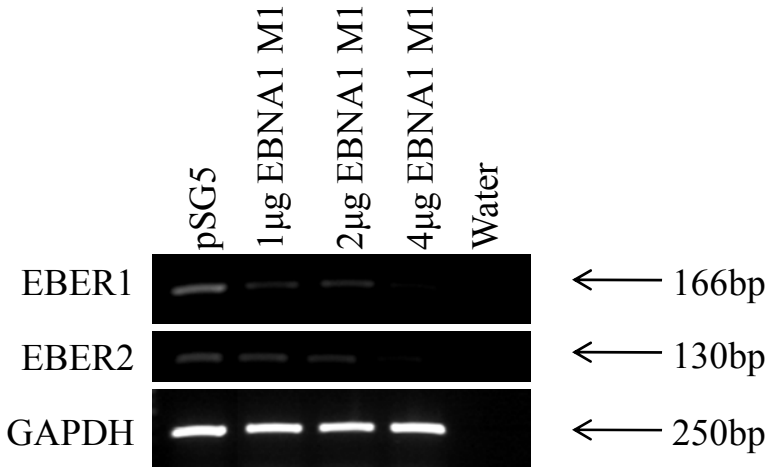

Figure 4.49

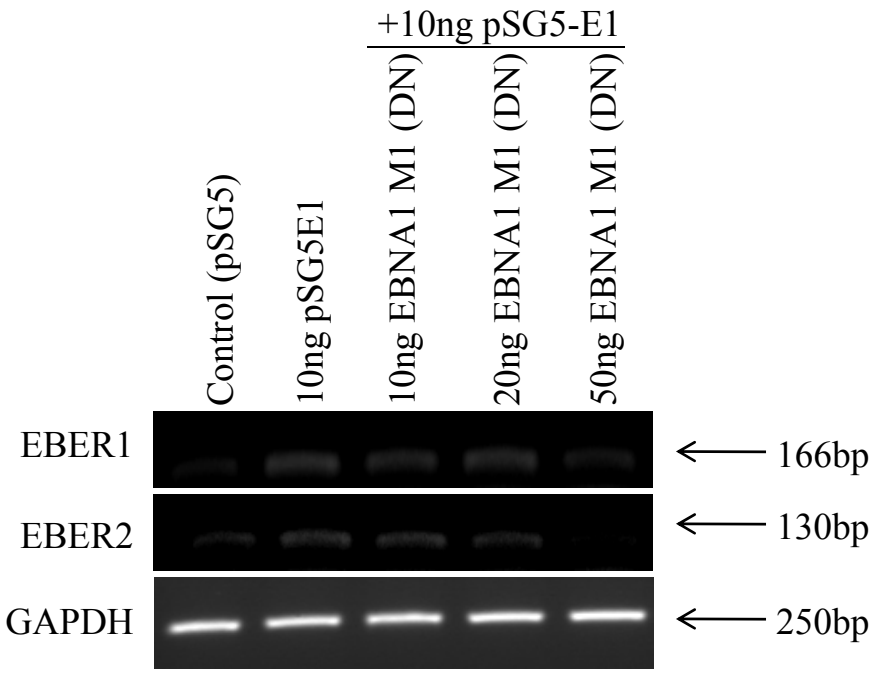

Figure 4.50

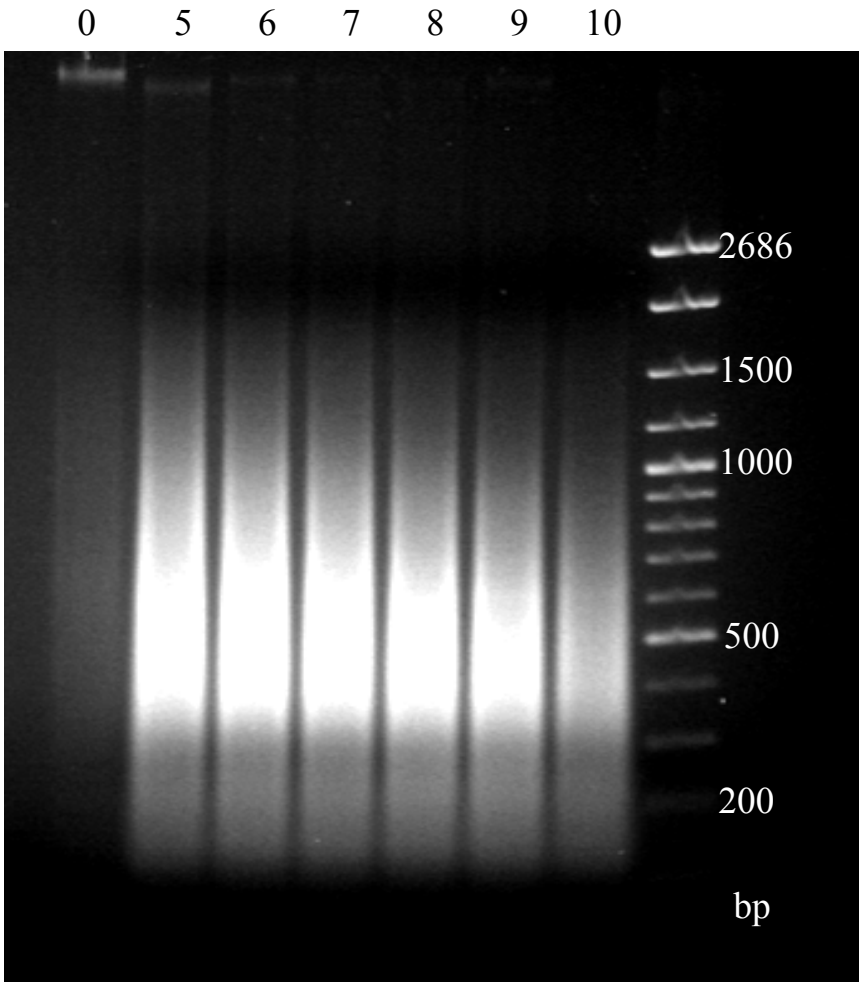

Figure 5.1

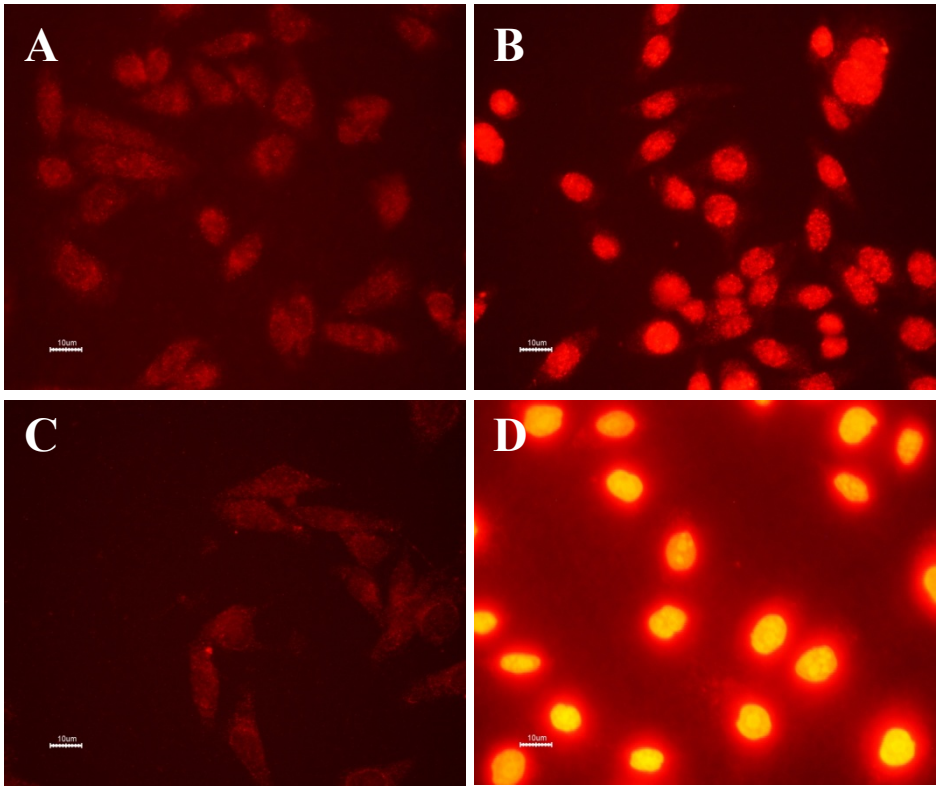

Figure 5.2

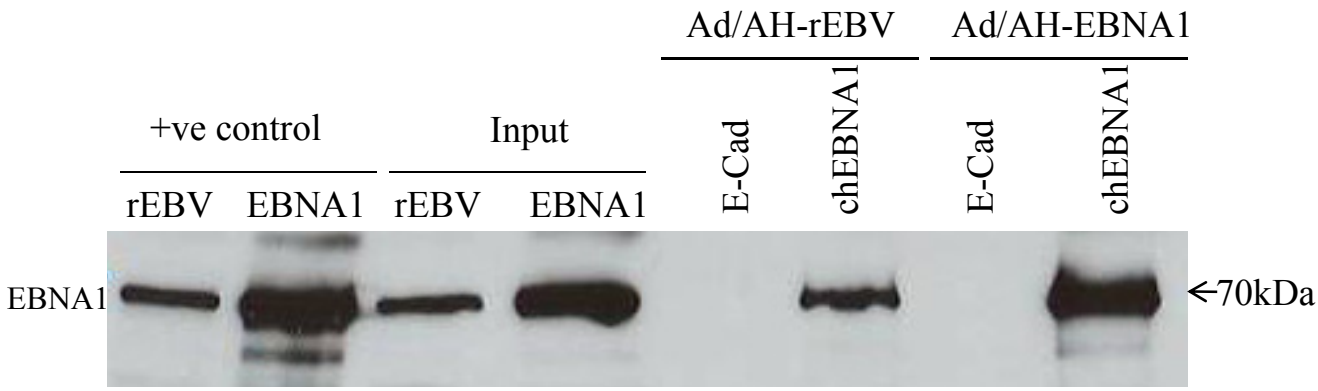

Figure 5.3

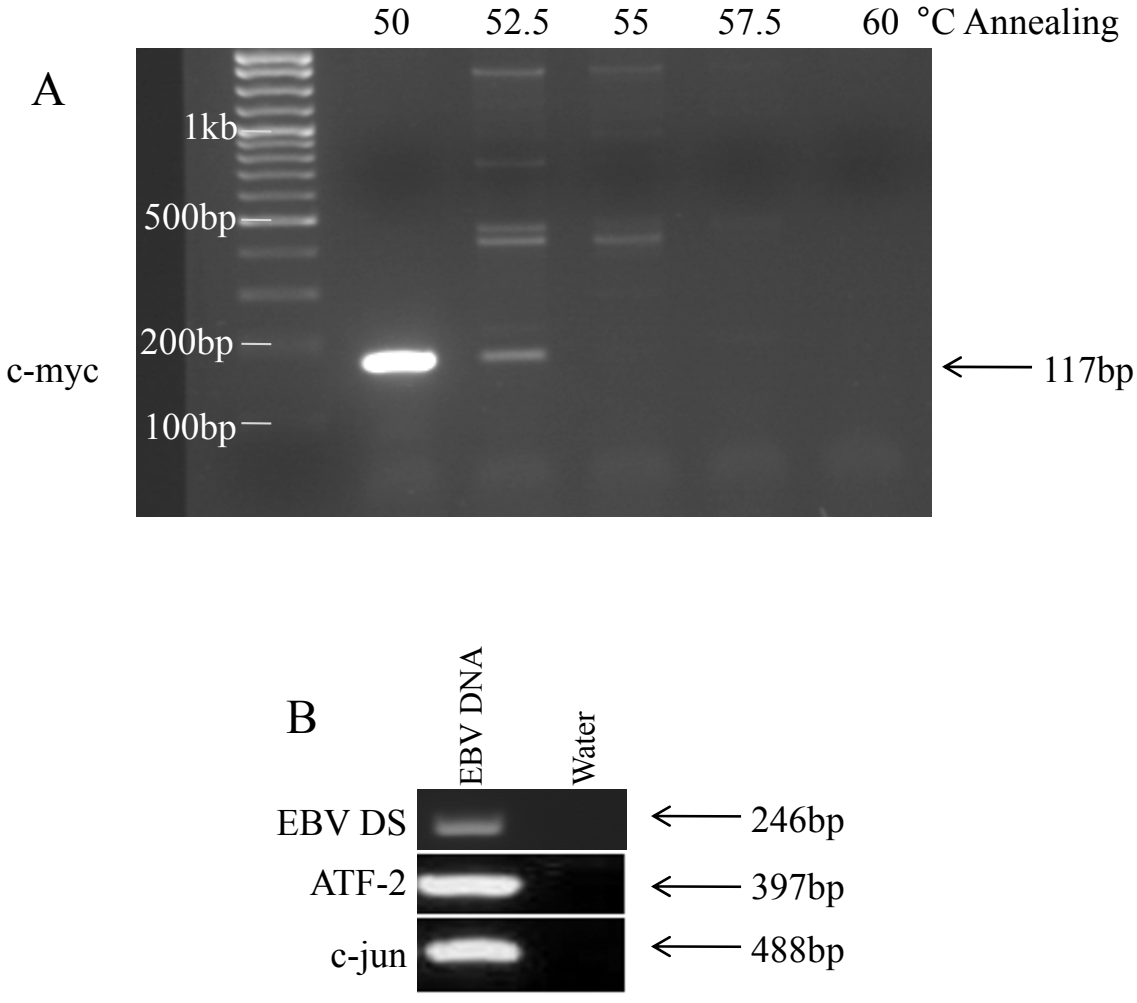

Figure 5.4

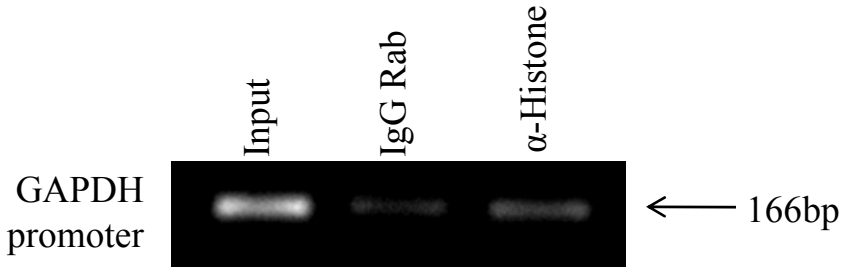

Figure 5.5A

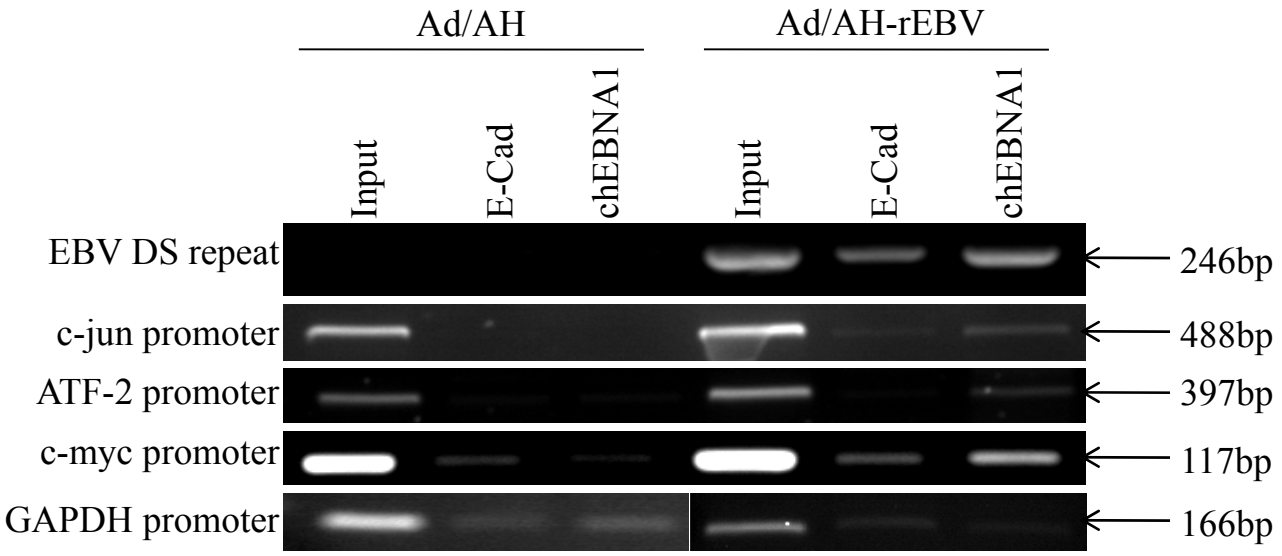

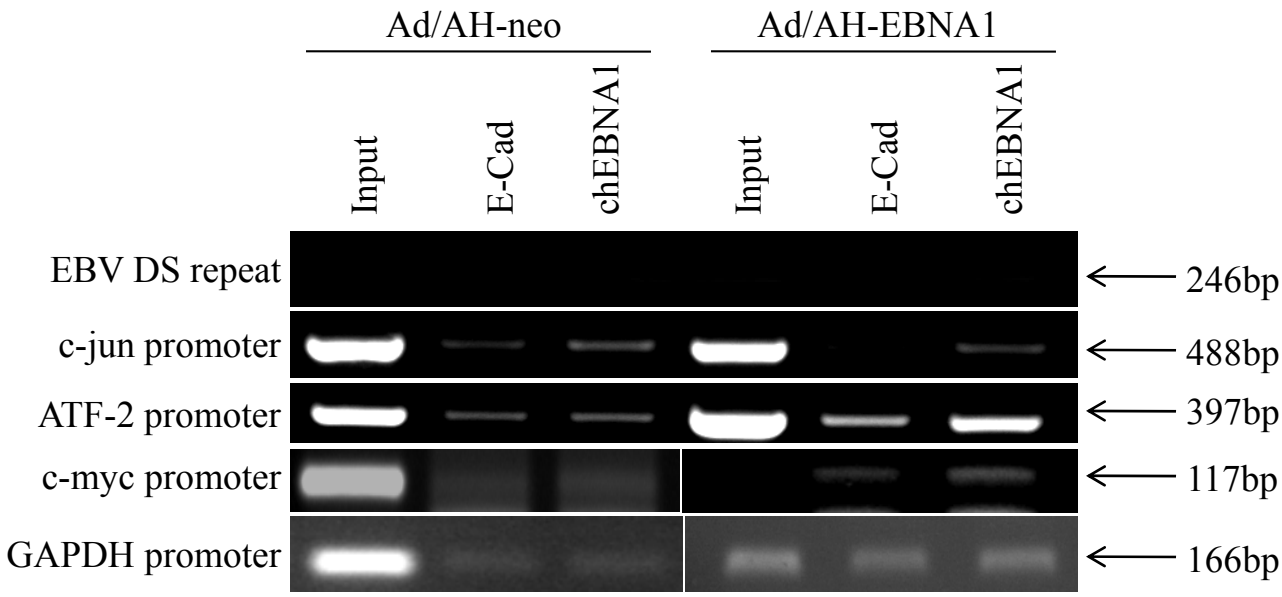

Figure 5.5B

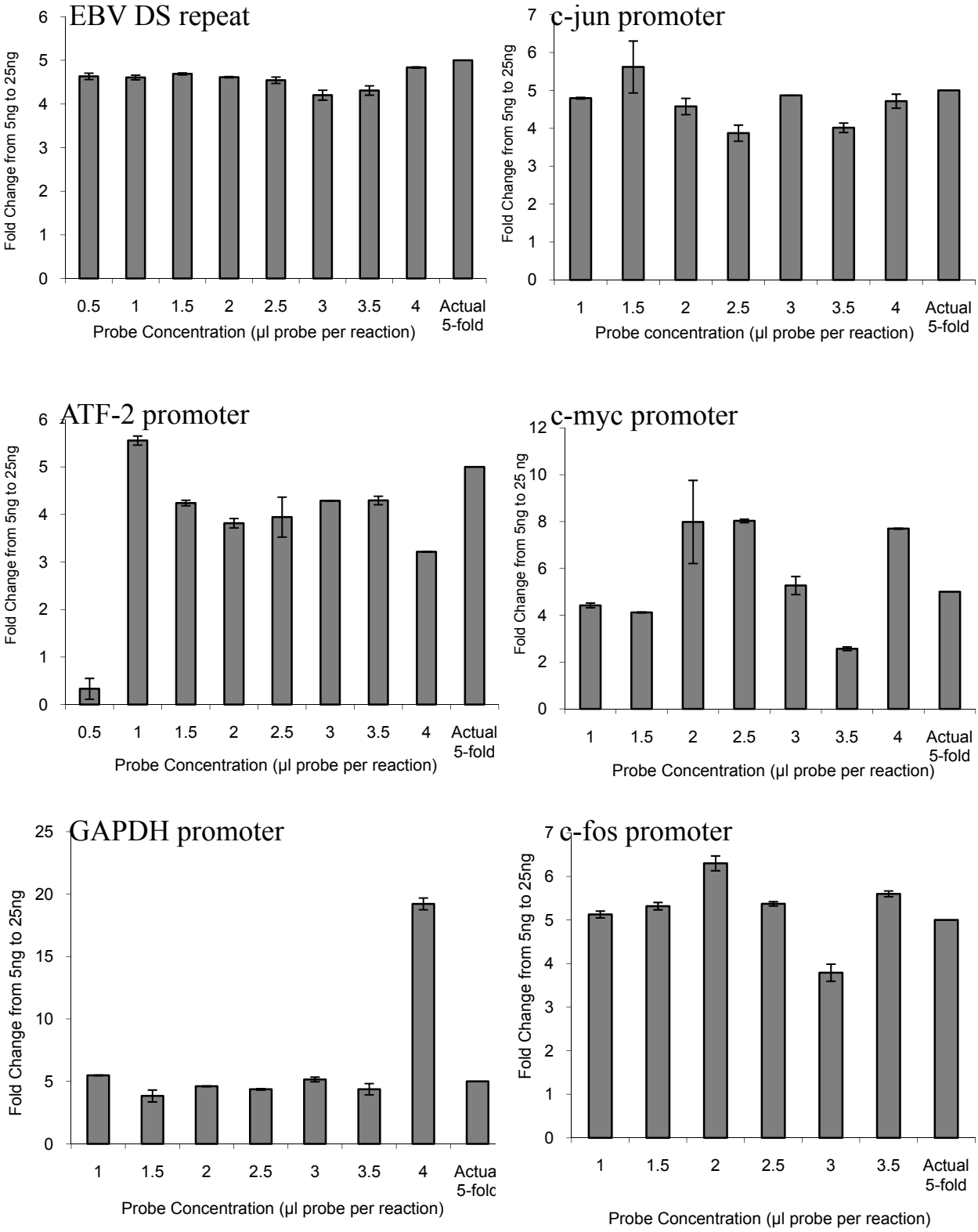
EBV DS repeat
Fold Change from 5ng to 25ng
0 1 2 3 4 5 6
0.5 1 1.5 2 2.5 3 3.5 4 Actual 5-fold
Probe Concentration (µl probe per reaction)
c-jun promoter
Fold Change from 5ng to 25ng
0 1 2 3 4 5 6 7
1 1.5 2 2.5 3 3.5 4 Actual 5-fold
Probe concentration (µl probe per reaction)
ATF-2 promoter
Fold Change from 5ng to 25ng
0 1 2 3 4 5 6
0.5 1 1.5 2 2.5 3 3.5 4 Actual 5-fold
Probe Concentration (µl probe per reaction)
c-myc promoter
Fold Change from 5ng to 25 ng
0 2 4 6 8 10 12
1 1.5 2 2.5 3 3.5 4 Actual 5-fold
Probe Concentration (µl probe per reaction)
GAPDH promoter
Fold Change from 5ng to 25ng
0 5 10 15 20 25
1 1.5 2 2.5 3 3.5 4 Actua 5-fold
Probe Concentration (µl probe per reaction)
c-fos promoter
Fold Change from 5ng to 25ng
0 1 2 3 4 5 6 7
1 1.5 2 2.5 3 3.5 Actual 5-fold
Probe Concentration (µl probe per reaction)

Figure 5.6

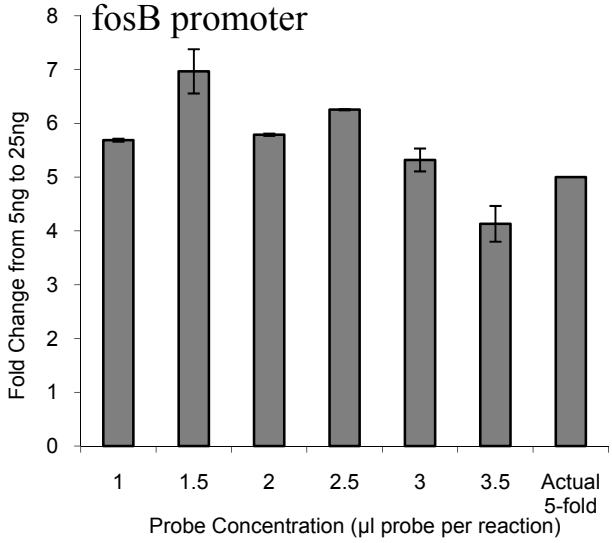

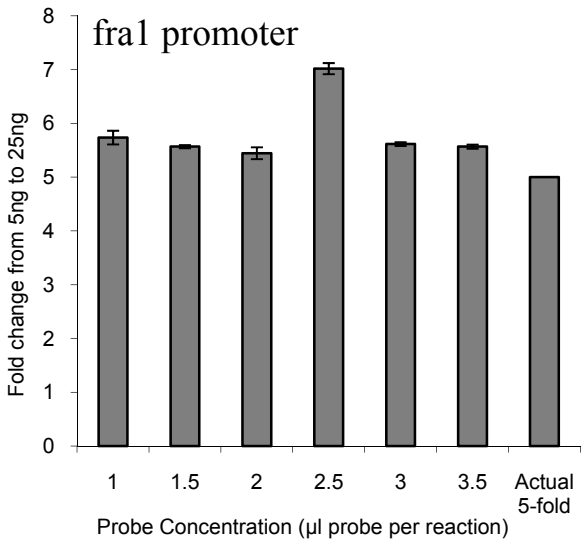

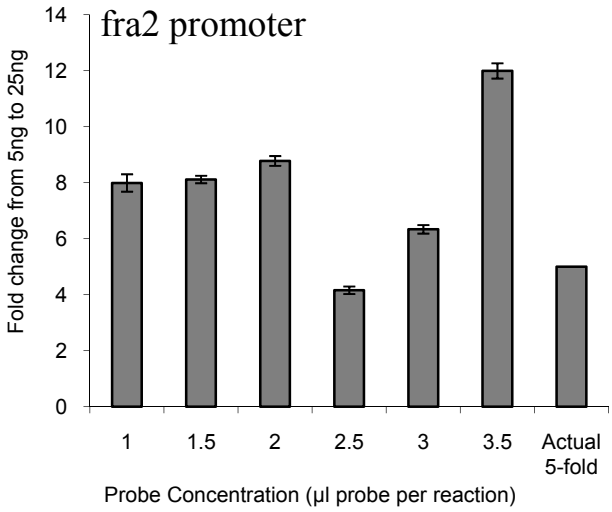

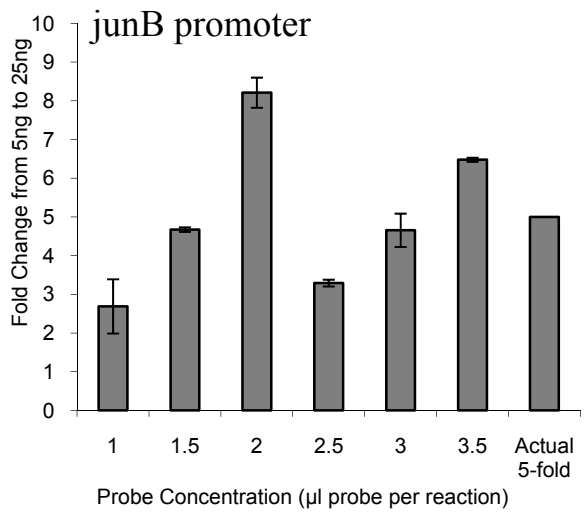

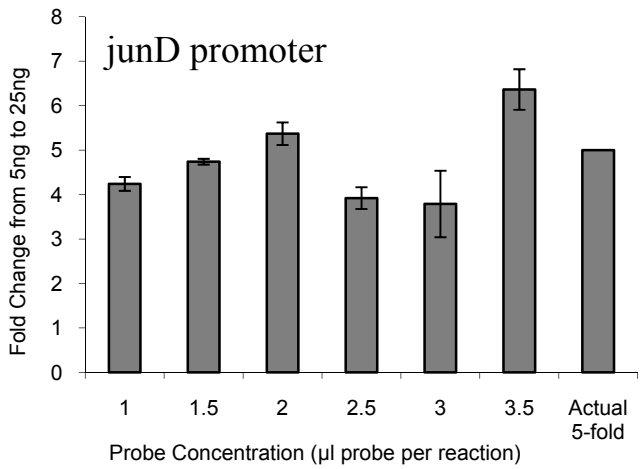

Figure 5.6 ctd.

A

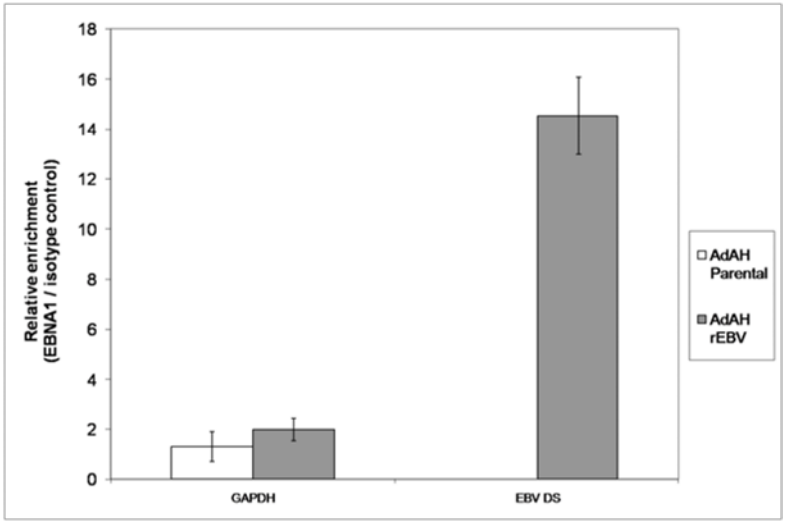

B

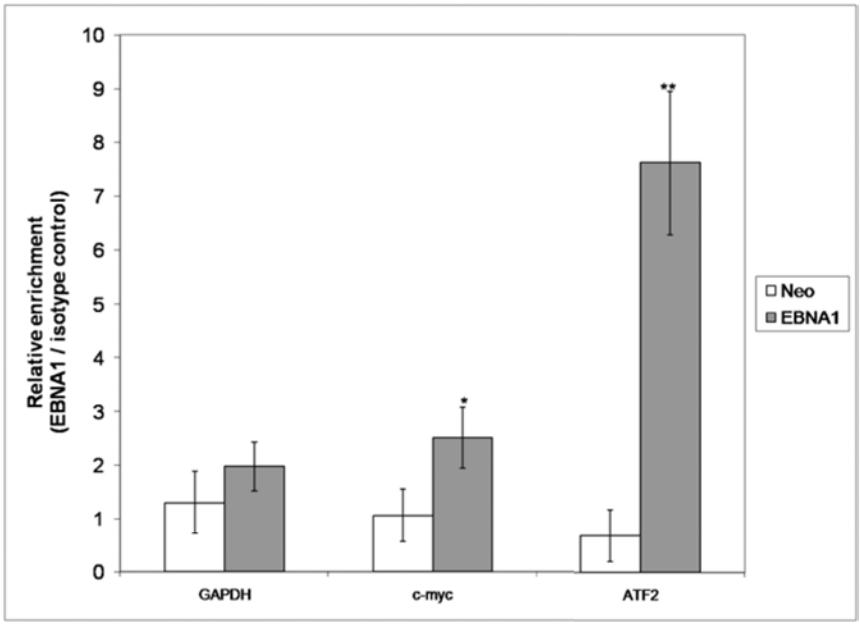

C

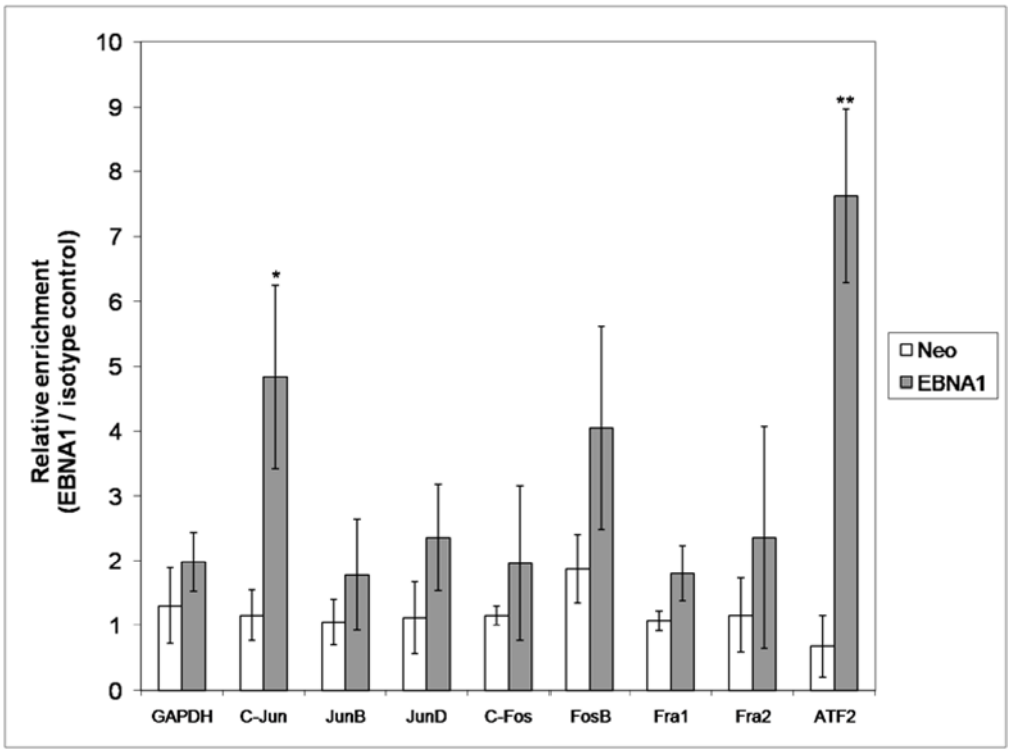

Figure 5.7

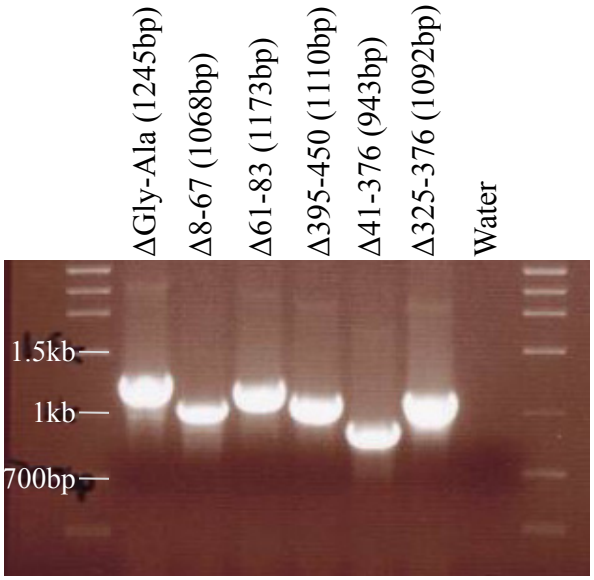

Figure 5.8

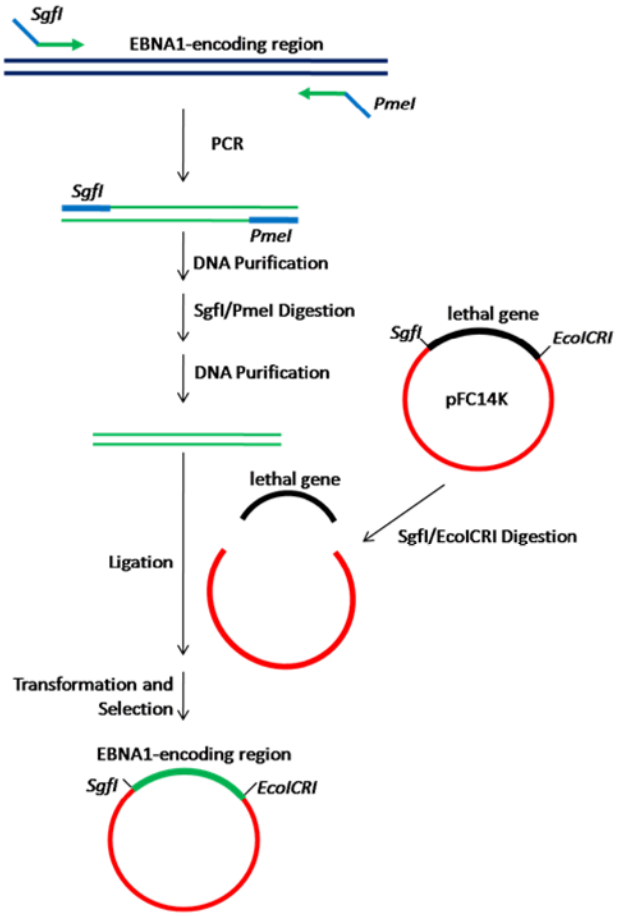

Figure 5.9

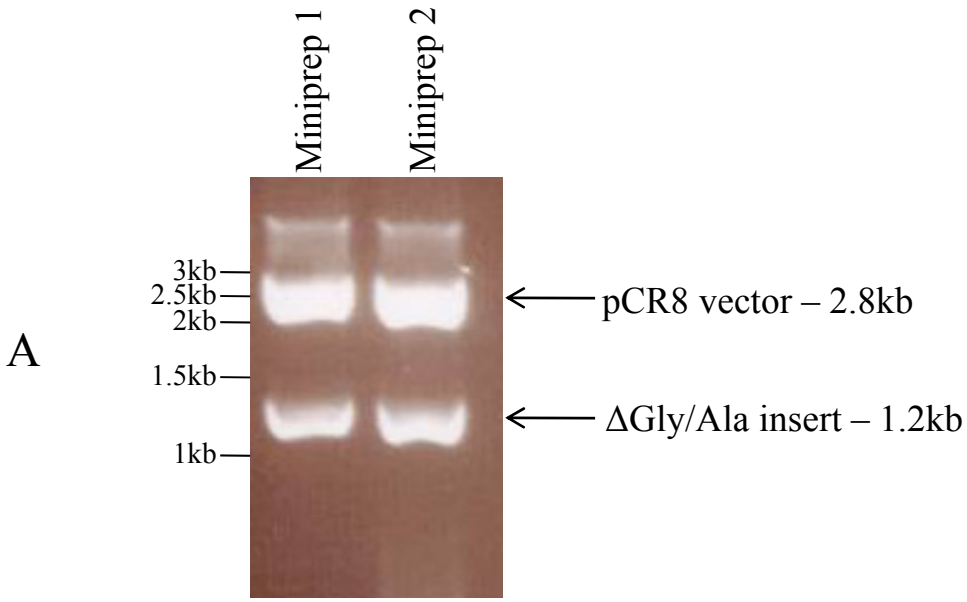
Miniprep 1
Miniprep 2
A
3kb
2.5kb
2kb
1.5kb
1kb
pCR8 vector – 2.8kb
ΔGly/Ala insert – 1.2kb

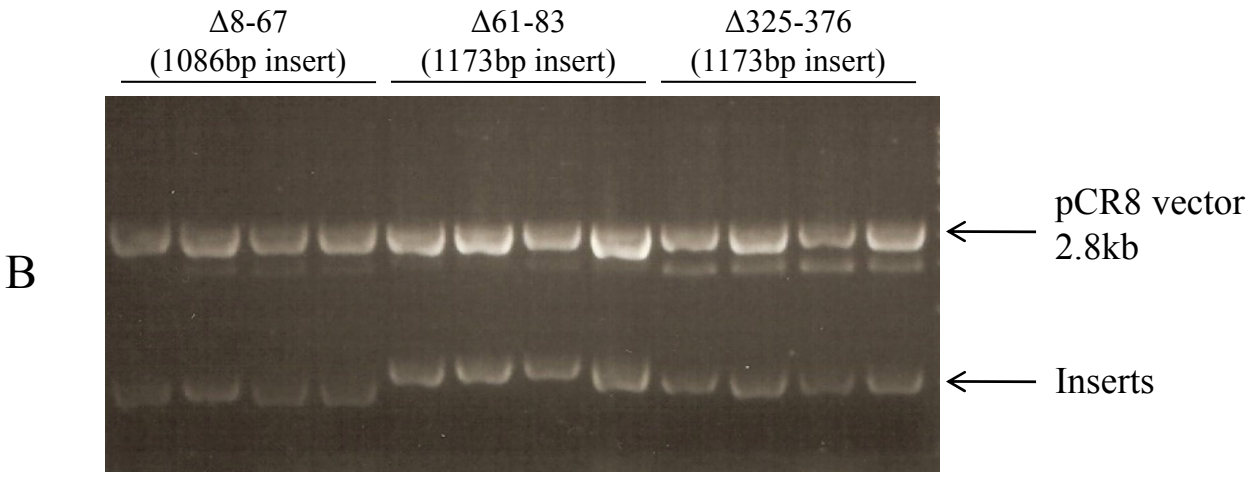
Δ8-67
(1086bp insert)
Δ61-83
(1173bp insert)
Δ325-376
(1173bp insert)
B
pCR8 vector
2.8kb
Inserts

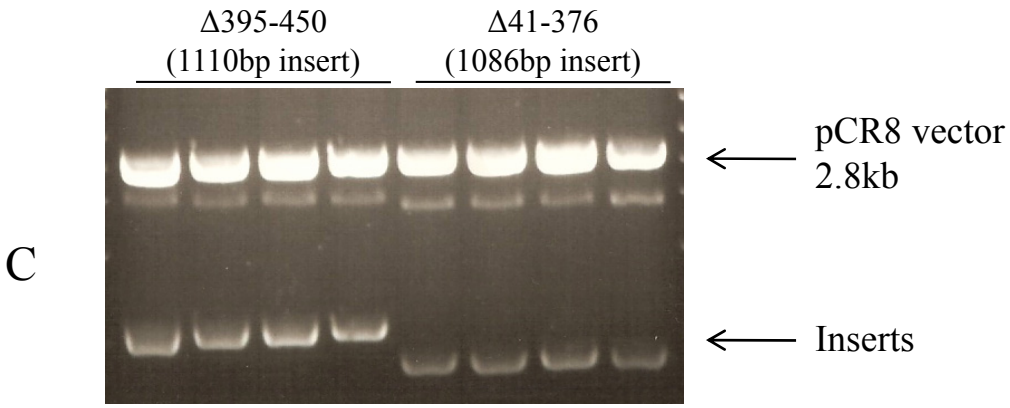
Δ395-450
(1110bp insert)
Δ41-376
(1086bp insert)
C
pCR8 vector
2.8kb
Inserts

Figure 5.10

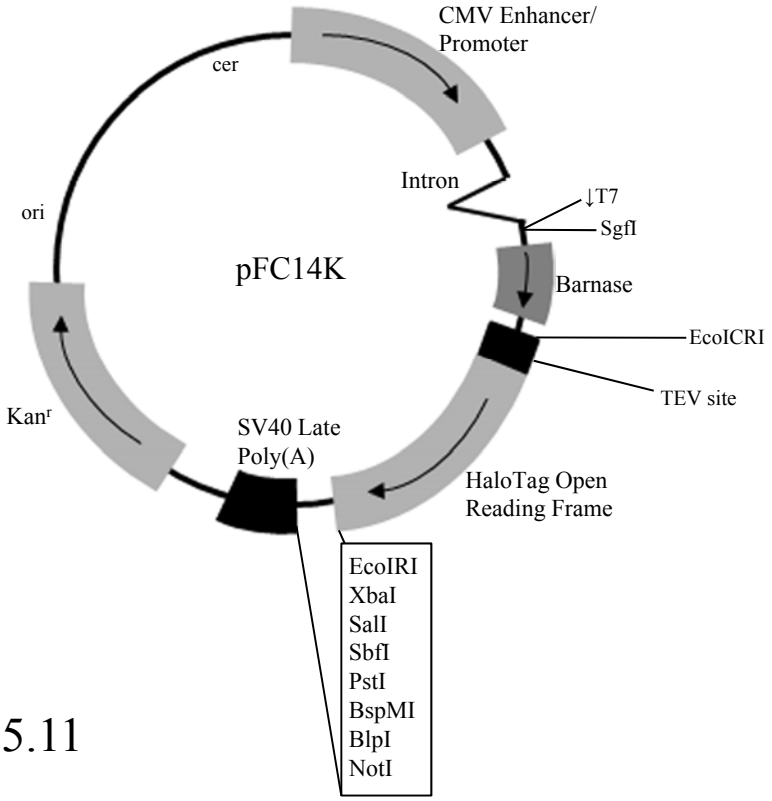

Figure 5.11

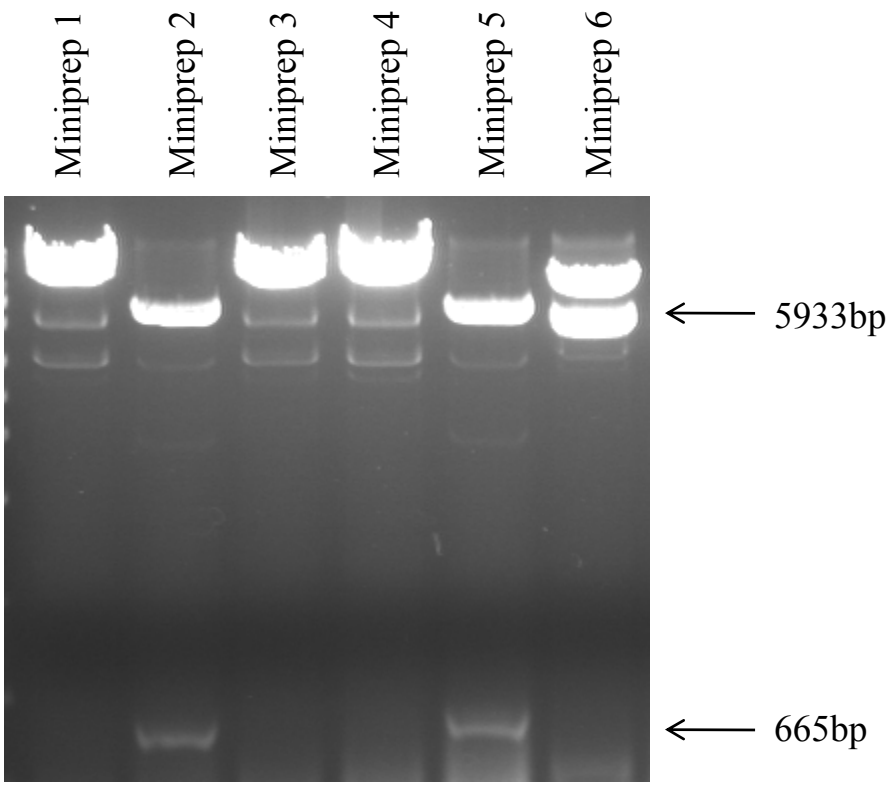

Figure 5.12

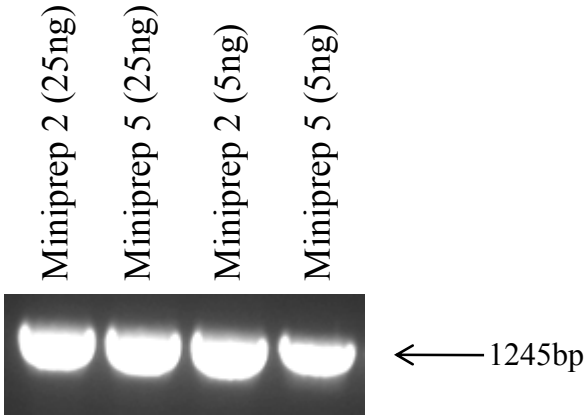

Figure 5.13

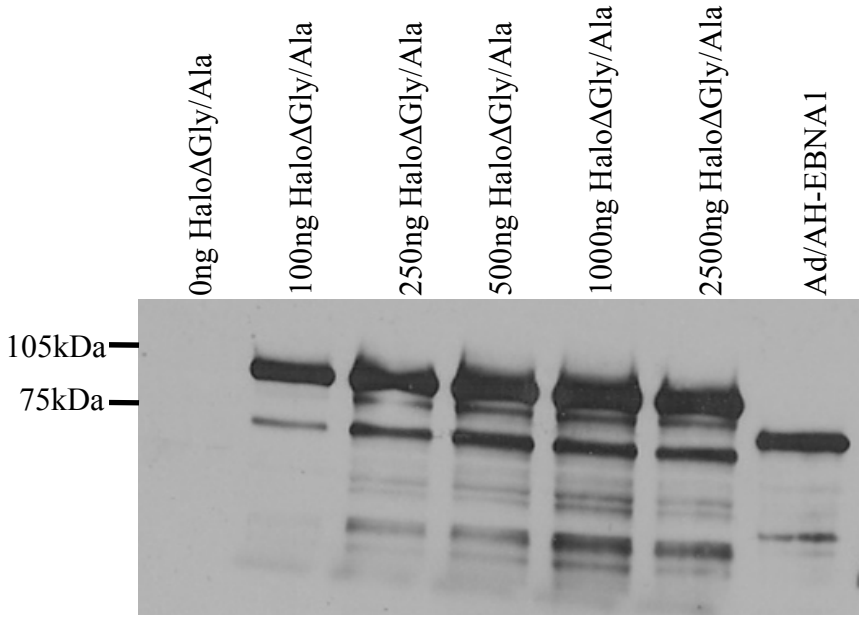

Figure 5.14

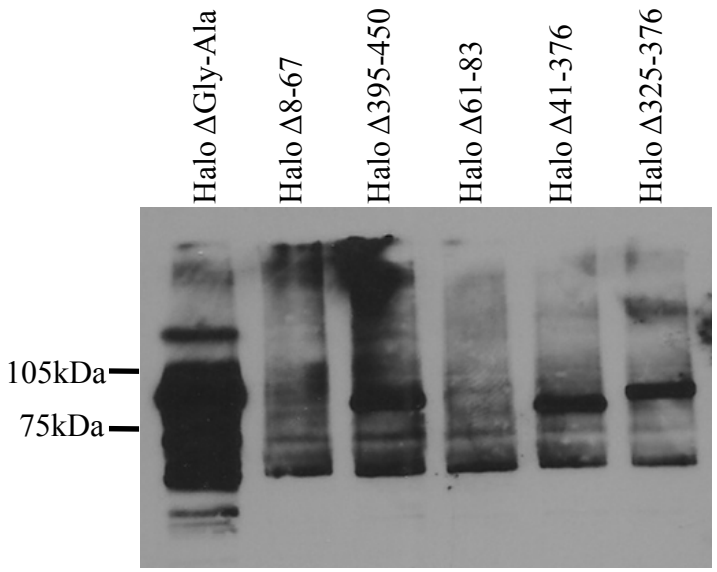

Figure 5.15

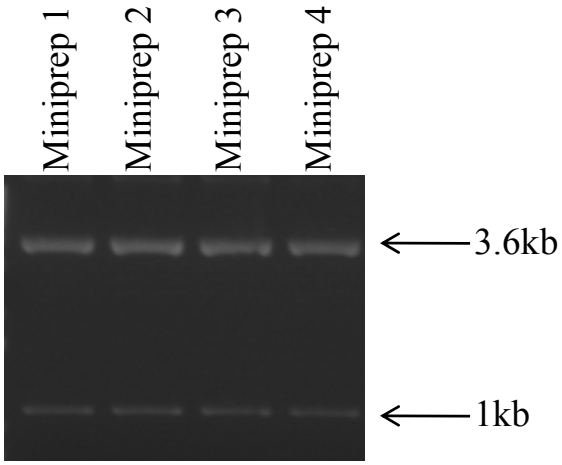

Figure 5.16

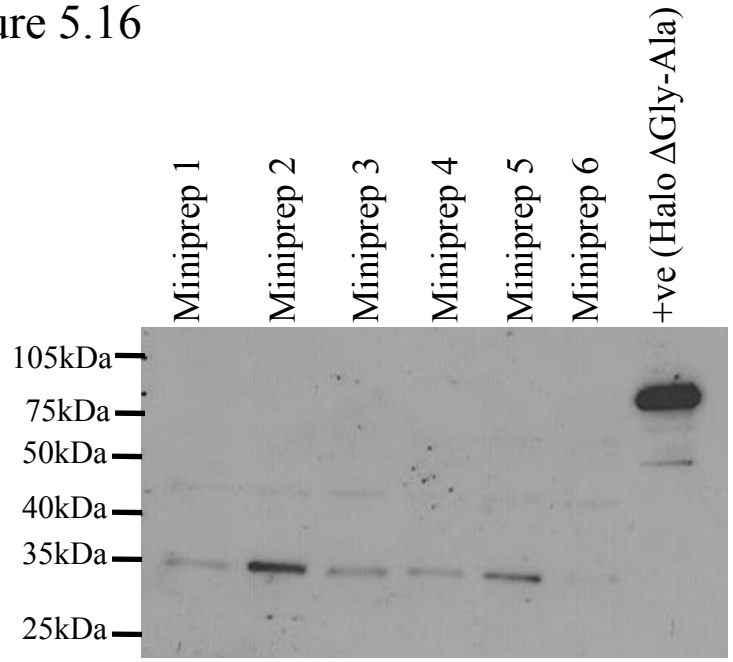

Figure 5.17

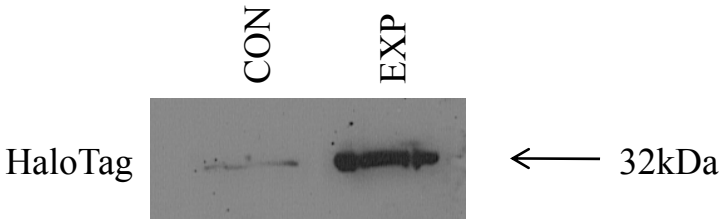

Figure 5.18

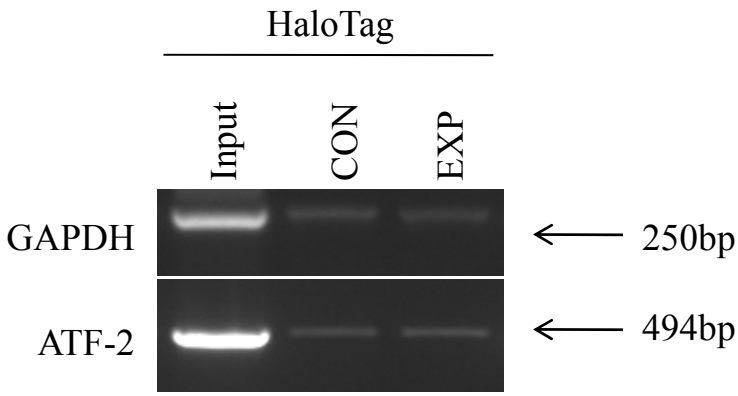

Figure 5.19

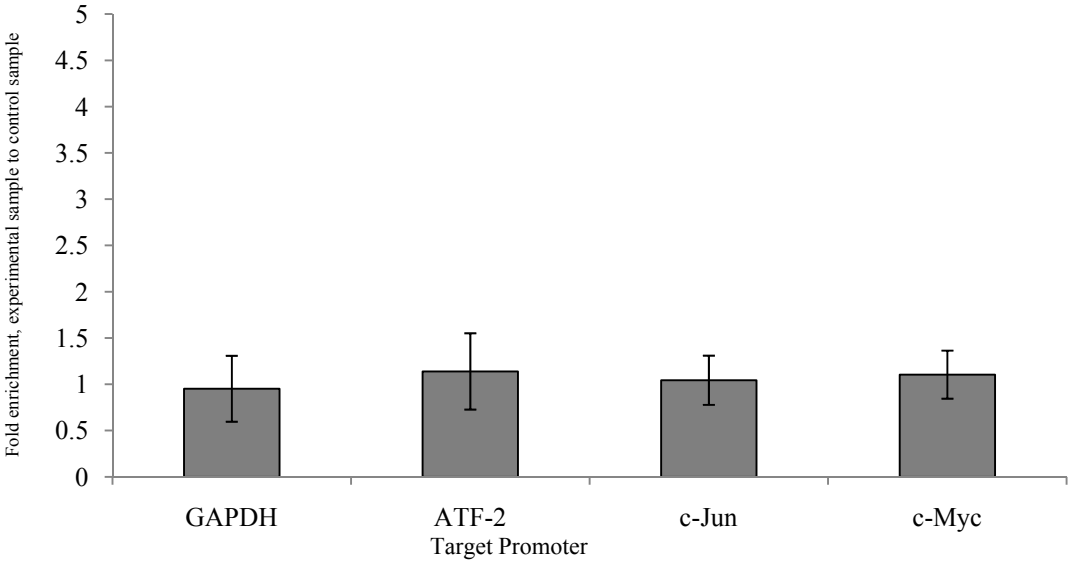

Figure 5.20

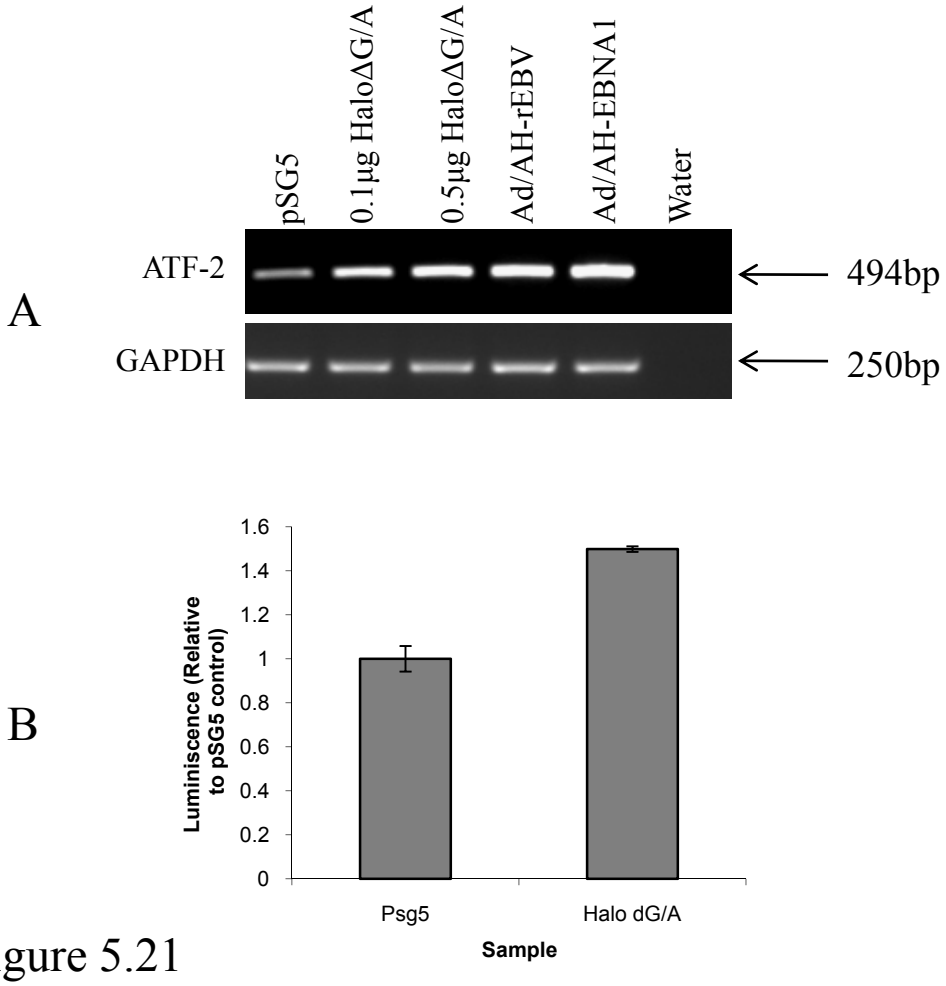

Figure 5.21

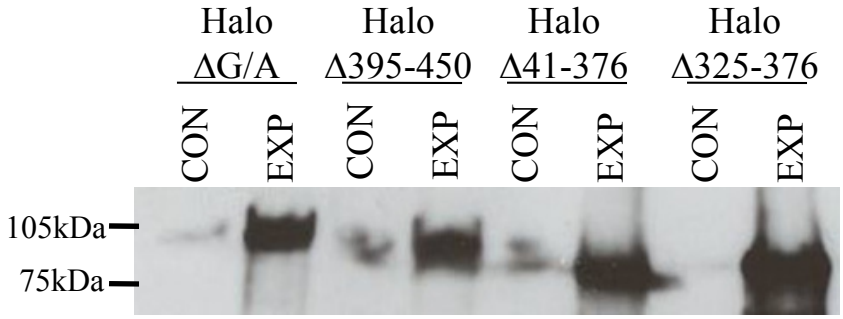

Figure 5.22

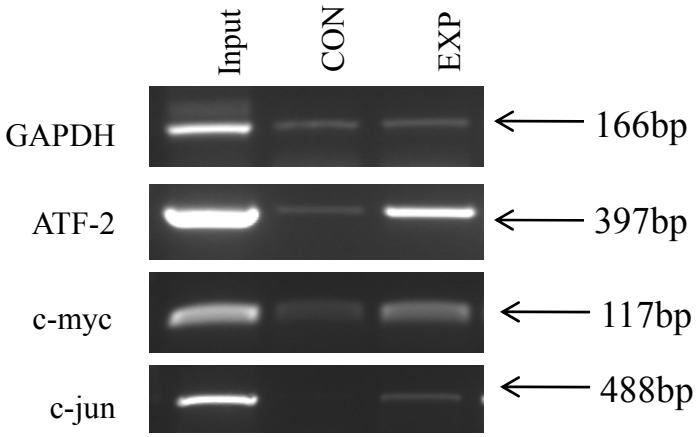

Figure 5.23

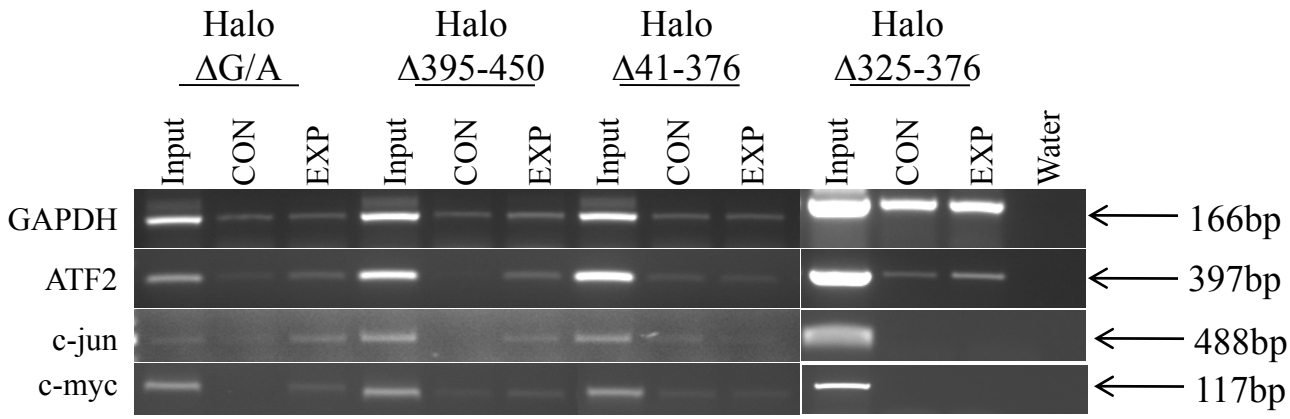

Figure 5.24

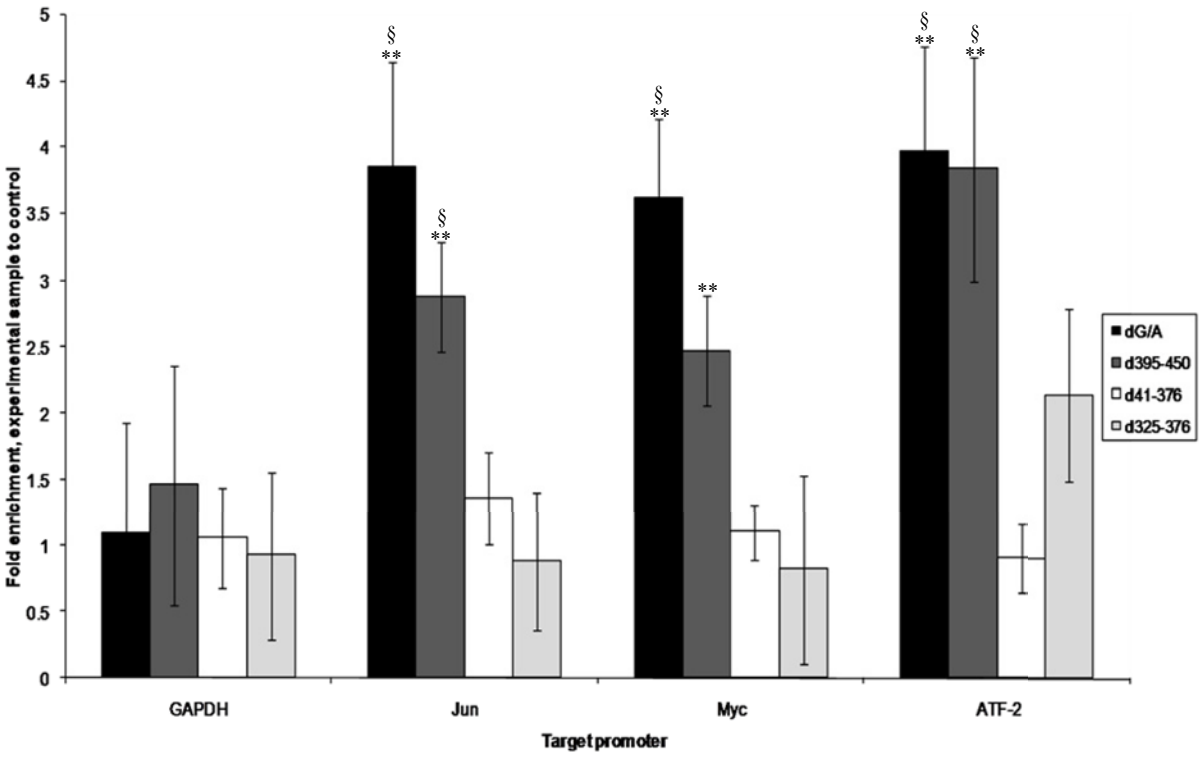

Figure 5.25

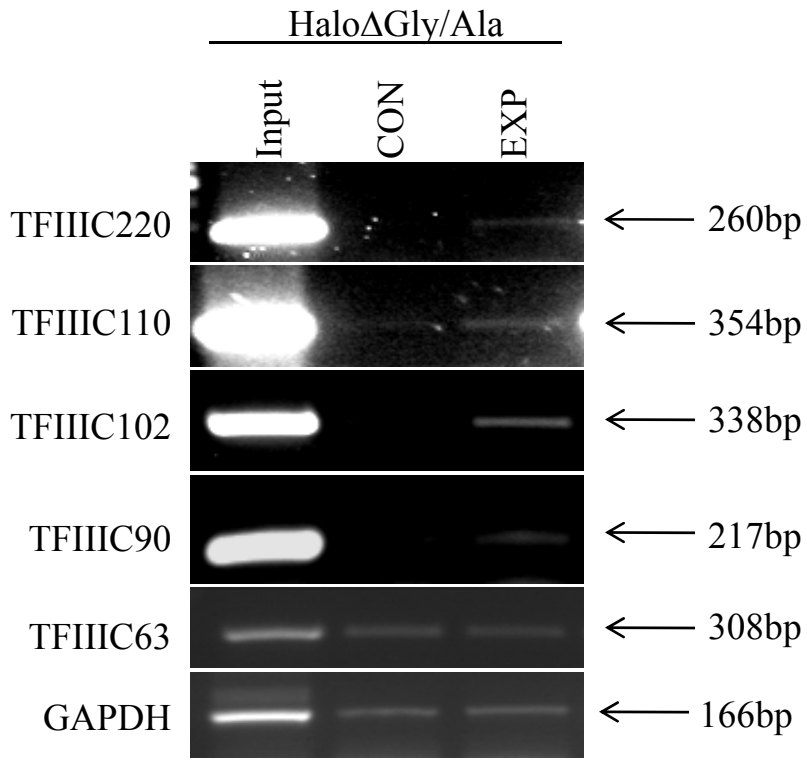

Figure 5.26

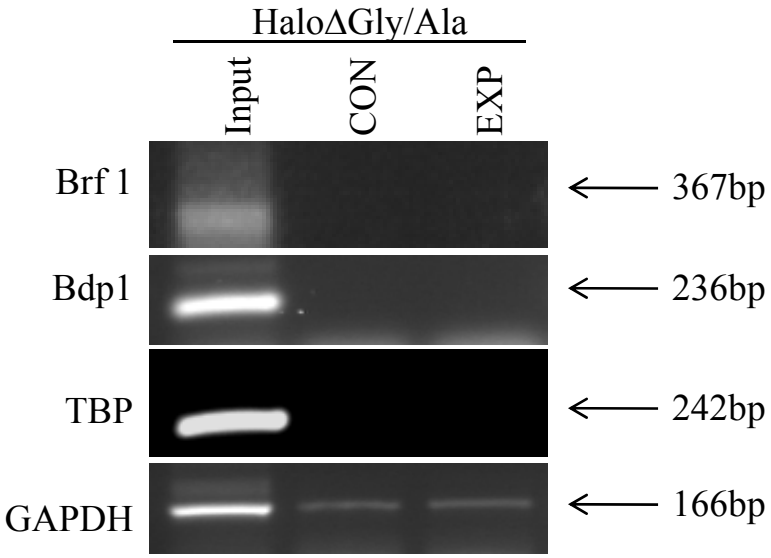

Figure 5.27

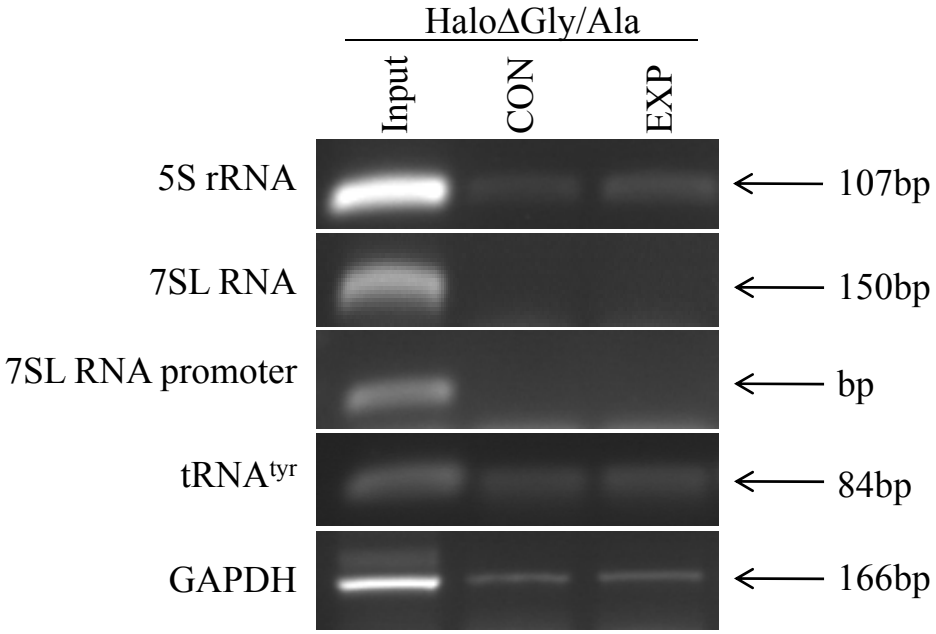

Figure 5.28

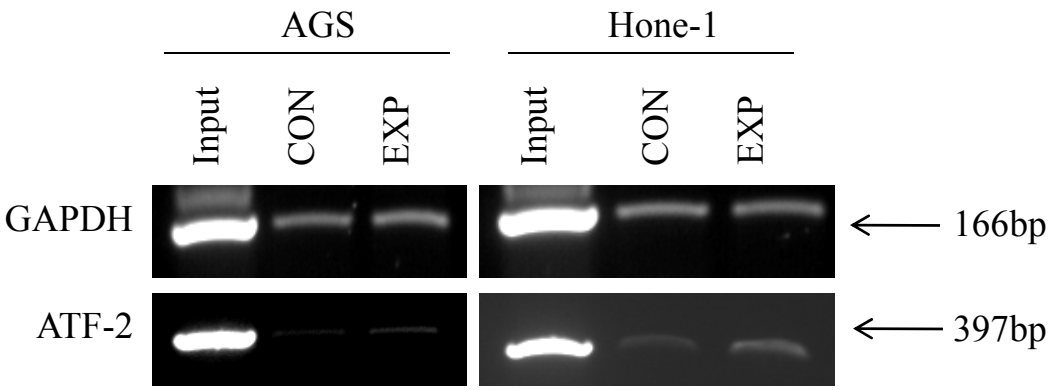

Figure 5.29

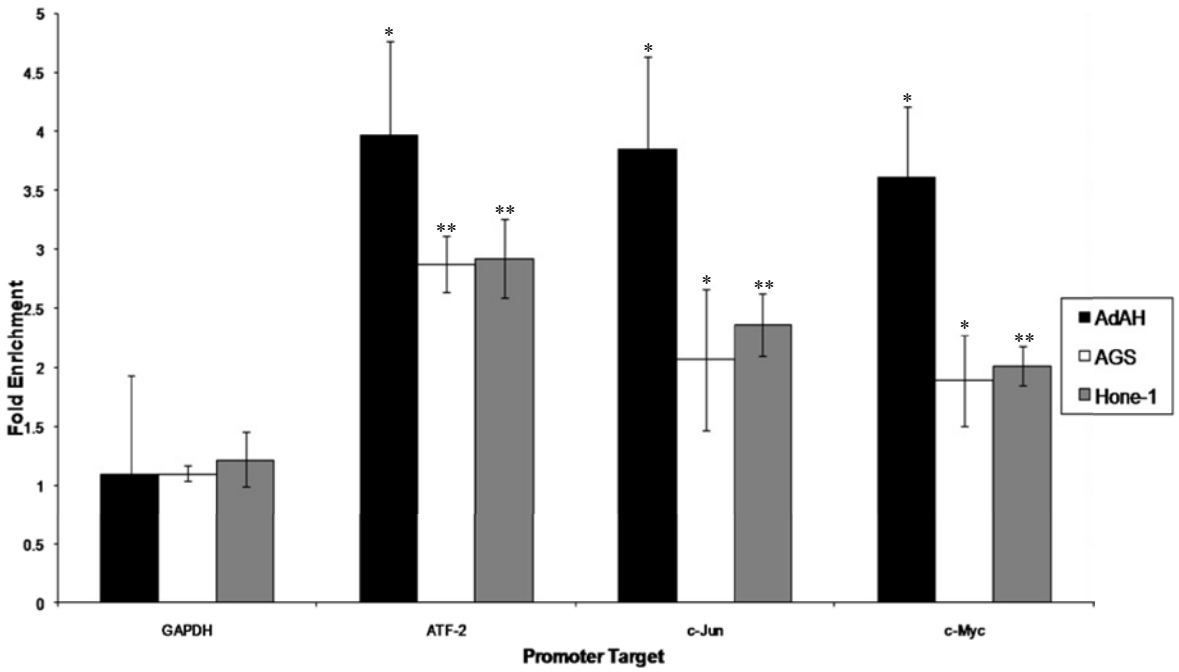

Figure 5.30

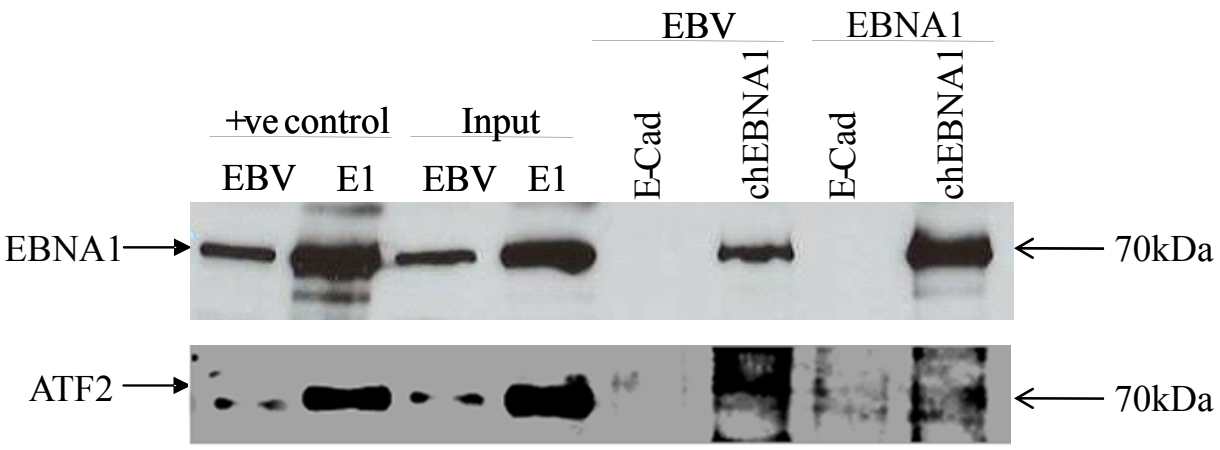

Figure 5.31

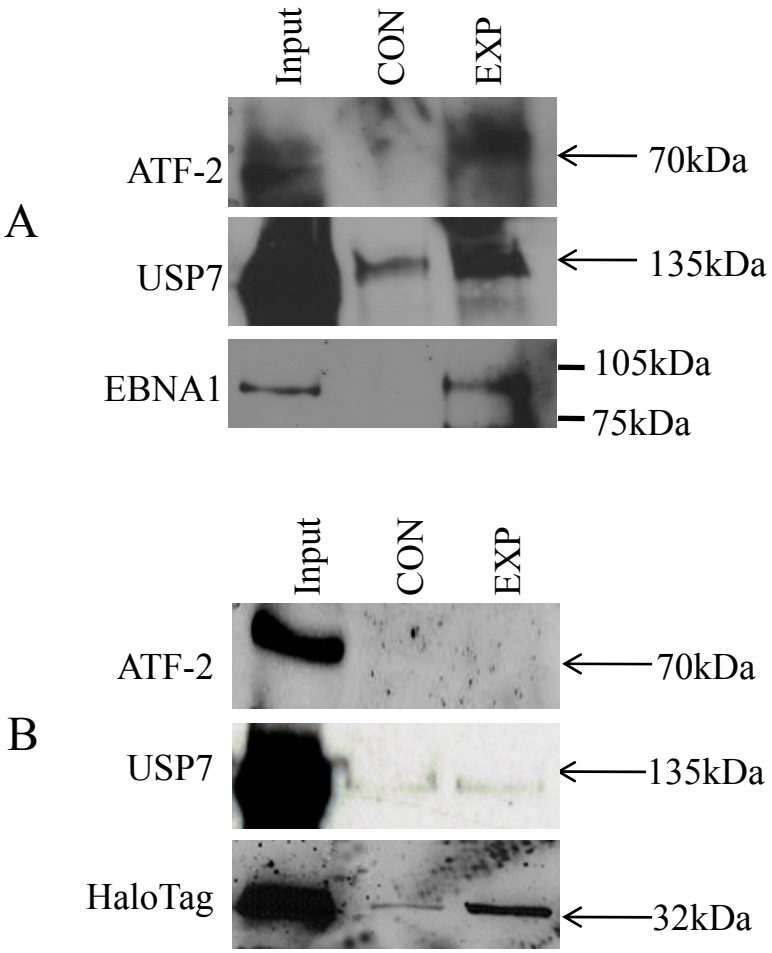
A
Input
CON
EXP
ATF-2
70kDa
USP7
135kDa
EBNA1
105kDa
75kDa
B
Input
CON
EXP
ATF-2
70kDa
USP7
135kDa
HaloTag
32kDa

Figure 5.32

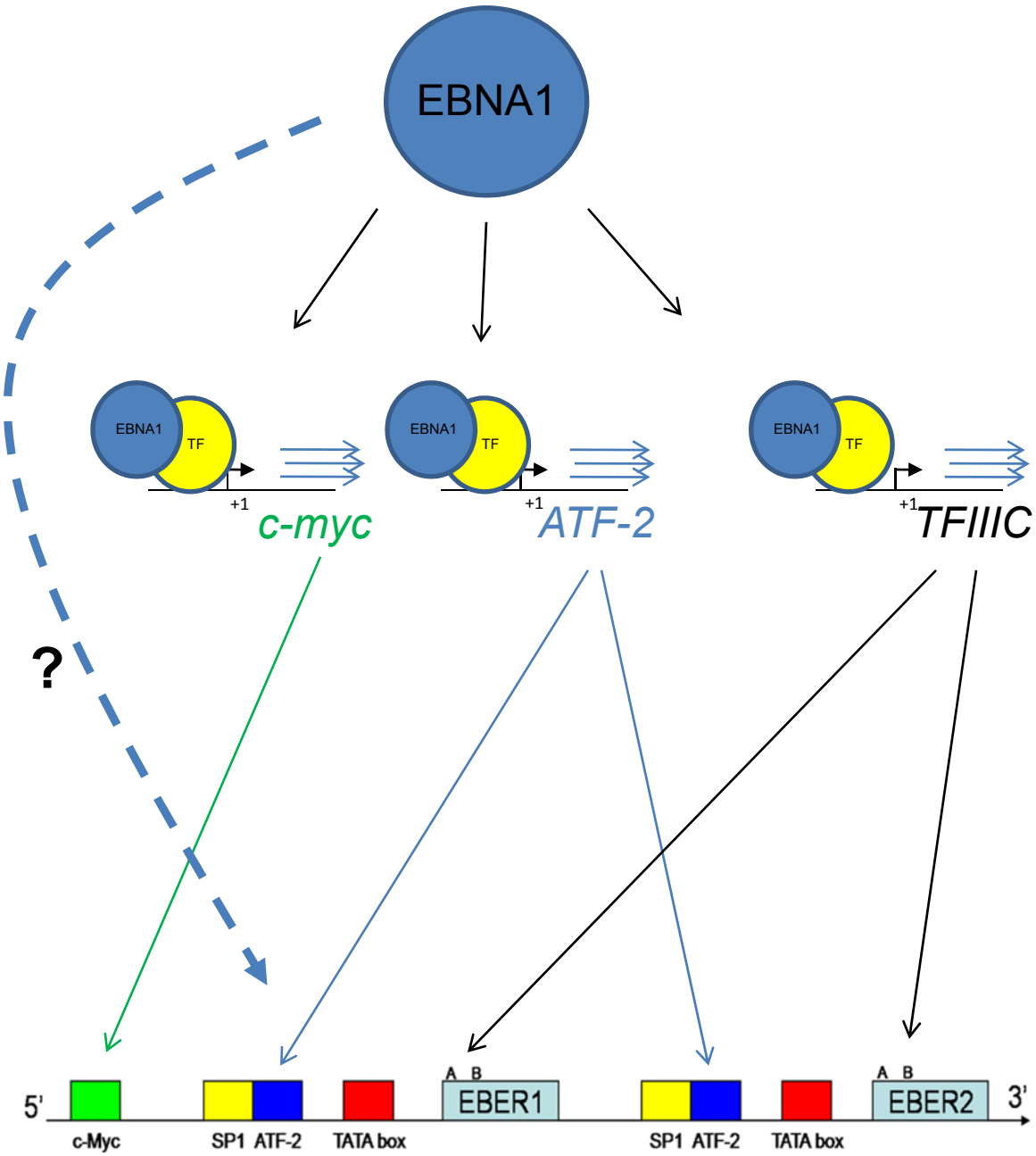
EBNA1
EBNA1
TF
+1
c-myc
EBNA1
TF
+1
ATF-2
EBNA1
TF
+1
TFIIIC
?
5'
c-Myc
SP1
ATF-2
TATA box
A
B
EBER1
SP1
ATF-2
TATA box
A
B
EBER2
3'

Figure 6.1